

Copyright
by
Megan Courtney Mears
2022

**The Dissertation Committee for Megan Courtney Mears
Certifies that this is the approved version of the following dissertation:**

**Vaccine Development Strategies for Crimean-Congo Hemorrhagic
Fever Virus and its Tick Vector**

Committee:

Dennis Bente, D.V.M., Ph.D., Supervisor

Alan Barrett, Ph.D.

Lynn Soong, M.D., Ph.D.

David Beasley, Ph.D.

Jose de la Fuente, Ph.D.

**Vaccine Development Strategies for Crimean-Congo Hemorrhagic
Fever Virus and its Tick Vector**

by

Megan Courtney Mears, B.S., M.P.H.

Dissertation

Presented to the Faculty of the Graduate School of

The University of Texas Medical Branch

in Partial Fulfillment

of the Requirements

for the Degree of

Doctor of Philosophy

The University of Texas Medical Branch

July 2022

Dedication

This dissertation is dedicated to my family, to whom I could never express enough gratitude for their constant support throughout this journey.

Acknowledgements

First, I would like to acknowledge my mentors and committee members for their guidance over the past five years. When I first started as a student at UTMB, I was drawn to Dennis Bente's lab, at first because I thought the work was fascinating, but secondly, and most importantly, because of the fantastic lab members who welcomed me in as a member of the Bente Lab family. Dennis, you continuously fostered my curiosity, and I think I could count on one hand the number of times that I heard something other than "Sure, try it and see what happens!" when I brought up a new experiment. I faced many difficulties with the studies for this dissertation, and I would not have made it to the end of this journey without the additional mentorship of Alan Barrett. It has been through your guidance and "molding" that I have grown so much as a scientist in such a short time. Thank you to both Dennis and Alan for encouraging me to aim high, but making sure that I learned how to map out every step to create a path I could follow to be successful. My other committee members, Jose de la Fuente, Lynn Soong, and David Beasley, have all been instrumental to my success, and I am so grateful for their help.

I want to thank all the current and former, official and unofficial, members of the Bente Lab. Maria Cajimat has been the best research scientist, lab manager, mentor, confidant, cheerleader, and friend that anyone could be so lucky to have. I will be forever indebted to you and the whole Dondonay clan for taking in not only me, but also Michael and Ivy, as members of your family. Sergio Rodriguez took me under his wing, much to his initial dismay with my overeager younger self. Our daily debates about viruses, experiments, and life are some of my favorite graduate school memories, and it has truly

been a joy to have you as such an amazing colleague and friend over the years. Nathen Bopp, an unofficial Bente Lab member, has always encouraged me to think outside of the box and was always there to lend a hand, reagents, and advice when something seemed wrong. The comedic relief from Sergio and Nathen always helped me keep a level head when studies were stressful, and I'm so thankful for you both. I could write pages about how much help I received from my other lab members, but I will end with a very broad 'Thank you for everything!' for my remaining lab members and other colleagues over the years: Chao Shan, Angel Padilla, Corey Fulton, Gabe Haila, Isolde Schuster, Sirri Kar, Aysen Gargili Keles, Tais Saito, Maureen Laroche, Vilma Ortiz, Diana Fdez Echeverri, Maricela Torres, and Balmoris Garcia.

This dissertation would not have been possible without the help of multiple institutions. Grant McFadden and Masmudur Rahman at Arizona State University provided guidance throughout my work with myxoma virus. I worked with many of Jose de la Fuente's lab members for the Subolesin studies. Sara Artigas Jeronimo, Margarita Villar, and especially, Marinela Contreras Rojo, all of your help is greatly appreciated. It was also a great experience working with Gabrielle Scher and Matthias Schnell on rabies and CCHFV studies. Finally, many other students, staff, and faculty at UTMB were instrumental in helping me complete my studies. I would not have been able to complete some of my studies without Jing Zhou, Antonio Muruato, Jennifer Smith, Trevor Brasel, Stephanea Sotcheff, Jill Thompson, Steve Widen, Kassandra Carpio, Clairissa Hansen, and Ashley Strother.

I would be remiss not to acknowledge the people who pushed me to pursue science and graduate school in the first place: Lori Warren and Marina Eremeeva. Lori Warren first

introduced me to science fair, and I've been fascinated by biology and research since the sixth grade. Marina Eremeeva, thank you for taking a chance on an undergraduate student interested in science. It is because of you that I wanted to pursue graduate school and a career as a scientist. Your encouragement, support, and belief in my abilities to accomplish these studies helped me never give up on my dream of obtaining this degree.

One piece of advice passed down to new students is the importance of having a group of friends that will support you through all of the stressful times of graduate school. For the friendships that I've made at UTMB, I couldn't be more thankful. Rachel Reyna, Corri Levine, Stephanie Foster, Angel Padilla, and Megan Files, thank you for always being there to make me laugh or let me cry, to get coffee and talk about science or life, and for sharing and celebrating huge successes and failures.

Last but certainly not least, I have had an amazing support system in my family over the years. David and Sharon Mears, Mom and Dad, there are no words to describe how grateful I am for *everything* you have done for me. Michael Bailey, you have been the best friend and partner I could have ever asked for, and I can't thank you enough for your unconditional patience and love while I finished these studies. My family, both Mears and Bailey, and my friends back home who are a part of the Mears family, have made sure that I made it through this journey. David, Sharon, Dave, Jamie, Kennedy, Cecilia, Brandon, Michael, Tammy, Jeff, Bill, Erin, Matthew, Nikki, and Ivy, thank you all for being there when I needed it most. Even though none of you really understood why I wanted to pursue this degree and work with dangerous things you can't see, you never faltered in your support. I love you all.

Vaccine Development Strategies for Crimean-Congo Hemorrhagic Fever Virus and its Tick Vector

Publication No. _____

Megan Courtney Mears, PhD

The University of Texas Medical Branch, 2022

Supervisor: Dennis A. Bente

Crimean-Congo hemorrhagic fever virus (CCHFV) is a tick-borne bunyavirus with an extensive geographic range and complex ecology. Ticks within the *Hyalomma* genera are the primary vector and reservoir of the virus and maintain the virus through a cryptic tick-vertebrate-tick cycle in nature. However, infection of humans with CCHFV can result in the severe disease known as Crimean-Congo hemorrhagic fever (CCHF). As humans are the only species that display clinical signs of disease from infection with CCHFV, vaccine development has focused on preventing human disease. Despite extensive research, no vaccine candidates have advanced to clinical trials. This dissertation aimed to utilize different vaccine platform technologies to target unique points in the CCHFV transmission cycle as new strategies for vaccine development for CCHFV. Vaccine candidates were developed against ticks for the preferred hosts of immature and adult *H. marginatum* ticks, and against the virus for prevention of human CCHF. The two anti-tick vaccine candidates utilized viral-vectored vaccine technology encoding the concealed tick antigen Subolesin

or a chimeric Subolesin and rabies virus glycoprotein antigen. Neither vaccine candidate induced stronger humoral immunity than the conventional approach of purified protein in adjuvant. These studies showed that the vaccine type, specific viral vector used and the generation of a chimeric Subolesin antigen are key considerations for developing future anti-tick vaccines. For prevention of human CCHF, a candidate multi-epitope antigen for CCHFV was developed using bioinformatics and a plasmid-based DNA vaccine was evaluated *in vitro* and *in vivo*. Although the multi-epitope antigen was not immunogenic, these studies provide information about predicted immunogenic regions of the CCHFV glycoprotein precursor that should be evaluated for inclusion in rational vaccine development. Overall, this dissertation has evaluated three different vaccine development strategies, and provides information for future tick and CCHFV vaccine development research.

TABLE OF CONTENTS

List of Tables	xv
List of Figures	xvii
List of Supplementary Tables	xx
List of Supplementary Figures.....	xxi
List of Abbreviations	xxiii
Chapter 1: Introduction	28
1.1 Crimean-Congo Hemorrhagic Fever Virus.....	28
1.1.1 History.....	28
1.1.2 Public Health Significance.....	29
1.1.3 Genome Organization and Virion Structure	30
1.1.4 Replication Cycle.....	31
1.1.5 Phylogeny	32
1.1.6 Pathogenesis and Immune Response to CCHFV Infection	33
1.1.7 Animal Models of CCHF	35
1.1.8 Difficulties in Vaccine Development to Prevent CCHF.....	36
1.2 Ticks.....	39
1.2.1 <i>Hyalomma</i> Life Cycle and CCHFV Transmission Cycle.....	39
1.2.2 The Tick Bite Site, Feeding, and Bloodmeal Metabolism.....	41
1.2.3 Tick Control Measures.....	43
1.2.3.1 Acaricides	43
1.2.3.2 Tick Vaccines Against Exposed and Concealed Antigens	43
1.3 Subolesin.....	46
1.3.1 Protein Discovery and Homology Across Species	46
1.3.2 Function of Subolesin and Impact of Subolesin Impairment.....	47
1.3.3 Subolesin as an Anti-Tick Vaccine Antigen.....	48
1.4 Myxoma Virus	51
1.5 Rabies Virus.....	55
1.6 Goals of Dissertation.....	57
Chapter 2: Materials and Methods.....	74
2.1 <i>In silico</i> Analyses.....	74

2.1.1 Subolesin Codon Optimization	74
2.1.2 Nucleotide Alignments and Homology Calculations	74
2.1.3 Cytotoxic T-Lymphocyte Epitope Prediction.....	74
2.1.4 Helper T-Lymphocyte Epitope Prediction.....	75
2.1.5 Alignment and Graphing of Predicted Epitopes to the CCHFV GPC	76
2.1.6 Amino Acid Alignments, Phylogenetic Tree, and Homology Calculations	76
2.1.6.1 Full-length GPC and Phylogenetic Tree	76
2.1.6.2 Individual GPC Proteins	76
2.1.6.3 Multi-Epitope Regions.....	77
2.1.6.4 Homology Calculations	77
2.1.7 Generation of the Multi-Epitope Antigen and Plasmid	77
2.1.8 Subcellular Localization Prediction.....	78
2.2 Biological Assays.....	78
2.2.1 Cell Lines and Cell Culture.....	78
2.2.1.1 Mammalian Cell Lines	78
2.2.1.2 Tick Cell Lines	79
2.2.2 Plasmids	79
2.2.3 Proteins	81
2.2.3.1 Antibodies	81
2.2.3.2 Purified Recombinant Protein	82
2.2.3.3 Generation of Whole-Cell Protein Lysates	82
2.2.4 Viruses	83
2.2.4.1 Recombinant Myxoma Viruses.....	83
2.2.4.1.1 Generation of Recombinant Myxoma Viruses	83
2.2.4.1.2 Production of Recombinant Myxoma Virus Stocks	83
2.2.4.1.3 Sucrose Purification of Recombinant Myxoma Virus	84
2.2.4.1.4 Titration by Fluorescent Focus Forming Assay.....	84
2.2.4.1.5 Multiplication Kinetics	85
2.2.4.1.6 Myxoma Virus Fluorescence Reduction Neutralization Test.....	86

2.3.2 Immunogenicity of Recombinant Rabies Viruses	100
2.3.3 Tolerability and Immunogenicity of the DNA Vaccine Candidate	101
2.4 Statistics	102
Chapter 3: A Poxvirus-Vectored Anti-Tick Vaccine for Hosts of Immature <i>Hyalomma marginatum</i>	108
3.1 Abstract	108
3.2 Introduction	109
3.3 Results	1011
3.3.1 Antigen Selection, Synthesis, and Evaluation of <i>H. marginatum</i> Subolesin from a Mammalian Expression Plasmid	1011
3.3.1.1 Codon Optimization and Antigen Synthesis	1011
3.3.1.2 Antigen Expression and Detection with Anti-Subolesin Antibodies	112
3.3.2 Generation and Characterization of Recombinant Myxoma Viruses	113
3.3.2.1 Generation of Recombinant Myxoma Viruses	113
3.3.2.2 Foci Morphology and Multiplication Kinetics are not Impacted by the Insertion of Subolesin into wtMYXV	114
3.3.2.3 Antigen Expression and Detection with Anti-Subolesin Antibodies	115
3.3.3 Tolerability and Immunogenicity of the Vaccine Candidate in a Mouse Model	116
3.3.4 Detection of <i>H. marginatum</i> Subolesin with Mouse Anti-Subolesin Antibodies	118
3.3.5 Evaluation of Subolesin Expression from vMyx-GFP-Subolesin using Mouse Anti-Subolesin Antibodies	119
3.4 Discussion	120
Chapter 4: A Replication-Competent Rabies Virus-Vectored Anti-Tick Vaccine for Hosts of Adult <i>Hyalomma marginatum</i>	142
4.1 Abstract	142
4.2 Introduction	143
4.3 Results	144

4.3.1 Antigen Modification, Codon-Optimization, and Synthesis of Subolesin-RABV-G	144
4.3.2 The Subolesin-RABV-G Chimeric Protein is Recognized by Anti-Subolesin Antibodies and has an Altered Subcellular Localization	147
4.3.3 Recombinant Virus Generation and Expression of Subolesin-RABV-G	148
4.3.4 Immunogenicity of the Vaccine Candidate in a Mouse Model	149
4.4 Discussion	153
Chapter 5: An Immunoinformatics Guided Approach for Rational Design of a Crimean-Congo Hemorrhagic Fever Virus Multi-Epitope DNA Vaccine	165
5.1 Abstract	165
5.2 Introduction	166
5.3 Results	167
5.3.1 Identification of Epitopes Across the CCHFV GPC using Bioinformatic Servers	167
5.3.2 Conservation of Multi-Epitope GPC Regions Between CCHFV Strains	169
5.3.3 Generation of the Multi-Epitope Antigen	170
5.3.4 Evaluation of Antigen Expression and Detection with CCHFV Antibodies	172
5.3.4.1 Recognition of <i>EPIC</i> by Anti-6XHis and Anti-CCHFV Polyclonal Antibodies	172
5.3.4.2 Recognition of <i>EPIC</i> by Anti-CCHFV mAbs	173
5.3.5 Tolerability of the DNA Vaccine Candidate in a Mouse Model	174
5.3.6 Immunogenicity of the DNA Vaccine Candidate in a Mouse Model	176
5.3.6.1 Assessment of Humoral Immunogenicity	176
5.3.6.2 Assessment of Cellular Immunogenicity	177
5.4 Discussion	182
Chapter 6: An <i>in vitro</i> Approach to Evaluate the Biological Impact of Subolesin Antisera	213
6.1 Abstract	213
6.2 Introduction	214

6.3 Results.....	215
6.3.1 Antibodies from <i>R. microplus</i> Subolesin Protein in Adjuvant Immunization Recognize <i>I. scapularis</i> Subolesin	215
6.3.2 Anti-Subolesin Antibodies Can Enter Nonpermeabilized ISE6 Cells to Bind Subolesin.....	217
6.3.3 Internalization of Anti-Subolesin Antibodies in ISE6 Cells is Concentration-Dependent	218
6.3.4 Starvation of ISE6 Cells Before Incubation with Anti-Subolesin Antibodies Increases Antibody Internalization.....	220
6.3.5 Anti-Subolesin Antibodies from Vaccination with RABV-Subolesin Can Enter ISE6 Cells to Bind Subolesin	221
6.3.6 Incubation of Tick Cells with Anti-Subolesin Antibodies Does Not Impact Cell Metabolism.....	222
6.3.7 Evaluation of Downregulated Genes in Response to Subolesin Knockdown.....	223
6.3.8 Incubation of Tick Cells with Subolesin Antisera Does Not Impact the Cell Transcriptome.....	226
6.4 Discussion	231
Chapter 7: Final Discussion	259
7.1 Vaccine Development to Prevent CCHF	260
7.2 Development of Anti-Tick Vaccines	263
7.3 Understanding the Mechanism of Action of Anti-Tick Vaccines	267
7.4 Conclusion	269
Appendix A: Supplementary Figures for Chapter 3	270
Appendix B: Supplementary Figures for Chapter 4	278
Appendix C: Supplementary Tables and Figures for Chapter 5	285
Appendix D: Supplementary Figures for Chapter 6	347
References	358
Vita	383

List of Tables

Table 1.1: CCHFV vaccine candidates that have demonstrated 100% protection from lethal challenge in mouse models and protection from disease in the <i>C. macaque</i> model.....	61
Table 1.2: Candidate protective antigens for anti-tick vaccine development.	63
Table 1.3: Subolesin anti-tick vaccine candidates and efficacy.....	65
Table 2.1: GPC sequences used for evaluation of CCHFV homology.....	103
Table 2.2: Primers used for cloning, PCR, Sanger sequencing, and qRT-PCR.	105
Table 3.1: Summary of IFA results.....	130
Table 5.1: Total CTL and HTL predicted epitopes by GPC region.....	191
Table 5.2: Total CTL and HTL predicted epitopes in each selected multi-epitope region	192
Table 5.3: Percent identity of each multi-epitope region between 50 different CCHFV GPC sequences.....	193
Table 5.4: Percent similarity of each multi-epitope region between 50 different CCHFV GPC sequences.....	194
Table 5.5: Percent identity and similarity of each GPC protein between 50 different CCHFV GPC sequences	195
Table 5.6: Summary of residue conservation between GPC proteins and multi-epitope regions.....	196
Table 5.7: <i>EPIC</i> is not recognized by CCHFV monoclonal antibodies.....	197
Table 5.8: Total mouse CTL and HTL predicted epitopes in each selected multi-epitope region	198

Table 5.9: Summary of results that differed from expectations, and potential explanations199

Table 6.1: Most significantly downregulated genes in response to Subolesin knockdown in ISE6 cells243

Table 6.2: Number of reads of genes of interest from NGS of ISE6 cells.....244

Table 6.3: Number of reads and read counts per sample and group from RNA-seq.245

Table 6.4: Differentially expressed genes between the rabbit mock serum treated and rabbit Subolesin antiserum treated ISE6 cells.246

List of Figures

Figure 1.1: Geographic distribution of <i>Hyalomma</i> ticks and CCHF cases.....	70
Figure 1.2: CCHFV genome organization and virion structure.....	71
Figure 1.3: Replication cycle of CCHFV	72
Figure 1.4: Transmission cycle of CCHFV.	73
Figure 2.1: Subolesin codon-optimization and sequences.....	106
Figure 3.1: Subolesin expression and detection in mammalian cells using antibodies to the C-terminal polyhistidine tag and rabbit anti-Subolesin serum.....	131
Figure 3.2: Schematic diagrams of wild-type and recombinant myxoma viruses.....	132
Figure 3.3: There are no differences in focus morphology between vMyx-GFP-Empty and vMyx-GFP-Subolesin	133
Figure 3.4: Insertion of Subolesin into wtMYXV does not impact virus multiplication kinetics	134
Figure 3.5: Rabbit anti-Subolesin serum cross-reacts with wtMYXV	135
Figure 3.6: Vaccination with vMyx-GFP-Subolesin does not elicit anti-Subolesin binding antibodies.....	136
Figure 3.7: wtMYXV-neutralizing antibodies were not detected in serum from vMyx- GFP-Empty, or vMyx-GFP-Subolesin vaccinated mice.....	138
Figure 3.8: Mouse anti-Subolesin antibodies recognize <i>H. marginatum</i> Subolesin expressed in mammalian cells by IFA	139
Figure 3.9: Mouse anti-Subolesin antibodies recognize <i>H. marginatum</i> Subolesin expressed in mammalian cells by western blot.....	140

Figure 3.10: Subolesin expression is not detected from the recombinant virus vMyx-GFP-Subolesin	141
Figure 4.1: The Subolesin-RABV-G chimeric protein is recognized by anti-Subolesin antibodies and has an altered subcellular localization	160
Figure 4.2: Schematic diagrams of recombinant RABV vaccines	161
Figure 4.3: Subolesin is expressed from RABV-Subolesin.....	162
Figure 4.4: Immunogenicity of live recombinant RABV vaccines	163
Figure 5.1: Alignment of all included epitopes to the GPC.....	200
Figure 5.2: <i>EPIC</i> is expressed in mammalian cells and is detectable with antibodies to the C-terminal polyhistidine tag and polyclonal CCHFV serum.....	202
Figure 5.3: <i>EPIC</i> is well-tolerated as a DNA vaccine given via IM-EP	203
Figure 5.4: Vaccinated mouse serum does not recognize <i>EPIC</i> or GPC expressed in mammalian cells	205
Figure 5.5: Alignment of all mouse epitopes to the GPC.....	206
Figure 5.6: IFN- γ + T cells quantified by ELISpot after polyclonal stimulation with ConA	207
Figure 5.7: HisPur™ Ni-NTA resin purification of <i>EPIC</i>	208
Figure 5.8: His.H8 western blot of HEK293T cell lysates	209
Figure 5.9: The NP, but not G _C , is recognized in R430 lysate by ELISA	210
Figure 5.10: CCHFV HMAF western blot of HEK293T cell lysates and R430 lysate..	211
Figure 5.11: Stimulation of naïve splenocytes with R430 lysate does not produce IFN- γ	212

Figure 6.1: Antibodies generated by immunization with <i>R. microplus</i> Subolesin protein in adjuvant recognize Subolesin in ISE6 cells	247
Figure 6.2: Anti-Subolesin antibodies can enter ISE6 cells to bind Subolesin without permeabilization.....	248
Figure 6.3: Large cytoplasmic puncta are present in ISE6 cells incubated with mouse Subolesin antiserum, but not in ISE6 cells stained post-fixation.....	249
Figure 6.4: Antibody internalization and binding is concentration-dependent	250
Figure 6.5: Starvation of the tick cells before incubation with anti-Subolesin antibodies increases antibody internalization	251
Figure 6.6: Antibodies from RABV-Subolesin immunization can enter ISE6 Tick cells and bind Subolesin.....	253
Figure 6.7: Incubation of tick cells with anti-Subolesin antibodies does not reduce cell metabolism	255
Figure 6.8: Total counts of reads that correspond to annotated genes of the <i>I. scapularis</i> genome.....	256
Figure 6.9: Analysis of differentially expressed genes from Subolesin antiserum treated ISE6 cells	257

List of Supplementary Tables

Supplementary Table 5.1: CTL epitopes identified in the CCHFV Turkey2004 GPC sequence	286
Supplementary Table 5.2: HTL epitopes of HLA locus DR identified in the CCHFV Turkey2004 GPC sequence.....	293
Supplementary Table 5.3: HTL epitopes of HLA locus DQ identified in the CCHFV Turkey2004 GPC sequence.....	302
Supplementary Table 5.4: HTL epitopes of HLA locus DP identified in the CCHFV Turkey2004 GPC sequence.....	3011
Supplementary Table 5.5: Mouse CTL epitopes identified in the CCHFV Turkey2004 GPC sequence	315
Supplementary Table 5.6: Mouse HTL epitopes identified in the CCHFV Turkey2004 GPC sequence	316
Supplementary Table 6.1: Differentially expressed genes between ISE6 cells treated with mouse mock and rabbit mock sera.....	348

List of Supplementary Figures

Supplementary Figure 3.1: Overview of Subolesin plasmid generation, plasmid uses, and plasmid maps of pMA-Subolesin and pcDNA3.1(+)-Subolesin-6XHis	271
Supplementary Figure 3.2: Nucleotide differences between tick and rabbit codon-optimized Subolesin.....	273
Supplementary Figure 3.3: Outputs of Subolesin localization prediction and residues important for localization.....	274
Supplementary Figure 3.4: Homology of Subolesin between <i>Rhipicephalus microplus</i> and <i>Hyalomma marginatum</i>	275
Supplementary Figure 3.5: Schematic diagram of wtMYXV genome.	276
Supplementary Figure 3.6: Sequence of vMyx-GFP-Subolesin	277
Supplementary Figure 4.1: Modification of the Subolesin antigen.....	279
Supplementary Figure 4.2: Outputs of Subolesin-RABV-G localization prediction and residues important for localization.....	280
Supplementary Figure 4.3: Nucleotide differences between tick and mammalian codon-optimized Subolesin.....	281
Supplementary Figure 4.4: Plasmid map of pCAGGS-Subolesin-RVG	284
Supplementary Figure 5.1: Alignment of all predicted CTL and HTL epitopes to the CCHFV Turkey2004 GPC	317
Supplementary Figure 5.2: Method of graphing overlapping epitopes	340
Supplementary Figure 5.3: Geneious Tree Builder output of 50 GPC sequences.....	341
Supplementary Figure 5.4: Amino acid sequence of <i>EPIC</i>	342
Supplementary Figure 5.5: pTWIST-CMV- <i>EPIC</i> DNA plasmid map.....	343

Supplementary Figure 5.6: Outputs of multi-epitope antigen localization prediction and residues important for localization	344
Supplementary Figure 5.7: Alignment of all predicted mouse CTL and HTL epitopes to the CCHFV Turkey2004 GPC	345
Supplementary Figure 6.1: Homology of Subolesin between <i>Rhipicephalus microplus</i> , <i>Hyalomma marginatum</i> , and <i>Ixodes scapularis</i>	349
Supplementary Figure 6.2: Comparison of mouse antisera and rabbit antiserum anti-Subolesin ELISA results	351
Supplementary Figure 6.3: Amplification curves and cycle threshold values from qRT-PCR experiments	352
Supplementary Figure 6.4: IFA of ISE6 cells treated with anti-Subolesin antibodies in parallel to the cells treated for RNA-seq.....	355
Supplementary Figure 6.5: Analysis of differentially expressed genes between rabbit and mouse sera treated groups	357

List of Abbreviations

μg	Micrograms
μL	Microliters
13G8	GP38 mAb
1C5	RABV-G mAb
6XHis	6 residue polyhistidine epitope tag
AAALAC	Association for Assessment and Accreditation of Laboratory Animal Care International
ABTS	2,2'-azinobis [3-ethylbenzthiazoline-6-sulfonic acid] diammonium salt
ANOVA	Analysis of variance
APC	Antigen presenting cells
ASU	Arizona State University
BCA	Bicinchoninic acid
BEI	Biodefense and Emerging Infections Research Resources Repository
BNSP/BNSP333	Derivative of SAD B19 with RABV-G attenuating mutation at residue 333
CCHF	Crimean-Congo hemorrhagic fever
CCHFV	Crimean-Congo hemorrhagic fever virus
cDNA	Complementary DNA
CDS	Coding sequence
CEV	Cell-associated enveloped virus
CMV	Cytomegalovirus
ConA	Concanavalin A
Ct	Cycle threshold value
CT	Cytoplasmic tail
C-terminus	Carboxy terminus
CTL	Cytotoxic T-lymphocyte
DAPI	4',6-diamidino-2-phenylindole
DDT	Dichlorodiphenyltrichloroethane
DIC	Disseminated intravascular coagulopathy
DNA	Deoxyribonucleic acid
DPBS	Dulbecco's Phosphate Buffered Saline
DPBST	Dulbecco's Phosphate Buffered Saline with 0.05% Tween-20
EC ₅₀	50% effective concentration
ED51	51 residue ectodomain of RABV-G
EEV	Extracellular enveloped virus
ELISA	Enzyme-linked immunosorbent assay
ELISpot	Enzyme-linked immunospot assay
EmGFP	Emerald green fluorescent protein
<i>EPIC</i>	<u>EP</u> Itope <u>C</u> onstruct
ER	Endoplasmic reticulum

ERK	Extracellular Regulated Kinases
FFU	Focus forming units (RABV)
FFU/mL	Fluorescent focus forming units per milliliter (MYXV)
G	Glycoprotein (RABV)
GAG	Glycosaminoglycans
G _C	Mature form of C-terminal glycoprotein (CCHFV)
GFP	Green fluorescent protein
GLUT-1	Solute carrier family 2, facilitated glucose transporter member 1
G _N	Mature form of N-terminal glycoprotein (CCHFV)
GP38	Glycoprotein of 38 kilodaltons in size (CCHFV)
GP85	Pre-cleavage glycoprotein of MLD and GP38 (CCHFV)
GPC	Glycoprotein precursor
HBSS	Hanks' Balanced Salt Solution
HEK293T/F	Human embryonic kidney cell lines
His.H8	Monoclonal antibody that binds 6XHis
HLA	Human leukocyte antigen
HMAF	Hyper-immune mouse ascitic fluid
HTL	Helper T-lymphocyte
HTNV	Hantaan virus
HRP	Horseradish peroxidase
IACUC	Institutional Animal Care and Use Committee
IC50	50% inhibitory concentration
IDE8	<i>Ixodes scapularis</i> embryonic cell line
IEV	Intracellular enveloped virus
IFA	Indirect immunofluorescence assay
IFNAR	Interferon α/β receptor
IFN- γ	Interferon-gamma
IM	Intramuscular
IMD	Immune deficiency pathway
IM-EP	Intramuscular-electroporation
IMV	Intracellular mature virus
ISE6	<i>Ixodes scapularis</i> embryonic cell line
ITR	Intergenic region
I κ B	NF- κ B binding inhibitory protein
kDa	Kilodaltons
L	Large segment-CCHFV genome
L	RNA-dependent RNA polymerase (RABV)
L-15	Leibovitz's L-15 medium
LB	Luria-Bertani medium
Lu	Lausanne strain of myxoma virus
M	Matrix protein (RABV)
M	Medium segment-CCHFV genome
mAb	Monoclonal antibody
Malic	NADP-dependent malic enzyme
MHC	Major Histocompatibility Complex
mL	Milliliters

MLD	Mucin-like domain (CCHFV)
MOI	Multiplicity of Infection
mRNA	Messenger RNA
MSP1a	Major surface protein 1a (<i>Anaplasma marginale</i>)
MTT	3-(4, 5-dimethylthiazolyl-2)-2, 5-diphenyltetrazolium bromide
MVA	Modified vaccinia Ankara
MYXV/wtMYXV	Myxoma virus/wild-type myxoma virus
N	Nucleoprotein (RABV)
NADP	Nicotinamide adenine dinucleotide phosphate
NF-κB	Nuclear factor-κB
NGS	Next Generation Sequencing
NI-NTA	Nickel-nitrilotriacetic acid
NIH-NIAID	National Institutes of Health-National Institute of Allergy and Infectious Diseases
Ni-NTA	Nickel-nitrilotriacetic acid
NLS	Nuclear localization signal
nM	Nanomolar
NP	Nucleoprotein (CCHFV)
NS _M	Non-structural M-segment protein (CCHFV)
NS _S	Nonstructural protein S (CCHFV)
nt	Nucleotide
NTC	No template control
N-terminus	Amino terminus
OATP-74D	Solute carrier organic anion transporter family member 74D
OPD	O-Phenylenediamine dihydrochloride
ORF	Open reading frame
P	Phosphoprotein (RABV)
PCR	Polymerase chain reaction
PLAAT3	Phospholipase A and acyltransferase 3
PUUV	Puumala virus
PVDF	Polyvinylidene difluoride
RABV	Rabies virus
RABV-G	Rabies virus Glycoprotein
RdRp	RNA-dependent RNA polymerase
RHD	Rabbit hemorrhagic disease
RIPA	Radioimmunoprecipitation assay buffer
RK-13	Rabbit kidney cell line
RNA	Ribonucleic acid
RNAi	RNA interference
RNAi	RNA interference
RNP	Ribonucleoprotein
ROBO1	Roundabout homolog 1
RPM	Revolutions per minute
RPMI 1640	Roswell Park Memorial Institute 1640 medium
RT	reverse transcription
S	Small segment-CCHFV genome

SAD B19	Street Alabama Dufferin B19
SDS	Sodium dodecyl sulphate
sE/L	Vaccinia virus synthetic early/late promoter
SEOV	Seoul virus
Slc26a6	Solute carrier family 26 member 6
STAT1	Signal transducer and activator of transcription 1
TAP	Transporter associated with antigen processing
TBST	5% nonfat milk in tris-buffered saline with 0.05% Tween-20
TEN	Buffer of 0.1M Tris-Cl, 0.01M EDTA, and 1M NaCl
TIR	Terminal inverted repeats
TJU	Thomas Jefferson University
T _m	Melting temperature
TMD	Transmembrane Domain
TNF/TLR	Tumor necrosis factor/toll-like receptor
USAMRIID	United States Armed Forces Research Institute for Infectious Diseases
UTMB	University of Texas Medical Branch at Galveston
VACV	Vaccinia virus
VLP	Virus-like particle
vMyx	Recombinant Myxoma virus
VRP	Virus replicon particle
WHO	World Health Organization
wt	Wild-type
x g	Times gravity

Chapter 1: Introduction

1.1 Crimean-Congo Hemorrhagic Fever Virus

1.1.1 History

During World War II in 1944, Soviet troops re-occupied the Crimean Peninsula and developed an acute febrile illness with a high incidence of bleeding and shock¹⁻⁴. The disease was termed “Crimean hemorrhagic fever” due to the location of the outbreak. It was later determined that the outbreak was linked to bites from *Hyalomma* ticks and that a tick-borne viral infection caused the disease. Unfortunately, the virus could not be isolated at this time¹⁻⁴. In 1956, a similar outbreak of a tick-borne disease occurred in Belgian Congo (now the Democratic Republic of the Congo), and the disease was termed “Congo hemorrhagic fever”^{1-3,5,6}. Advances in virus propagation led to the isolation of the tick-borne virus responsible for the Crimean hemorrhagic fever outbreak by intracranial inoculation of infected patient material into suckling mice in 1967^{2,3}. This isolate, the Drozdov strain of Crimean hemorrhagic fever virus (named for its region of origin in the former Soviet Union), was then used to show that tick-borne hemorrhagic diseases occurring throughout the Soviet Union and Bulgaria were related to Crimean hemorrhagic fever^{2,3}. In 1969, virus characterization efforts by the Yale Arbovirus Research Unit determined that the causative agents of Crimean hemorrhagic fever and Congo hemorrhagic fever were indistinguishable based on complement-fixation tests using convalescent patient sera¹⁻³. The virus became known as Crimean hemorrhagic fever-Congo virus in 1970, and the name was then standardized to Crimean-Congo hemorrhagic fever virus (CCHFV) with the disease known as Crimean-Congo hemorrhagic fever

(CCHF)^{2,3}. The Drozdov strain of CCHFV was commonly used in early studies, as it was isolated from a human case of CCHF³. However, the reference strain of CCHFV used by western scientists is IbAr10200, which was isolated from a tick removed from a camel in Nigeria in 1966².

1.1.2 Public Health Significance

The geographic range of CCHFV is the most extensive of the medically significant tick-borne viruses, and it is the second most widespread of all hemorrhagic fever viruses, after dengue virus (**Figure 1.1**)^{2,3,7-9}. CCHFV is endemic to 30 countries in Western Asia, Southeast Europe, the Middle East, and Africa^{2,7-9}. The European Centre for Disease Prevention and Control estimates that there are 10,000-15,000 cases per year, including 500 deaths, and an estimated three billion people are at risk of infection⁹. Consequently, CCHFV poses a high risk to public health and has been classified as an National Institutes of Health-National Institute of Allergy and Infectious Diseases (NIH/NIAID) Category A and World Health Organization (WHO) high-priority pathogen^{10,11}. Transmission to humans occurs through a tick bite, crushing of engorged ticks, or contact with infected animal or human fluids. About two weeks post-infection, severe and fatal hemorrhagic disease occurs, and case fatality rates can be as high as 70%².

Over the last two decades, an increase in CCHF case numbers in endemic areas and new foci of CCHFV have emerged in several parts of the world^{2,12,13}. This is most likely due to anthropogenic factors such as changes in agricultural activities, land fragmentation, importation of infected animals and ticks, and the potential influence of climate change

influencing the ecology and disease dynamics^{12,14–18}. CCHFV circulates cryptically in a tick-vertebrate-tick cycle in nature, with ixodid ticks of the genera *Hyalomma* being both the reservoir and vector. Invasive *Hyalomma* ticks have been detected in several countries beyond the typical vector range, which has partially been attributed to spread via migratory birds and emphasizes the risk of *Hyalomma* spreading further and establishing new foci of CCHFV^{2,12,13,19–23}.

1.1.3 Genome Organization and Virion Structure

CCHFV has a tri-segmented, negative sense, and single-stranded RNA genome and is classified within the genus *Orthonairovirus* of the family Nairoviridae²⁴. The three segments are known as the small (S), medium (M), and large (L) segments, with names reflecting their relative nucleotide length^{25,26}. Each segment encodes untranslated regions at the 3' and 5' termini that are partially complementary, forming closed circular viral RNA molecules with an RNA panhandle required for transcription, replication, and packaging^{25–28}.

The S-segment contains two ambisense open reading frames (ORFs) that encode either the structural nucleoprotein (NP) or nonstructural protein S (NS_S)^{25,29,30} (**Figure 1.2A**). The L-segment contains one ORF that encodes the RNA-dependent RNA polymerase^{2,25} (**Figure 1.2A**). The M-segment contains one ORF that encodes a polyprotein referred to as the glycoprotein precursor (GPC)^{25,31} (**Figure 1.2A**). The CCHFV GPC undergoes the most extensive cleavage and processing of viruses in the order Bunyavirales. The N-terminal signal peptide targets the M segment mRNA to the endoplasmic reticulum (ER), where it

is translated into the ER. The five transmembrane domains weave the polyprotein through the ER lumen^{28,31-33}. The GPC is post-translationally cleaved and processed throughout the secretory pathway to initially form the two precursor proteins, Pre-G_N and Pre-G_C. Pre-G_N is cleaved to produce GP85 and the mature structural glycoprotein G_N. GP85 is either cleaved into the mucin-like domain (MLD) and GP38 or forms a dimer, which is referred to as GP160. Pre-G_C is cleaved to form the nonstructural protein M (NS_M) and the mature structural glycoprotein G_C. The precursor proteins Pre-G_N and Pre-G_C and the nonstructural proteins MLD, GP38, and NS_M, aid in the maturation of G_N and G_C^{25,31-39}. Overall, the complex processing of the GPC includes N-linked glycosylation, complex folding from the presence of many cysteine residues that may form disulfide bonds, and numerous O-linked glycosylations³¹.

The C-terminal cytoplasmic tail of mature G_N contains two zinc finger domains that can bind viral RNA and are thought to mediate the assembly of genomic segments within virions^{40,41}. CCHFV virions are spherical and approximately 80-100 nm in diameter² (**Figure 1.2B**). Heterodimers of G_N and G_C are found throughout the host cell derived lipid envelope^{26,28,34,39,41}. Within the envelope, viral RNA is bound by the NP and RdRp, forming ribonucleoprotein (RNP) complexes for each segment^{25,26,28}.

1.1.4 Replication Cycle

Heterodimers of G_N and G_C on the viral envelope are responsible for binding to unknown cellular receptors and initiating the infection cycle of CCHFV^{2,26,31} (**Figure 1.3**). It is thought that mature G_C is the primary glycoprotein responsible for cell binding and entry

and is a class II fusion protein⁴²⁻⁴⁵. Virions enter host cells by receptor-mediated endocytosis, which is dependent on clathrin, cholesterol, microtubules, early endosome compartmentalization, and pH⁴⁶⁻⁴⁸. Fusion of the viral envelope with the acidified endosome releases the viral genome into the cytoplasm^{2,25}. The segment associated RdRp synthesizes complementary positive-sense RNA molecules that can act as mRNA for translation of viral proteins and as a template for transcription of negative-sense viral RNA^{2,25}. The NP, NS_S, and RdRp proteins are translated by cytoplasmic ribosomes, whereas the GPC is targeted to the ER for processing and maturation of the glycoproteins^{28,31-33}. Host microtubules aid in the association of new RNPs with the cytoplasmic tails of mature G_N and G_C heterodimers for the budding of virus particles into the Golgi body^{25,26,32,34,41}. Mature virus particles are then released from infected cells via exocytosis into the extracellular space^{25,26}.

1.1.5 Phylogeny

CCHFV is the most genetically diverse arbovirus, and phylogenetic analysis is complicated by differences in the diversity of the three genomic segments^{2,49}. The M segment demonstrates the largest nucleotide divergence of the three segments at 31%, the L segment has a 22% nucleotide divergence, and the S-segment is the most conserved with 20% nucleotide divergence². CCHFV clade nomenclature varies within the field and is described using a Roman numeral system or by their geographic region². There are either six or seven clades of CCHFV, depending on the publication^{2,50}. Throughout this dissertation, M segment clades will be discussed using the seven-clade grouping method

and both Roman numeral and geographic terms: Clade I-Africa 1, II-Africa 2, III-Africa 3, IV-Asia 1, IV-Asia 2, V-Europe 1, and VI-Europe 2.

1.1.6 Pathogenesis and Immune Response to CCHFV Infection

Many human infections with CCHFV result in a mild, nonspecific febrile illness^{1,2}. However, some patients develop severe CCHF, which can result in hemorrhaging, multi-organ failure, shock, and death². Human cases of severe CCHF are divided into four phases: incubation, prehemorrhagic, hemorrhagic, and convalescent¹⁻³. The tick vector plays a key role in the early pathogenesis of CCHFV^{51,52}. Immunomodulation of the immune response at the tick bite site by salivary proteins may aid in dissemination of the virus upon introduction⁵¹⁻⁵³. After the bite of an infected tick, the incubation period is approximately one to five days^{1,2}. It is thought that antigen presenting cells (APCs), such as dendritic cells, monocytes, and macrophages, are early targets of infection of CCHFV^{54,55}. Infection of these early target cells triggers innate immune activation and release of interferon, which is critical for controlling early viral replication^{54,56}. Infected APCs migrate to draining lymph nodes, where virus replication continues⁵⁶.

When entering the prehemorrhagic phase of disease, viremia becomes detectable, and peripheral tissues, primarily the liver and spleen, begin to be infected^{1,2,7,54,56,57}. The prehemorrhagic period is marked by nonspecific symptoms such as fever in the first few days of illness. The transition into the hemorrhagic phase of disease begins between days three and five of illness². As the name suggests, patients begin to display characteristic hemorrhagic manifestations during this time, including petechial rashes that progress to

large bruises and bleeding from the gastrointestinal and urinary tracts^{2,57}. This phase is also associated with hepatic damage, elevated serum levels of liver enzymes, and high viral loads from the inability to control viral replication^{1,2,7,54,56-58}. It is thought that significant expression of proinflammatory cytokines in response to infection leads to vascular dysfunction, disseminated intravascular coagulopathy (DIC), multi-organ failure, and shock^{2,54,56,58-60}. Progression to this state often results in a fatal outcome, occurring between days five and 14 of illness^{1,2,56}.

The detection of antibodies in patient serum samples is associated with positive outcomes, whereas humoral responses remain undetectable in fatal cases^{2,54,61-63}. Detection of serum antibody levels and a decrease in viral load indicates a transition into the convalescent phase. Production of IgM can be detected between days four and eight after symptom onset, and IgG becomes detectable between days seven and nine after symptom onset^{54,62,63}. These antibody responses are primarily binding antibodies targeted to the NP, but neutralizing antibodies are also often present^{54,63}. Neutralizing antibody titers can be highly variable between patients⁶², and no correlation has been made between antibody titers and survival or protection from infection^{43,64-66}. While a decrease in viral load is seen with increasing antibody levels, a decrease in viral load has also been seen independent of IgG production⁶⁷, implicating the role of cellular immunity in addition to humoral immunity. Evaluation of the T cell recall responses of human survivors of CCHF has shown that survivors have long-lived (>10 years) CD8+ T cell recall responses to the NP and GPC⁶⁸, but more information is needed to understand the role of T cells in CCHFV infection⁵⁴.

1.1.7 Animal Models of CCHF

Early innate immune responses and interferon are critical for controlling viral replication, and small animal models of CCHF require the use of immunocompromised mice lacking signal transducer and activator of transcription 1 (STAT1^{-/-}) or interferon α/β receptor (IFNAR^{-/-})^{69,70}. In animal models, morbidity and mortality are rapid, and mice succumb to infection by approximately four days post infection⁶⁹⁻⁷¹. Disease in these animal models is characterized by hyperthermia followed by hypothermia, weight loss, elevated liver enzymes, elevated proinflammatory cytokines, thrombocytopenia, coagulopathy, and histopathologic changes in the liver and spleen, all of which recapitulate clinical findings of severe human CCHF⁶⁹⁻⁷¹. These animal models have been used to evaluate the immunogenicity and efficacy of CCHFV vaccines to determine the type of immune response that is protective from lethal CCHF.

Vaccine development for CCHFV was hindered by the lack of a lethal animal model for assessment of vaccine efficacy until 2010^{69,70}. Following the development of immunocompromised (STAT1^{-/-} and IFNAR^{-/-}) mouse models, advances were made in evaluating candidate vaccines. However, the initial mouse models developed were not ideal for assessing vaccine immunogenicity, as the animals are immunocompromised. In 2017, Garrison, et al. demonstrated the use of transient immunosuppression using an anti-IFNAR monoclonal antibody (mAb) in immunocompetent mice to generate a lethal model⁷², allowing for the evaluation of vaccine immunogenicity followed by vaccine efficacy in the same animals, providing a better model for vaccine assessment. A nonlethal non-human primate (NHP) model was first described in 2018⁶⁴. This model provides a tremendous

advantage for future pre-clinical vaccine assessments of CCHFV vaccine candidates for human use.

1.1.8 Difficulties in Vaccine Development to Prevent CCHF

There is currently no approved vaccine widely available for human use to prevent CCHF, and the only vaccine available for human use is not licensed by the FDA. This vaccine was developed in Russia and Bulgaria in 1974 and will be referred to as the ‘Bulgarian vaccine’ throughout this dissertation^{2,73}. The Bulgarian vaccine was developed by passaging CCHFV in the brains of newborn mice, then inactivating the material with chloroform and heat⁷³. This vaccine is given in multiple doses and has not been evaluated in clinical trials for efficacy. It is unlikely that this vaccine will receive approval for use in countries beyond Bulgaria due to safety concerns regarding the mouse neural tissue content and inactivation mechanism⁷⁴.

A significant amount of work has been done over the past decade towards the development of a vaccine for CCHFV after the development of lethal animal models⁷⁴. Vaccine development for CCHFV has assessed the whole virus, the full-length GPC, individual proteins, or a combination of proteins as potential antigens, with no consensus on the most efficacious antigen⁷³. The majority of vaccine development research has evaluated the use of the NP or glycoproteins due to the development of binding and neutralizing antibodies to these proteins during natural infections^{54,73}. It is logical to target the surface glycoproteins with the thought of inducing neutralizing antibody responses. However, as the glycoproteins are the most antigenically diverse between strains of CCHFV², and

neutralizing antibody titers don't correlate with protection from CCHF⁵⁴, neutralizing antibody production may not be the key for CCHFV vaccine development⁵⁴. As a different strategy, the NP has been a common antigen evaluated for CCHFV vaccine development, as the NP is expressed in the highest abundance during infection and has the greatest homology between strains of CCHFV².

Numerous vaccine candidates utilizing nine different types of vaccine platform technology have been assessed without a human vaccine candidate reaching clinical trials⁷³. CCHFV antigens have been used in inactivated, transgenic plants (oral administration), virus-like particle (VLP), virus replicon particle (VRP), subunit, viral-vectored, DNA, DNA/VLP blend, and mRNA vaccine platforms⁷³. Of the vaccine candidates assessed, only recombinant viral-vectored, VRP, mRNA, and DNA vaccines have demonstrated 100% protection from lethal challenge in animal models, but not all constructs of a particular platform. Of the ten vaccine candidates that have completely protected animals against lethal CCHFV challenge, four of these are DNA vaccines⁷⁵⁻⁷⁸, three are recombinant viral-vectored vaccines⁷⁹⁻⁸¹, two are mRNA vaccines^{82,83}, and one is a VRP vaccine⁸⁴ (**Table 1.1**).

Vaccine immunogenicity and efficacy studies have provided information on the immune responses necessary for protection from lethal challenge with CCHFV, although correlate(s) of protection have not been established. These studies have shown that protective antibodies, both neutralizing and non-neutralizing, can be induced by vaccination and that T cells can be robustly activated^{66,68,72,77-79,85}. Other studies in

CCHFV animal models have demonstrated that passive transfer of CCHFV antiserum alone does not provide clinical benefit, but the transfer of CCHFV antiserum and CD3+ T cells significantly increases the mean time to death, and depletion of CD4+ and/or CD8+ T cells exacerbates morbidity and mortality during acute CCHFV infection^{66,85}. Together, these studies suggest the need for both humoral and cellular immune responses for protection against lethal CCHFV infection.

Recent research has been interested in trying to identify protective epitopes within CCHFV. Various mAbs that recognize epitopes on different CCHFV proteins, some of which are protective against lethal challenge, have been available since 2005^{38,45,86-88}. The epitopes of these antibodies have not been fully elucidated. Some antibody binding sites of polyclonal CCHFV antiserum have been identified throughout the NP and GPC using peptide-binding enzyme-linked immunosorbent assays (ELISAs) or structural studies^{45,89-95}. Experiments attempting antibody epitope mapping have shown limited reactivity and variability in immune reactivity between CCHFV strains, where slight sequence variation ablated antibody binding of convalescent sera to peptides^{54,89}. It is thought that most antibodies to CCHFV bind to conformational rather than linear epitopes, and much of the problem with CCHFV vaccine candidates is related to incorrect folding of the expressed viral proteins due to the complex processing of the GPC³¹.

When assessing vaccine immunogenicity, splenocytes from vaccinated animals can be restimulated with peptide pools generated from the GPC to measure T cell recall responses^{66,77-79,96}. It has been demonstrated that immunogenicity is not evenly distributed

across the antigen, as the nonstructural proteins and N-terminal region of G_C generates the strongest recall responses. This pattern has been seen in both mice and *Cynomolgus macaques*^{77,78}. Recall responses are variable depending on whether the stimulating peptide pool is generated from a CCHFV strain that is homologous or heterologous to the vaccine sequence⁷⁷. The nonstructural proteins display the greatest recall responses when using homologous peptide sequences, whereas these recall responses are nearly absent when using peptides from a heterologous strain of CCHFV. In contrast, significant recall responses to the N-terminal region of G_C are maintained when peptides from both homologous and heterologous strains of CCHFV are used. Despite the abundance of data showing the importance of T cells in immunity to CCHFV, the development of vaccines geared towards enhancing T cell immunity have yet to be investigated.

1.2 Ticks

Multiple genera of ixodid, or “hard” ticks, are implicated as vectors for CCHFV and are considered the true natural reservoir of the virus^{1,2,14,97}. Ticks are hematophagous arthropods, and they must acquire nutrients via a blood meal to undergo metamorphosis to the next stage in their life cycle². CCHFV cases and virus transmission peak in the spring and summer, corresponding to tick feeding activity².

1.2.1 *Hyalomma* Life Cycle and CCHFV Transmission Cycle

Multiple genera of ticks overlap the geographic distribution of CCHFV, and ticks in the genera of *Amblyomma*, *Dermacentor*, *Ixodes*, and *Rhipicephalus* have been implicated as vectors of CCHFV⁹⁸. However, ticks of the genus *Hyalomma* are considered the primary

vector and reservoir of CCHFV and maintain CCHFV through transstadial, transovarial, and venereal transmission² (**Figure 1.4**). These ticks have strict host preferences and parasitize fewer host families than ticks of other genera⁹⁸. Additionally, *Hyalomma* are “hunting” ticks, which can quest long distances to find a preferred host for feeding². Completing the life cycle for *Hyalomma* ticks can take multiple years. Ticks in various life cycle stages provide a large population for virus maintenance in endemic areas¹⁴. CCHFV replicates to high titers within reproductive organs of female *Hyalomma* ticks and is transovarially transmitted². Female *Hyalomma* ticks can lay thousands of eggs, some of which can be infected with CCHFV. The newly hatched larva must find a host to take a blood meal to acquire nutrients to grow. Different species of *Hyalomma* ticks have different life cycles and can act as one-host ticks, two-host ticks, or three-host ticks, such as *H. scupense*, *H. marginatum*, and *H. anatolicum*, respectively⁹⁹. Different ticks of the same species may have different life cycles and follow either a two-host or three-host feeding pattern, which can depend on numerous factors, including climate^{99–101}.

This dissertation focuses on *H. marginatum* ticks, which are one of the principal species implicated in the transmission of CCHFV in Eurasia, including the highly endemic country of Turkey⁹⁹. *H. marginatum* are two-host ticks, and upon completion of feeding during the larva instar, the ticks will stay on the same host while molting to the nymph instar. On the same host, nymphs will complete a second feeding before dropping off to molt into an adult. Both the larva and nymph instars are considered immature ticks, and these stages prefer to feed on small hosts, such as rabbits, mice, ground-feeding birds, hedgehogs, and lizards, in preferential order⁹⁸. After feeding, nymphs of both two-host or three-host ticks

will drop off the host and molt into adults. Newly molted adult ticks will commonly overwinter prior to feeding. Warm temperatures increase the activity of adult *H. marginatum* ticks, and they will begin to actively seek out a host in the spring and summer months^{1,2}. Adult *H. marginatum* ticks prefer to feed on large hosts such as cattle, sheep, and camels but can also be found on birds and tortoises, although these hosts are less preferred⁹⁸. Humans are incidental hosts for adult *H. marginatum* ticks². While on the large host, CCHFV can also be transmitted from infected males to females during copulation². Engorged female ticks will drop off the host, produce eggs, then undergo oviposition.

While some ticks may be infected with CCHFV upon hatching, uninfected ticks may acquire CCHFV from any vector-host interaction during their life cycle, either from feeding on a viremic host or through co-feeding with infected ticks on the same host^{1,2,51,102,103}. The number of different tick species and genera that feed on the same host or have similar host preferences and close human interaction with domestic animals adds layers of complexity to the transmission cycle⁹⁸. CCHFV transmission to humans occurs through the bite of an infected tick, or contact with infectious fluids, either from animal interactions or in patient care settings. Consequently, humans with agricultural or slaughterhouse professions are at the highest risk of infection from increased contact with CCHFV-infected ticks or fluids^{2,7}.

1.2.2 The Tick Bite Site, Feeding, and Bloodmeal Metabolism

Natural immunity to tick proteins can be acquired from repeated feedings of ticks on a host¹⁰⁴. As ixodid ticks initiate feeding, they will use their hypostome to penetrate the skin,

anchor at the bite site, and create a hemorrhagic pool for feeding. During this process, tick saliva is secreted into the tick bite site⁵³. Tick saliva is a potent immunomodulator that contains hundreds of salivary proteins, many with redundant functions, involved in the modulation of pain, coagulation, vasodilation, and inflammatory responses at the tick bite site⁵³. These salivary proteins are referred to as “exposed” antigens because hosts are naturally exposed to these antigens from each tick feeding^{105,106}. Repeated exposure to these antigens, through repeated tick feedings, stimulates an immunological resistance to the parasite^{104–106}. During feeding, ticks alternate between salivating and ingesting the bloodmeal from the pool¹⁰⁷. As fluids are ingested, the tick must concentrate the nutritious components for digestion, and excess water and other ions such as sodium, cross the midgut barrier to enter the hemocoel¹⁰⁷. This excess fluid is taken up by the salivary glands and returned to the host during salivation¹⁰⁷. The concentrated bloodmeal components are endocytosed and metabolized intracellularly by midgut cells^{108,109}. Proteins in the bloodmeal, such as antibodies, can interact with tick proteins that are not exposed to the host during feeding, otherwise referred to as “concealed” antigens¹⁰⁵. Concealed antigens are not limited to midgut proteins. Host antibodies can be found in the hemocoel after feeding, likely from the bloodmeal concentration process. This demonstrates that larger proteins can cross the midgut barrier, and host antibodies can interact with numerous tick tissues from their location within the hemocoel^{106,110–113}.

1.2.3 Tick Control Measures

1.2.3.1 Acaricides

Tick control measures were developed to combat the economic impact of ticks on cattle production. Ticks negatively impact cattle production by directly damaging animal hides, reducing animal production due to blood loss, and introducing vector-borne diseases¹¹⁴. Before the discovery of dichlorodiphenyltrichloroethane (DDT) having insecticide properties in 1939, there were very limited options for controlling ectoparasites¹¹⁵. Over the years, ticks began to acquire resistance to the insecticide, and new insecticides and acaricides were developed. This resulted in a pattern of tick control measure development followed by acquired acaricide resistance, for DDT and organochlorines, organophosphates, amidines, and pyrethroids, throughout the twentieth century¹¹⁵. In addition to acquired resistance, these compounds had numerous issues, including toxicity to animal hosts, consumers, and the environment^{114,115}. Current research for new control measures is based on immunological control of ticks through the development of anti-tick vaccines¹¹⁴. Unlike acaricide use, this method is largely exempt from environmental problems and can be used to target both ticks and tick-borne pathogens¹¹⁴.

1.2.3.2 Tick Vaccines Against Exposed and Concealed Antigens

Efforts to develop anti-tick vaccines have focused on controlling the cattle tick *Rhipicephalus (Boophilus) microplus* due to its economic importance¹¹⁶. This tick species serves as an excellent model for anti-tick vaccines since it is a one-host tick that will remain on its host throughout its life cycle and does not have multiple vector-host interactions. Control of *R. microplus* ticks by vaccination using *R. microplus* protein was first reported

in 1989¹¹⁷. This vaccination strategy used the 86kDa midgut membrane-bound glycoprotein (Bm86), and antibodies against Bm86 were shown to interact with the tick proteins following ingestion of the blood meal, destroying midgut cells and rendering the ticks unable to digest their blood meal¹¹⁸. This resulted in high tick mortality and significantly decreased egg-laying capacity, which in turn reduced populations in subsequent generations. Two anti-tick vaccines utilizing Bm86 have been licensed for commercial use in cattle; TickGARD in Australia plus Gavac in Cuba and parts of South America¹¹⁹. Integrated use of TickGARD in bovine tick control programs has reduced the cost of chemical acaricides by 83.7% per bovine per year¹²⁰. Unfortunately, Bm86-based vaccines have had a limited impact on tick control efforts due to the inefficacy of the vaccine against multiple tick species¹¹⁶.

To improve the Bm86 vaccination strategy, various candidate anti-tick vaccines have been developed utilizing both exposed and concealed antigens (**Table 1.2**)¹¹⁴. These antigens have been developed from *Rhipicephalus*, *Ixodes*, and *Hyalomma* tick species. Immunization with some of these antigens has been shown to reduce tick feeding and reproduction of multiple tick species and reduce the infection and transmission of pathogens from the tick to the vertebrate host¹²¹. These candidate antigens have been evaluated as recombinant protein in adjuvant formulations, but other vaccine strategies, such as viral-vectored vaccines, are also being explored. However, none of these vaccine candidates have advanced toward commercial development.

Anti-tick vaccine candidates utilizing exposed antigens have different hypothesized mechanisms of action than vaccine candidates using concealed antigens. Since exposed antigens are present within the salivary components that are secreted into the host upon feeding, it is hypothesized that host antibodies to these proteins would alter the immunomodulation of the tick bite site to prevent tick attachment and feeding. Additionally, it is thought that after immunization with these antigens, subsequent exposure to the antigen during tick feedings would act as an immunological boost, and repeated tick exposure would continuously boost the immune response. Unfortunately, due to the copious amount of secreted immunomodulatory proteins within tick saliva, it is also thought that immunization with a single exposed antigen is overcome by the redundancy of immunomodulatory components^{53,106}. As described above, immunization with concealed antigens induces humoral responses that are taken up during feeding and interact with internal proteins. While Bm86 is located only in the midgut membrane and has direct contact with the bloodmeal, other concealed antigens, such as Subolesin, are found in other tick tissues such as the ovaries. It has been hypothesized that immunoglobulins crossing the midgut membrane into the hemocoel can interact with concealed antigens found in other tick tissues¹⁰⁶. Thus far, studies have not shown that ticks are able to overcome the effects of antibodies against concealed antigens from the presence of redundant proteins, as seen with exposed antigens, which is encouraging for the continued development of anti-tick vaccines utilizing concealed antigens.

While anti-tick vaccine candidates utilizing exposed versus concealed antigens have different mechanisms of action, the protective effect of anti-tick antigens is evaluated using

the same parameters: reduced numbers of engorged ticks, increased mortality, reduced engorged weight, and reduced oviposition in females¹⁰⁶. Additional studies may be undertaken to evaluate the role of the anti-tick antigen in the prevention of tick-borne pathogen transmission. The ideal anti-tick candidate vaccine would be highly immunogenic using a single dose, and the resulting immune response would demonstrate a significant reduction in ectoparasite infestation, survival, oviposition, and pathogen transmission.

1.3 Subolesin

1.3.1 Protein Discovery and Homology Across Species

Subolesin, originally known as 4D8, was first identified as a candidate tick protective antigen in 2003 from immunization of mice with cDNA clones from an *I. scapularis* embryonic cell line (IDE8) derived expression library¹²². Subolesin displays reductive evolution, and the protein is shorter in tick genera that have most recently diverged, such as *Rhipicephalus* and *Hyalomma*, compared to *Ixodes*¹²³. Although the protein length differs, Subolesin is highly conserved. Subolesin has 84.7% residue identity or greater among the five tick genera within the geographical range of CCHFV that are implicated in CCHFV transmission (*Hyalomma*, *Dermacentor*, *Amblyomma*, *Rhipicephalus*, and *Ixodes*)^{98,124}, and 77.3% identity or greater when analyses are expanded to include *Haemaphysalis* and *Ornithodoros* genera. The conservation of Subolesin poises it to act as a broad-spectrum anti-tick antigen. Subolesin has lower levels of conservation when compared to other dipterans, with 53.4% identity between *Hyalomma anatolicum* and *Aedes aegypti* and 47.2% identity between *Hyalomma anatolicum* and *Glossina*

*morsitans*¹²⁴. Subolesin in ticks is the functional homolog of Akirin2 in vertebrates¹²³. The conservation of Subolesin with homologous proteins in other species is consistent, with a 48.0% identity to Akirin2 from rats¹²³.

1.3.2 Function of Subolesin and Impact of Subolesin Impairment

Subolesin/Akirin2 is a transcription cofactor that acts with Relish/Nuclear-factor kappa-light-chain-enhancer of activated B-cells (NF- κ B) in the immune deficiency (IMD) and tumor necrosis factor/toll-like receptor (TNF/TLR) signaling pathways, which are critical in stimulating expression of genes involved in the tick immune response^{123,125–129}. Subolesin is expressed in the cytoplasm and is also found in the nucleus of tick cells¹²³. Nuclear localization of the protein is required for its function as a transcription cofactor. There are two nuclear localization signal (NLS) sequences within Subolesin, which are conserved in the Akirin2 protein¹²³. It is thought that these NLS domains are post-translationally modified through phosphorylation, similar to Relish/NF- κ B, which triggers interaction with Importin- α for import into the nucleus, but Subolesin can also localize to the nucleus to exert its function in an Importin- α independent manner^{123,130,131}. Within the nucleus, the extent of Subolesin's binding partners remains unknown^{123,130}. However, Subolesin has been implicated in having a role in numerous cellular processes beyond its role in the tick immune response.

RNA interference (RNAi) studies have demonstrated that Subolesin plays an important role in gene expression, tick survival, and completion of the tick life cycle. Subolesin is involved in tick stress, feeding, and reproduction, and lack of Subolesin protein function

results in the deterioration of the midgut, salivary glands, reproductive tissues, and embryos^{123,132–137}. These studies have also determined that Subolesin and Relish (NF- κ B) are involved in reciprocal regulation¹²⁷, and numerous genes are differentially expressed following Subolesin knockdown¹²⁵.

1.3.3 Subolesin as an Anti-Tick Vaccine Antigen

The long-term goal of anti-tick vaccines is the reduction of tick populations and viral, bacterial, and protozoan tick-borne diseases¹¹⁴. Immunogenicity of these vaccines is based on the induction of humoral responses, with the hypothesis that the interaction of antibodies with the protein of interest impacts protein function, exerting a negative impact on the tick, as seen with the Bm86 vaccine^{118,138}. Efficacy of anti-tick vaccines is measured by comparing ectoparasite infestation (number of ectoparasites completing feeding), weight (weight of engorged female ectoparasites), oviposition (number of eggs per female), and fertility (number of larvae per female) between ticks placed on vaccinated or unvaccinated animals¹³⁹. These measures show the impact of the anti-tick vaccine on different points of the life cycle of ticks and allows for straight-forward evaluation of the protective capacity of these vaccines against multiple types of ectoparasites.

The protective capacity of Subolesin as an anti-tick antigen has been shown through feeding of ticks on vaccinated animals and by force-feeding of ticks using serum from vaccinated animals, emphasizing the importance of the humoral response to vaccination^{114,123,132,139–144}. A summary of studies evaluating Subolesin as an anti-tick antigen can be found in **Table 1.3**. Subolesin has primarily been evaluated as a recombinant

purified protein or chimeric protein that has been adjuvanted with Freund's Complete Adjuvant (FCA), Freund's Incomplete Adjuvant (FIA), Montanide ISA 50 V2, or 10% Montanide 888 in vaccination trials of mice, rabbits, sheep, deer, and cattle (**Table 1.3**)^{123,139}. Impacts on various stages of multiple ectoparasites in the genera of *Aedes*, *Anopheles*, *Phlebotomus*, *Caligus*, *Dermanyssus*, *Ornithodoros*, *Ixodes*, *Haemaphysalis*, *Amblyomma*, *Dermacentor*, *Hyalomma* and *Rhipicephalus* have been shown, including heterologous protection against multiple species due to the highly conserved nature of the protein^{123,139}. Despite Subolesin being the most promising anti-tick vaccine candidate, vaccine efficacy ranges significantly from none to 99% depending on experimental conditions, including the use of different doses, adjuvants, animal models, tick challenge species and stage, and measurement of vaccine efficacy (overall efficacy versus efficacy of individual measurements: infestation, weight, molting, oviposition, or fertility).

Immunization of animals with Subolesin has been shown to reduce ectoparasite infection when feeding on hosts infected with *Anaplasma marginale*, *Anaplasma phagocytophilum*, *Borrelia burgdorferi*, and *Babesia bigemina*^{145,146}. In contrast, vaccination with Subolesin has very limited data on its protective capacity against tick-borne viruses. Mice immunized with Subolesin were not protected from the transmission of tick-borne encephalitis virus (TBEV; Central European subtype, strain Hypr) from infected female *Ixodes scapularis* ticks feeding on the mice¹⁴⁷. The difference in protection against these diseases may be attributable to the duration of tick attachment for transmission or the directionality of transmission¹⁴⁸⁻¹⁵¹. Since Subolesin immunization significantly impacts ectoparasite infestation, many ticks may not remain attached for a time sufficient to internalize or

transmit bacteria and protozoans. In contrast, it is thought that tick-borne viruses are transmitted more rapidly (less than 24 hours of attachment) than bacterial pathogens (greater than 24 hours of attachment)^{148–151}. However, research to determine the duration of tick attachment needed for transmission of viruses has been limited to Thogoto virus and Powassan virus¹⁴⁹. Thus, the impact of Subolesin immunization on ectoparasite infestation may play a greater role in reducing bacterial and protozoan tick-borne diseases than viral tick-borne diseases. These data suggest that while Subolesin is an excellent candidate for a universal protective antigen against tick infestations and bacterial and protozoan infections¹⁵², pathogen-specific vaccine development is needed to protect tick hosts against various tick-borne viruses¹⁴⁷.

Subolesin immunogenicity is evaluated by measuring binding antibody titers using enzyme-linked immunosorbent assays. Unfortunately, the vaccination regime of Subolesin as a protein in adjuvant vaccine requires multiple doses. Two studies have attempted to increase the immunogenicity of Subolesin to reduce the number of needed doses by generating a chimeric Subolesin antigen or by delivering Subolesin within a viral vector. In the first study, the fusion of Subolesin to the N-terminal region of the major surface protein 1a (MSP1a) of *Anaplasma marginale* generated a SUB-MSP1a chimeric antigen that localized to the membrane of *Escherichia coli* during expression, making the chimeric protein membrane-bound^{153,154}. Immunization of animals with this membrane-bound preparation in Montanide ISA 50 V2 significantly increased the immunogenicity and protective capacity of the vaccine compared to Subolesin only¹⁵³. In the second study, a recombinant Vaccinia virus expressing Subolesin was generated¹⁴⁶. This recombinant virus

did not include a modified form of the Subolesin protein. Similar to the protein in adjuvant approach, anti-Subolesin antibodies were generated in vaccinated mice, and there was a 52% reduction in tick infestation compared to control mice. These two studies provide important proof of concept studies, and avenues, for improving Subolesin's immunogenicity and efficacy as an anti-tick vaccine.

1.4 Myxoma Virus

Myxoma virus (MYXV) was first described in 1896 by Sanarelli as the causative agent of a fatal disease of imported European rabbits of the genus *Oryctolagus*¹⁵⁵. MYXV was later found to be an endemic pathogen of North and South American rabbit species in the genus *Sylvilagus*¹⁵⁵⁻¹⁵⁷. In *Sylvilagus* species, MYXV causes a benign fibroma at the inoculation site, with no further clinical signs. However, in *Oryctolagus* species, MYXV causes the severe disease myxomatosis, which has a nearly 100% fatality rate. In the 1950's MYXV was explored as a means of controlling the wild *Oryctolagus* population and was introduced to Europe and Australia, where it is now endemic. MYXV spreads between rabbits through direct contact or contact with contaminated surfaces, but most commonly through mechanical transmission by biting insects such as mosquitos, fleas, and ticks¹⁵⁵⁻¹⁵⁷. Due to its high mortality, numerous vaccines have been developed since the 1950s to prevent myxomatosis in farmed, pet, and wild rabbits¹⁵⁵⁻¹⁵⁸.

MYXV is the prototype species of the *Leporipoxvirus* genus that is found within the Chordopoxvirinae subfamily of the Poxviridae family¹⁵⁹. The Lausanne strain (Lu) of MYXV (isolated in Brazil in 1949) was the first MYXV genome to be sequenced and is

considered the reference strain¹⁵⁹. Other members of the Leporipoxvirus genus include Shope fibroma virus (also known as rabbit fibroma virus), hare fibroma virus, and squirrel fibroma virus¹⁵⁹. MYXV has a double-stranded DNA genome of 161,774 nucleotides in length and contains terminal inverted repeats (TIRs)¹⁵⁹. The single-stranded ends form covalently closed hairpin loops at each end of the linear genome. ORFs are found on both strands of the genome, and MYXV has 159 unique ORFs, with 12 genes duplicated within the TIRs, for a total of 171 proteins expressed from MYXV¹⁵⁹. Genes were named in numerical order beginning at the left-most end of the genome in the TIR, starting with M001L. After the numerical designation, genes are named with L or R, meaning left or right, indicating the direction of transcription of the gene. The homologous gene to M001L in the right-most end of the genome within the TIR is designated as M001R, allowing for differentiation of the same protein that is present within two locations of the genome. Each gene is transcribed from a unique promoter, which are classified into early, intermediate, and late categories based on the time at which the genes are transcribed during the replication process¹⁵⁹. There are numerous genetic similarities of MYXV to other poxviruses, such as VACV, and most often, these similar genes (at least 90¹⁶⁰) are found within the center of the genome and are involved in virus replication and structure¹⁵⁹. Genes found closer to the termini of the genome encode host-range and virulence factors that are key for the strict species-specific nature of poxviruses¹⁵⁷. Of these, 42 MYXV genes have demonstrated immunomodulatory effects within the host¹⁵⁷.

The MYXV virion follows the characteristic morphology of poxviruses; it is approximately 200-300nm in diameter and brick-shaped^{160,161}. Specific cellular receptors for many

poxviruses have not been identified, but poxviruses are thought to bind primarily to glycosaminoglycans (GAGs) on the host cell membrane for internalization¹⁶⁰. Since GAGs are found in a variety of cell types, poxviruses can bind and enter a variety of both permissive and restrictive cells, and the ability of the virus to complete the replication cycle is dependent on the host-range and virulence factors encoded by the specific poxvirus¹⁶⁰. Two different virion forms are considered mature virions that can initiate the infection cycle: the intracellular mature virus (IMV) and extracellular enveloped virus (EEV)^{160,161}. In both forms, the biconcave virion core containing the genome is flanked by two lateral bodies. These forms differ by the number of enveloping membranes^{160,161}. IMV particles are the first form of the virion produced during the replication cycle and are shuttled through the Golgi apparatus, where they are wrapped with another membrane, forming intracellular enveloped virions (IEV)^{160,161}. IEV particles are exocytosed to form cell-associated enveloped virus particles (CEV) or free EEV particles, or EEV particles are formed by direct budding of IMV particles from the cell membrane^{160,161}. Production of viral stocks in laboratories uses cell lysis to release IMV particles rather than collecting EEV particles from cell supernatant¹⁶². Virus replication occurs exclusively in the cytoplasm of infected cells in specialized sites known as replication factories¹⁶². During replication, viral DNA is subject to high levels of homologous recombination^{163,164}, providing an efficient mechanism for removing or inserting desired genes within poxvirus genomes.

Host-restricted poxviruses have been viewed as attractive vaccine vectors because they lack replication competency in nonpermissive species¹⁶⁰ and are tolerant of large

insertions¹⁶⁵. Poxviruses such as VACV Modified Vaccinia Ankara (MVA) strain, fowlpox, canarypox, and lumpy skin disease virus, have all been assessed for their use as non-replicative vaccine vectors. Four veterinary vaccines using poxviral vectors have been licensed for use in the United States¹⁶⁶. Recombitek® by Boehringer-Ingelheim encodes two glycoproteins from canine distemper virus and is licensed for use in dogs. PUREVAX® FeLV by Boehringer-Ingelheim encodes four proteins from feline leukemia virus (FeLV) and is licensed for use in cats. PUREVAX® Rabies by Boehringer-Ingelheim encodes the Rabies virus (RABV) glycoprotein (G) and is licensed for use in cats. RABORAL V-RG® by Boehringer-Ingelheim encodes the RABV-G and is licensed for use in wildlife such as raccoons and coyotes.

MYXV has been explored as a host-restricted vaccine vector through the removal of immunomodulatory genes and insertion of foreign genes using homologous recombination¹⁵⁸. As an attenuated replication-competent vaccine vector in rabbits, MYXV has been used as a backbone for the internationally licensed bivalent vaccine Nobivac Myxo-RHD®, targeting myxomatosis and rabbit hemorrhagic disease (RHD)¹⁶⁷. MYXV is replication-competent only in rabbits, giving this vector a robust safety profile for use in other species. MYXV is safe and immunogenic as a recombinant vaccine against rabbit hemorrhagic disease virus in sheep¹⁶⁵ and feline calicivirus in cats¹⁶⁸. These were important proof-of-concept experiments demonstrating that simple heterologous antigens expressed by MYXV can be immunogenic in nonpermissive species.

1.5 Rabies Virus

Rabies was first described in the fourth century using the Greek term ‘lyssa’ as a disease of madness^{169,170}. The disease was shown to be of infectious nature in the early 1800s by injecting saliva of diseased animals into healthy animals¹⁶⁹. This research became of interest to Louis Pasteur, and in 1885, Pasteur began treating individuals who had been bitten by rabid dogs¹⁷¹. This work demonstrated the use of a live attenuated vaccine for preventing rabies, although it wasn’t until 1936 that the rabies virus was isolated¹⁷¹.

Rabies virus (RABV) is the prototype species of the *Lyssavirus* genus within the Rhabdoviridae family¹⁷². This family of viruses was named for their characteristic virion shape, which is the shape of a bullet or rod¹⁷². Rabies virus has a single-stranded, negative-sense RNA genome that encodes five genes: the nucleoprotein (N), phosphoprotein (P), matrix protein (M), glycoprotein (G), and RNA-dependent RNA polymerase (L)^{170,172}. These five genes are transcribed in a gradient, with genes at the 3’ end of the genome (N) being transcribed more than genes at the 5’ end of the genome (L)^{170,172}. The RABV G is the only protein expressed on the surface of the virion and is found as a trimer throughout the host-derived lipid membrane^{170,172}. RABV G is anchored in the membrane via a transmembrane domain, and the cytoplasmic tail within the virion interacts with the matrix protein, which is associated with N, P, L, and the RNA genome to form the bullet virion shape^{170,172}.

All mammals are considered permissive to RABV, and despite available vaccines for humans and animals, RABV is maintained in enzootic cycles throughout the world¹⁷³. In

areas with large-scale vaccination campaigns, human RABV infections have been eliminated by eliminating RABV infections in dogs¹⁷³. RABV vaccines have been greatly improved since their development in 1885. Current vaccines have extensive safety and efficacy profiles after being administered for decades and have been shown to be safe and immunogenic, with long-lasting immunogenicity¹⁷³. Human RABV vaccines are inactivated preparations with adjuvant and require at least two doses for pre-exposure prophylaxis or four doses for the post-exposure prevention of rabies¹⁷⁴. Vaccines for animals include adjuvanted inactivated viruses or modified live viruses that can be given intramuscularly or orally using bait distribution for wildlife^{173,175}.

Since the development of the reverse genetics system for RABV¹⁷⁶, next-generation vaccines for RABV include recombinant vaccines and the use of RABV as a vaccine vector¹⁷⁶. RABV has been researched as a recombinant vaccine vector for decades since large foreign antigens can be stably incorporated into the RABV genome without the loss of RABV replication function¹⁷⁷. The major concern with using RABV as a vaccine vector is its pathogenicity. The RABV G determines the viral tropism and is believed to be the main determinant of viral pathogenicity. Studies have shown that the introduction of mutations can abolish the neurotropism of RABV, specifically mutating the amino acid residue 333, generating a safe, replication-competent vaccine vector¹⁷⁷. This is an attractive vaccination platform, as it generates high levels of immunogenicity to both the inserted foreign antigens and the RABV G from a single dose¹⁷⁷. RABV-vectored vaccines, encoding antigens from Lassa virus¹⁷⁸, Ebola virus^{179,180}, Nipah virus¹⁸¹, or Severe Acute Respiratory Syndrome coronavirus 2 (SARS-CoV-2)¹⁸² are in preclinical development.

1.6 Goals of Dissertation

CCHFV has a complex transmission cycle, where *Hyalomma marginatum* is the primary vector and reservoir of the virus, and humans are the only species that develop clinical disease². *Hyalomma marginatum* relies on mammals for bloodmeals, and these vector-host interactions provide an exploitation point to target for vaccine development. While a significant amount of research has been conducted in attempts to develop a vaccine to prevent CCHF, no candidates have advanced to clinical trials⁷³. No efforts have been directed at the development of vaccines targeting each vector-host interaction point of the CCHFV transmission cycle. The overall goal of this dissertation was to develop and evaluate tick and virus targeting vaccine candidates for both the tick vector and vertebrate host interaction points in the CCHFV transmission cycle. The hypothesis being tested is that utilizing diverse vaccine technologies for the development of vaccine candidates that target unique points of the CCHFV transmission cycle is the optimum vaccine development strategy for CCHFV. These studies are divided into four specific aims:

Specific Aim 1: Develop and evaluate a poxvirus-vectored anti-tick vaccine for hosts of immature *Hyalomma marginatum*.

Hypothesis: Subolesin will not alter the replication of the viral vector, and the recombinant virus expressing Subolesin will be an immunogenic vaccine candidate.

Rationale: Previous studies have demonstrated that Subolesin is a highly conserved, immunogenic, and efficacious tick antigen when used as a protein in adjuvant vaccine formulation¹³⁹. One proof-of-concept study demonstrated that Subolesin could be immunogenic and efficacious when expressed from a poxvirus vector¹⁴⁶. Immature stages

of *H. marginatum* ticks have a predominant host preference for small mammals such as rabbits⁹⁸. It is proposed to use a poxvirus with a strict host restriction to rabbits to develop a vaccine candidate targeting the hosts of the immature stages of *H. marginatum* ticks.

Specific Aim 2: Evaluate the expression and immunogenicity of a rabies virus-vectored anti-tick vaccine for hosts of adult *Hyalomma marginatum*.

Hypothesis: The utilization of rabies virus as a replication-competent vector for Subolesin will produce an immunogenic vaccine candidate.

Rationale: The live-attenuated rabies virus is a well-established vaccine strain with worldwide use in a variety of mammals¹⁷⁷. Rabies virus has been used as a viral vector for vaccine development, and previous vaccine candidates have been developed by generating chimeric antigens using the C-terminus of the rabies virus glycoprotein¹⁷⁷. A different chimeric protein strategy has previously demonstrated an increase in immunogenicity and efficacy of Subolesin¹⁵³. It is proposed to generate a Subolesin and rabies virus glycoprotein chimeric antigen for use within a recombinant rabies virus as a vaccine candidate targeting large mammals, which are the preferential hosts for adult *H. marginatum* ticks⁹⁸.

Specific Aim 3: Identify potential epitopes in the CCHFV GPC to create a novel CCHFV DNA vaccine candidate and assess vaccine characteristics *in vitro* and *in vivo*.

Hypothesis: Reducing antigen size and processing from the full-length CCHFV GPC by generation of a multi-epitope antigen will result in an immunogenic DNA vaccine candidate.

Rationale: The CCHFV GPC undergoes complex cleavage and processing for the maturation of the structural glycoproteins, and the GPC sequence is the most diverse of the three virus segments². Due to the complicated nature of this process, in addition to a lack of mapping of protective epitopes, the whole CCHFV GPC has been used as a common antigen for CCHFV vaccine development rather than using immunogenic regions^{54,73}. Current research in the field highlights the utility of DNA vaccines for CCHFV, as they offer a safe, easily scalable, cost-effective, and stable approach for human vaccination. DNA vaccines encoding the whole GPC robustly stimulate both humoral and cellular responses. T cell recall responses are unevenly distributed across the GPC and are diminished when using peptides from heterologous strains of CCHFV for stimulation^{66,77-79,96}. Multi-epitope antigens have been proposed to overcome the size and complex processing associated with using the whole GPC as a DNA vaccine antigen and to increase immunogenicity across diverse CCHFV strains⁷³.

Specific Aim 4: Evaluate the biological impact of anti-Subolesin antibodies on tick cells.

Hypothesis: Anti-Subolesin antibodies can enter tick cells to prevent the function of Subolesin, therefore leading to measurable changes in gene expression or metabolism of tick cells.

Rationale: Subolesin binding antibodies are the protective mechanism of Subolesin protein-in-adjuvant vaccines. However, it is unknown how antibodies exert an effect on this intracellular protein. Previous research has shown that antibodies can cross cell membranes during feeding as part of the bloodmeal concentration mechanism^{106,110-113} and

that incubation of tick cells with antibodies to actin leads to intracellular protein binding¹⁴². When Subolesin is silenced using RNAi, there are numerous differentially expressed genes that are involved in multiple biological processes, similar to the effects seen in ticks that have fed on Subolesin vaccinated animals^{123,125,127,132-137}. Intracellular antibody binding to Subolesin may exert differential gene expression, as seen with RNAi studies.

Table 1.1: CCHFV vaccine candidates that have demonstrated 100% protection from lethal challenge in mouse models and protection from disease in the *C. macaque* model.

Vaccine Platform	Antigen(s) Encoded	Vaccine Dose	Animal Model	Challenge Dose	Challenge Strain	Reference(s)
VRP	GPC (Oman-98) RdRp and NP (IbAr10200)	One dose of 1 or 2.15 10^5 TCID ₅₀	IFNAR ^{-/-} mice	100 TCID ₅₀ or 373 TCID ₅₀	IbAr10200, Turkey2004, Oman-97	Scholte, et al., 2019 ⁸⁴ Spengler, et al., 2019 ¹⁸³ Spengler, et al., 2021 ¹⁸⁴
mRNA	NP (Ank-2)	Two doses of 25 μ g	IFN $\alpha/\beta/\gamma$ R ^{-/-} mice	1000TCID ₅₀	Ank-2	Farzani, et al., 2019 ⁸³
	G _N +G _C alone, NP alone, or G _N +G _C and NP combination	Two doses of 10 μ g (single antigens) or 20 μ g (combination)	IFNAR ^{-/-} mice	400 FFU	IbAr10200	Appelberg, et al., 2022 ⁸²
Viral-Vectored	GPC (Ibar10200) in Vesicular Stomatitis virus	One or two doses of 10^7 PFU	STAT-1 ^{-/-} mice	50 PFU	Turkey-2004	Rodriguez, et al., 2019 ⁸⁰

	GPC (IbAr10200) in Modified Vaccinia Ankara	Two doses of 10^7 PFU	IFNAR ^{-/-} mice	200 TCID ₅₀	IbAr10200	Buttigieg, et al., 2014 ⁷⁹
	NP (Ank-2) in Bovine Herpesvirus Type 4	Two doses of 100TCID ₅₀	IFN α / β / γ R ^{-/-} mice	1000TCID ₅₀	Ank-2	Farzani, et al., 2019 ⁸¹
	NP (Ank-2) in Adenovirus type 5	Two doses of 100TCID ₅₀	IFN α / β / γ R ^{-/-} mice	1000TCID ₅₀	Ank-2	Farzani, et al., 2019 ⁸¹
DNA	Ubiquitin-linked GN, GC, and NP (IbAr10200)	Three doses of 50 μ g	IFNAR ^{-/-} mice	400 FFU	IbAr10200	Hinkula, et al., 2017 ⁷⁵
	NP (Ank-2) alone or co-delivered with CD24	Two doses of 50 μ g	IFNAR ^{-/-} mice	1000 TCID ₅₀	Ank-2	Farzani, et al., 2019 ⁷⁶
	GPC (IbAr10200)	Three doses of 50 μ g	Transient immune suppressed C57BL/6 mice	100 PFU	IbAr10200	Suschak, et al., 2021 ⁷⁷
	Ubiquitin-linked NP and GPC (Hoti)	Three doses of one mg of each plasmid	<i>Cynomolgus macaque</i>	1×10^5 TCID ₅₀	Hoti	Hawman, et al., 2020 ⁷⁸

Table 1.2: Candidate protective antigens for anti-tick vaccine development.

Antigen	Antigen Type	Species of Antigen Origin	Reference(s)
15kDa salivary gland protein (Salp15)	Exposed	<i>I. scapularis</i> and <i>I. ricinus</i>	Garcia, et al., 2014 ¹⁸⁵ Anguita, et al., 2002 ¹⁸⁶ Hovius, et al., 2007 ¹⁸⁷
64P	Exposed	<i>R. appendiculatus</i>	Nuttall, et al., 2006 ¹⁰⁶ Havlikova, et al., 2009 ¹⁸⁸ Trimnell, et al., 2005 Labuda, et al., 2006
Aquaporin (AQP)	Concealed	<i>R. microplus</i>	Campbell, et al., 2010 ¹⁸⁹ Hussein, et al., 2015 ¹⁹⁰ Guerrero, et al., 2014 ¹⁹¹
86kDa midgut protein (Bm86)	Concealed	<i>R. microplus</i> (also <i>R. annalatus</i> , <i>R. sanguineus</i> , and <i>H. anaticum</i>)	Willadsen, et al., 1989 ¹¹⁷
Bm91	Concealed	<i>R. microplus</i>	Willadsen, et al., 1996 ¹⁹²
Bm95	Concealed	<i>R. microplus</i>	Garcia-Garcia, et al., 2000 ¹⁹³
Calreticulin (CRT)	Exposed	<i>H. anaticum</i>	Kumar, et al., 2017 ¹²⁴
Cathepsin L-like cysteine proteinase (CathL)	Concealed	<i>I. ricinus</i> and <i>H. anaticum</i>	Kumar, et al., 2017 ¹²⁴
Elongation factor 1a (EF1a)	Concealed	<i>R. microplus</i>	Almazan, et al., 2010 ¹⁹⁴ Almazan, et al., 2012 ¹⁹⁵
Ferritin 2	Concealed	<i>H. anaticum</i>	Manjunathachar, et al., 2019 ¹⁹⁶
Glutathione-S transferase (GST)	Concealed	<i>R. microplus</i>	Almazan, et al., 2010 ¹⁹⁴
Salp16	Exposed	<i>I. scapularis</i>	Das, et al., 2000 ¹⁹⁷ Sukumaran, et al., 2006 ¹⁹⁸
Salp25D	Exposed	<i>I. scapularis</i>	Das, et al., 2001 ¹⁹⁹ Narasimhan, et al., 2006 ²⁰⁰
Selenoprotein W	Concealed	<i>R. microplus</i>	Almazan, et al., 2010 ¹⁹⁴
Serpins (RAS-3, RAS-4, RIM36 cocktail)	Concealed	<i>R. appendiculatus</i> and <i>Haemaphysalis longicornis</i>	Imamura, et al., 2005 ²⁰¹ Imamura, et al., 2006 ²⁰²

Silk	Exposed	<i>R. microplus</i>	Merino, et al., 2013 ¹⁴⁴ Antunes, et al., 2014 ¹⁴⁰
Subolesin	Concealed	<i>I. scapularis</i>	Almazan, et al., 2003 ¹²²
Tick histamine release factor (tHRF)	Exposed	<i>I. scapularis</i>	Dai, et al., 2010 ²⁰³
Tick salivary lectin pathway inhibitor (TSLPI)	Exposed	<i>I. scapularis</i>	Schuijt, et al., 2011 ²⁰⁴ Schuijt, et al., 2011 ²⁰⁵
Tropomyosin	Concealed	<i>H. anatolicum</i>	Manjunathachar, et al., 2019 ¹⁹⁶
TROSPA	Concealed	<i>I. scapularis</i>	Pal, et al., 2004 ²⁰⁶
Ubiquitin	Concealed	<i>R. microplus</i> and <i>R. annalatus</i>	Almazan, et al., 2010 ¹⁹⁴ Almazan, et al., 2012 ¹⁹⁵

Table 1.3: Subolesin anti-tick vaccine candidates and efficacy.

* Percent values were rounded to the nearest whole number for consistency between studies.

Vaccine Platform	Subolesin Antigen Species	Dosage	Animal Model	Challenge Species and Stage	Vaccine Efficacy (Overall, % Reduction of Each Measurement, or % Mortality) *	Reference
Purified protein in Freud's complete adjuvant (FCA)	<i>R. haemaphysaloides</i>	Three doses of 100 µg	Balb/c mice	<i>R. haemaphysaloides</i> larvae	Engorgement: 29%	Lu, et al., 2016 ²⁰⁷
	<i>R. haemaphysaloides</i>	Three doses of 100 µg	Balb/c mice	<i>R. haemaphysaloides</i> nymphs	Attachment: 20% Engorgement: 16% Weight: 26% Molting: 3%	
	<i>R. haemaphysaloides</i>	Three doses of 250 µg	New Zealand white rabbits	<i>R. haemaphysaloides</i> adults	Attachment: 14% Engorgement: 43% Weight: 43% Egg weight: 53%	
Purified protein in Freud's incomplete adjuvant (FIA)	<i>I. scapularis</i>	Two doses of 10 µg	CD-1 Mice	<i>I. scapularis</i> larvae	Overall: 71%	Almazan, et al., 2003 ¹²²
	<i>I. scapularis</i>	Three doses of 50 µg	New Zealand white rabbits	<i>I. scapularis</i> , <i>D. variabilis</i> , and <i>A. americanum</i> nymphs	Infestation: 35% (<i>I. scapularis</i>) 22% (<i>D. variabilis</i>) 17% (<i>A. americanum</i>) Engorged Weight: 0% (<i>I. scapularis</i>) 32% (<i>D. variabilis</i>) 3% (<i>A. americanum</i>)	Almazan, et al., 2005 ²⁰⁸

	<i>I. scapularis</i>	Four doses of 100 µg	Sheep	<i>I. scapularis</i> adults	Overall: 99% Infestation: 90% Oviposition: 87%	Almazan., et al., 2005 ²⁰⁹
Purified protein 1 st dose in FCA 2 nd dose in FIA 3 rd dose: no adjuvant	<i>O. erraticus</i>	Three doses of 100 µg	New Zealand white rabbits	<i>O. erraticus</i> and <i>O.moubata</i> adults and nymphs	<i>O. erraticus</i> Oviposition: 22% Fertility: 9%	Manzano-Roman, et al., 2012 ²¹⁰
	<i>O. moubata</i>				<i>O. moubata</i> Oviposition: 8% Fertility: 6%	
Purified protein in Montanide ISA 50 V2 adjuvant	<i>R. microplus</i>	Three doses of 100 µg	Crossbred calves	<i>R. annalatus</i> and <i>R. microplus</i> larva	<i>R. microplus</i> Overall: 51% Infestation: 43% Weight: 0% Oviposition: 0% Fertility: 15%	Almazan, et al., 2010 ¹⁹⁴
	<i>A. americanum</i>	Three doses of 100 µg	Crossbred calves	<i>A. americanum</i> nymphs and adults	<i>R. annalatus</i> Overall: 60% Infestation: 18% Weight 17% Oviposition 23% Fertility 37%	Nymphs: Overall: 12% Infestation 12% Weight: 10%
						de la Fuente, et al., 2010 ²¹¹

					Molting 5% Adults: Overall: 66% Infestation: 7% Weight: 33% Oviposition: 41% Fertility: 38%	
	<i>I. scapularis</i>	Two doses of 100 µg	Sheep	<i>I. scapularis</i> and <i>A. americanum</i> adults	<i>I. scapularis</i> Infestations: 12% Weight: 15% <i>A. americanum</i> Infestation: -4% Weight: 5%	Canales, et al., 2009 ²¹²
	<i>R. microplus</i>	Three doses of 25 µg	Balb/c mice	<i>I. ricinus</i> larvae	Mortality: -4% Molting: 48%	Moreno-Cid, et al., 2013 ²¹³
	<i>R. microplus</i>	Three doses of 100 µg	Crossbred calves	<i>R. microplus</i> larvae	Overall: 60% Infestation: 47% Weight: 9% Oviposition: 18%	Merino, et al., 2013 ¹⁴⁴
	<i>R. microplus</i>	Three doses of 100 µg	Crossbred calves	<i>R. microplus</i> larvae	Overall: 44% Infestation: 42% Weight: 2% Oviposition: 3%	Merino, et al., 2011 ²¹⁴
	<i>R. microplus</i>	Three doses of 100 µg	White-tailed deer	<i>R. microplus</i> larvae	Overall: 83% Infestation: 56% Weight: 11% Oviposition: 21% Fertility: 51%	Carreon, et al., 2012 ²¹⁵

	<i>H. anatolicum</i>	Three doses of 200 µg	Crossbred calves	<i>H. anatolicum</i> and <i>R. microplus</i> larvae	<i>H. anatolicum</i> Overall: 65% Infestation: 40% Mortality: 42% <i>R. microplus</i> Overall: 54% Infestation: 39% Weight: 20% Egg weight: 25%	Kumar, et al., 2017 ¹²⁴
Purified protein in 10% Montanide 888	<i>R. microplus</i>	Three doses of 100 µg	Crossbred calves	<i>R. microplus</i> larvae 15 days after the final dose	Overall: 44% Infestation: 16% Weight: 8% Oviposition: 9% Fertility: 26%	Shakya., et al., 2014 ²¹⁶
				<i>R. microplus</i> larvae 45 days after the final dose	Overall: 37% Infestation: 9% Weight: 4% Oviposition: 9% Fertility: 24%	
SUB-MSP1a chimeric protein, <i>E. coli</i> membrane bound, in Montanide ISA 50 V2	<i>R. microplus</i>	Three doses of 120 µg	Crossbred calves	<i>R. microplus</i> and <i>R. annalatus</i> larvae	<i>R. microplus</i> Overall: 81% Infestation: 34% Weight: 37% Oviposition: 11% Fertility: 67% <i>R. annalatus</i> Overall: 67% Infestation: 20% Weight: 38%	Almazan, et al., 2012 ¹⁹⁵

					Oviposition: -15% Fertility: 67%	
Subolesin/Akirin multi-epitope antigen (Q38) chimeric purified protein in Montanide ISA 50 V2	<i>R. microplus</i> and <i>A. albopictus</i>	Three doses of 100 µg	Crossbred calves	<i>R. microplus</i> larvae	Overall: 75% Infestation: 69% Weight: 5% Oviposition: 20%	Merino, et al., 2013 ¹⁴⁴
	<i>R. microplus</i> and <i>A. albopictus</i>	Three doses of 25 µg	Balb/c mice	<i>I. ricinus</i> larva	Mortality: -8% Molting: 28%	Moreno-Cid, et al., 2013 ²¹³
	<i>R. microplus</i> and <i>A. albopictus</i>	Two doses of 50 µg	New Zealand white rabbits	<i>D. reticulatus</i> and <i>I. ricinus</i> larvae	<i>D. reticulatus</i> Mortality: 13% Weight: 25% Molting: 15% <i>I. ricinus</i> Mortality: 8% Weight: -15% Molting: 38%	Contreras and de la Fuente, 2016 ²¹⁷
Subolesin/Akirin multi-epitope antigen (Q41) chimeric purified protein in Montanide ISA 50 V2	<i>R. Microplus</i> and <i>A. albopictus</i>	Three doses of 25 µg	Balb/c mice	<i>I. ricinus</i> larvae	Mortality: 10% Molting: 14%	Moreno-Cid, et al., 2013 ²¹³
Vaccinia virus- vectored	<i>I. scapularis</i>	1 x 10 ⁸ PFU	C3H/HeN mice	<i>I. scapularis</i> larvae	Infestation: 52%	Bensaci, et al., 2012 ¹⁴⁶

Figure 1.1: Geographic distribution of *Hyalomma* ticks and CCHF cases.

Used and modified from a 2017 World Health Organization (WHO) CCHFV distribution map⁸ under the Creative Commons license:

CC BY-NC-SA 3.0 IGO.

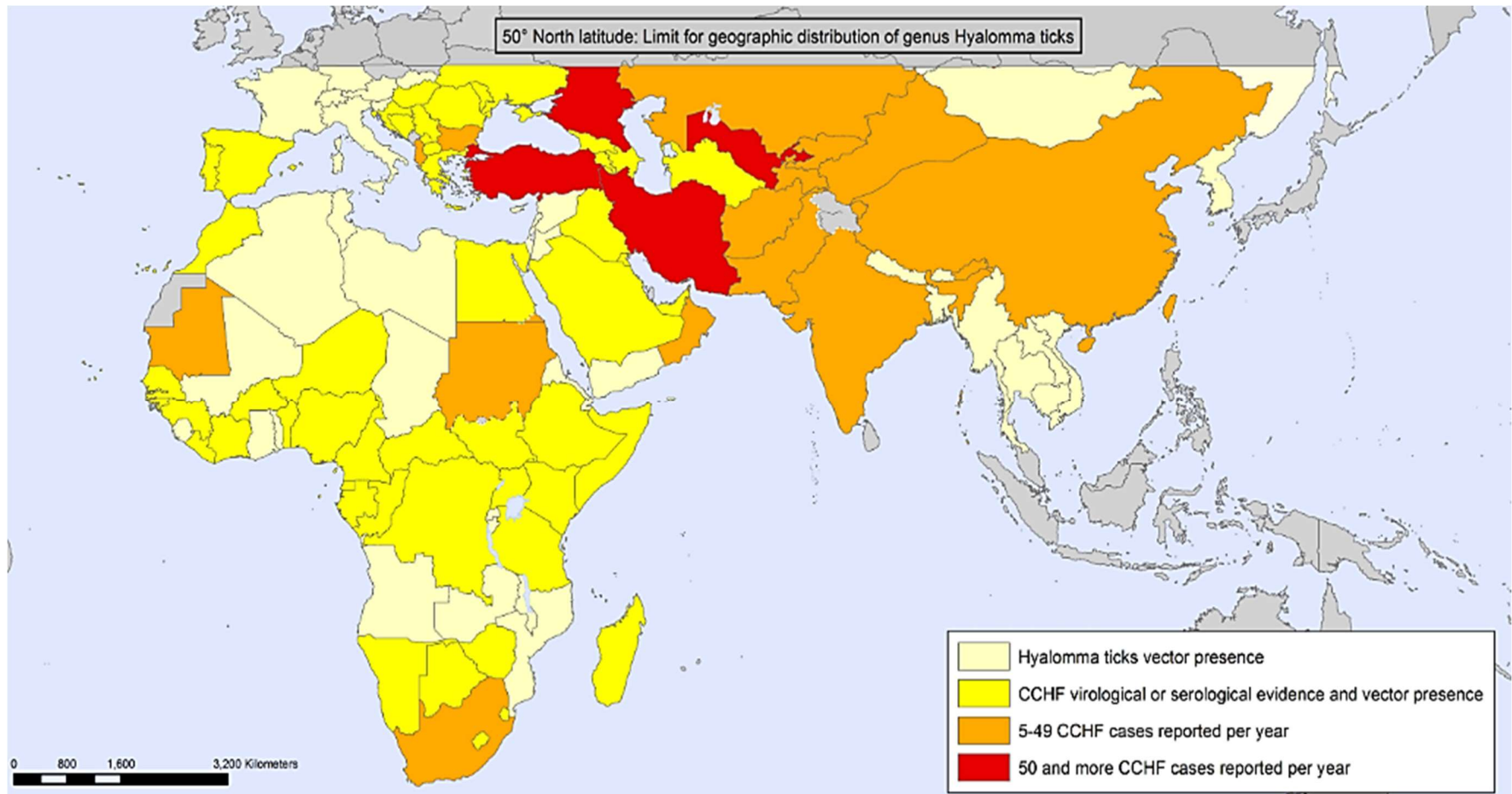


Figure 1.2: CCHFV genome organization and virion structure².

A) Schematic diagram of CCHFV genome organization and protein products. Generated using BioRender. B) Schematic diagram of CCHFV virion. Used with permission from Elsevier Publishing Group; License: 5322200635394.

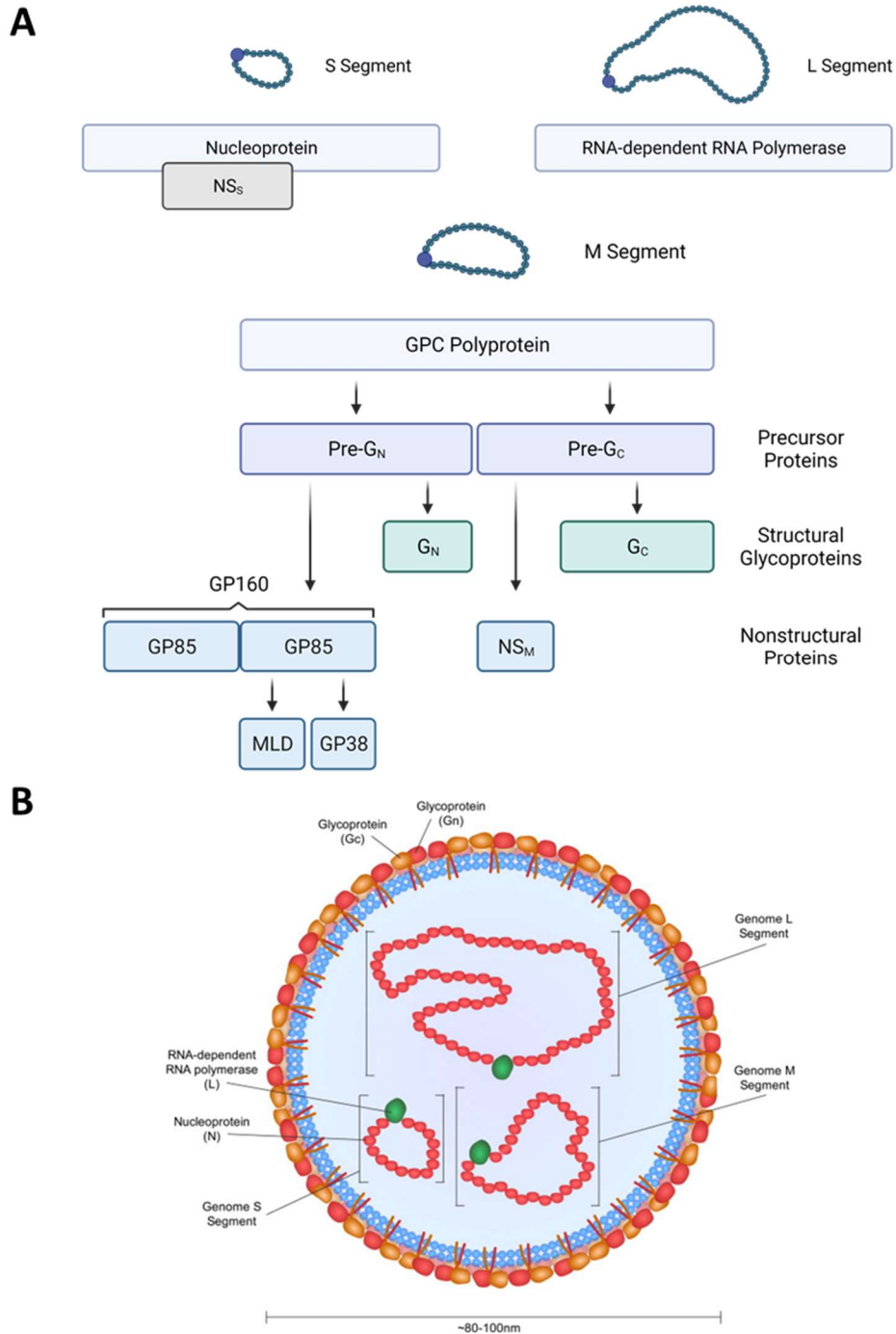


Figure 1.3: Replication cycle of CCHFV².

Used with permission from Elsevier Publishing Group; License: 5322200635394.

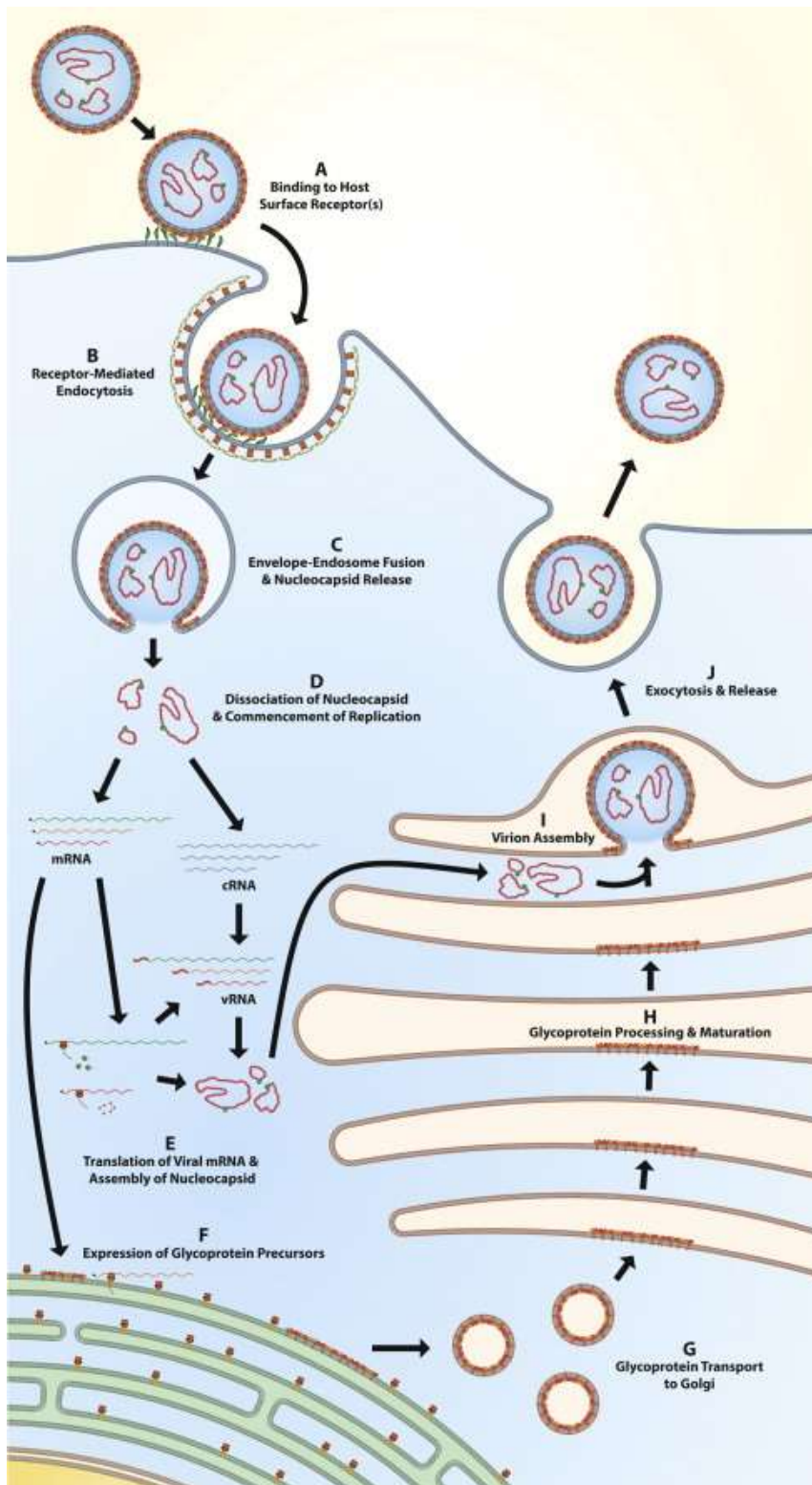
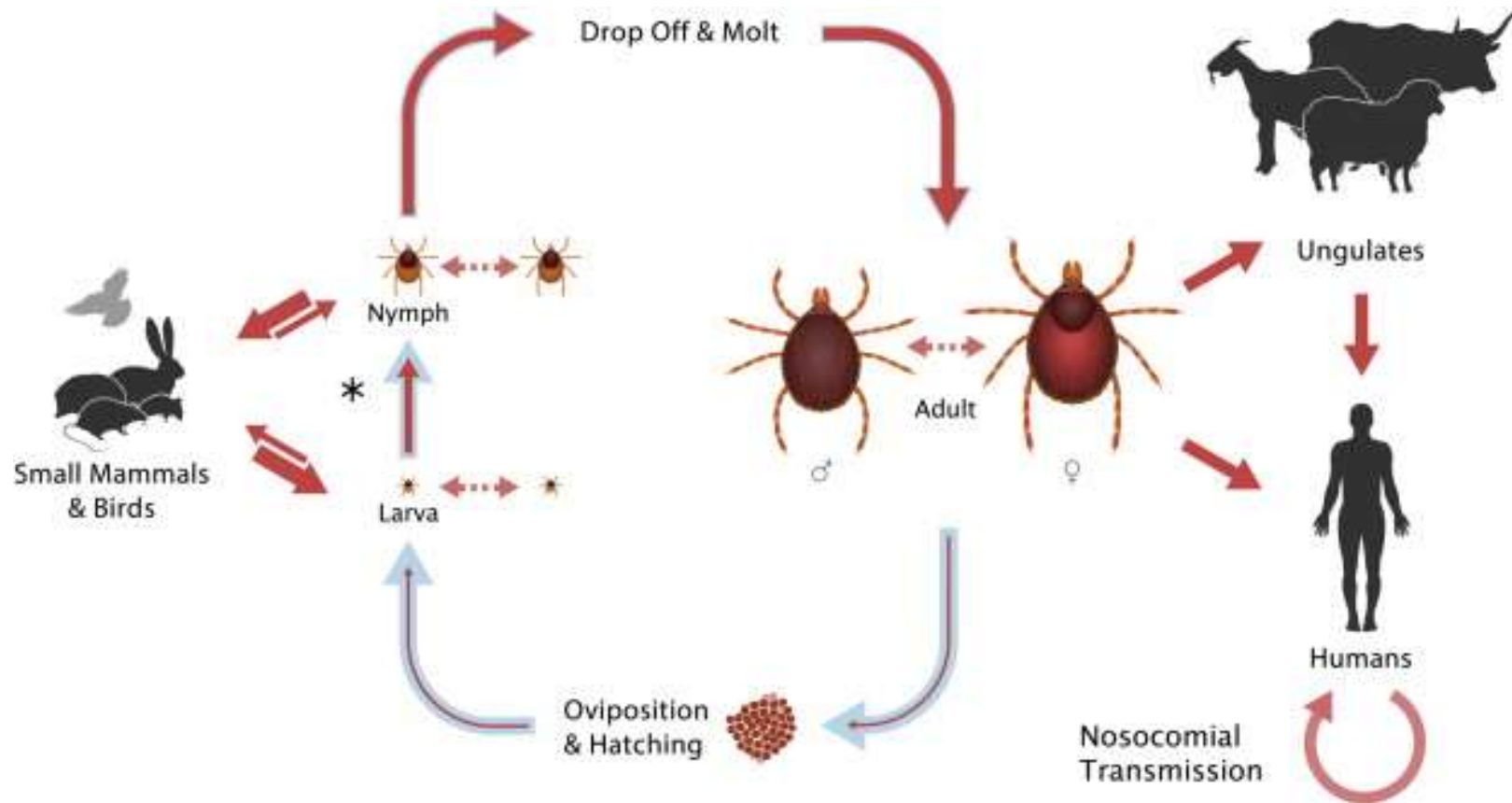


Figure 1.4: Transmission cycle of CCHFV².

Blue arrows show the life cycle of *H. marginatum* ticks, and red arrows within the blue arrows indicate the efficiency of virus transmission between life cycle stages. The * indicates the difference in feeding patterns between two and three-host ticks. Used with permission from Elsevier Publishing Group; License: 5322200635394.



Chapter 2: Materials and Methods

2.1 *In silico* Analyses

2.1.1 Subolesin Codon Optimization

The Subolesin coding sequence was codon-optimized for rabbits (*Oryctolagus cuniculus*) using the GeneArt system through Thermo Fisher Scientific or mice (*Mus musculus*) using the Integrated DNA Technologies codon-optimization tool. The coding sequence for the Subolesin-RABV-G chimeric antigen was codon-optimized for cattle (*Bos taurus*) using GenScript (**Figure 2.1**).

2.1.2 Nucleotide Alignments and Homology Calculations

Nucleotide sequences were aligned using Geneious Prime software (www.geneious.com) with default settings. The number and percent of identical nucleotides between given sequences was calculated by the software during the alignment.

2.1.3 Cytotoxic T-Lymphocyte Epitope Prediction

The translation of the GPC of CCHFV strain Turkey200406546, designated throughout this work as Turkey2004 (Accession # KY362519.1) was used for bioinformatic server predictions to identify epitopes likely to be presented by human major histocompatibility complex (MHC) class I molecules to CD8⁺ cytotoxic T-lymphocytes (CTL). CTL epitopes were predicted using the NetCTL 1.2 Server (<https://services.healthtech.dtu.dk/service.php?NetCTL-1.2>) powered by the Department of Bio and Health Informatics at the Technical University of Denmark. The NetCTL 1.2

Server was used to predict binding of 9-mer CTL peptides to 12 MHC class I supertypes (A1, A2, A3, A24, A26, B7, B8, B27, B39, B44, B58, and B62) using neural networks. Predicted peptides were selected based on an inclusion criterion of a combined score of >1.0 given from the prediction of MHC class I binding, proteasomal C-terminal cleavage, and transporter associated with antigen processing (TAP) transport efficiency. A combined score of >1.0 yields 70% sensitivity and 98.5% specificity of CTL ligand prediction accuracy, where sensitivity and specificity refer to the probability of identifying true positives and true negatives, respectively²¹⁸. Peptides were excluded if they fell across known cleavage sites on the GPC polyprotein.

2.1.4 Helper T-Lymphocyte Epitope Prediction

The translation of the GPC of CCHFV strain Turkey2004 was used for bioinformatic server predictions to identify epitopes likely to be presented by human MHC class II molecules to CD4⁺ helper T-lymphocytes (HTL). HTL epitopes were predicted using the NetMHCII 2.3 Server (<https://services.healthtech.dtu.dk/service.php?NetMHCII-2.3>) powered by the Department of Bio and Health Informatics at the Technical University of Denmark. The NetMHCII 2.3 Server was used to predict binding of 15-mer HTL peptides to 25 HLA-DR, 20 HLA-DQ, and 9 HLA-DP alleles using artificial neural networks. Predicted peptides were selected if they met both inclusion criteria of (1) a strong binder threshold of <2.00%-rank to a set of 1,000,000 random natural peptides and (2) a predicted IC50 value <50 nM. Peptides were excluded if they fell across known cleavage sites on the GPC polyprotein.

2.1.5 Alignment and Graphing of Predicted Epitopes to the CCHFV GPC

All predicted CTL and HTL peptides that met the above inclusion criteria were aligned to the Turkey2004 GPC sequence using Clustal Omega (<https://www.ebi.ac.uk/Tools/msa/clustalo/>). Groups of peptides were assigned numerical values for the number of peptides that overlapped a given residue in the GPC alignment, and peptides were graphed in GraphPad Prism using these assigned values. Regions with the highest number of overlapping predicted peptides and regions including two previously demonstrated T cell epitopes⁶⁸ were selected as multi-epitope regions.

2.1.6 Amino Acid Alignments, Phylogenetic Tree, and Homology Calculations

2.1.6.1 Full-length GPC and Phylogenetic Tree

Sequences of 50 CCHFV glycoprotein precursors were imported into Geneious Prime software from Genbank (**Table 2.1**). The open-reading frame was translated to obtain the amino acid sequence of each CCHFV GPC. A phylogenetic tree was constructed from all 50 sequences using Geneious Tree Builder with default parameters, and clades were assigned based on previous publications^{2,50}.

2.1.6.2 Individual GPC Proteins

An alignment of the translations of all 50 GPC sequences was generated using a Geneious alignment with default parameters. This alignment was used to identify the known cleavage sites between GPC proteins (MLD-RS/KR-GP38; GP38-RK/LL-G_N; G_N-RK/LL-NS_M; NS_M-RK/PL-G_C) to make alignments for the individual GPC proteins.

2.1.6.3 Multi-Epitope Regions

Multi-epitope regions were chosen based on bioinformatic predictions using the Turkey2004 sequence. An alignment of the translations of all 50 GPC sequences was generated using a Geneious alignment with default parameters. Using the alignment with the Turkey2004 sequence, the corresponding sequence from the remaining 49 sequences of each multi-epitope region was identified and saved as an individual document for homology calculations.

2.1.6.4 Homology Calculations

Sequence conservation was assessed at the residue level for both percent identity and percent similarity. The percent identity and percent similarity of each selected sequence to the Turkey2004 sequence was determined using William Pearson's *lalign* program run through the Swiss Institute of Bioinformatics ExPASy Bioinformatics Resource Portal, (https://embnet.vital-it.ch/software/LALIGN_form.html; now available at <https://www.ebi.ac.uk/Tools/psa/lalign/>). The percent identity and similarity to the Turkey2004 sequence was calculated for each GPC protein, and each multi-epitope region. The percent of amino acid identity and similarity were averaged for each protein or epitope region from the 50 sequence comparisons.

2.1.7 Generation of the Multi-Epitope Antigen and Plasmid

The 11 multi-epitope regions were joined together *in silico* using a flexible linker of -glycine-glycine-glycine-serine- (-GGGS-). A start codon was placed at the N-terminus, and a six residue polyhistidine tag (6XHis) was added before a stop codon at the C-terminus.

A signal peptide was not included at the N-terminus of the antigen. The final EPItope Construct (*EPIC*) product with linkers and tag was 853 amino acid residues in length and will be referred to as *EPIC* throughout. *EPIC* was synthesized and subcloned behind a cytomegalovirus (CMV) promoter in the mammalian expression vector pTWIST-CMV using the restriction enzyme sites *NotI* and *BamHI* to create pTWIST-CMV-EPIC (TWIST Biosciences).

2.1.8 Subcellular Localization Prediction

Subcellular localization and the residues important for localization were predicted using the DeepLoc-1.0 server run through the Department of Bio and Health Informatics at the Technical University of Denmark (<https://services.healthtech.dtu.dk/service.php?DeepLoc-1.0>).

2.2 Biological Assays

2.2.1 Cell Lines and Cell Culture

2.2.1.1 Mammalian Cell Lines

Rabbit kidney epithelial cells (RK13; ATCC CCL-37) and human embryonic kidney 293T cells (HEK293T; ATCC CRL-3216; provided by the laboratory of Dr. Pei-Yong Shi, UTMB, Galveston, TX) were cultured in Minimum Essential Medium Eagle (MEM) supplemented with 1% penicillin-streptomycin and 10% fetal bovine serum (FBS), cumulatively termed E10 medium, at 37°C with 5% CO₂.

2.2.1.2 Tick Cell Lines

Ixodes scapularis embryonic cells (ISE6; ATCC CRL-11974; provided by the laboratory of Dr. Jere McBride, UTMB, Galveston, TX) were cultured at 34°C without CO₂ in L15B-300 medium containing 5% FBS, 10% tryptose phosphate broth, and 0.1% lipoprotein concentrate (referred to as complete medium).

Generation of complete medium required multiple steps, and was prepared according to the publication by Munderloh and Kurtti²¹⁹. First, L-15 medium (Gibco) was supplemented with L-aspartic acid, α -ketoglutaric acid, L-glutamine, L-proline, L-glutamic acid, D-glucose, Mineral Stock D, and Vitamin Stock^{219,220}. The pH was adjusted to 6.5 using NaOH, then sterile filtered. This is referred to as Base Medium. Next, three parts of Base Medium was combined with one part of sterile water to reduce the osmolarity, and the FBS, tryptose phosphate broth, and lipoprotein concentrate was added. The pH was adjusted to 7.4 using NaOH, then sterile filtered.

2.2.2 Plasmids

The pCAGGS-GPC plasmid containing the CCHFV GPC of strain Turkey2004 was kindly provided by Dr. Eric Bergeron (Centers for Disease Control and Prevention, Atlanta, GA). Plasmids containing Subolesin (pMA-Subolesin and pcDNA3.1(+)-Subolesin-6XHis) were synthesized by TWIST Biosciences. The plasmid containing the Subolesin-RABV-G chimeric antigen (pCAGGS-Subolesin-RABV-G) was synthesized by GenScript and was kindly provided by Dr. Schnell's laboratory (Thomas Jefferson University, Philadelphia, PA). The plasmid containing green fluorescent protein (pCAGGS-GFP) was generated

using PCR amplification and restriction enzyme digestion. The GFP gene was PCR amplified using 2X DreamTaq PCR Master Mix (Thermo Fisher Scientific) and the primers GFP-*EcoRI*-F and GFP-*BglII*-R, which included the restriction enzyme sites for *EcoRI* and *BglII* on the 5' and 3' of the gene during amplification, respectively. The pCAGGS-GPC plasmid and PCR product were digested using the restriction enzymes *EcoRI* and *BglII* (New England Biolabs), then purified after separation on a 1% agarose gel. The digested PCR product was then ligated into the pCAGGS plasmid backbone using T4 DNA ligase (New England Biolabs). The ligation mixture was then transformed into *Escherichia coli* (Mix & Go Competent Cells - Strain DH5 Alpha, Zymo Research) according to the manufacturer's instructions and plated on Luria-Bertani (LB) agar plates supplemented with 100µg/mL ampicillin (LB and ampicillin: Thermo Fisher Scientific; plates made in house). Cultures were incubated at 37°C for 24 hours, then individual colonies were picked using sterile pipet tips and placed into 5.0 mL LB broth supplemented with 100µg/mL ampicillin. Liquid cultures were incubated at 37°C for 24 hours with shaking at 250rpm. After incubation, the culture was vortexed, then 0.5mL of culture was mixed with 0.5mL of sterile 50% glycerol (Thermo Fisher Scientific) and stored at -80°C. The remaining 4.5mL of liquid cultures were lysed and purified using the QIAprep Spin Miniprep Kit (QIAGEN) according to the manufacturer's instructions, and plasmids were eluted using sterile molecular grade water. All plasmid sequences were confirmed using Sanger sequencing at the UTMB Molecular Genomics Core Facility. The frozen glycerol/suspension mixture was used for large-scale plasmid preparations to inoculate 250mL of LB broth supplemented with 100µg/mL ampicillin. These cultures were incubated at 37°C for 24 hours with shaking at 250rpm. Cultures of *E. coli* were lysed, and

plasmids were purified using the ZymoPURE™ II Plasmid Maxiprep Kit (Zymo Research) according to the manufacturer's instructions, and eluted using sterile molecular grade water. Plasmid suspensions were quantified using a Tecan NanoQuant plate and a Tecan infinite 200Pro plate reader.

2.2.3 Proteins

2.2.3.1 Antibodies

A monoclonal antibody (mAb) recognizing a six residue polyhistidine tag was obtained from Thermo Fisher Scientific (His.H8, Cat # MA1-21315). The mouse anti-CCHFV mAbs 9D5 (NR-40270), 2B11 (NR-40257), 11F6 (NR-40283), 13G8 (NR-40294), 5A5 (NR-40249), 8F10 (NR-40282), 10E11 (NR-40276), 7F5 (NR-40281), 6B12 (NR-40259), 11E7 (NR-40277), 3E3 (NR-40273), 1H6 (NR-40296), 30F7 (NR-40288), 12A9 (NR-40254), and 13G5 (NR-40293) were obtained from the Biodefense and Emerging Infections Research Resources Repository (BEI resources, ATCC, Manassas, VA). The mouse anti-CCHFV mAb 8A1 was kindly provided by United States Armed Forces Research Institute for Infectious Diseases (USAMRIID), Frederick, MD from the Peters-Dalrymple Collection. Hyperimmune mouse ascitic fluid (HMAF) was kindly provided by Dr. Tom Ksiazek (World Reference Center for Emerging Viruses and Arboviruses, UTMB, Galveston, TX). Goat-anti-mouse-IgG conjugated to horseradish peroxidase (HRP) (Abcam, Cat # ab6789), goat-anti-mouse-IgG conjugated to Alexa Fluor™ 488 (Invitrogen, Cat # A11029), goat-anti-mouse-IgG conjugated to Alexa Fluor™ 594 (Invitrogen, Cat # 10680), goat-anti-rabbit-IgG conjugated to Alexa Fluor™ 488 (Invitrogen, Cat # A11034), and goat-anti-rabbit conjugated to Alexa Fluor™ 594

(Invitrogen, Cat # A11037) were used as secondary antibodies for ELISA and IFAs. Mouse anti-RABV-G mAb 1C5 (Novus Biologicals, Cat # NBP2-11630), goat-anti-mouse conjugated to HRP (Jackson ImmunoResearch, Cat # 115-053-146), and donkey-anti-rabbit-IgG conjugated to HRP (Jackson ImmunoResearch, Cat # 711-035-152) were used in the laboratory of Dr. Matthias Schnell. Rabbit anti-Subolesin serum was generated by immunization of rabbits with three doses of purified *Rhipicephalus microplus* Subolesin protein (50 µg per dose) in Montanide ISA 50 V2 adjuvant (Seppic, France). Rabbit anti-Subolesin serum was kindly provided by Dr. Jose de la Fuente (University of Castilla-La Mancha, Ciudad Real, Spain). Rabbit anti-West Nile virus serum was kindly provided by Dr. Alan Barrett (University of Texas Medical Branch, Galveston, TX).

2.2.3.2 Purified Recombinant Protein

Purified *R. microplus* Subolesin protein was kindly provided by Dr. Jose de la Fuente.

2.2.3.3 Generation of Whole-Cell Protein Lysates

HEK293T cells seeded to 80% confluency in 6-well plates were transfected with either pTWIST-CMV-EPIC or pCAGGS-GPC using Lipofectamine 3000 according to the manufacturer's instructions. The cell and transfection mixtures were incubated at 37°C with 5% CO₂ for four hours; then medium was replaced with fresh growth medium. At 48 hours post-transfection the media was removed, and cells were washed with DPBS. Radioimmunoprecipitation assay (RIPA) buffer (25mM Tris-HCl, 150mM NaCl, 1% NP-40, 1% sodium deoxycholate, 0.1% SDS, Pierce) supplemented with 1X Halt Protease Inhibitor Cocktail (Thermo Fisher Scientific) was applied to each well to lyse the cells, and

the protein slurry was pipetted into a labeled vial. DNA was sheared by passing the lysate through a 29-gauge needle attached to an insulin syringe ten times. Cell debris was pelleted by centrifugation for five minutes at 16,000 x g and the supernatant was transferred into a new vial for storage at -20°C until use.

2.2.4 Viruses

2.2.4.1 Recombinant Myxoma Viruses

2.2.4.1.1 Generation of Recombinant Viruses

Recombinant myxoma viruses were generated by the laboratory of Dr. Grant McFadden (Arizona State University (ASU), Tempe, AZ) using gateway cloning and homologous recombination. Foreign antigens were cloned into a recombination plasmid behind individual Vaccinia virus synthetic early/late (sE/L) promoters. The final recombination plasmid encoded part of the M135R and M136R genes flanking the foreign antigens. Briefly, RK13 cells were infected with wild-type myxoma virus, Lausanne strain, then transfected with the final recombination plasmid. Recombinant viruses were purified three times by fluorescent foci selection before purified stock aliquots were shipped to UTMB.

2.2.4.1.2 Production of Recombinant Myxoma Virus Stocks

Virus aliquots provided by ASU were passaged once to make working stocks for all subsequent experiments. Viruses were grown by infecting RK13 cells at 80% confluency at a multiplicity of infection (MOI) of 0.1. Virus was allowed to adsorb for one hour at 37°C with 5% CO₂ with rocking at 15-minute intervals, after which MEM supplemented with 10% FBS was added to the flask. Flasks were incubated at 37°C with 5% CO₂ until

48 hours post-infection. At this point, media was removed from the flask, and cell monolayers were washed once with DPBS. DPBS was added to the flask, and cells were scraped off of the flask into the solution using a cell scraper. The cell suspension was pipetted into a conical tube, and flash-frozen in a slurry of dry ice and 70% ethanol. The suspension was thawed and then vigorously vortexed. This process was repeated for a total of three freeze-thaw cycles. Cell debris was then pelleted by centrifuging for 30 minutes at 3,000 x g. The supernatant was then aliquoted and stored at -80°C for future use.

2.2.4.1.3 Sucrose Purification of Recombinant Myxoma Virus

Viruses were semi-purified over a 36% sucrose cushion as described previously¹⁶². Briefly, 20mL of clarified virus supernatants were pipetted over 16mL of 36% sucrose in 10mM Tris-HCl in a polycarbonate centrifuge tube (Beckman Coulter). Samples were centrifuged in a SW28 rotor at 18,000 revolutions per minute (RPM) for 80 minutes. The supernatant was removed, and the virus pellet was resuspended in DPBS then aliquoted and stored at -80°C for future use.

2.2.4.1.4 Titration by Fluorescent Focus Forming Assay

Twelve-well plates were seeded to approximately 80% confluency with RK13 cells. Cells were infected with 10-fold dilutions (10^0 - 10^{-5}) of the virus. Virus was allowed to adsorb for one hour at 37°C with 5% CO₂ with rocking at 15-minute intervals. E10 medium was added to each well, and plates were incubated until 48 hours post-infection at 37°C with 5% CO₂. Media was removed, and cells were washed with DPBS. Plates were then fixed with 10% neutral-buffered formalin for one hour at room temperature. The fixative was

decanted, and plates were allowed to dry. Fluorescent foci were viewed and counted using a Dino-Lite EDGE AM4115T-YFGW digital microscope and DinoCapture 2.0 software, or a Cytation 7 imaging plate reader (BioTek). The titer of the virus was determined using fluorescent focus forming units per milliliter (FFU/mL).

2.2.4.1.5 Multiplication Kinetics

Twelve-well plates were seeded to approximately 80% confluency with RK13 cells, then infected with either vMyx-GFP-Empty or vMyx-GFP-Subolesin diluted to an MOI of 0.1 in serum-free MEM. Virus was allowed to adsorb for one hour at 37°C with rocking at 15-minute intervals. The inoculum was removed, and cells were washed with DPBS before E10 medium was added to each well. Samples were collected at 0, 12, 24, 36, 48, 72, and 96 hours post-infection in triplicate. To harvest virus at each time point, E10 medium was removed from the well, and 500µl of cold DPBS was added to each well. A sterile pipette tip was used to scrape cells from the bottom of each well into solution. The DPBS and cell slurry was pipetted into a labeled screw cap vial and stored at -80°C until titration. Prior to titration, samples were removed from -80°C and allowed to thaw. This served as one round of freeze-thaw. Tubes were then submerged into a dry ice and 70% ethanol slurry to rapidly freeze the samples, then allowed to thaw. This was repeated once more for a total of three freeze-thaw cycles for each sample. Samples were then centrifuged at 16,000 x g for five minutes, then supernatant was transferred into a new labeled tube for titration then storage at -80°C.

2.2.4.1.6 Myxoma Virus Fluorescence Reduction Neutralization Test

Serum from one mouse from the vMyx-GFP-Subolesin, vMyx-GFP-Empty, and Saline groups was serially diluted 1:2 in serum free MEM starting at a 1 in 10 dilution, for a total of five dilutions. Sera dilutions were combined with vMyx-GFP-Empty and incubated on ice for one hour. The serum and virus mixtures were inoculated onto duplicate wells of RK13 cells seeded to 80% confluency in a 96-well plate. Virus was allowed to adsorb for one hour at 37°C with 5% CO₂, then growth media was added to each well. The plate was then incubated at 37°C with 5% CO₂ for 48 hours. The relative fluorescence of each well was measured using the Tecan Infinite M200 Pro plate reader. Values for 100% and 0% fluorescence were obtained by duplicate wells inoculated with virus only and media only without virus, respectively.

2.2.4.2 Recombinant Rabies Viruses

Recombinant rabies viruses were generated by the laboratory of Dr. Matthias Schnell (Thomas Jefferson University [TJU]) using a well-established reverse genetics system¹⁷⁶. The Subolesin-RABV-G chimeric antigen or the GP85 chimeric antigen was inserted between the nucleoprotein (N) and phosphoprotein (P) of the BNSP333 vaccine vector. All work with recombinant rabies viruses was conducted in the Schnell laboratory at TJU.

2.2.5 Nucleotide Sequence Analysis

2.2.5.1 DNA Extraction

Viral DNA was extracted from recombinant myxoma viruses using the Zymo ZR-Duet DNA/RNA Miniprep kit (Zymo) according to the manufacturer's instructions. The

insertion site of Subolesin was PCR amplified using 2X DreamTaq PCR Master Mix (Thermo Fisher Scientific) according to manufacturer's recommendations with primers that flanked the M135R-M136R intergenic region (M136R-F [CGATAACCGAGGTATGTGTT] and M136R-R [ACGTCAACGTGTTCTCTTTA]). The PCR product of the intergenic region was submitted to the UTMB Molecular Genomics Core Facility for Sanger sequencing using the flanking primers above and internal primers (Subolesin-F [ATGGCTTGCGCAACATTAAAGC], Subolesin-R [TTGGTCGTACGTAAACTTGAC], GFP-*EcoRI*-F [GAGTCGAATTCACCATGGTGAGCAAGGG], and GFP-*BglII*-R [GACATAGATCTCATCTTGTACAGCTCG]).

2.2.5.2 Sanger Sequencing

Sanger sequencing of purified plasmid or PCR products was completed by the UTMB Molecular Genomics Core Facility. Chromatograms were visually inspected, and sequences were aligned to reference sequences using Geneious Prime software.

2.2.5.3 RNA Extraction

To obtain total RNA from ISE6 cells, growth media was removed, and cells were lysed with Trizol reagent (Invitrogen). RNA was extracted using the Zymo Direct-Zol RNA miniprep kit. After extraction, RNA was stored at -80°C until use.

2.2.5.4 Two-Step qRT-PCR

Total RNA extracted from ISE6 cells was used as a template for generation of cDNA. cDNA was generated using random hexamers with the SuperScript™ III First-Strand Synthesis System (Invitrogen). cDNA was quantified using a NanoQuant Plate and Tecan Infinite M200 Pro plate reader. The qRT-PCR was completed using iTaq™ Universal SYBR® Green Supermix (BioRad) and the LightCycler 96 real-time PCR system (Roche). Primers were designed for each gene of interest using Geneious Prime software and Primer3 software (<https://bioinfo.ut.ee/primer3-0.4.0/>) (**Table 2.2**).

2.2.5.5 Next Generation Sequencing

Total RNA was extracted from ISE6 cells and submitted to the UTMB Next Generation Sequencing Core. cDNA libraries were prepared using the NEBNext Ultra II RNA Library Prep Kit for Illumina (New England Biolabs, Ipswich, MA) and random hexamer primers, following manufacturers instructions. Libraries were sequenced on the NextSeq550 Illumina platform, using 400-million read lanes with paired-end 75 nt read lengths.

2.2.5.6 RNA-seq

Total RNA was extracted from biological triplicates of mock antisera and Subolesin antisera treated ISE6 cells and was transported to the UTMB Next Generation Sequencing Core. Poly-A sample RNAs were purified with the NEBNext® Poly(A) mRNA Magnetic Isolation Module before cDNA libraries were prepared using the NEBNext Ultra II RNA Library Prep Kit for Illumina and random hexamer primers, following manufacturers instructions. Libraries were sequenced on the NextSeq550 Illumina platform, using 400-

million read lanes with single-end 75 nt read lengths. Raw reads were aligned to the *I. scapularis* genome assembly GCA_016920785.2 and a counts table was provided by the UTMB Molecular Genomics Core Facility for analysis of differentially expressed genes between mock and Subolesin antiserum treated samples.

2.2.6 Immunofluorescence Assays (IFA)

All IFA experiments used the 8-well Lab-Tek II chamber slide system (Nunc/Thermo Fisher Scientific), and images were collected using either an Olympus IX71 or BX61 fluorescent microscope.

2.2.6.1 One-Step Method for Fixation and Permeabilization of Cells

At the chosen time point, cell culture media was removed from cells, and cells were washed once with DPBS. The DPBS was decanted, and cells were fixed and permeabilized using a cold (-20°C) 50/50 mixture of acetone/methanol for 10 minutes at 4°C. The mixture was decanted, and cells were washed three times in DPBS-100mM glycine for five minutes each wash. Cells were blocked using 3% normal goat serum (Gibco) in DPBS-100mM glycine for one hour at room temperature.

2.2.6.2 Two-Step Method for Fixation and Permeabilization of Cells

At the chosen time point, cell culture media was removed from cells, and cells were washed once with DPBS. The DPBS was decanted, and cells were fixed using 4% paraformaldehyde for 10 minutes at room temperature. The fixative was decanted, and the reaction was quenched by incubation with DPBS-100mM glycine for 15 minutes at room

temperature. Cells were washed twice more with DPBS-100mM glycine for five minutes each. Cells were then permeabilized using 1% Triton-X in DPBS-100mM glycine for 15 minutes at room temperature. The permeabilization solution was decanted, and cells were washed three times in DPBS-100mM glycine for five minutes each wash. Cells were then blocked using 3% normal goat serum (Gibco) in DPBS-100mM glycine for one hour at room temperature.

2.2.6.3 IFA of Plasmid Transfected Cells

Chamber slides were seeded with RK13 or HEK293T cells the day prior to transfection, both at 100,000 cells per well. Plasmids were transfected using Lipofectamine 3000 according to manufacturer's recommendations. Cell culture media containing the transfection solution (DNA/liposome mixture) was removed at four hours post-transfection and replaced with fresh media. Cells were then incubated until 24 hours post-transfection. IFA experiments using RK13 cells were fixed and permeabilized using a two-step method of fixation and permeabilization. IFA experiments using HEK293T cells were fixed and permeabilized using a one-step method of fixation and permeabilization. Cells were then probed with primary antibodies for one hour, washed three times with blocking solution for five minutes each wash, then probed with the secondary antibody for one hour. Cells were then washed three times in blocking solution for five minutes each wash. Chambers were removed and ProLong™ Diamond Antifade Mountant with DAPI (4',6-diamidino-2-phenylindole) was applied to each well before slides were covered with a glass coverslip. Slides were allowed to cure in the dark for 24-48 hours prior to imaging.

2.2.6.4 IFA of Recombinant Myxoma Virus Infected Cells

Chamber slides were seeded with RK13 cells the day prior to infection. Cells were infected with vMyx-GFP-Subolesin or vMyx-GFP-Empty viruses at a MOI of 0.1, or mock infected, and incubated until 24 hours post infection. Cells were fixed and permeabilized using the two-step method, then blocked, probed, mounted, and imaged as described above.

2.2.6.5 IFA of ISE6 Cells

Chamber slides were seeded with ISE6 cells at 150,000 cells per well. Cells were incubated for 24 hours prior to fixation and permeabilization with the one-step 50/50 Acetone/Methanol method. Cells were then blocked, probed, mounted, and imaged as described above.

2.2.6.6 IFA of Antibody Internalization by ISE6 Cells

Chamber slides were seeded with ISE6 cells and incubated for 24 hours. For non-starved cells, the media was removed then replaced with media containing anti-Subolesin antibodies diluted in complete medium and incubated for 24 hours. For starved cells, the media was removed then replaced with L-15 medium and incubated for 24 hours. The L-15 medium was removed then replaced with media containing anti-Subolesin antibodies diluted in complete medium and incubated for 24 hours. After cells were incubated with the anti-Subolesin antibodies, the media was removed. The cells were fixed and permeabilized with the one-step method, then blocked, probed, mounted, and imaged as described above.

2.2.7 Enzyme-Linked Immunosorbent Assays (ELISA)

2.2.7.1 Anti-Subolesin ELISA

Purified *R. microplus* Subolesin protein was provided by Dr. Jose de la Fuente for the anti-Subolesin ELISA. The purified protein was diluted in BupH Carbonate-Bicarbonate Buffer (Pierce) to coat Nunc MaxiSorp high protein-binding capacity 96 well ELISA plates with 0.5µg per well overnight at 4°C with rocking. Unbound protein was removed by washing three times with 0.05% Tween-20 in DPBS (DPBST). Wells were then blocked with 5% non-fat milk in DPBST (blocking buffer) for one hour at room temperature with rocking. Mouse sera were diluted in blocking buffer, then inoculated onto the wells and incubated for one hour at room temperature with rocking. The primary antibody was removed, and wells were washed three times with DPBST. The secondary antibody, Goat-anti-mouse-IgG-HRP, was diluted in blocking buffer, then inoculated onto the wells and incubated for one hour at room temperature with rocking. The secondary antibody was removed, and wells were washed three times with DPBST. Wells were then washed three times with DPBS. Pierce 1-Step ABTS (2,2'-azinobis [3-ethylbenzthiazoline-6-sulfonic acid] diammonium salt) Solution was used as the HRP substrate, and the reaction was stopped using 1% sodium dodecyl sulphate (SDS) in water. Absorbance at 450nm was measured on a plate reader.

2.2.7.2 Gamma-Irradiated CCHFV Lysate ELISA

Gamma-irradiated CCHFV Ibar10200 Lysate (R430) was obtained from Dr. Tom Ksiazek (UTMB, Galveston, TX). The protein slurry was diluted in BupH Carbonate-Bicarbonate Buffer (Pierce) to coat Nunc MaxiSorp high protein-binding capacity 96 well ELISA plates

with 1 µg, 5 µg, or 10 µg per well overnight at 4°C with rocking. Unbound protein was removed by washing three times with DPBST, then wells were blocked with blocking buffer for one hour at room temperature with rocking. The R430 lysate was probed with one of three mAbs, His.H8 (nonspecific binding control), 9D5 (CCHFV NP-specific), and 11E7 (CCHFV G_C specific), or no primary (negative control), that were diluted in blocking buffer at 1:500, 1:1000, and 1:2000. The primary antibody was incubated for one hour at room temperature with rocking, then unbound antibody was removed with three washes with DBPST. The secondary antibody, Goat-anti-mouse-IgG-HRP (Abcam), was diluted in blocking buffer, then inoculated onto the wells and incubated for one hour at room temperature with rocking. The secondary antibody was washed away, and colorimetric signal was developed and measured as described above.

2.2.7.3 ELISAs at Thomas Jefferson University

RABV-G and GP38 proteins were generated from Gabrielle Scherr in the Schnell laboratory at TJU. Immulon 4 HBX 96 well flat bottom microtiter plates were coated in either protein diluted in carbonate coating buffer overnight at 4°C. Excess protein was washed away with DPBST, wells were blocked with blocking buffer, washed, then incubated with the primary antibody. Mouse sera were serially diluted 1:3 starting at a 1 in 50 dilution, for a total of eight dilutions. Plates were then washed and probed with an anti-mouse HRP conjugated secondary antibody, incubated, then washed. A colorimetric product was generated using o-Phenylenediamine dihydrochloride (OPD) peroxidase substrate solution, and the reaction was stopped with sulfuric acid. Absorbance at 490nm

and 630nm was measured on a plate reader, and the delta value was calculated from subtraction of the 630nm absorbance from the 430nm absorbance.

2.2.8 Protein Purification

Clarified protein lysates were purified under native conditions using HisPur™ Nickel-nitrilotriacetic acid (Ni-NTA) resin according to manufacturer's instructions for purification using the batch method. All centrifugation steps were carried out at 700 x g for two minutes. A sample of HisPur™ Ni-NTA resin was aliquoted into a tube, then centrifuged to pellet the resin. The resin storage buffer was removed and discarded. The resin pellet was resuspended in two resin bed volumes of equilibration buffer (10mM imidazole in DPBS) then pelleted by centrifugation. The sample of clarified protein lysate was mixed with an equal volume of equilibration buffer then added to the resin pellet. The resin pellet was resuspended in the sample and incubated for 30 minutes with constant rocking. The resin was pelleted by centrifugation, and the supernatant was removed and stored as the sample post-resin binding. The resin pellet was washed twice with wash buffer (25mM imidazole in DPBS). Supernatant after each wash step was saved. The protein was removed from the resin by resuspension of the resin bed in elution buffer (250 mM imidazole in DPBS) then pelleting the resin. This was repeated two additional times to generate three elution fractions.

2.2.9 Protein Gels and SYPRO Ruby Protein Gel Stain

Clarified protein lysates and samples from throughout the protein purification process were mixed 1:1 with 2X Laemmli Sample Buffer (BioRad) and boiled at 95°C for five minutes.

Proteins were separated using a NuPAGE 4-12% Bis-Tris gel (Invitrogen). The gel was fixed using a solution of 50% methanol and 7% acetic acid for one hour. The gel was then incubated in 60mL of SYPRO Ruby Protein Gel Stain (Thermo Fisher Scientific) overnight with gentle rocking. The gel was washed in a solution of 10% methanol and 7% acetic acid for 30 minutes, rinsed twice in ultrapure water, then imaged using the Bio-Rad Molecular Imager VersaDoc MP system.

2.2.10 Dot Blot

Five microliters of clarified protein lysates and samples from throughout the protein purification process were pipetted onto a nitrocellulose membrane and allowed to dry. The membrane was blocked using blocking buffer (5% nonfat milk in tris-buffered saline with 0.05% Tween-20 [TBST]) for 30 minutes at room temperature. The membrane was then incubated with the His.H8 mAb diluted at 1:2000 in blocking buffer for 30 minutes at room temperature with rocking. Unbound primary antibody was removed by three washes with TBST. The membrane was probed with Goat-anti-mouse-IgG-HRP for 30 minutes at room temperature with rocking, then washed three times with TBST. The membrane was submerged in a working solution of SuperSignal West Femto Maximum Sensitivity Substrate (Thermo Fisher Scientific) then imaged using the Bio-Rad Molecular Imager VersaDoc MP system.

2.2.11 Western Blots

Protein samples were prepared and separated using NuPAGE 4-12% Bis-Tris gels as above. Proteins were transferred onto a polyvinylidene difluoride membrane (PVDF;

Immobilon) using a semi-dry transfer method. Prior to transfer, the gel, membrane, and filter paper were soaked in transfer buffer for 10 minutes. The transfer sandwich was stacked on the bottom plate of a Trans-Blot® SD Semi-Dry Transfer Cell in the following order: extra thick filter paper, filter paper, membrane, gel, filter paper, then extra thick filter paper. A roller was used to ensure no bubbles were present between each layer. The top plate was placed on top of the transfer sandwich and proteins were transferred for one hour at 12 volts. After transfer, the membrane was removed and rinsed with water, then blocked in blocking buffer for one hour at room temperature with rocking. The membrane was probed with the primary antibody diluted in blocking buffer for one hour at room temperature, then washed three times with TBST. The membrane was then probed with goat-anti-mouse-IgG-HRP for one hour at room temperature with rocking, then washed three times with TBST. The membrane was submerged in a working solution of SuperSignal West Femto Maximum Sensitivity Substrate then imaged using the Bio-Rad Molecular Imager VersaDoc MP system.

2.2.12 Western Blot of Purified RABV Virions

The western blot confirming the presence of Subolesin-RABV-G within RABV virions was completed at TJU. Briefly, RABV virions were purified by pelleting through a 20% sucrose cushion using a SW28 rotor at 22,000 RPM for 1 hour at 4°C. Virus pellets were resuspended in TEN buffer (0.1M Tris-Cl, 0.01M EDTA, and 1M NaCl), lysed with RIPA buffer, then quantified using a bicinchoninic acid (BCA) assay. One microgram of each virion lysate was boiled for five minutes at 95°C in 2X urea sample buffer supplemented with 5% beta-mercaptoethanol, then proteins were separated using a 4-20% Mini-

PROTEAN® TGX gel (BioRad). Proteins were transferred onto a nitrocellulose membrane using a semi-dry transfer method, then the membrane was blocked using blocking buffer for one hour at room temperature. The membrane was then probed with the primary antibody overnight at 4°C, then washed three times with DPBST. The membrane was probed with donkey-anti-rabbit-IgG-HRP for one hour at room temperature, then washed five times with DPBST. The membrane was submerged in a working solution of SuperSignal Dura West Extended Duration Substrate then imaged using a FluorChem M imager.

2.2.13 MTT Cell Proliferation Assay

The effect of anti-Subolesin antibodies on the metabolism of ISE6 cells was assessed using the MTT Cell Proliferation Assay (ATCC). ISE6 cells were seeded into a 96-well plate in triplicate for each condition. Cells were incubated for 24 hours before the media was removed and replaced with L-15 without additives to starve the cells for 24 hours. The L-15 was then removed and replaced with anti-Subolesin antibodies diluted in complete medium, or complete medium without anti-Subolesin antibodies for mock cells. Cells were then incubated for 24 hours. Manufacturer's instructions were followed for the addition of the MTT reagent (3-(4, 5-dimethylthiazolyl-2)-2, 5-diphenyltetrazolium bromide), incubation, and cell lysis. The absorbance at 570nm was measured using a Tecan Infinite M200 Pro plate reader. As a measurement for cellular metabolism, the percent of cellular proliferation was normalized to mock cells that were not incubated with anti-Subolesin antibodies.

2.2.14 Preparation of Single-Cell Splenocyte Suspensions

Spleens were harvested from C57Bl/6 mice into serum-free Roswell Park Memorial Institute (RPMI) 1640 medium (Gibco). The spleens in medium were poured into a 70 μ m cell strainer (Falcon) placed into a sterile petri dish. The flat presser end of a sterile syringe was used to gently push the spleen through the cell strainer. The cell strainer was then rinsed using a sterile bulb pipet and medium from the petri dish. The single cell suspension in medium was transferred from the petri dish to a conical tube, where cells were pelleted. The media was decanted, and the cells were resuspended in 1mL of Red Blood Cell Lysing Buffer Hybri-Max (Sigma), then incubated for 10 minutes. The solution was diluted with DPBS then cells were pelleted, solution decanted, and splenocytes resuspended in DPBS for use in ELISpot analyses. Splenocyte concentration was determined from counting using a hemocytometer.

2.2.15 ELISpots

ELISpot analyses were completed using the Murine Interferon-gamma (IFN- γ) Single-Color Enzymatic ELISPOT kit (ImmunoSpot), following manufacturers recommendations. Concanavalin A (ConA) was used as a positive control for stimulation of splenocytes from naïve mice. Briefly, the antigen stimulant (ConA or R430) was diluted in CTL-Test Medium and plated at 100 μ l per well onto anti-IFN- γ antibody coated ELISpot plates. Single cell splenocyte suspensions were diluted to the desired concentration in CTL-Test Medium, then added to each well. The cell and antigen mixtures were incubated for 24 hours then removed. The captured IFN- γ was detected and spots

were developed using the provided antibody and substrate solutions. Spots were automatically counted using the ImmunoSpot Analyzer and software.

2.3 Animal Studies

Animal studies were approved by either the UTMB or TJU Institutional Animal Care and Use Committees (IACUC), depending on where the studies were undertaken. Animal research was carried out in compliance with the Animal Welfare Act and other federally regulated stipulations regarding animals and adherences to the Guide for the Care and Use of Laboratory Animals, National Research Council, 2013. The animal facilities where this research was conducted are accredited by the Association for Assessment and Accreditation of Laboratory Animal Care International (AAALAC International). All mice were anesthetized using inhalational isoflurane prior to any procedure.

2.3.1 Tolerability and Immunogenicity of Recombinant Myxoma Viruses

Female, six-week-old, BALBc/J mice (Stock #000651; The Jackson Laboratory, Bar Harbor, ME) were split into five groups with five mice per group: Saline, Adjuvant Only, Subolesin in Adjuvant, vMyx-GFP-Empty, or vMyx-GFP-Subolesin. Mice in the Saline group served as the negative control group. Mice in the Adjuvant Only or Subolesin in Adjuvant groups received water or 25 µg of purified *R. microplus* Subolesin protein in Montanide ISA 50 V2 adjuvant (Seppic, Paris, France), respectively. Mice in the vMyx-GFP-Empty or vMyx-GFP-Subolesin groups received a target of 1.0 million sucrose-purified virus particles. All inocula were given subcutaneously, and mice received a homologous boost 21 days after the primary dose. Mice were assessed daily for 14 days

after the primary dose for clinical scores and weights. Serum was collected from each mouse 20 days after the first and second doses, aliquoted, and stored frozen ($\leq -20^{\circ}\text{C}$) until use.

2.3.1.1 Preparation of Emulsions using Montanide ISA 50 V2 Adjuvant

The protein in water, or water only, was mixed with adjuvant in a 50/50 ratio (volume) then emulsified. The mixture was loaded into a syringe with a luer-lok tip, and the syringe was secured to a Hi-Flo™ 3-way stopcock with an additional syringe secured in the adjacent connector to form an “L” shape from both syringes. The mixture was passed from one syringe to the other and back to form one cycle of emulsion. The mixture was emulsified for 20 cycles at low speed and 80 cycles at high speed. The emulsified mixture was then ready for inoculation.

2.3.2 Immunogenicity of Recombinant Rabies Viruses

The immunogenicity of the recombinant rabies viruses was evaluated at TJU. Female, C57Bl/6 mice were split into five groups with five mice per group: Saline, RABV-Empty, RABV-Subolesin, RABV-GP85, and Mixture (50/50 mixture of RABV-Subolesin and RABV-GP85 constructs). Each mouse received 50 μL via intramuscular injection (IM) into each hind leg, totaling 100 μL . The target dose was 1.0 billion focus forming units (FFU) for each mouse, or 100 μL of saline for the negative control group. Serum was collected from each mouse at 28 days post infection, aliquoted, and stored frozen ($\leq -20^{\circ}\text{C}$) until use.

2.3.3 Tolerability and Immunogenicity of the DNA Vaccine Candidate

Female, six-week-old, C57BL/6J mice (Stock #000664; The Jackson Laboratory, Bar Harbor, ME) were split into two groups: Vaccinated (N=18) or Not Vaccinated (N=10). Mice were implanted with electronic ID transponders (Bio Medic Data Systems, Inc.) programmed with unique identifiers for each mouse. Vaccinated mice received three doses of the DNA plasmid pTWIST-CMV-EPIC at 21-day intervals. Each dose delivered 25 µg of plasmid in 20 µL of DPBS via intramuscular electroporation (IM-EP) into the anterior tibialis muscle using the Ichor Intramuscular TriGrid Delivery System (Ichor Medical Systems). The left hind leg was shaved using electric clippers followed by area disinfection using an alcohol preparation pad. The preloaded syringe was placed into the rodent TriGrid array prior to visualization of the anterior tibialis muscle. The skin around the muscle was pulled taut to anchor the muscle and the TriGrid electrodes were positioned over the muscle site with the long axis of the array parallel to the long axis of the muscle. The array was inserted into the muscle with the full length of the electrodes implanted into the tissue while avoiding contact with the tibia bone. The inoculum was injected into the muscle and the electroporation sequence was started approximately four seconds after the DNA injection. The array was removed from the tissue upon completion of the electroporation sequence and the vaccination site was visually inspected for any vaccine leakage before mice were returned to their housing. Five parameters were assessed daily for 63 days: body weight, temperature, clinical score, redness at the vaccination site, and vaccination limb paralysis. Serum was collected from each mouse at 20 days after the first and second doses, aliquoted, and stored frozen ($\leq -20^{\circ}\text{C}$) until use.

2.4 Statistics

T-tests, analysis of variance (ANOVA) tests, and nonlinear regression curve fitting were completed using GraphPad Prism software (version 8.0). Differential expression analyses for the RNA-seq experiment were completed using the DESeq2 package in R (version 4.2.0).

Table 2.1: GPC sequences used for evaluation of CCHFV homology.

Accession #	Country/Region	Strain	Clade
AB069670	China	7001	I-Africa 1
AB069673	China	79121	I-Africa 1
AY900143	Zaire	UG3010	II-Africa 2
DQ019222	Zaire	UG3010	II-Africa 2
DQ211637	Zaire	UG3010	II-Africa 2
DQ094832	Uganda	Semunya	II-Africa 2
DQ211625	Greece	AP92	VI-Europe 2
MG516212	Greece	Pentalofos-Greece-2015	VI-Europe 2
AY675511	Kosovo	Kosovo/9553/2001	V-Europe 1
EU037902	Kosovo	Kosovo Hoti	V-Europe 1
MH483985	RML Isolate	Hoti	V-Europe 1
DQ211630	Astrakhan	Drozdov	V-Europe 1
KY982866	Russia	Kalmykia 2016	V-Europe 1
DQ206448	Russia, Rostov	ROS/HUVLV-100	V-Europe 1
DQ211631	Stavropol	Kashmanov	V-Europe 1
KY362519	Turkey	Turkey 2004	V-Europe 1
MF511224	Turkey	Turkey 813048	V-Europe 1
DQ211636	Turkey	Turkey200310849	V-Europe 1
GQ337054	Turkey	Turkey-Kelkit06	V-Europe 1
GU477490	Bulgaria	V42/81	V-Europe 1
AB069669	China	66019	IV-Asia 2
KC344856	UK ex Afghanistan	SCT	IV-Asia 2
AB069674	China	8402	IV-Asia 2
AB069675	China	88166	IV-Asia 2
AF467769	Pakistan	Matin	IV-Asia 2
DQ211632	Oman	Oman	IV-Asia 2
KY362518	Oman	Oman_812956	IV-Asia 2
DQ211633	South Africa	SPU97/85	IV-Asia 2
DQ211635	South Africa	SPU415/85	IV-Asia 2
AY900142	South Africa	SPU41/84	III-Africa 3
DQ211634	South Africa	SPU103/87	III-Africa 3
DQ157175	South Africa	SPU4/81	III-Africa 3
HQ378184	Sudan	Al-Fulah 3	III-Africa 3
HQ378185	Sudan	Al-Fulah 9	III-Africa 3
HQ378187	Sudan	Ab1-2009	III-Africa 3
MH483988	RML Isolate	10200	III-Africa 3
MF547416	Spain	Caceres 2014	III-Africa 3
AB069671	China	75024	IV-Asia 1
AB069672	China	7803	IV-Asia 1
AJ538197	Iraq	Baghdad-12	IV-Asia 1
AY179962	Tajikistan	TAJ/HU8966	IV-Asia 1
AY223476	Uzbekistan	Hodzha	IV-Asia 1

JN572085	India	NIV/112143	IV-Asia 1
JN572086	India	NIV/11703	IV-Asia 1
MH461098	Iran	Iran 5900	IV-Asia 1
AJ538199	Pakistan	SR3	IV-Asia 1
HM452306	Germany ex Afghanistan	Afg09-2990	IV-Asia 1
KC867273	Iran	Zahedan 2007	IV-Asia 1
DQ446216	Iran	Iran-53	IV-Asia 1
MF289415	United Arab Emirates	813040 UAE	IV-Asia 1

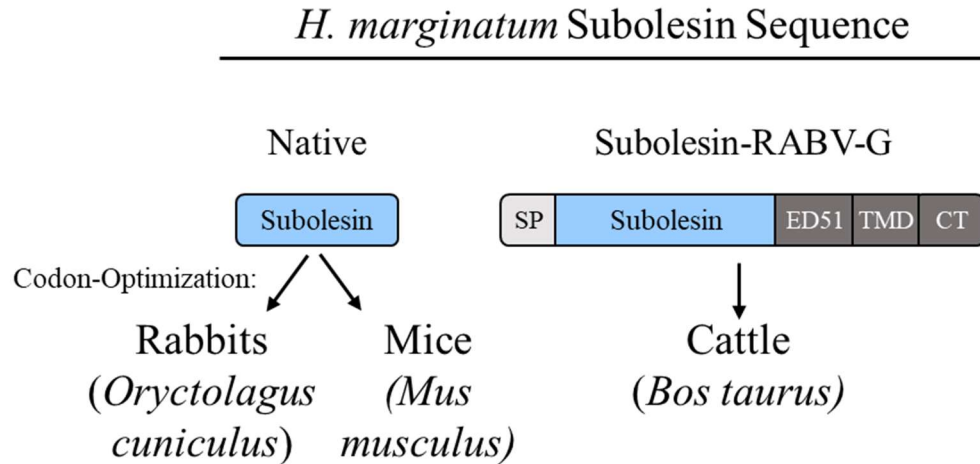
Table 2.2: Primers used for cloning, PCR, Sanger sequencing, and qRT-PCR.

Use	Primer Name	Orientation	Sequence
Cloning, PCR, and Sanger Sequencing	M135R-F	Forward	CGATAACCGAGGTATGTGTT
	M136R-R	Reverse	ACGTCAACGTGTTCTCTTTA
	Subolesin-F	Forward	ATGGCTTGCGCAACATTAAAGC
	Subolesin-R	Reverse	TTGGTCGTACGTAAACTTGAC
	GFP-EcoRI-F	Forward	GAGTCGAATTCACCATGGTGAGCAAGGG
	GFP-BglII-R	Reverse	GACATAGATCTCATCTTGTACAGCTCG
qRT-PCR	Actin-F	Forward	CTACCTGATGAAGATCCTCACCG
	Actin-R	Reverse	TCCAGGGAAGAAGAGGAGGC
	I.scap-SUB-F	Forward	TCCAAACGGAAGATCGCCC
	I.scap-SUB-R	Reverse	ATGTTGGCCGCTATCTCCTC
	OATP-74D-F	Forward	CTATCCCGAAGACCCGCATG
	OATP-74D-R	Reverse	TTGGGCCGTATCTTCTTGGG
	GLUT-1-F	Forward	TCCGAGCGTCTTCATGTTGG
	GLUT-1-R	Reverse	CGCATCTCGTCCATCTCGTC
	Slc26a6-F	Forward	CGTTGTATGCCTTCTTCGCG
	Slc26a6-R	Reverse	ATGAGCTCGATGGGAATGGG
	PLAAT3-F	Forward	CGAGTTCAACTTCCTCACCC
	PLAAT3-R	Reverse	CTCGTCAGGAAGGTGGTGTG
	Malic-F	Forward	ACTGCGTGACGGAAGGTAAC
	Malic-R	Reverse	TCTTGTCCTTTGGTTCGGGC

Figure 2.1: Subolesin codon-optimization and sequences.

(A) Schematic diagram of Subolesin codon-optimization. (B) Codon-optimized sequences of each Subolesin sequence.

A



B

Subolesin: *H. marginatum* Sequence, No Codon-Optimization

ATGGCCTTGCGCAACATTAAGCGAACACACGACTGGGATCCCCTGCACAGTC
CGAATGGCCGATCGCCAAAGAGACGGAGGTGTATGCCCTTGTCCCCACCAGC
ACCTCCAACCAGGGCTCACCAGATGAATCCATCGCCCTTCGGAGAAGTGCCG
CCCAAGATGACTTCAGAGGAGATAGCAGCCAACATTCGCGAGGAGATGCGA
CGGCTACAACGGCGCAAGCAGCTCTGTTTCCAGGGGACAGACCCAGAATCGC
AGCAGACGAGTGGCCTCTTGTTCGCTGTCCGTCGAGACCAGCCACTGTTTAC
CTTCGCCAGGTGGGCCTCATTTGCGAACGGATGATGAAGGAGCGAGAGAGC
CAGATACGGGAGGAGTATGACCATGTGCTTCTACCAAGCTTGCAGGACAGT
ACGACACATTTGTCAAGTTTACGTACGACCAA

Subolesin: Codon-Optimized for Rabbits

ATGGCCTTGCGCCACACTGAAGCGCACCCACGATTGGGATCCTCTGCACTCTC
CTAACGGACGCAGCCCTAAAAGACGCCGCTGCATGCCTCTGTCTCCACCAGC
TCCTCCAACAAGGGCCCACCAGATGAACCCATCTCCATTCGGCGAGGTGCCA
CCTAAGATGACCAGCGAAGAAATCGCCGCCAACATCCGCGAGGAAATGAGA
AGGCTGCAGCGCAGAAAGCAGCTGTGCTTCCAGGGCACCGATCCTGAGTCTC
AGCAGACCTCTGGACTGCTGTCTCCAGTGCGAAGAGATCAGCCCCTGTTTAC
CTTTCGCCAGGTTCGGACTGATCTGCGAGCGCATGATGAAGGAACGCGAGAGC
CAGATCCGCGAAGAGTACGATCACGTGCTGAGCACCAAACCTGGCCGGGCAGT
ACGACACCTTCGTGAAGTTCACCTACGACCAGTGA

Subolesin: Codon-Optimized for Mice

ATGCTTGCGCCACTTTGAAACGCACACATGACTGGGACCCCCTTCACTCCCCA
AATGGTTCGGAGCCCTAAAAGGCGAAGATGTATGCCACTCTCTCCACCTGCAC
CTCCCCTCGGGCTCACCAAATGAATCCCTCCCCATTCGGGGAAGTTCCACCT
AAGATGACTTCCGAAGAAATAGCTGCAAACATACGCGAAGAAATGCGCCGG
CTTCAAAGACGGAAGCAACTGTGTTTTTCAGGGCACTGACCCCGAGTCTCAGC
AGACCAGTGGTTTTGCTTAGTCCAGTTCGCAGGGATCAACCTTTGTTACCTTT
AGACAAGTTGGCCTGATATGTGAACGAATGATGAAAGAACGCGAGTCCCAA
ATCCGAGAAGAGTATGATCACGTACTGAGTACAAAGCTTGCTGGGCAGTATG
ATACTTTTGTCAAGTTTACCTATGATCAA

Subolesin-RABV-G: Codon-Optimized for Cattle

ATGGAGACGGACACACTTCTTCTTTGGGTGCTCCTGCTGTGGGTCCCTGGGTC
CACTGGAGATGCATGTGCCACCCTGAAAAGAACACATGACTGGGACCCCCTG
CACAGCCCAAATGGGCGCAGCCCCAAGCGGCGCCGGTGATGCCCTTTGTCCC
CACCTGCCCCGCCAACGCGAGCCCACCAGATGAACCCCTCTCCTTTTGGAGA
AGTGCCCCCAAATGACATCAGAAGAAATTGCTGCCAACATCCGAGAGGA
GATGAGGCGACTGCAGAGGAGAAAGCAGCTGTGTTTCCAGGGCACTGATCCA
GAATCCCAGCAGACCAGCGGTCTCCTAAGTCCGGTAAGGCGGGACCAGCCGC
TCTTACATTCCGGCAAGTGGGCCTCATCTGTGAGCGCATGATGAAGGAAAG
GGAGTCTCAAATACGTGAAGAGTACGATCACGTGCTGAGCACCAAGCTGGCA
GGCCAGTATGACACCTTTGTCAAGTTCACCTATGATCAAGAGAGCTCTGTTAT
CCCCTGGTGCATCCTTTGGCTGACCCATCAACTGTATTTAAAGATGGAGATG
AAGCAGAGGACTTTGTGGAGGTACATCTGCCTGATGTGCACAACCAGGTCAG
CGGCGTGGACCTGGGCCTACCCAAGTGGGGCAAGTACGTGCTTCTCAGTGCT
GGGGCGTTGACAGCCCTGATGCTGATCATTTTCTCATGACCTGCTGCAGGCG
CGTCAATAGATCAGAGCCCACCCAGCACAAATTTAAGAGGTACAGGCCGGGA
AGTTTTCAGTCACGCCCCAGTCTGGAAAATTATATCGTCCTGGGAGTCCCATA
AAAGTGGTGGGGAAACTCGTTTATGA

Chapter 3: A Poxvirus-Vectored Anti-Tick Vaccine for Hosts of Immature

Hyalomma marginatum

3.1 Abstract

Vector-host interactions in the CCHFV transmission cycle provide unique targets for developing veterinary anti-tick vaccines. To improve upon the conventional protein in adjuvant approach of licensed anti-tick vaccines, this chapter sought to utilize the highly conserved tick antigen, Subolesin, expressed via a viral vector. It was hypothesized that using myxoma virus (wtMYXV), which is only replication-competent in rabbits, would be an ideal vaccine vector to target small mammals of the Leporidae, Erinaceidae, and Muridae families, that are the preferred hosts of immature stages of *Hyalomma marginatum* ticks. Expression of *H. marginatum* Subolesin in RK13 cells was recognized by polyclonal serum generated using *Rhipicephalus microplus* Subolesin, lending further information to support the cross-reactivity of Subolesin between the *Rhipicephalus* and *Hyalomma* genera. The recombinant virus was evaluated as a non-replication-competent vaccine in mice, which are nonpermissive to wtMYXV. Subolesin-binding antibodies were below the detection limit in vaccinated mice, likely due to low levels of Subolesin expression from the recombinant virus. Ultimately, the results presented in this chapter suggest that the use of an attenuated strain of wtMYXV lacking host immunomodulatory genes, modification of Subolesin to change the subcellular localization, or the use of a vector that is replication-competent in multiple mammalian species may be better vaccine development strategies for a viral-vectored anti-tick vaccine.

3.2 Introduction

A recent WHO blue print analysis has emphasized the need to develop a livestock or wildlife vaccine to prevent the spread of CCHFV to humans, rather than focusing solely on human vaccine development^{221,222}. Each vector-host interaction point in the transmission cycle of CCHFV provides a target for vaccine development for the preferred hosts of each tick life stage. *H. marginatum* larva and nymphs prefer small mammalian hosts of the Leporidae, Erinaceidae, and Muridae families⁹⁸. It was hypothesized that the leporipoxvirus, myxoma virus (wtMYXV), would be an ideal vector for developing an anti-tick vaccine against the immature stages of *H. marginatum* since it is only replication-competent in rabbits, the most preferred host of immature *H. marginatum*⁹⁸.

Host-restricted poxviruses, such as wtMYXV, are viewed as attractive vaccine vectors because they can enter multiple mammalian cell types, including nonpermissive cells, and begin expressing early viral proteins before virion formation is restricted by host-cell factors¹⁶⁰. The promiscuous entry of host-restricted poxviruses to multiple cell types allows for the expression and presentation of foreign antigens to induce an immune response within target species, with reduced safety concerns compared to poxvirus vectors that can replicate in multiple species such as Vaccinia virus (VACV). As an attenuated replication-competent vector in rabbits or non-replication-competent vector in sheep and cats, wtMYXV has been used for vaccines against myxomatosis, rabbit hemorrhagic disease, bluetongue, and feline calicivirus^{165,167,168,223}. These proof-of-concept experiments in sheep and cats demonstrated that simple heterologous antigens expressed by wtMYXV are immunogenic in nonpermissive species.

The highly conserved tick protein, Subolesin, has greater than 84% residue homology among the five tick genera within the geographical range of CCHFV^{98,124} (*Hyalomma*, *Rhipicephalus*, *Dermacentor*, *Amblyomma*, and *Ixodes*^{2,98}) and has demonstrated great potential as an anti-tick antigen for each tick life stage when administered as an adjuvanted purified protein vaccine. However, this approach requires multiple doses to induce an immune response, which is not ideal for a veterinary vaccine, especially for wildlife. It was hypothesized that a viral-vectored Subolesin vaccine would yield a vaccine candidate superior to the protein in the adjuvant approach. Only one study has evaluated a viral vectored Subolesin vaccine, which showed that Subolesin could be expressed from a mouse-adapted, replication-competent strain of VACV. This vaccine candidate was immunogenic in mice, which provides a proof-of-concept for using Subolesin in a viral-vectored vaccine¹⁴⁶.

This chapter aims to utilize wtMYXV to develop a viral-vectored anti-tick vaccine for hosts of immature *H. marginatum* ticks and assess this vaccine candidate as a non-replication-competent virus in mice. The results presented in this chapter show the first work with *H. marginatum* Subolesin, the generation and characterization of the recombinant myxoma virus including Subolesin, and the tolerability and immunogenicity of this vaccine candidate in a nonpermissive mouse model.

3.3 Results

3.3.1 Antigen Selection, Synthesis, and Evaluation of *H. marginatum* Subolesin from a Mammalian Expression Plasmid

Previous work with Subolesin has primarily used the Subolesin sequence from *Rhipicephalus microplus* ticks (Accession # ABA62330). To generate an anti-tick vaccine specifically to target *H. marginatum* ticks, the sequence of Subolesin from *H. marginatum* submitted to GenBank by Dr. Jose de la Fuente's laboratory (University of Castilla-La Mancha, Ciudad Real, Spain) was used (Accession # DQ159970). Throughout this dissertation, discussion of Subolesin from *R. microplus* or *H. marginatum* refers to these sequences.

3.3.1.1 Codon Optimization and Antigen Synthesis

Subolesin from *H. marginatum* was codon-optimized, synthesized, and subcloned into two different plasmids to be used for rescue of the recombinant virus or transfection studies (**Supplementary Figure 3.1A**). The sequence of Subolesin from *H. marginatum* was submitted to the GeneArt system through Thermo Fisher Scientific for synthesis. The Subolesin sequence was codon-optimized by the GeneArt system for codon usage by the European rabbit, *Oryctolagus cuniculus*, which is used for the laboratory disease model of myxomatosis, and the origin species of the rabbit kidney epithelial cell line (RK13 cells), which are used for *in vitro* experiments throughout this dissertation. Two different versions of the gene were synthesized, either with or without a C-terminal six-residue polyhistidine epitope tag (6XHis). The version of Subolesin without the polyhistidine tag was subcloned into a basic plasmid for amplification in *E. coli* and to be used for cloning and rescue of

the recombinant virus (pMA-Subolesin) (**Supplementary Figures 3.1A and 3.1B**). The version of Subolesin including the C-terminal polyhistidine epitope tag was subcloned into a mammalian expression plasmid to be used for transfection studies (pcDNA3.1(+)-Subolesin-6XHis) (**Supplementary Figures 3.1A and 3.1C**). Codon-optimization of the Subolesin sequence modified 103 of 447 nucleotides for pMA-Subolesin and 94 of 447 nucleotides for pcDNA3.1(+)-Subolesin-6XHis (**Supplementary Figure 3.2**). Sanger sequencing of the inserts was completed by Invitrogen and reads confirming product insertion were provided with the plasmid shipment.

3.3.1.2 Antigen Expression and Detection with Anti-Subolesin Antibodies

Subolesin is found in both the cytoplasm and nucleus of tick cells¹²³. However, the expression and localization of Subolesin in mammalian cells had not been previously evaluated. Subcellular localization prediction of Subolesin in mammalian cells by the DeepLoc 1.0 server (<https://services.healthtech.dtu.dk/service.php?DeepLoc-1.0>) predicted that Subolesin would be localized to the nucleus with a 94.9% likelihood, with the residues important for localization corresponding to the two nuclear localization signals found in the N-terminus of the protein (**Supplementary Figure 3.3**)¹²³.

Subolesin-6XHis expression from the mammalian expression plasmid (pcDNA3.1(+)-Subolesin-6XHis) was assessed using an indirect immunofluorescence assay (IFA) in RK13 cells. At 24 hours post-transfection, cells were fixed, permeabilized, then probed with a mAb to the 6XHis tag (His.H8) or polyclonal rabbit serum from a rabbit immunized with prokaryotic-expressed *R. microplus* Subolesin purified protein in adjuvant, which was

kindly provided by Dr. Jose de la Fuente's laboratory. Since the 6XHis epitope tag is on the C-terminus of the protein, it was predicted that cells that are fluorescing when probed with His.H8 are expressing the full-length Subolesin-6XHis protein. The amino acid sequences of Subolesin from *R. microplus* and *H. marginatum* are 91.3% identical (**Supplementary Figure 3.4**), so it was hypothesized that expression of *H. marginatum* Subolesin would be recognized by the rabbit serum generated against *R. microplus* Subolesin. Fluorescent signal was detected from pcDNA3.1(+)-Subolesin-6XHis transfected RK13 cells that were probed with both His.H8 and the rabbit anti-Subolesin serum (**Figure 3.1**). This suggests that the full-length Subolesin-6XHis protein was being expressed in the RK13 cells and that the *H. marginatum* antigen was recognized by sera raised against *R. microplus* Subolesin. The signal from probing for Subolesin-6XHis in transfected cells seemed to overlap with the signal from the nuclei stained with 4',6-diamidino-2-phenylindole (DAPI), which was expected from the localization prediction (**Supplementary Figure 3.3**).

3.3.2 Generation and Characterization of Recombinant Myxoma Viruses

3.3.2.1 Generation of Recombinant Myxoma Viruses

The pMA-Subolesin plasmid, encoding Subolesin without the C-terminal polyhistidine tag, was shipped to Dr. Grant McFadden's laboratory at Arizona State University, Tempe, AZ, (ASU) to insert Subolesin into wtMYXV using gateway cloning and homologous recombination (**Supplementary Figure 3.1A**). Dr. McFadden's laboratory generated two recombinant myxoma viruses from the Lausanne strain of wtMYXV, identified using vMyx (**Figure 3.2** and **Supplementary Figure 3.5**). The first recombinant virus generated,

vMyx-GFP-Empty, encoded the emerald green fluorescent protein (EmGFP) behind a VACV synthetic early/late (sE/L) promoter. This gene was inserted into the intergenic region (ITR) between the M135R and M136R genes. The second recombinant virus, vMyx-GFP-Subolesin, encoded both EmGFP and Subolesin behind separate sE/L promoters within the M135R-M136R ITR. The two recombinant viruses were purified three times by fluorescent foci selection before stocks were prepared and shipped to UTMB for further characterization. Stocks of each virus were expanded, and the insertion sequence of vMyx-GFP-Subolesin was confirmed by Sanger sequencing at the UTMB Molecular Genomics Core Facility. No nucleotide differences between the virus sequence and the plasmid sequence used for rescue were observed. The genes were in the proper orientation with promoters and start and stop codons present (**Supplementary Figure 3.6**).

3.3.2.2 Foci Morphology and Multiplication Kinetics are not Impacted by the Insertion of Subolesin into wtMYXV

It was hypothesized that there would be no significant differences in viral replication of vMyx-GFP-Subolesin compared to vMyx-GFP-Empty in permissive RK13 cells. Therefore, RK13 cells were infected with vMyx-GFP-Empty or vMyx-GFP-Subolesin at a multiplicity of infection (MOI) of 0.1 in biological triplicates. Samples were collected every 12 hours until 96 hours post-infection, then titrated to quantify the fluorescent focus forming units per milliliter (FFU/mL). Wells of infected RK13 cells from titration were imaged using a Cytation 7 to compare foci morphology. Representative images of vMyx-GFP-Empty and vMyx-GFP-Subolesin foci in RK13 cells at 48 hours post-infection are shown in **Figure 3.3**. No differences in foci morphology were visualized from infection

with the two viruses, suggesting that insertion of Subolesin does not impact vMyx-GFP-Subolesin focus morphology. The vMyx-GFP-Empty and vMyx-GFP-Subolesin recombinant viruses did not display significant differences in multiplication through 24 hours post-infection (**Figure 3.4**). One difference in titer between the two viruses was seen at 36 hours post-infection (*, $p = 0.02$), but this was no longer statistically different at 48 hours post-infection or throughout the rest of the time points collected, suggesting that this difference was not biologically relevant. Both viruses displayed a peak infectivity titer at 72 hours post-infection, with decreasing titers at the following two timepoints. There was no difference in the peak infectivity titer between the two recombinant viruses. Together, these results suggested that the insertion of Subolesin into wtMYXV did not affect focus morphology or multiplication kinetics.

3.3.2.3 Antigen Expression and Detection with Anti-Subolesin Antibodies

Given that the vMyx-GFP-Subolesin foci displayed a bright green signal from the EmGFP reporter protein, it was hypothesized that Subolesin would be expressed from vMyx-GFP-Subolesin since EmGFP and Subolesin are both encoded behind the same type of promoter within the same ITR. To assess Subolesin expression from the recombinant virus, vMyx-GFP-Empty and vMyx-GFP-Subolesin viruses were infected at a MOI of 0.1 in RK13 cells until 24 hours post-infection. Cells were then fixed, permeabilized, and probed with rabbit serum to detect Subolesin, with the EmGFP reporter protein serving as a marker for vMyx infected cells. Fluorescent cells were seen in the vMyx-GFP-Empty and vMyx-GFP-Subolesin infected cells around EmGFP expressing cells. Since the vMyx-GFP-Empty infected cells served as a control for reactivity to wtMYXV proteins, the fluorescent signal

in the vMyx-GFP-Empty infected cells suggested that the serum was binding to wtMYXV proteins. As the synthesized *H. marginatum* Subolesin without the polyhistidine epitope tag was inserted into vMyx-GFP-Subolesin, no other reagents were available to assess the expression of Subolesin from vMyx-GFP-Subolesin. Given that the EmGFP reporter protein was expressed from the same type of promoter within the same intergenic region as Subolesin, it was hypothesized that Subolesin was also being expressed. However, this was not confirmed.

3.3.3 Tolerability and Immunogenicity of the Vaccine Candidate in a Mouse Model

This study used six-week-old female BALB/cJ mice to assess vaccine tolerability and immunogenicity, as this strain of mice responds to immunization with robust humoral responses²²⁴. Mice were separated into five groups of five mice each. Purified *R. microplus* Subolesin protein (25 µg/dose) emulsified in Montanide ISA 50 V2 adjuvant served as the positive control, water emulsified in adjuvant served as a vehicle control, saline served as a negative control, vMyx-GFP-Empty (0.9 million FFU/dose) served as a vector control, and vMyx-GFP-Subolesin (0.685 million FFU/dose) was the test article. Mice were immunized with 100 µL of test or control article subcutaneously then given a homologous boost 21 days post-prime.

wtMYXV is not replication-competent in mice. With the involvement of Subolesin in the tick innate immune response, there was a concern that vMyx-GFP-Subolesin may impact the host-restriction of wtMYXV. If the inclusion of Subolesin in vMyx-GFP-Subolesin altered the host restriction of the virus, clinical signs and significant weight changes would

be expected. Therefore, mice were monitored daily for clinical signs and changes in weight for two weeks post-prime immunization, which served as a surrogate for vaccine tolerability. During the observation period, at no point did any mice in this study exhibit any clinical signs or significant changes in weight. These results suggested that the vaccines were well-tolerated in BALB/cJ mice.

Serum was collected from each mouse at 21 days post-prime and 21 days post-boost immunization to analyze Subolesin-binding antibodies. Purified *R. microplus* Subolesin protein was used as a coat for an anti-Subolesin indirect ELISA, as serum cross-reactivity between *R. microplus* and *H. marginatum* antigens had already been demonstrated. Serum from each mouse was diluted at 1:20 then used to detect Subolesin binding IgG (**Figure 3.6**). No anti-Subolesin IgG was detected in any group, except for the positive control group, where there was a significant increase in signal after boost as tested by as tested by one-way ANOVA with Tukey's post-hoc correction for multiple comparisons (***, $p = 0.0001$). These results suggested that vMyx-GFP-Subolesin was not immunogenic in this animal model. Sera from the five mice in the positive control group were subsequently analyzed using the same anti-Subolesin ELISA to determine the concentration of antibody that gives half-maximal binding (EC_{50}), which was 1682 (reciprocal dilution).

To determine if mice in this study generated wtMYXV-neutralizing antibodies, a preliminary fluorescence reduction neutralization test (FRNT) against vMyx-GFP-Empty was conducted using serum from one mouse each from the vMyx-GFP-Empty, vMyx-GFP-Subolesin, and saline groups (**Figure 3.7**). Serum from the vMyx-GFP-Subolesin

vaccinated mouse exhibited a low level (~17%) of neutralization of vMyx-GFP-Empty, but this was not concentration-dependent, which suggests that this neutralization was nonspecific. No neutralization was detected using serum from either the vMyx-GFP-Empty or saline vaccinated mice. Sera from the remaining mice were not evaluated for neutralizing antibody responses. Together, these results suggest that the recombinant viruses did not induce wtMYXV-neutralizing antibodies after two doses in BALB/cJ mice.

3.3.4 Detection of *H. marginatum* Subolesin with Mouse Anti-Subolesin Antibodies

By including a group of mice immunized with purified Subolesin protein in adjuvant as the positive control in this study, mouse anti-Subolesin polyclonal serum was generated that would not cross-react with wtMYXV. This serum was generated from immunization with purified *R. microplus* Subolesin protein and was assessed using homologous purified *R. microplus* Subolesin protein as the ELISA coat. To confirm that these mouse anti-Subolesin antibodies would recognize *H. marginatum* Subolesin, the pcDNA3.1(+)-Subolesin-6XHis plasmid was transfected into RK13 cells, and the mouse serum was used as a primary antibody for IFA in addition to His.H8 (**Figure 3.8**). To control for nonspecific binding of the serum, a transfection control plasmid expressing green fluorescent protein (GFP; pCAGGS-GFP) was used. Probing the pcDNA3.1(+)-Subolesin-6XHis transfected cells with the mouse serum gave a fluorescent signal with a similar number of fluorescent cells as the His.H8 probed pcDNA3.1(+)-Subolesin-6XHis transfected cells. The mouse serum probed cells also had a similar fluorescent pattern to the His.H8 probed transfected cells. No staining was present in the mouse serum probed pCAGGS-GFP transfected wells.

Together these results suggested that the mouse serum recognized *H. marginatum* Subolesin without giving nonspecific signal in pCAGGS-GFP transfected RK13 cells.

Mouse serum recognition of *H. marginatum* Subolesin was confirmed using a western blot. Whole-cell lysates of untransfected human embryonic kidney (HEK293T) cells or pcDNA3.1(+)-Subolesin-6XHis transfected HEK293T cells were probed with either His.H8 or mouse serum (**Figure 3.9**). The molecular weight of Subolesin-6XHis was predicted to be 18kDa (Geneious Prime Software). One band of this expected size was seen in the pcDNA3.1(+)-Subolesin-6XHis transfected HEK293T cell lysate, but not the untransfected lysate when probed with both His.H8 and mouse serum. Together, these blots suggest that expression of *H. marginatum* Subolesin from pcDNA3.1(+)-Subolesin-6XHis is recognized by mouse serum generated from *R. microplus* Subolesin.

3.3.5 Evaluation of Subolesin Expression from vMyx-GFP-Subolesin using Mouse Anti-Subolesin Antibodies

The results from IFA and western blots suggested that the mouse anti-Subolesin polyclonal serum can detect expression of *H. marginatum* Subolesin from pcDNA3.1(+)-Subolesin-6XHis. This reagent was then used to assess the expression of Subolesin from vMyx-GFP-Subolesin (**Figure 3.10**). vMyx-GFP-Empty and vMyx-GFP-Subolesin viruses were infected at an MOI of 0.1 in RK13 cells, and pcDNA3.1(+)-Subolesin-6XHis transfected RK13 cells were used as a positive control. Cells were then probed with mouse serum to detect Subolesin. The EmGFP reporter protein served as a marker for vMyx infected cells. No anti-Subolesin fluorescent signal was detected from vMyx-GFP-Subolesin infected

cells. Since a fluorescent signal was detected from the pcDNA3.1(+)-Subolesin-6XHis transfected cells, but not the vMyx-GFP-Subolesin infected cells, these results suggested that the mouse serum recognized Subolesin in this experiment, but Subolesin was not being expressed from the vMyx-GFP-Subolesin construct.

3.4 Discussion

Developing an anti-tick vaccine for veterinary use provides a unique advantage for targeting the vector-host interactions in the CCHFV transmission cycle. The vaccine approach used in this chapter aimed to develop a live attenuated, viral-vectored, anti-tick vaccine for small mammals in the families of Leporidae, Erinaceidae, and Muridae, which are the preferred hosts of *H. marginatum* larva and nymphs⁹⁸. It was hypothesized that a single-dose viral-vectored anti-tick vaccine would yield superior immunogenicity to the current protein in adjuvant approach, which requires multiple doses and is not ideal for wildlife vaccination. In addition, this chapter provides further information on serological cross-reactivity between *R. microplus* and *H. marginatum* Subolesin, and suggests that the recombinant virus vMyx-GFP-Subolesin is not an immunogenic vaccine candidate, at least in Balb/c mice.

The highly conserved tick protein, Subolesin, was chosen as an anti-tick antigen for its ability to negatively impact tick infestation, female weight, fertility, and oviposition when it is used to immunize hosts of different tick life stages¹²³. No prior work had evaluated the expression of Subolesin within mammalian cells. RK13 cells were used for transfection studies to show that rabbit codon-optimized Subolesin could be expressed in mammalian

cells. However, these cells have previously been shown to have low transfection efficiency (approximately 20%)^{225,226}. Overall, few pcDNA3.1(+)-Subolesin-6XHis transfected cells gave a positive fluorescent signal when probed with either His.H8 or rabbit serum, which is thought likely due to the low transfection efficiency of RK13 cells^{225,226}. The staining pattern of the fluorescent cells differed when probing with His.H8 or rabbit serum; it is thought that this is likely due to using a mouse mAb, which recognizes a single epitope, compared to rabbit polyclonal serum, rather than a difference in protein recognition. Previous work has shown that immunization of animals with purified Subolesin protein from *H. anatolicum* ticks protects against *R. microplus* tick infestation, indicating serologic cross-reactivity between the *Rhipicephalus* and *Hyalomma* genera¹²⁴. Recognition of the *H. marginatum* Subolesin protein with the rabbit serum generated against *R. microplus* Subolesin suggested that the processing of the mammalian expressed protein is suitable for antibody recognition from animals vaccinated with prokaryotic expressed protein (**Figure 3.1**). Further, this lends additional support to the cross-reactivity of Subolesin antibodies between the *Rhipicephalus* and *Hyalomma* genera and highlights the utility of using Subolesin to generate an anti-tick vaccine for multiple genera of ticks that overlap in the geographic distribution of CCHFV.

Subolesin is thought to act as a transcription factor in tick cells and, upon phosphorylation, translocates to the nucleus from the cytoplasm to impact gene expression and play a role in the tick innate immune response¹²³. Subolesin has approximate 48% residue homology to its mammalian ortholog, Akirin2, which is involved in nuclear factor- κ B (NF- κ B) signal transduction¹²³. As Subolesin expression had previously not been evaluated in mammalian

cells, it was unknown whether or not Subolesin would localize to the nucleus or exert a similar function to its mammalian ortholog. The presence of the two nuclear localization signals in Subolesin¹²³ suggested that Subolesin would localize to the nucleus of mammalian cells (**Supplementary Figure 3.3**). Expression of *H. marginatum* Subolesin from pcDNA3.1(+)-Subolesin-6XHis appeared to have a fluorescent signal that overlapped with the nuclear DAPI stain, suggesting that Subolesin localizes to the nucleus of transfected mammalian cells (**Figure 3.1**). In contrast to endogenous expression of Subolesin in tick cells where it is detected in both the cytoplasm and nucleus¹²³, Subolesin was only detected in the nucleus of transfected RK13 cells in these studies. As transfection of dsDNA is known to trigger innate immune responses²²⁷, the localization of Subolesin in the nucleus of transfected mammalian cells may suggest that Subolesin interacts with the Akirin2/NF- κ B signal transduction pathway in mammalian cells but this remains to be demonstrated.

Two recombinant myxoma viruses, vMyx-GFP-Empty and vMyx-GFP-Subolesin, were generated by Dr. Grant McFadden's laboratory at ASU using the Lausanne strain of wtMYXV (**Figure 3.2**). The wtMYXV Lausanne strain was chosen as the vMyx backbone since removing virulence factors to attenuate wtMYXV is known to impact virus replication and gene expression¹⁶⁰. Since Subolesin was localizing to the nucleus in transfection studies, allowing for potential interactions with the Akirin2/NF- κ B signal transduction pathway, it was unknown if Subolesin would alter vMyx-GFP-Subolesin replication, as host-cell factors involved in signal transduction such as interferon, extracellular regulated kinases (ERK), and NF- κ B, play a role in cell tropism and regulation

of poxvirus replication^{158,160,228}. However, since insertion of Subolesin within VACV did not impact the replication of VACV in a previous study¹⁴⁶, it was hypothesized that there would be no differences in focus morphology or multiplication kinetics between vMyx-GFP-Empty and vMyxGFP-Subolesin in cells permissive to wtMYXV infection. The impact of insertion of Subolesin within wtMYXV was evaluated by assessing differences in focus morphology and multiplication kinetics between vMyx-GFP-Empty and vMyx-GFP-Subolesin in RK13 cells, which are permissive to wtMYXV. As expected, there were no differences in focus morphology (**Figure 3.3**) or multiplication kinetics (**Figure 3.4**) between vMyx-GFP-Subolesin and vMyx-GFP-Empty. These results suggested that the inclusion of Subolesin within vMyx-GFP-Subolesin did not affect the replication of the virus in a permissive cell type.

The first attempt to evaluate Subolesin expression from the recombinant virus used rabbit serum as the primary antibody for an IFA (**Figure 3.5**). Fluorescent signal was seen from cells expressing the EmGFP reporter protein in both vMyx-GFP-Empty and vMyx-GFP-Subolesin infected RK13 cells. This suggested that the rabbit serum was cross-reacting with wtMYXV proteins. It was later determined that the rabbits used to generate the reagent had also been vaccinated against wtMYXV. Due to the cross-reactivity of the serum, this reagent could not be used to evaluate the expression of Subolesin from vMyx-GFP-Subolesin. The Subolesin antigen encoded within vMyx-GFP-Subolesin did not include the C-terminal polyhistidine epitope tag, so the His.H8 mAb could not be used to assess protein expression. Therefore, it was hypothesized that Subolesin was being expressed

from the recombinant virus, and evaluation of the recombinant virus continued with *in vivo* studies without confirmation of Subolesin expression.

Leporidae, which are permissive to wtMYXV, are the most preferred host of immature *H. marginatum*⁹⁸. Since the recombinant viruses used in these studies were generated using wtMYXV as the backbone, rabbits could not be used to evaluate the vMyx-GFP-Subolesin vaccine candidate because wtMYXV is nearly 100% lethal in rabbits¹⁵⁵. Therefore, this vaccine candidate was evaluated as a non-replicating vector in mice, which are nonpermissive to wtMYXV infection. Previous studies using wild-type or attenuated MYXV-vectored vaccines in nonpermissive species used doses of at least 1 million virus particles, ranging up to 600 million particles^{146,165,168,223,229}. The production of wtMYXV stocks for use *in vitro* involves lysing infected cells to release virus particles through repeated freezing and thawing, then removal of cellular debris through centrifugation. However, this is not adequate for the production of stocks to be used *in vivo* where the virus-containing supernatant post centrifugation must be semi-purified by pelleting the virus particles through a 36% sucrose cushion¹⁶². This additional purification step made generating high-titer stocks difficult, which resulted in low inocula (0.6-0.9 million FFU) used for this mouse study. After immunization, no mice exhibited any clinical signs or significant changes in weight for two weeks post-prime immunization, which suggested that the five different inocula used in this study were well-tolerated by the mice. With the involvement of Subolesin in the tick innate immune response, there was a concern that vMyx-GFP-Subolesin may impact the strict host-restriction of wtMYXV. The lack of either clinical signs or weight loss suggested that the inclusion of Subolesin within the

recombinant virus did not impact host-restriction at the dose of virus used to immunize the mice.

The generation of Subolesin-binding antibodies in vaccinated mice was evaluated using an anti-Subolesin ELISA (**Figure 3.6A**). Subolesin-binding antibodies were only generated in mice that served as the positive control for this study, which received purified *R. microplus* Subolesin protein in adjuvant. A significant increase in binding antibodies was generated in this group after the second dose. It was surprising that there were no Subolesin binding antibodies detected from the vMyx-GFP-Subolesin vaccinated group, given the high anti-Subolesin titers of mice vaccinated with the recombinant VACV expressing Subolesin in a previous study¹⁴⁶. By including a group of mice immunized with purified Subolesin protein in adjuvant as the positive control in this study, the possibility of mice not being able to mount an immune response to Subolesin can be excluded. Further, it was unlikely that using *R. microplus* purified Subolesin protein as the ELISA coat limited binding antibody detection due to the known cross-reactivity of Subolesin between the *Rhipicephalus* and *Hyalomma* genera. It was expected that no anti-Subolesin antibodies would be generated in the mice that received either saline, adjuvant only, or vMyx-GFP-Empty, since these groups served as negative, vehicle, and vector controls, respectively, and the inocula did not contain Subolesin. These results suggested that the lack of Subolesin immunogenicity may be related to using wtMYXV as the viral vector.

Previous work has exclusively used attenuated strains of wtMYXV when assessing MYXV-vectored vaccines or MYXV as an oncolytic therapy in species nonpermissive to

wtMYXV^{165,167,168,223,229,230}, rather than using wtMYXV like the studies in this chapter. These previous studies detected wtMYXV-neutralizing antibodies in sheep, mice, and dogs post-vaccination^{165,223,229,230}. To determine if mice in this study developed wtMYXV-neutralizing antibody responses, serum from one mouse from each group that received saline, vMyx-GFP-Empty, and vMyx-GFP-Subolesin was chosen for evaluation using a FRNT. Incubation of vMyx-GFP-Empty with mouse serum did not result in any detectable neutralization by serum from the vMyx-GFP-Empty or saline vaccinated mice and serum from the vMyx-GFP-Subolesin group did not demonstrate a concentration-dependent reduction in fluorescence, which suggested that the limited neutralization activity from this group was nonspecific. This experiment only used serum from one mouse from each group, so it is unknown if the remaining mice developed wtMYXV-neutralizing antibodies. Moreover, a wtMYXV-neutralizing antibody control was not available for use in this assay, so it is unknown if the neutralization of wtMYXV is detectable with the FRNT method rather than the conventional plaque reduction neutralization test (PRNT) used in previous studies. These results suggest that a combination of using wtMYXV as the vaccine vector and the low-titer dose of recombinant virus resulted in a lack of immunogenicity in this study.

The lack of development of Subolesin-binding antibodies in vMyx-GFP-Subolesin vaccinated mice was unexpected. This result could be due to either the low quantity of virus used in the inoculum or lack of Subolesin expression from the recombinant virus. The anti-Subolesin EC₅₀ of the serum from protein in adjuvant vaccinated mice was determined to be a reciprocal dilution of 1682 (**Figure 3.6B**). This titer suggested that this serum could

act as a tool to evaluate Subolesin expression without cross-reactivity to wtMYXV proteins like the rabbit serum. While this mouse serum was generated from immunization with *R. microplus* Subolesin protein, this serum was shown to recognize *H. marginatum* Subolesin by both IFA (**Figure 3.8**) and western blot (**Figure 3.9**). When vMyx-GFP-Subolesin infected RK13 cells were probed with the mouse serum generated by Subolesin protein in adjuvant immunization, no fluorescent signal was detected (**Figure 3.10**), suggesting that Subolesin was not being expressed by the recombinant virus, rather than poor immunogenicity. The lack of Subolesin expression from the recombinant virus explains the lack of Subolesin immunogenicity in the vaccinated mice. Immunogenicity of this vaccine candidate could not be evaluated in rabbits, which are permissive to wtMYXV infection, since the wtMYXV backbone used for vMyx-GFP-Subolesin is nearly 100% lethal in rabbits¹⁵⁵. However, it is considered unlikely that using rabbits would have yielded different immunogenicity results since expression of the Subolesin protein from vMyx-GFP-Subolesin was not detected in rabbit cells, but this was not investigated experimentally. The lack of Subolesin expression from vMyx-GFP-Subolesin was surprising since Subolesin was codon-optimized for rabbits to avoid differences of codon usage between rabbits and ticks inhibiting Subolesin translation. Sequencing of the virus stock confirmed that Subolesin was indeed inserted in the construct behind a sE/L promoter in the proper orientation with start and stop codons in the correct open reading frame (**Supplementary Figure 3.6**). Also, the EmGFP reporter protein was expressed from the same ITR behind the same type of promoter. Together, this suggested that the lack of Subolesin expression from vMyx-GFP-Subolesin was due to the Subolesin protein itself.

As previously discussed, the nuclear localization of Subolesin in pcDNA3.1(+)-Subolesin-6XHis transfected RK13 cells may suggest interaction of Subolesin with the Akirin2/NF- κ B signal transduction pathway in mammalian cells. Previous research has shown that some poxviruses can interfere with the NF- κ B signaling pathway through protein similarity to NF- κ B binding inhibitory proteins (I κ Bs) or play a role in modulating the host ubiquitin-proteasome system to degrade host proteins due to the protein function redundancy of poxviruses to evade host innate immune responses and prevent apoptosis¹⁵⁸. In wtMYXV, there are two proteins known to inhibit NF- κ B function (M150R and M13L), although the function of all wtMYXV proteins is not known^{155,158}. It is hypothesized that the immunomodulatory proteins in the wtMYXV backbone used for vMyx-GFP-Subolesin may have interfered with the expression of Subolesin as part of the wtMYXV host innate immune evasion strategies. One limitation of these studies is that vMyx-GFP-Subolesin infected RK13 cells were not analyzed at different time points post-infection for the presence of both Subolesin mRNA and protein. The current studies only examined the presence of protein at 24 hours post-infection. It is interesting to consider the possibility that some of the early immunomodulatory genes of wtMYXV could have inhibited translation of Subolesin or that Subolesin would be tagged for proteasomal degradation quickly after translation due to its similarity to Akirin2 and its role in the NF- κ B pathway. It is possible that protein similarity between Subolesin and Akirin2 and modulation of the host innate immune response by wtMYXV may have prevented the detection of Subolesin expression by IFA at 24 hours post-infection. It would be interesting to assess the use of an attenuated strain of MYXV lacking one, or both, of the known NF- κ B inhibitory proteins to see if Subolesin would be expressed from a different vMyx. It is important to

note that the previous study demonstrating expression of Subolesin from VACV and immunogenicity of the vaccine candidate in mice may be explained by VACV lacking strict host-restriction and being permissive in numerous species, in contrast to wtMYXV¹⁶⁰.

Overall, the most likely explanation for the lack of vMyx-GFP-Subolesin immunogenicity in vaccinated mice is the lack of detection of the Subolesin protein expression from the viral vector. It is possible that Subolesin expression was not detected from the recombinant virus due to the use of wtMYXV as the viral vector, as no immunomodulatory genes were removed from the genome. It is hypothesized that the nuclear localization of Subolesin in pcDNA3.1(+)-Subolesin-6XHis transfected RK13 cells suggests that Subolesin may interact with the Akirin2/NF- κ B pathway in mammalian cells. Thus, the immunomodulatory proteins known to downregulate NF- κ B in permissive cells may prevent the expression of Subolesin from the wtMYXV vector. Evaluation of Subolesin in an attenuated strain of wtMYXV lacking the NF- κ B-interacting proteins should not be ruled out for future vaccine development strategies.

In conclusion, the use of wtMYXV as a viral vector of Subolesin did not result in an immunogenic vaccine candidate. Modifying the Subolesin antigen to either change the subcellular localization to the cytoplasm for exposure to the host immune system or using a vaccine vector that is replication-competent in multiple mammalian species may be a better vaccine development strategy for the development of an anti-tick vaccine.

Table 3.1: Summary of IFA results.

RK13 cells were transfected with pcDNA3.1(+)-Subolesin-6XHis or pCAGGS-GFP or infected with vMyx-GFP-Subolesin or vMyx-GFP-Empty, then probed with His.H8, rabbit serum, or mouse serum.

Transfected Plasmid or Virus Infected	Fluorescent Protein	Subolesin	Fluorescent Cells When Probed With:		
			His.H8	Rabbit Serum	Mouse Serum
pcDNA3.1(+)-Subolesin-6XHis	N/A	Yes	Yes	Yes	Yes
pCAGGS-GFP	GFP	No	No	N/A	No
vMyx-GFP-Subolesin	EmGFP	Yes	N/A	Yes	No
vMyx-GFP-Empty	EmGFP	No	N/A	Yes	No

Figure 3.1: Subolesin expression and detection in mammalian cells using antibodies to the C-terminal polyhistidine tag and rabbit anti-Subolesin serum.

RK13 cells were fixed and stained 24 hours after transfection with pcDNA3.1(+)-Subolesin-6XHis. Cells were then probed with His.H8 or rabbit serum produced from vaccination with bacterially expressed *Rhipicephalus microplus* Subolesin. Subolesin was recognized by both antibodies, suggesting the full-length protein was being expressed, and *Hyalomma marginatum* Subolesin can be recognized by serum generated by Subolesin from a different tick species.

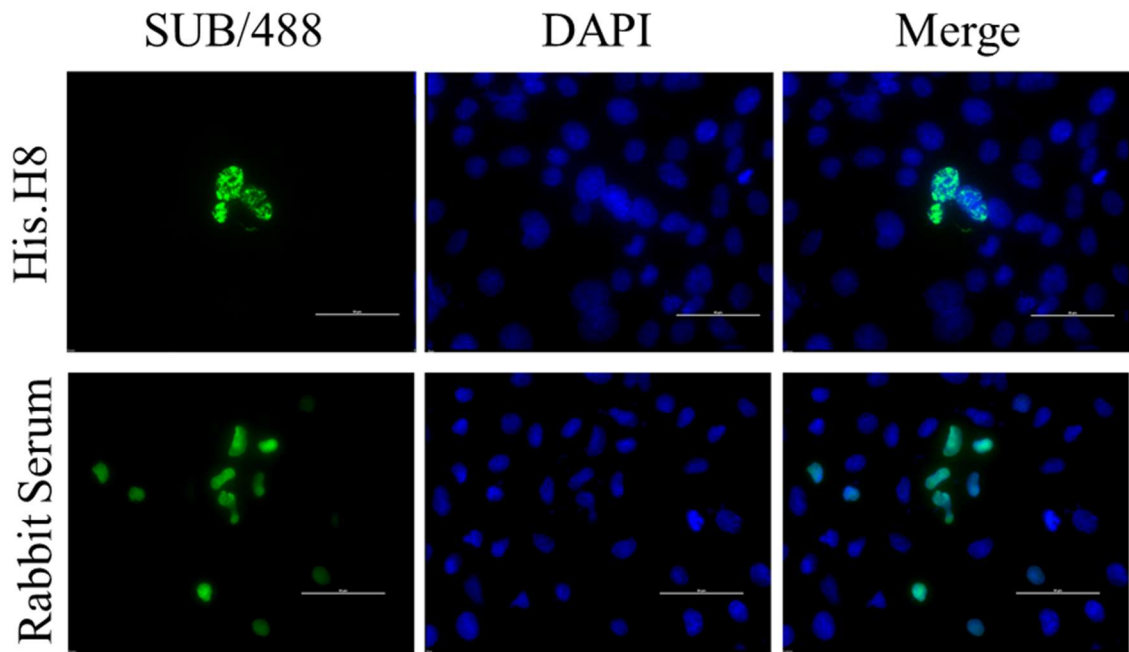


Figure 3.2: Schematic diagrams of wild-type and recombinant myxoma viruses.

Schematic diagrams of the M135R – Intergenic Region (ITR) – M136R region of the wild-type virus (wtMYXV) and recombinant viruses, with GFP only (vMyx-GFP-Empty), and both Subolesin and GFP (vMyx-GFP-Subolesin), with individual Vaccinia virus synthetic early/late promoters (sE/L).

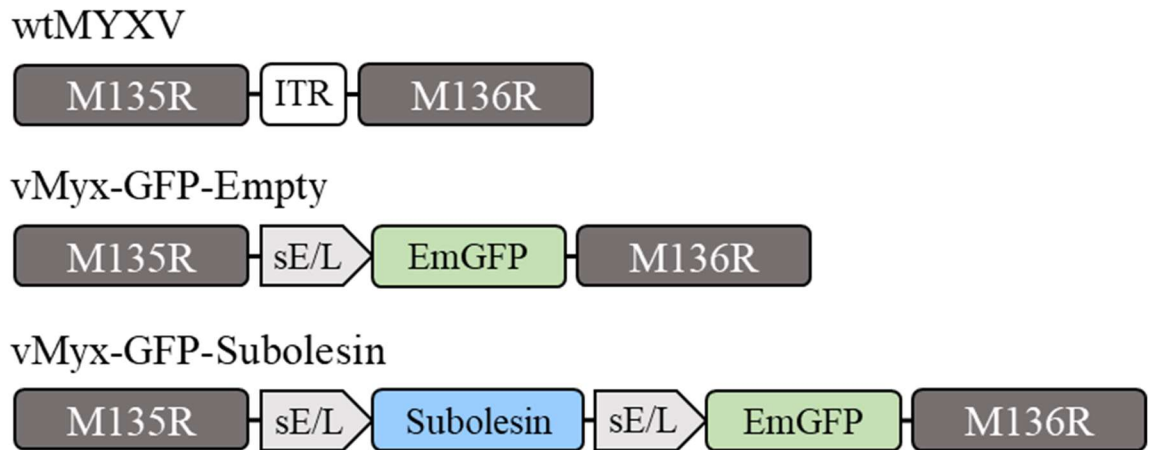
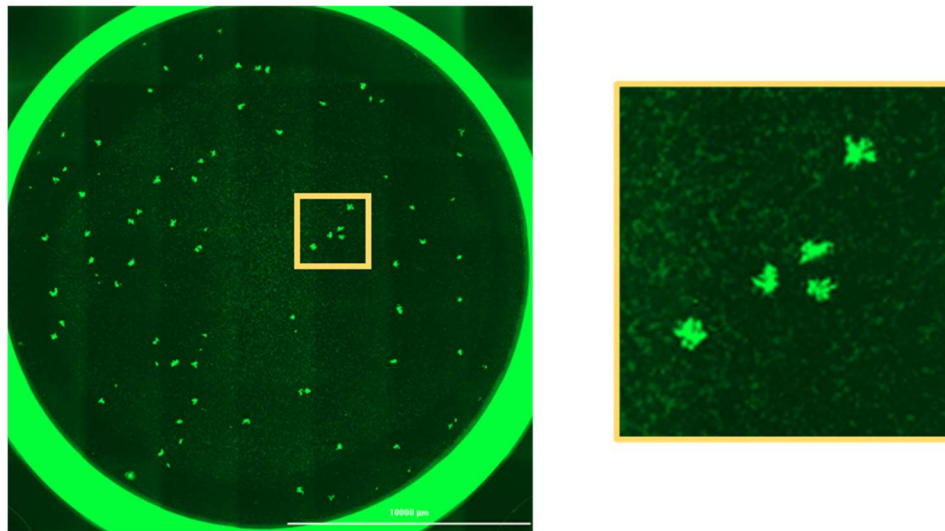


Figure 3.3: There are no differences in focus morphology between vMyx-GFP-Empty and vMyx-GFP-Subolesin.

Representative images of vMyx-GFP-Empty and vMyx-GFP-Subolesin foci in RK13 cells at 48 hours post-infection. Images on the left are of a whole well of a 12-well plate, and the box in yellow is magnified in the right image.

vMYX-GFP-Empty



vMYX-GFP-Subolesin

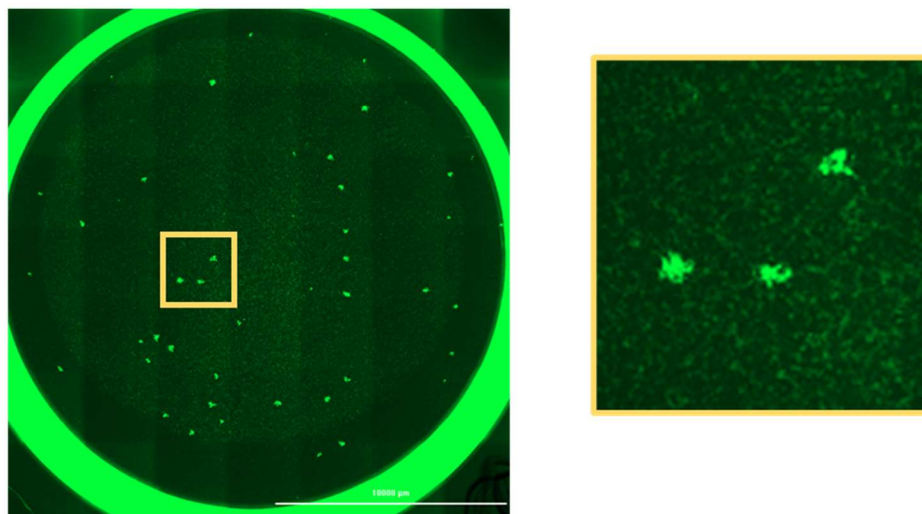


Figure 3.4: Insertion of Subolesin into wtMYXV does not impact virus multiplication kinetics.

vMyx-GFP-Empty and vMyx-GFP-Subolesin viruses were infected at a MOI of 0.1 in RK13 cells. Points and error bars represent the mean and standard deviation of the focus forming units per milliliter (FFU/mL) from biological triplicates. Only one significant difference in the mean was seen ($p=0.02$) between the two viruses at 36 hours post-infection from multiple t-tests, which were corrected for multiple comparisons using the Bonferroni-Dunn method. Although this difference was statistically significant, it does not appear to be biologically significant.

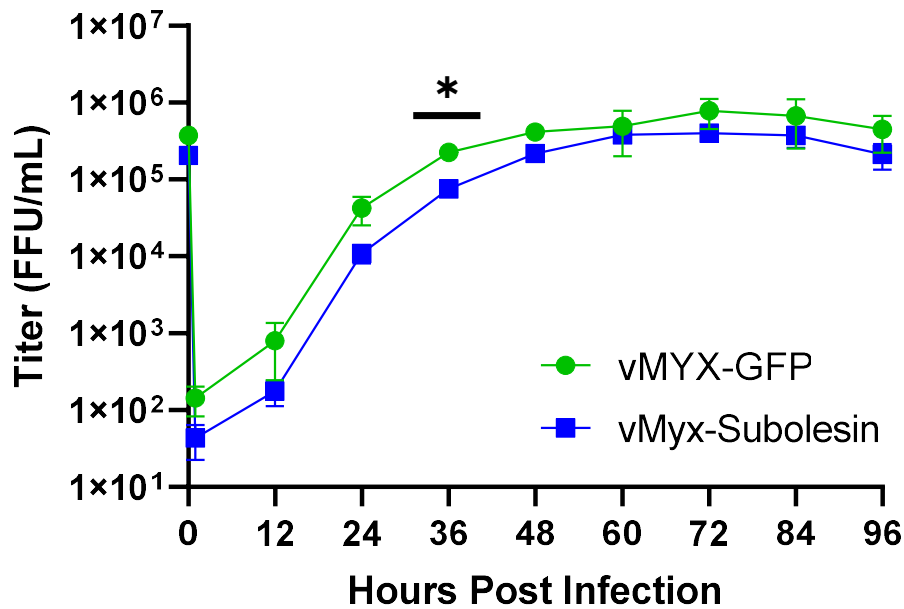


Figure 3.5: Rabbit anti-Subolesin serum cross-reacts with wtMYXV proteins.

vMyx-GFP-Empty (top) and vMyx-GFP-Subolesin (bottom) viruses were infected at a MOI of 0.1 in RK13 cells until 24 hours post-infection. Wells were stained with anti-Subolesin rabbit serum. Staining in the vMyx-GFP-Empty wells around the GFP expressing cells suggested that the rabbit serum was reacting to wtMYXV proteins and expression of Subolesin from vMyx-GFP-Subolesin could not be assessed using this reagent.

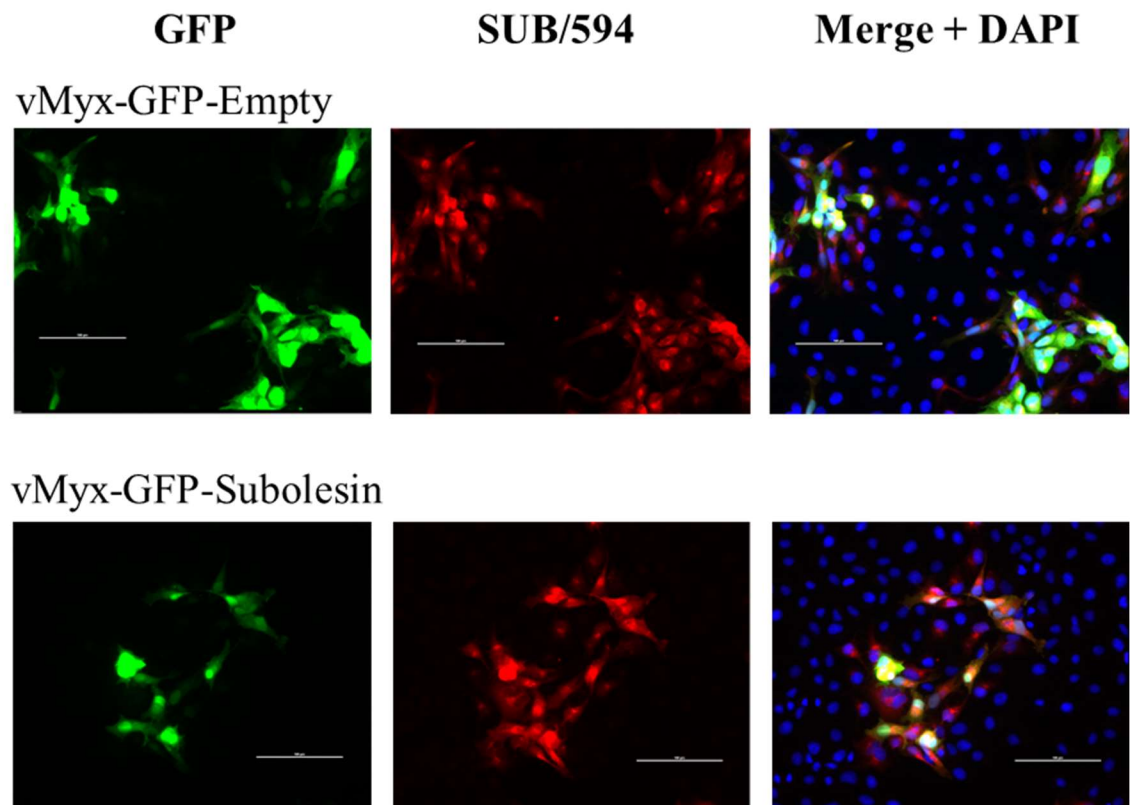
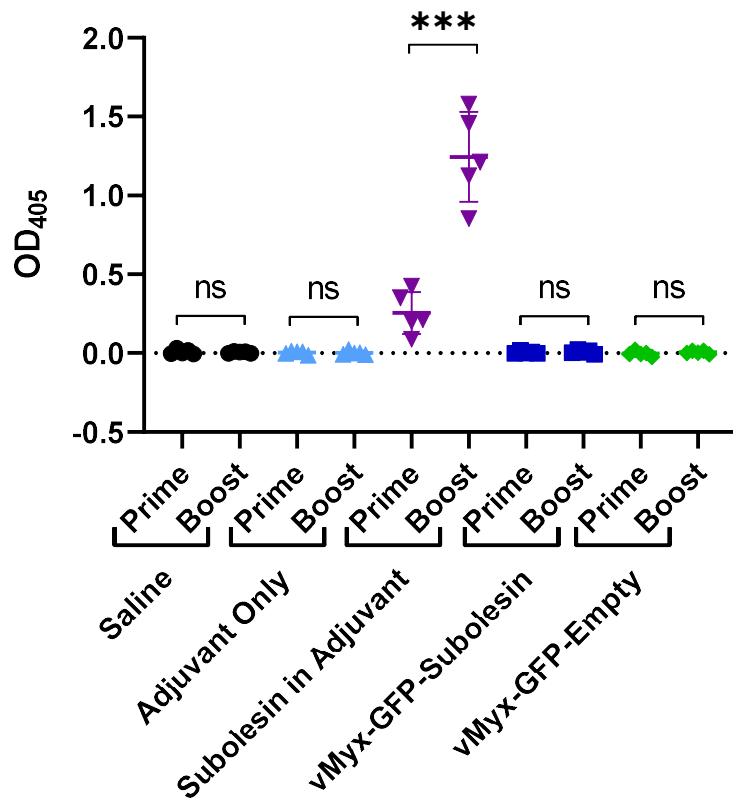


Figure 3.6: Vaccination with vMyx-GFP-Subolesin does not elicit anti-Subolesin binding antibodies.

Bacterially expressed purified *R. microplus* Subolesin protein was used as a protein coat for an anti-Subolesin ELISA. (A) Serum collected from BALB/cJ mice immunized with purified *R. microplus* Subolesin in adjuvant, adjuvant only, vMyx-GFP-Subolesin, vMyx-GFP-Empty, or saline was diluted at 1:20 for use in the anti-Subolesin ELISA. There was a significant increase in signal after boost in the Subolesin in adjuvant group as tested by one-way ANOVA with Tukey's post-hoc correction for multiple comparisons. (B) Determination of the EC50 of serum from Subolesin in adjuvant vaccinated mice. The EC50 was calculated using a curve fit to a nonlinear regression with a variable slope in GraphPad PRISM.

A



B

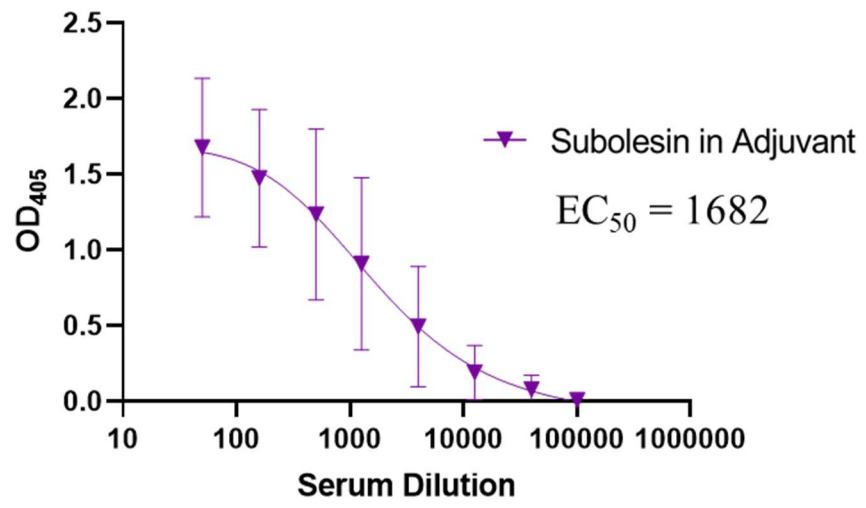


Figure 3.7: wtMYXV-neutralizing antibodies were not detected in serum from vMyx-GFP-Empty or vMyx-GFP-Subolesin vaccinated mice.

A preliminary fluorescence reduction neutralization test (FRNT) against vMyx-GFP-Empty was conducted using serum from one mouse from the vMyx-GFP-Empty, vMyx-GFP-Subolesin, and saline groups. Serum from the remaining mice was not evaluated for neutralizing antibody responses.

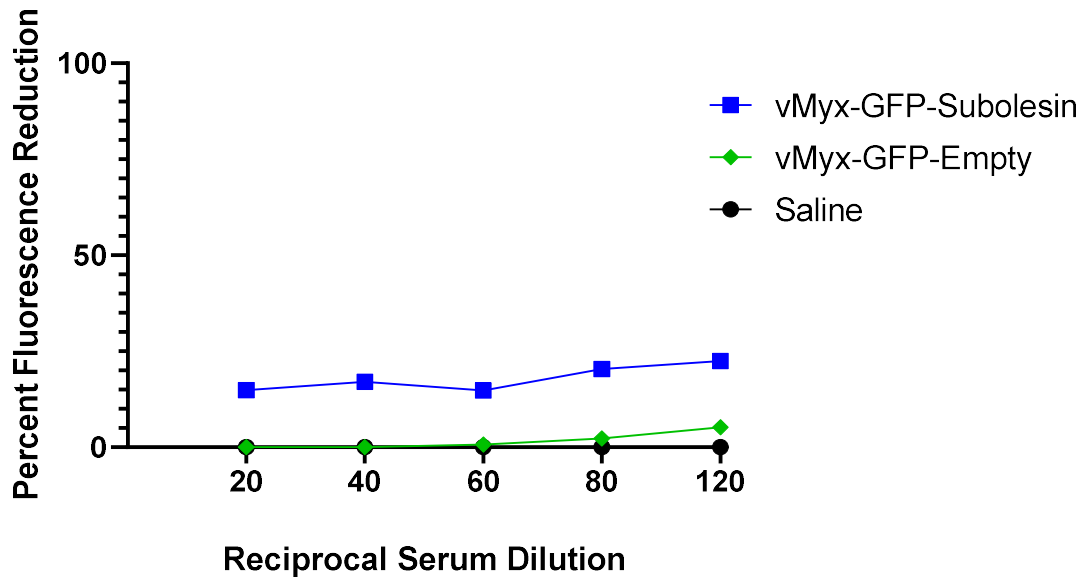


Figure 3.8: Mouse anti-Subolesin antibodies recognize *H. marginatum* Subolesin expressed in mammalian cells by IFA.

RK13 cells were transfected with pcDNA3.1(+)-Subolesin-6XHis or pCAGGS-GFP for 24 hours then probed with mouse serum or His.H8. Subolesin expression was recognized by the mouse serum, with a fluorescent pattern similar to His.H8 probed cells.

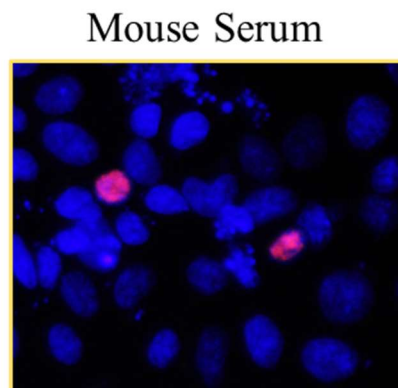
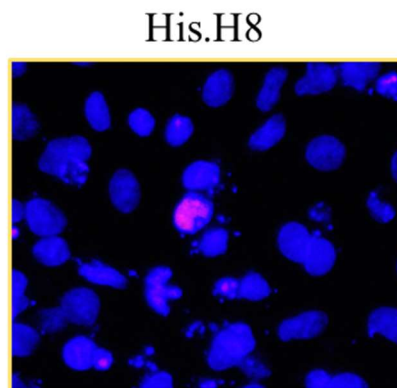
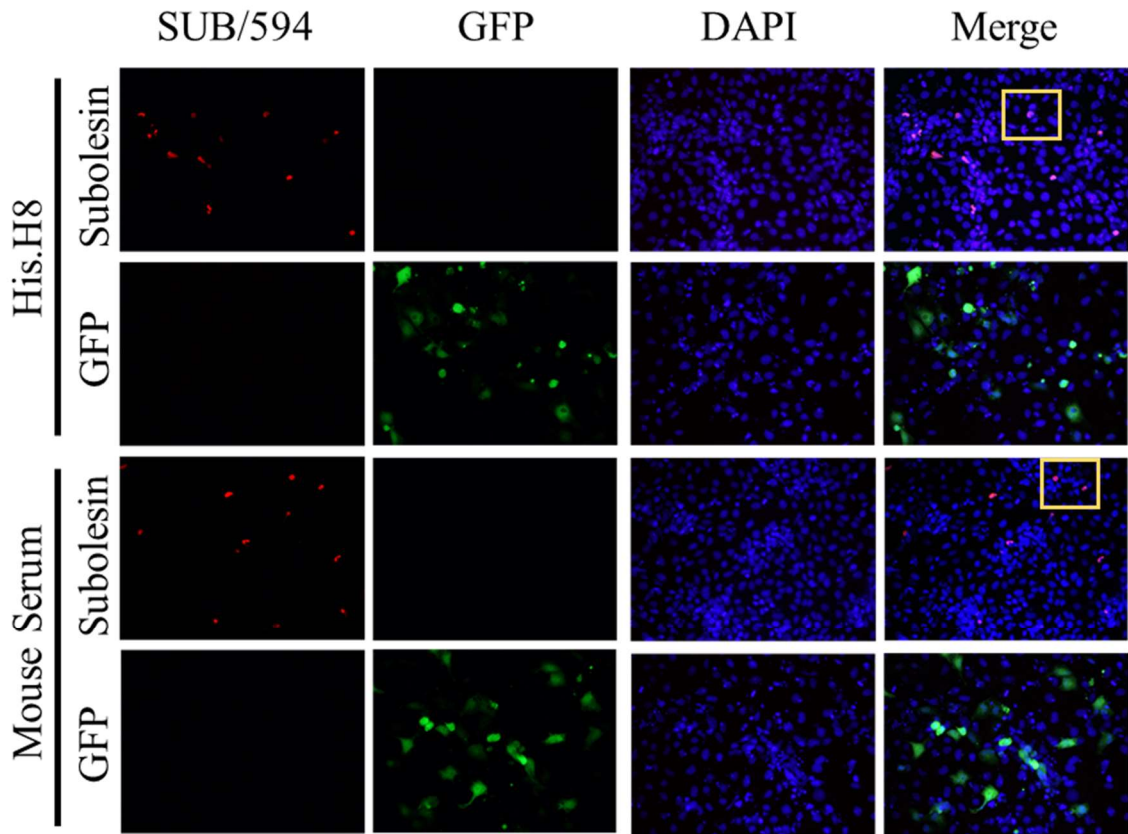


Figure 3.9: Mouse anti-Subolesin antibodies recognize *H. marginatum* Subolesin expressed in mammalian cells by western blot.

Whole-cell lysates of untransfected HEK293T cells or pcDNA3.1(+)-Subolesin-6XHis transfected HEK293T cells were probed with His.H8 or mouse serum. The molecular weight of Subolesin with the 6X polyhistidine epitope tag was predicted to be 18kDa. The same band was seen in both the His.H8 and mouse serum probed blots.

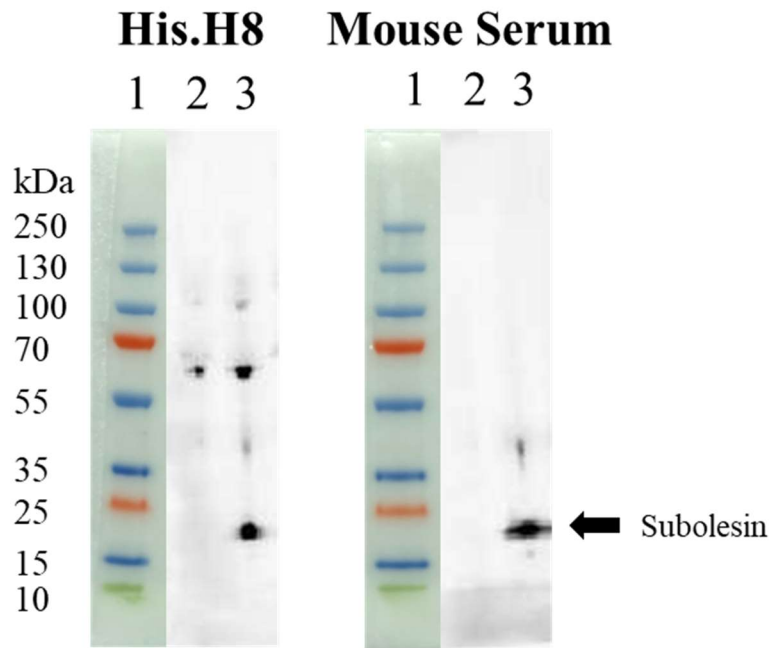
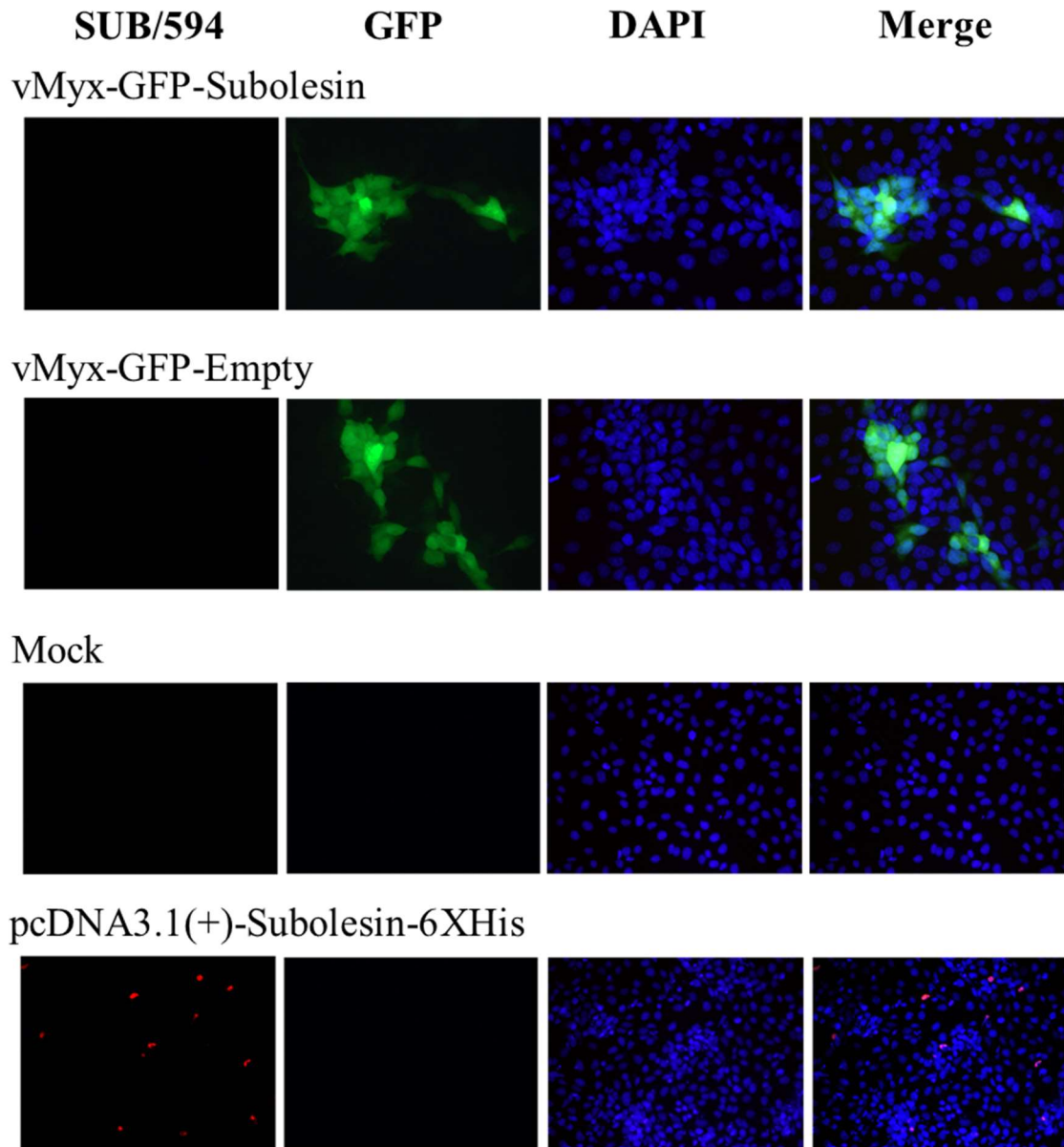


Figure 3.10: Subolesin expression is not detected from the recombinant virus vMyx-GFP-Subolesin.

vMyx-GFP-Subolesin and vMyx-GFP-Empty viruses were infected at a MOI of 0.1 in RK13 cells until 24 hours post-infection. Cells were stained with anti-Subolesin mouse serum. Subolesin was detected from the transfected cells, but not vMyx-GFP-Subolesin infected cells, suggesting that Subolesin was not transfected from the recombinant virus.



Chapter 4: A Replication-Competent Rabies Virus-Vectored Anti-Tick Vaccine for Hosts of Adult *Hyalomma marginatum*

4.1 Abstract

This chapter describes efforts to target the second vector-host interaction point in the *H. marginatum* life cycle by developing an anti-tick vaccine for livestock, such as cattle, which are the preferred hosts of adult *H. marginatum*. Live attenuated and inactivated rabies virus (RABV) vaccines have been developed as human and veterinary vaccines and have a well-established record of safety and immunogenicity^{173,177,231}. Several candidate recombinant vaccines have been developed that express foreign antigens, demonstrating that chimeric RABV glycoprotein (G) antigens can increase the immunogenicity of foreign antigens within RABV-vectored vaccines by incorporating them into the RABV virion²³². It was hypothesized that the generation of a Subolesin-RABV-G chimeric protein for use in a recombinant, replication-competent RABV vaccine would result in a candidate that produces robust humoral immunogenicity to Subolesin from a single dose. The results presented in this chapter show that anti-Subolesin antibodies recognize a Subolesin-RABV-G chimeric protein, the subcellular localization of the chimeric protein is different from native Subolesin, and the chimeric protein was detected in recombinant RABV virions. Assessment of immunogenicity after a single dose of the replication-competent vaccine candidate in mice revealed low levels of Subolesin-binding antibodies. This chapter provides a proof-of-concept study that a chimeric Subolesin antigen in a RABV-vectored vaccine can be developed. However, it has limited immunogenicity, and further work is necessary to develop an anti-tick vaccine that generates robust humoral responses from a single dose.

4.2 Introduction

Hyalomma marginatum is a two-host tick, giving two vector-host interaction points that can be exploited to develop an anti-tick vaccine. The work presented in Chapter 3 aimed to target the first vector-host interaction point by developing an anti-tick vaccine for preferred hosts of the immature stages of *H. marginatum* ticks, and the results suggested that modification of Subolesin to change the subcellular localization, or the use of a less complex and replication-competent viral vector, may be a better strategy for the development of an anti-tick vaccine. This chapter targets the second vector-host interaction point in the *H. marginatum* life cycle by developing a replication-competent viral-vectored anti-tick vaccine for large mammalian ungulates of the Bovidae family, the preferred hosts of adult *H. marginatum*⁹⁸.

Rabies virus (RABV) has been used as a safe and immunogenic live attenuated vaccine in wildlife for decades^{233,234}, and it is an attractive recombinant vaccine platform as all mammalian species are permissive to RABV. Recombinant RABV generates high levels of immunogenicity to both the inserted foreign antigens and the RABV glycoprotein (G) from a single dose¹⁷³. Recent research has focused on the generation of RABV G chimeric proteins²³² to incorporate foreign antigens into RABV virions without the loss of RABV replication¹⁷⁷. These chimeric proteins within recombinant live RABV have been assessed for foreign antigens that need a robust humoral response for protection¹⁷⁷ and are an appropriate vector for immunogens such as Subolesin. Previous work has shown that generation of an *Anaplasma marginale* Major Surface Protein 1a (MSP1a)-Subolesin chimeric protein for insertion into bacterial membranes significantly increased humoral

immunogenicity from a single dose of the membrane-bound modified protein^{153,154}. This suggested that Subolesin would be a good candidate for generating a RABV-G chimeric antigen.

The goal of this chapter is to utilize the RABV-G chimeric protein method to develop a replication-competent RABV-vectored Subolesin vaccine for hosts of adult *H. marginatum* ticks. It was hypothesized that a Subolesin-RABV-G chimeric antigen incorporated within RABV would result in a replication-competent vaccine candidate that produces robust humoral immunogenicity from a single dose. This chapter investigates the generation of a Subolesin-RABV-G chimeric protein and recombinant RABV vaccine, and the immunogenicity of this vaccine candidate in a mouse model.

4.3 Results

4.3.1 Antigen Modification, Codon-Optimization, and Synthesis of Subolesin-RABV-G

It was hypothesized that nuclear localization of Subolesin would negatively affect its immunogenicity and, therefore, modification of Subolesin for presentation on the cell membrane for incorporation into RABV virions would increase its immunogenicity. Modifications to the amino acid sequence of *H. marginatum* Subolesin (Accession # DQ159970) were made by Dr. Matthias Schnell's laboratory at Thomas Jefferson University, Philadelphia, PA (TJU). The Subolesin-RABV-G chimeric protein was generated *in silico* using both N- and C-terminal modifications to localize the protein to the cell membrane for incorporation into RABV virions. The modifications chosen for

Subolesin have previously been used to incorporate other antigens within RABV virions^{177,231,232}. Specifically, the human immunoglobulin κ chain signal peptide (21 residues) was added to the N-terminus of Subolesin and the 118 residues of the C-terminus of RABV-G, which includes 51 residues of the G ectodomain (ED51), the transmembrane domain (TMD), and the cytoplasmic tail (CT), were added to the C-terminus of Subolesin (**Supplementary Figure 4.1A**). Together, these modifications increased the size of Subolesin from 150 residues to 286 residues (**Supplementary Figure 4.1B**), and the chimeric antigen was referred to as Subolesin-RABV-G. The amino acid sequence of Subolesin-RABV-G was submitted to the DeepLoc 1.0 server (<https://services.healthtech.dtu.dk/service.php?DeepLoc-1.0>) for prediction of subcellular localization, and results were compared to the subcellular localization prediction of the native Subolesin protein. Native Subolesin is predicted to localize to the nucleus of mammalian cells due to two nuclear localization signals (**Supplementary Figure 3.3**). However, Subolesin-RABV-G was predicted to localize to the cell membrane with an 86.8% likelihood, with the RABV-G TMD residues overpowering the nuclear localization signal sequence that was not removed in Subolesin-RABV-G (**Supplementary Figure 4.2**).

The amino acid sequence of Subolesin-RABV-G was submitted to GenScript for codon optimization and synthesis. The nucleotide sequence was codon-optimized by GenScript for expression in cattle, as the targeted organisms for this vaccine development strategy are members of the family Bovidae, which are the preferred hosts for adult *H. marginatum* ticks⁹⁸. As the vaccine candidate discussed in this chapter was evaluated for

immunogenicity using a mouse model, codon-optimization of the antigen for cattle was compared to codon-optimization for mice using the IDT codon-optimization tool for *Mus musculus*. To align the nucleotide sequence of *H. marginatum* Subolesin to the rabbit, cattle, and mouse codon-optimized sequences, the starting methionine residue was removed from the tick, rabbit, and mouse codon-optimized sequences since this residue was removed to add the signal peptide in the Subolesin-RABV-G chimeric antigen. The C-terminal 6XHis or RABV-G antigen modifications in the rabbit or cattle codon-optimized sequences, respectively, were also removed. The alignment of the four sequences showed numerous nucleotide differences (**Supplementary Figure 4.3A**). There were 104/444 nucleotide differences between the tick and cattle codon-optimized sequence, 94/444 nucleotide differences between the tick and rabbit codon-optimized sequence, 110/444 nucleotide differences between the tick and mouse codon-optimized sequence, 107/444 nucleotide differences between the cattle and rabbit codon-optimized sequences, 99/444 nucleotide differences between the cattle and mouse codon-optimized sequences, and 112/444 nucleotide differences between the rabbit and mouse codon-optimized sequences (summarized in **Supplementary Figure 4.3B**). The cattle codon-optimized sequence of the Subolesin-RABV-G chimeric antigen was synthesized by GenScript and then shipped to Dr. Schnell's laboratory, where Subolesin-RABV-G was subcloned into a mammalian expression vector to produce the plasmid pCAGGS-Subolesin-RABV-G (**Supplementary Figure 4.4**). Dr. Schnell's laboratory supplied this mammalian expression plasmid to evaluate antigen expression.

4.3.2 The Subolesin-RABV-G Chimeric Protein is Recognized by Anti-Subolesin Antibodies and has an Altered Subcellular Localization

Generation of the Subolesin-RABV-G chimeric protein nearly doubled the size of the protein, from 150 residues in its native form to 286 residues in its chimeric form. It was hypothesized that the Subolesin-RABV-G chimeric protein would have a different subcellular localization than the native Subolesin protein. RK13 cells were transfected with either pcDNA3.1(+)-Subolesin-6XHis (containing the native form of Subolesin), pCAGGS-Subolesin-RABV-G (containing the Subolesin chimeric protein), or pCAGGS-GFP as a transfection and negative control (**Figure 4.1**). Transfected cells were probed with mouse anti-Subolesin serum (generated in Chapter 3) to detect Subolesin expression. Subolesin-RABV-G expression from pCAGGS-Subolesin-RABV-G was detected with the mouse antiserum, which suggested that modification of the antigen did not prevent recognition of Subolesin by polyclonal antibodies. The fluorescent pattern of RK13 cells expressing native Subolesin and Subolesin-RABV-G differed. The signal from pcDNA3.1(+) Subolesin-6XHis transfected RK13 cells primarily overlapped nuclei stained with DAPI, suggesting the expected nuclear localization of native Subolesin. The signal from pCAGGS-Subolesin-RABV-G was diffuse and displayed fluorescence within the RK13 cells that did not overlap with nuclei. This change in the fluorescent pattern suggested that the subcellular localization of Subolesin-RABV-G was altered, as it was not directly overlapping nuclei like the native form. Thus, the residue additions did not appear to significantly affect protein folding and there was little impact on antigen recognition. An IFA using nonpermeabilized cells to evaluate the presence of Subolesin-RABV-G on the cell surface was not undertaken.

4.3.3 Recombinant Virus Generation and Expression of Subolesin-RABV-G

Dr. Schnell's Laboratory uses a well-established reverse genetics system to generate recombinant RABV¹⁷⁶. Recombinant viruses generated for this work used the RABV BNSP333 vaccine vector, which is derived from the attenuated wildlife vaccine strain Street Alabama Dufferin (SAD) B19 and incorporates an additional attenuating mutation of arginine to glutamate at position 333 of RABV-G^{235,236}. This vector was engineered to contain a RABV stop-start transcription sequence flanked by restriction sites for the insertion of foreign genes between the nucleoprotein (N) and phosphoprotein (P) of RABV. Three versions of the BNSP333 recombinant virus were used in these studies; the first virus, RABV-Empty, is the control BNSP333 vector without any foreign genes, the second virus, RABV-Subolesin, is the BNSP333 vector encoding Subolesin-RABV-G, and the third virus, RABV-GP85, is the BNSP333 vector encoding CCHFV GP85 (**Figure 4.2**). All three viruses were rescued at TJU, and insertion of the foreign antigens was confirmed with Sanger sequencing.

To evaluate Subolesin-RABV-G expression from RABV-Subolesin, RABV-Empty and RABV-Subolesin virions were pelleted through a 20% sucrose cushion for purification. The virion pellets were then resuspended and lysed for use in a Western blot (**Figure 4.3**). Virion lysates were probed with rabbit anti-Subolesin serum, which was shown to recognize *H. marginatum* Subolesin in Chapter 3 (**Figure 3.1**). The predicted molecular weight of Subolesin-RABV-G is 32.3 kDa (Geneious Prime software). One band was visualized in the RABV-Subolesin lane, but not the RABV-Empty lane, close to the expected molecular weight, suggesting that RABV-Subolesin was expressing Subolesin-

RABV-G. An additional band unique to the RABV-Subolesin lysate was visualized above 72kDa, but the identification of this product is unknown. Since the lysates used in this blot were from purified virions, it further suggested that Subolesin-RABV-G was incorporated into the RABV-Subolesin virions.

4.3.4 Immunogenicity of the Vaccine Candidate in a Mouse Model

This study used C57Bl/6 mice to assess vaccine immunogenicity. Mice were separated into five groups with five mice per group. RABV-Empty served as a vector control, saline served as a negative control, and there were three test groups, RABV-Subolesin only, RABV-GP85 only, and a 50/50 mixture of RABV-Subolesin and RABV-GP85 (referred to as the “Mixture” group). Each mouse received 50 μ L via intramuscular injection (IM) into each hind leg, totaling a 100 μ L dose. The target dose was 1.0 billion focus forming units (FFU) for each mouse. Results of inoculum back-titration were as follows: RABV-Subolesin mice received 2.0 million FFU, RABV-GP85 mice received 5.3 million FFU, the Mixture group received 6.0 million FFU, and the RABV-Empty group received 0.087 million FFU. The FFU of each virus in the Mixture group was not determined, but it is assumed that the mice received 3.0 million FFU of each virus, equaling the 6.0 million FFU total dose. The negative control group received 100 μ L of saline. Mice received one dose of these replication-competent recombinant viruses or saline. Serum was collected from each mouse at 28 days post-infection to assess immunogenicity to three different antigens using indirect ELISAs at TJU. For each ELISA, sera were initially diluted to 1:50, then serially diluted at 1:3, for a total of eight dilutions. Statistical significance in signal or

EC₅₀ titers was determined using a one-way ANOVA with Tukey's post hoc correction for multiple comparisons.

Purified *R. microplus* Subolesin protein and mouse serum from purified *R. microplus* Subolesin protein in adjuvant mice (Chapter 3) were provided to Dr. Schnell's laboratory for use as a coat and positive control, respectively, for an anti-Subolesin ELISA (**Figure 4.4A**). For this ELISA, sera were pooled for the five mice in each group before dilution. In the anti-Subolesin ELISA undertaken by TJU, the EC₅₀ titer of the mouse antiserum was 1 in 17,017, which was different from the UTMB anti-Subolesin ELISA EC₅₀ of 1 in 1682. This approximately 10-fold difference in EC₅₀ titer calculations suggested that the TJU ELISA method was more sensitive than the UTMB method. Subolesin binding antibodies were generated in both the RABV-Subolesin only and Mixture groups, but no other groups. ELISA signal did not reach the maximum for the assay in either the RABV-Subolesin only or Mixture groups, so the EC₅₀ could not be determined. At the lowest dilution (1:50), there was a significant difference in signal between the RABV-Subolesin only, Mixture, and the Subolesin antiserum positive control groups (****, $p = < 0.0001$) (**Figure 4.4B**). The quantity of RABV-Subolesin received by mice in the RABV-Subolesin group and the Mixture group, 2.0 million FFU and approximately 3.0 million FFU, respectively, is likely not significantly different. Interestingly, there was a significantly greater signal from the RABV-Subolesin group than the Mixture group, despite the slightly lower quantity of immunogen. These results suggest that a greater immune response is generated to Subolesin when the RABV-Subolesin vaccine is given alone rather than in a mixture. These results also suggest that the Subolesin binding antibody responses in both groups were

significantly lower than the antibody levels induced by two doses of Subolesin protein in adjuvant.

Inclusion of the RABV-GP85 and Mixture groups allowed for the assessment of antibody responses to a different foreign antigen in the same insertion site as Subolesin-RABV-G. Purified GP38 from transfected HEK293F cells was used as a protein coat for an anti-GP38 ELISA (**Figure 4.4C**). For this ELISA, sera from each mouse were assessed individually, rather than pooling by group, and the GP38 specific mAb 13G8 was used as a positive control. GP38-binding antibodies were generated in the RABV-GP85 and Mixture groups, but no other groups. The maximum signal was achieved for both groups, and the EC_{50} was determined (**Figure 4.4D**). The mean EC_{50} titer of the RABV-GP85 group (861.6 ± 305.3) was greater than the Mixture group (551.9 ± 227.8), but this difference was not statistically significant. The quantity of RABV-GP85 received by mice in the RABV-GP85 group and the Mixture group, 5.3 million FFU and approximately 3.0 million FFU, respectively, is likely not significantly different, although the RABV-GP85 only group received slightly more GP85 immunogen than the Mixture group. There was a significant difference in the EC_{50} titers of both groups compared to the 13G8 control (****, $p = < 0.0001$). These results suggest that robust humoral immune responses can be generated to a foreign antigen inserted in the same genome location as Subolesin-RABV-G. While the EC_{50} titer of the Mixture group was lower than the RABV-GP85 group, this difference was not significant, unlike the significant difference in signal between the RABV-Subolesin and Mixture groups in the anti-Subolesin ELISA. These results suggest that the significant difference in signal seen in the anti-Subolesin ELISA may be due to the Subolesin antigen itself, since

a similar significant difference was not seen with the humoral responses to the GP38 antigen between the RABV-GP85 and Mixture groups.

An anti-RABV-G ELISA was used to evaluate vector immunogenicity (**Figure 4.4E**). For this ELISA, purified RABV-G was used as a protein coat, sera from each mouse were diluted individually, and the RABV-G mAb 1C5 was used as a positive control. The maximum signal was reached for the four groups that received RABV vaccines, and the EC_{50} was determined. There were no significant differences in the EC_{50} titers between the four vaccine groups (RABV-Subolesin [3115.0 ± 585.2], RABV-GP85 [2316.0 ± 993.0], Mixture [2270.0 ± 530.6], and RABV-Empty [3131.0 ± 729.8]) and no differences between the four groups and the mAb positive control (1C5 [5060.0 ± 142.8]). These results suggest that the immunogenicity elicited by the RABV vector was not different between any of the groups, despite differences in the quantity of immunogen used. These results further suggest that the differences in humoral responses against Subolesin and GP38 are due to the foreign antigens within RABV themselves.

Together, the results from these three ELISAs suggest that all recombinant viruses generated similar immunogenicity to RABV-G, and differences in ELISA signal or EC_{50} titers in the Subolesin and GP38 ELISAs were due to differences in immunogenicity of the foreign antigens included within RABV. A comparison of the GP38 and Subolesin ELISA results suggests that the Subolesin-RABV-G chimeric antigen is not as immunogenic as GP85 within RABV.

4.4 Discussion

The studies in Chapter 3 attempted to develop a candidate anti-tick vaccine using a non-replicating vector for small mammals that are the preferred hosts of immature stages of *H. marginatum*. The lack of immunogenicity of the previous vaccine candidate is hypothesized to be due to the nuclear localization of Subolesin and the complexity of the vaccine vector chosen for evaluation. This chapter aimed to develop a vaccine candidate for members of the family Bovidae, the preferred hosts of the adult stages of *H. marginatum*⁹⁸, by modifying the Subolesin antigen and using a less complex vaccine vector that is replication-competent in the animal model used for evaluation of immunogenicity. The research presented within this chapter suggests that the Subolesin-RABV-G chimeric protein has a different subcellular localization than native Subolesin, Subolesin-RABV-G can be incorporated within RABV virions, and the RABV-Subolesin replication-competent vaccine candidate can induce low levels of Subolesin binding antibodies.

The expression of *H. marginatum* Subolesin in mammalian cells appeared to localize to the nucleus (**Figure 3.1**), and it was hypothesized that the nuclear localization of Subolesin hindered its immunogenicity. Previous research has shown that C-terminal modifications of Subolesin incorporating the transmembrane domains of *A. marginale* MSP1a to form a membrane-bound protein significantly increased the immunogenicity of Subolesin^{153,154}. Dr. Schnell's laboratory at TJU has previously demonstrated that foreign antigen modification with the RABV-G ED51, TMD, and CT to form a chimeric protein, can incorporate the modified foreign antigens into RABV virions to increase immunogenicity^{231,232}. It was hypothesized that the generation of a Subolesin-RABV-G

chimeric protein would change the subcellular localization of Subolesin upon expression within mammalian cells, leading to increased immunogenicity of this vaccine candidate (**Supplementary Figure 4.1**). Subcellular localization prediction of the Subolesin-RABV-G chimeric protein predicted that Subolesin-RABV-G would localize to the cell membrane (**Supplementary Figure 4.2**), which would allow for incorporation into RABV virions²³¹. The Subolesin-RABV-G sequence was codon-optimized for cattle (**Supplementary Figure 4.3**), as the goal of this chapter was the development of a vaccine candidate for livestock, specifically members of the family Bovidae. The codon-optimized sequence was synthesized by GenScript and subcloned into a mammalian expression vector at TJU to yield pCAGGS-Subolesin-RVG (**Supplementary Figure 4.4**). Detection and localization of the Subolesin-RABV-G protein from pCAGGS-Subolesin-RVG was compared to the native Subolesin protein from pcDNA3.1(+) Subolesin-6XHis using IFA of transfected RK13 cells probed with mouse anti-Subolesin serum (**Figure 4.1**). The Subolesin-RABV-G protein was recognized by mouse antiserum raised against purified *R. microplus* Subolesin protein, which suggested that the modifications of Subolesin, which nearly doubled the length of the protein, did not ablate recognition by polyclonal antibodies. The fluorescent pattern differed between fluorescent cells transfected with the native or chimeric Subolesin proteins. Transfected cells expressing native Subolesin had fluorescent staining that primarily overlapped with the nuclear stain. In contrast, transfected cells expressing Subolesin-RABV-G displayed fluorescence that did not overlap with nuclei and was instead located throughout the cell. These differences in the fluorescent pattern suggested that the Subolesin-RABV-G protein has a different subcellular localization than Subolesin. While it was predicted that the Subolesin-RABV-G protein would localize to

the cell membrane, an IFA without cell permeabilization was not undertaken to assess this hypothesis.

Three recombinant rabies viruses, RABV-Empty, RABV-Subolesin, and RABV-GP85, with no foreign genes, Subolesin-RABV-G, or CCHFV GP85, respectively, between RABV N and P, were generated by Dr. Schnell's laboratory for use within this study (**Figure 4.2**). Rabies virus mRNA is independently transcribed for each gene from the start and stop signals between each gene, resulting in a transcript concentration gradient, with genes near the 3' of the viral RNA producing more transcripts than genes farthest from the 3' end²³⁷. Insertion of the foreign genes after N is meant to yield high expression levels of the antigen of interest since this position has the second most transcribed mRNAs. To evaluate the expression of Subolesin-RABV-G from the recombinant virus, purified RABV-Empty and RABV-Subolesin virions were probed with mouse anti-Subolesin serum using a Western blot (**Figure 4.3**). Using sucrose-cushion purified virions as the protein lysate allows for specific detection of proteins incorporated within RABV virions¹⁷⁸. The predicted molecular weight of Subolesin-RABV-G is 32.3 kDa. A single band was seen above the 34kDa marker in the RABV-Subolesin lane, but not the RABV-Empty lane, which is hypothesized to be Subolesin-RABV-G. The presence of this band suggested that not only was Subolesin-RABV-G being expressed from RABV-Subolesin but that it was also being incorporated into RABV-Subolesin virions. This blot was run using reducing conditions, so protein-protein interactions should not be present. Interestingly, the mouse serum recognized a second band unique to the RABV-Subolesin lane above the 72kDa marker. The approximate molecular weight of this band corresponds

to the weight of RABV-G; however, since a band was not visualized in the RABV-Empty virion lysate at this weight, it is unlikely that there is nonspecific binding to RABV-G. Further experiments to determine this protein product were not explored, and Western blots using polyclonal rabies antiserum were not undertaken.

The immunogenicity of the recombinant viruses generated for this chapter was assessed using a single dose of live virus in C57Bl/6 mice. Serum was collected from each mouse at 28 days post-infection to evaluate binding antibodies to Subolesin, GP38, and RABV-G (**Figure 4.4**). There were slight differences in the quantity of immunogen given to the RABV-Subolesin (2.0 million FFU), RABV-GP85 (5.3 million FFU), and Mixture groups (6.0 million FFU total, assuming 3.0 million of each virus), and a larger difference in the quantity of immunogen given to the RABV-Empty group (0.087 million FFU). Despite the differences in the quantity of immunogen between groups, there were no significant differences in binding antibody EC_{50} titers generated to RABV-G between the four groups that received a recombinant virus. This suggested that each group generated similar levels of anti-vector immunity and that it is unlikely that the differences in immunogen quantity between groups is an explanation for statistically significant differences in immunogenicity between groups in the Subolesin and GP38 ELISAs. This further suggested that the statistically significant differences in the Subolesin and GP38 ELISA results were due to the foreign antigens themselves.

The positive control for the anti-Subolesin ELISA was serum from a BALB/c mouse immunized twice with purified *R. microplus* Subolesin protein in adjuvant (generated in

Chapter 3). It is known that C57Bl/6J and BALB/c mice are immunologically biased for Th1- and Th2-type responses, respectively²³⁸. While samples from these two different strains of mice were assessed in the same ELISA, it is difficult to directly compare the RABV-Subolesin/Mixture groups and the mouse antiserum since the samples are from different mice genotypes in addition to a different vaccine. However, since it was hypothesized that this vaccine candidate would yield anti-Subolesin antibodies superior to the conventional protein in adjuvant method, this comparison, although flawed, was necessary. In the anti-Subolesin ELISA, only low levels of Subolesin binding antibodies were detected from the RABV-Subolesin or Mixture groups, and the maximum signal was not achieved at the lowest dilution. Since EC_{50} titers could not be calculated, differences between groups were assessed using signal at the 1:50 dilution. The signal from both the RABV-Subolesin and Mixture groups was significantly lower than the positive control mouse serum, and the signal from the Mixture group was significantly lower than the signal from the RABV-Subolesin group. While the RABV-Subolesin vaccine candidate generated anti-Subolesin antibodies, the levels were not superior to the conventional protein in adjuvant method, as hypothesized. An important point to consider is that purified *R. microplus* Subolesin protein was used as a coat for the anti-Subolesin ELISA rather than the Subolesin-RABV-G protein. This ELISA coat was chosen to measure antibody binding responses to the form of Subolesin expressed in ticks. With the extensive modifications made to Subolesin, it's possible that antibodies were generated that do not bind to the purified *R. microplus* Subolesin protein. Antibody responses to the Subolesin-RABV-G protein were not evaluated, but it would be interesting to assess the differences in antibody recognition to the two different antigens, although binding to the Subolesin-RABV-G

protein would not be biologically relevant. Further, it is also important to consider that different humoral responses would likely be seen if immunogenicity was evaluated in a mouse strain such as BALB/c, since they are immunologically biased for a Th2-type response. Comparison of immunogenicity of the viral-vectored and protein-in-adjuvant candidates would be stronger when evaluated using the same mouse strain.

In the GP38 ELISA, both the RABV-GP85 and Mixture groups had significantly lower EC_{50} titers than the 13G8 mAb positive control, but there was no significant difference between the EC_{50} titers of the RABV-GP85 and Mixture groups. These results, in combination with the results of the anti-Subolesin ELISA, suggest that the significantly lower signal in the Mixture group compared to the RABV-Subolesin group in the anti-Subolesin ELISA, and the lower EC_{50} titer in the Mixture group compared to RABV-GP85 group in the anti-GP38 ELISA, can be attributed to the use of two immunogens in the Mixture group, rather than the single immunogen used in the RABV-Subolesin or RABV-GP85 groups. Further, these results suggest that the immunogenicity of the Subolesin antigen is poorer than the GP85 antigen, as there was a significantly lower immune response generated to Subolesin than to GP85 in the Mixture group.

The Subolesin-binding antibodies generated by RABV-Subolesin were low, which gives one avenue for continued exploration of this vaccine construct. Since the recombinant viruses used in this chapter are replication-competent, substantially increasing the dose to generate robust antibody responses is not the best option. Previous work by Dr. Schnell's laboratory has shown that antigen-specific antibody responses can be significantly

increased by immunizing with inactivated recombinant RABV in adjuvant^{178,179}. Since the Western blot of RABV-Subolesin virion lysate suggests that Subolesin-RABV-G is incorporated into RABV-Subolesin virions, it would be interesting to evaluate Subolesin-binding antibody responses generated from immunization with inactivated RABV-Subolesin in adjuvant.

In conclusion, a Subolesin-RABV-G chimeric antigen within a replication-competent RABV vector resulted in a vaccine candidate that induced low levels of Subolesin-binding antibodies. The low levels of Subolesin-binding antibodies induced by this replication-competent vaccine suggests that further work is necessary to develop of this anti-tick vaccine candidate. These results provide a proof-of-concept that a chimeric Subolesin protein can induce humoral responses that recognize the native form of Subolesin, which offers new avenues of exploration for the use of a chimeric Subolesin antigen for anti-tick vaccine development.

Figure 4.1: The Subolesin-RABV-G chimeric protein is recognized by anti-Subolesin antibodies and has an altered subcellular localization.

RK13 cells were transfected with pcDNA3.1(+) Subolesin-6XHis, pCAGGS-Subolesin-RABV-G, or pCAGGS-GFP, then stained with mouse anti-Subolesin serum at 24 hours post-transfection. The yellow box on the merge images is magnified in the bottom images, which shows the change in fluorescent pattern that suggests the change in subcellular localization.

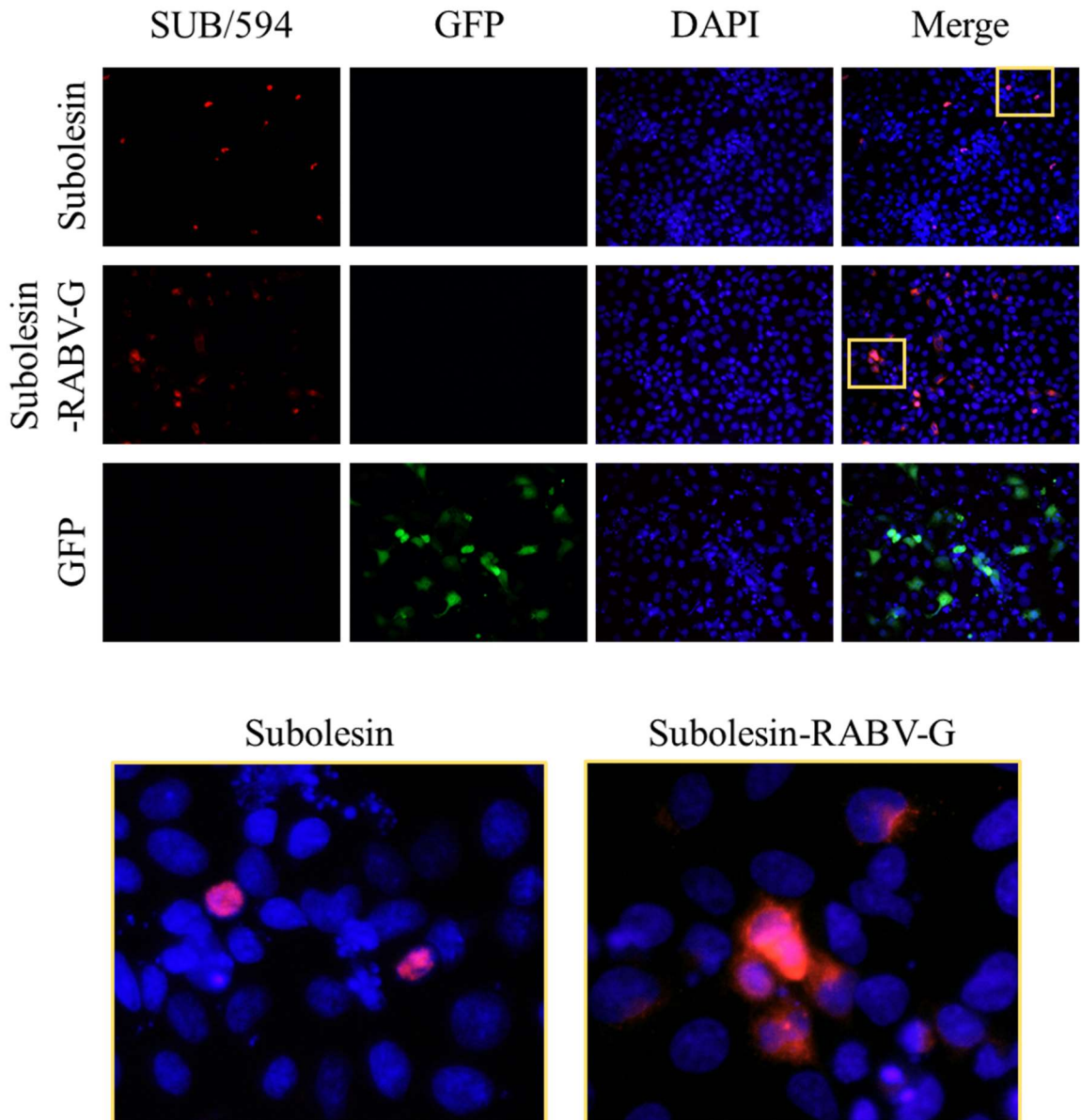


Figure 4.2: Schematic diagrams of recombinant RABV vaccines.

Schematic diagrams of the recombinant RABV vector without insertion of foreign antigens (RABV-Empty) and the recombinant viruses encoding Subolesin-RABV-G (RABV-Subolesin), or CCHFV GP85 (RABV-GP85).

RABV-Empty



RABV-Subolesin



RABV-GP85



Figure 4.3: Subolesin is expressed from RABV-Subolesin.

A western blot of RABV-Empty and RABV-Subolesin infected lysates was probed with rabbit anti-Subolesin serum. The predicted molecular weight of Subolesin-RABV-G is 32.3 kDa.

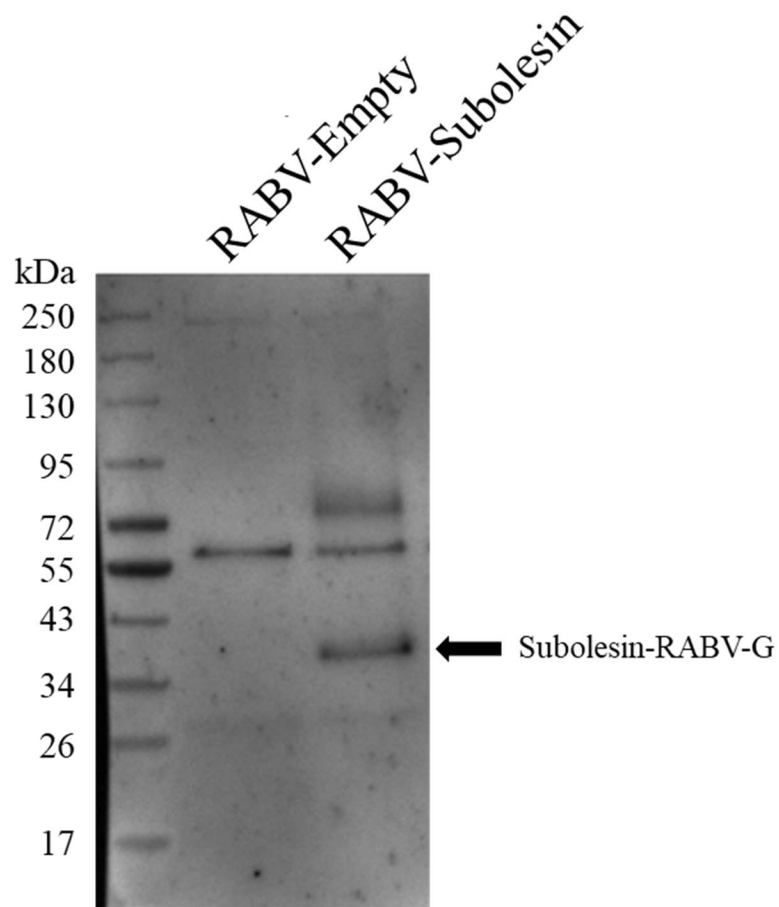
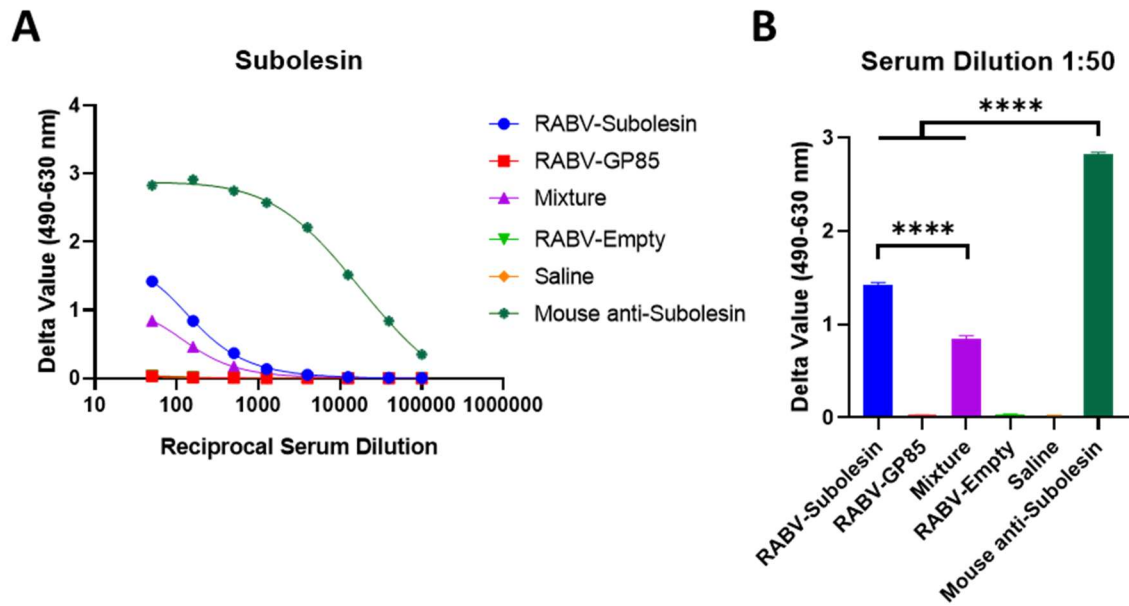
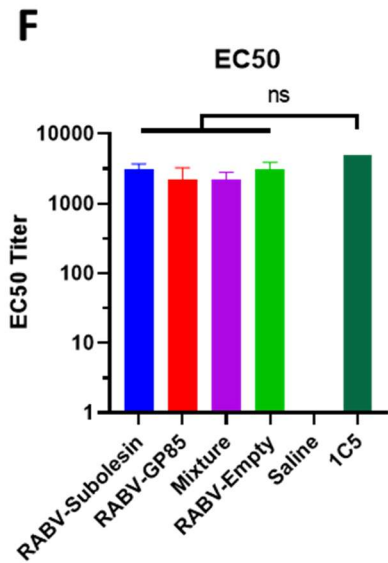
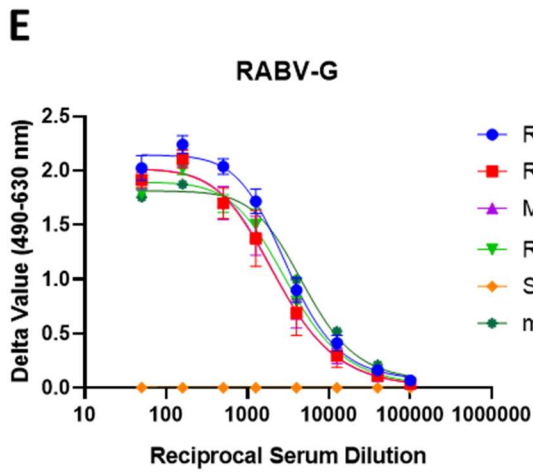
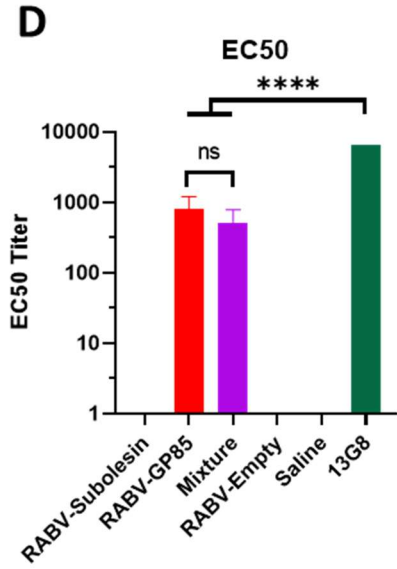
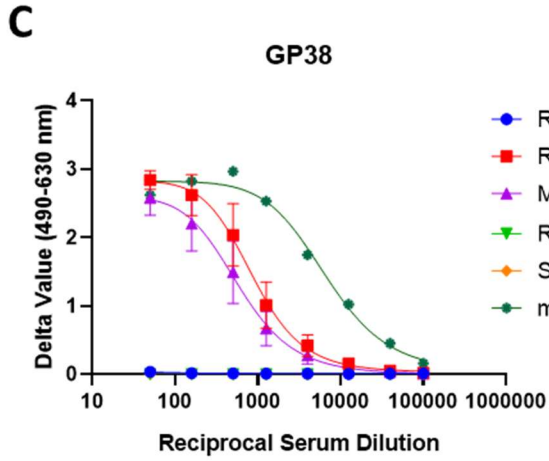


Figure 4.4: Immunogenicity of live recombinant RABV vaccines.

R. microplus Subolesin, GP38, or RABV-G, were used as a protein coat for indirect ELISAs. Serum was serially diluted 1:3, starting at a 1:50 dilution. (A) Anti-Subolesin ELISA using sera pooled by group. (B) ELISA signal from the starting 1:50 dilution. (C) Anti-GP38 ELISA. Serum from each mouse was run individually. (D) EC₅₀ titers of each group. (E) Anti-RABV-G ELISA. Serum from each mouse was run individually. (F) EC₅₀ titers of each group. For each ELISA graph, a curve was fit to a nonlinear regression with a variable slope in GraphPad PRISM. This curve was used to determine the EC₅₀. Statistical differences in graphs B, D, and F, were determined using an ordinary one-way ANOVA with Tukey's post hoc correction for multiple comparisons.





Chapter 5: An Immunoinformatics Guided Approach for Rational Design of a Crimean-Congo Hemorrhagic Fever Virus Multi-Epitope DNA Vaccine

5.1 Abstract

Work presented in this chapter explores the development of a multi-epitope antigen DNA vaccine to reduce antigen size and processing from the current full-length GPC DNA vaccine candidates. The multi-epitope antigen, termed *EPIC*, for Epitope Construct, was generated from a series of *in silico* predicted cytotoxic and helper T cell epitopes across the GPC. Furthermore, it was evaluated for sequence conservation, antigen expression, recognition by CCHFV antibodies, and assessed for tolerability and immunogenicity of the vaccine candidate in a mouse model. Overall, the multi-epitope regions in *EPIC* were not more conserved than their respective whole GPC proteins. *EPIC* expression was detected in transfected mammalian cells by IFA, but the number of cells transfected was low and had poor recognition by CCHFV antibodies. The bright signal of *EPIC* and GPC transfected cells by IFA did not correspond to high expression levels of the proteins when detected by western blot. The vaccine candidate was well-tolerated but did not produce either *EPIC* or GPC binding antibody responses in C57Bl6/J mice, although epitopes predicted to be recognized by the mouse immune system were included in the antigen. Ultimately, this chapter provides information for target regions of the GPC for future vaccine development and suggests that the use of the whole GPC or whole proteins of the GPC are superior antigens for CCHFV DNA vaccine development rather than a multi-epitope antigen until more information about protective CCHFV epitopes is known.

5.2 Introduction

Previous chapters in this dissertation have investigated viral vectored vaccines. This chapter explores a DNA vaccine as a different vaccine development strategy for CCHFV. Current CCHFV DNA vaccines being explored primarily encode the full-length GPC, but other whole protein-encoding sections from the GPC, including GP38, G_N, and G_C, have been used due to the complex processing of the glycoproteins^{72,75,77,78,239}. It has been suggested that the size and complex processing of the CCHFV GPC could hinder using the GPC as a DNA vaccine antigen and that the use of a multi-epitope antigen would be an improvement from current CCHFV DNA vaccine candidates^{73,240-242}. Combining plasmid-based multi-epitope DNA vaccines with electroporation at the vaccination site increases plasmid uptake by the muscle tissue and antigen-presenting cells, where expression and processing of the antigen by different cell types allow for the presentation of the multiple encoded epitopes by both Major Histocompatibility Complex (MHC) class I and MHC class II molecules. Stimulation of cytotoxic T-lymphocytes (CTL) and helper T-lymphocytes (HTL) generates memory T cells and activates B cells to generate humoral responses, respectively, required for protection from lethal CCHFV challenge^{66,72,77-79,243}. Previous research has demonstrated the feasibility of this vaccine development strategy for other members of *Bunyavirales* with complex glycoprotein processing; a multi-epitope DNA vaccine generated with conserved epitopes selected from alignment of the Hantaan virus (HTNV), Seoul virus (SEOV), and Puumala virus (PUUV) glycoproteins induced both humoral and cellular immunity against all three viruses in mice²⁴⁴.

Recently, computational studies have attempted to identify epitopes across the GPC; however, this work has yet to be explored beyond *in silico* analyses^{240–242}. The apparent uneven distribution of immunogenicity across the GPC suggests that generating an antigen using immunodominant regions may be a highly effective approach for CCHFV vaccine development. It was hypothesized that reducing antigen size and processing from the full-length CCHFV GPC by generating a multi-epitope antigen would produce an immunogenic DNA vaccine candidate. The results presented in this chapter show the first work on the development of a multi-epitope DNA vaccine for CCHFV that goes beyond *in silico* analyses to evaluate antigen expression and recognition by CCHFV antibodies using immunofluorescent microscopy and the tolerability and immunogenicity of the vaccine candidate in a mouse model.

5.3 Results

5.3.1 Identification of Epitopes Across the CCHFV GPC using Bioinformatic Servers

Dr. Éric Bergeron (CDC) provided the open reading frame of the CCHFV GPC strain Turkey2004 in the plasmid pCAGGS-GPC (Genbank # KY362519.1). The translation of the GPC was used for bioinformatic server predictions to identify epitopes likely to be presented by human MHC class I and MHC class II molecules to CD8⁺ cytotoxic T-lymphocyte (CTL) and CD4⁺ helper T-lymphocytes (HTL), respectively. Using the NetCTL 1.2 Server (<https://services.healthtech.dtu.dk/service.php?NetCTL-1.2>), CTL epitopes were identified for each of the 12 MHC class I supertypes in the server for a total of 256 predicted epitopes that met the inclusion criteria of a combined score of >1.0 (**Supplementary Table 5.1**). HTL epitopes were predicted using the NetMHCII 2.3 Server

(<https://services.healthtech.dtu.dk/service.php?NetMHCII-2.3>) for 20/25 (80%) Human Leukocyte Antigen (HLA)-DR alleles (**Supplementary Table 5.2**), 13/20 (65%) HLA-DQ alleles (**Supplementary Table 5.3**), and 6/9 (66.7%) HLA-DP alleles (**Supplementary Table 5.4**), for a total of 837 predicted HTL epitopes that met the inclusion criteria of (1) a strong binder threshold of <2.00%-rank to a set of 1,000,000 random natural peptides and (2) a predicted 50% effective concentration (EC50) value <50 nM. Together, these bioinformatic servers identified 1093 epitopes across the GPC that are predicted to bind to various MHC haplotypes.

All predicted CTL and HTL peptides that met the above inclusion criteria were aligned to the GPC using Clustal Omega (**Supplementary Figure 5.1**). Peptides were excluded if they fell across known cleavage sites on the GPC polyprotein, removing 21 of the 1093 total predicted peptides from consideration (**Supplementary Figure 5.1 and Table 5.1**). It was expected that the number of peptides aligned to the individual proteins would be relative to the proportion of the GPC that the individual proteins comprise. The individual GPC proteins, MLD (249 residues), GP38 (272 residues), G_N (288 residues), NS_M (233 residues), and G_C (647 residues), comprise 14.7%, 16.1%, 17.1%, 13.8%, and 38.3% of the polyprotein, respectively. The number of peptides aligned to the individual proteins resulted in similar proportions of 19.1%, 16.2%, 13.1%, 14.9%, and 34.8% for MLD, GP38, G_N, NS_M, and G_C, respectively. Interestingly, the peptides predicted for the nonstructural proteins MLD, GP38, and NSM resulted in peptide prediction proportions higher than the proportion of the polyprotein the proteins comprise. At the same time, there were a lower proportion of peptides predicted for the structural glycoproteins G_N and G_C.

Alignment of the 1072 peptides (total predicted peptides excluding the 21 located across cleavage sites) showed regions of the GPC that contained multiple predicted peptides that overlapped. To quantify this, groups of peptides were assigned numerical values for the number of peptides that overlapped the identical residues (**Supplementary Figure 5.2**). Alignment of the predicted epitopes allowed for comparison to experimentally demonstrated T cell epitopes⁶⁸ (**Figure 5.1A**) and to identify regions with the most predicted peptides (**Figure 5.1B**). All identified peptides aligned to the GPC sequence showed 11 regions with the highest number of overlapping predicted peptides, including the two experimentally shown T cell epitopes. These 11 regions were selected for construction of the multi-epitope antigen (**Figure 5.1C**). It was hypothesized that using large regions of the GPC (≥ 36 residues) would retain the cleavage sites for each predicted epitope to facilitate cleavage and MHC presentation. The 11 regions, referred to as GPC-01 through GPC-11, selected from the epitope alignment include 812 (75.7%) of all predicted CTL and HTL ligands and include 805 residues (47.7%) of the GPC sequence with regions selected from all five proteins of the GPC (**Table 5.2**).

5.3.2 Conservation of Multi-Epitope GPC Regions Between CCHFV Strains

Multiple studies have demonstrated variability of immune responses to homologous or heterologous CCHFV strains^{65,77,80,88,89,183,184,245}. Thus, it was essential to assess the residue conservation of the selected GPC regions between various CCHFV sequences. It was hypothesized that the 11 selected GPC regions would have more significant residue conservation than their originating GPC protein due to the significant diversity of the CCHFV M segment². Fifty GPC sequences from ticks, animals, and clinical cases were

selected with representative sequences from each clade of CCHFV and spanning the widespread geographical distribution of the virus (**Table 2.1 and Supplementary Figure 5.3**). Each of the 11 epitope sequences was compared individually to the same region in the 50 sequences using William Pearson's *lalign* program (https://embnet.vital-it.ch/software/LALIGN_form.html). Sequence conservation was assessed at the residue level for both identity (**Table 5.3**), and similarity (**Table 5.4**), where sequence identity considers only the residues that match strictly between two sequences, and sequence similarity considers residues that match exactly, and of the residues that differ, how similar the physicochemical properties of the residues are. The conservation of the individual GPC proteins was assessed using the same methodology (**Table 5.5**), and the conservation of each epitope region was compared to its respective GPC protein (**Table 5.6**). Assessment of the conservation of the multi-epitope regions showed 5/11 regions of the GPC (GPC-04, GPC-05, GPC-06, GPC-10, and GPC-11) were less conserved than their respective whole proteins, and 6/11 regions (GPC-01, GPC-02, GPC-03, GPC-07, GPC-08, and GPC-09) were more conserved than the whole proteins. While more regions had higher levels of conservation than their respective proteins, these analyses do not support the hypothesis that the 11 GPC regions will be more conserved than their respective GPC proteins, as 5/11 regions were less conserved.

5.3.3 Generation of the Multi-Epitope Antigen

To create the final multi-epitope antigen, the 11 epitope regions were joined together *in silico* using a flexible linker of -glycine-glycine-glycine-serine- (-GGGS-). A start codon was placed at the N-terminus, and a six residue polyhistidine tag (6XHis) was added before

a stop codon at the C-terminus. A signal peptide was not included at the N-terminus of the antigen. It was hypothesized that a lack of signal peptide would result in protein expression within the cytoplasm, to facilitate proteasomal degradation and presentation of cleaved epitopes. The final EPItope Construct (*EPIC*) product with linkers and tag was 853 residues in length and will be referred to as *EPIC* throughout this chapter (**Supplementary Figure 5.4**). *EPIC* was synthesized and subcloned into a mammalian expression vector behind a cytomegalovirus (CMV) promoter (pTWIST-CMV) to create the pTWIST-CMV-*EPIC* plasmid by TWIST Biosciences (**Supplementary Figure 5.5**). The sequence of *EPIC* was confirmed by Sanger sequencing at the UTMB Molecular Genomics Core.

The five transmembrane domains in the GPC play a vital role in the movement of the polyprotein through the ER lumen to facilitate the extensive post-translational cleavage and processing of the structural glycoproteins G_N and G_C ^{2,25,26}. Overexpression of the GPC from transfection of a mammalian expression plasmid or infection with a high multiplicity of infection (MOI) in mammalian cells can localize the structural glycoprotein G_C to the cell membrane^{72,246}. Localization prediction of the G_C by the DeepLoc 1.0 server (<https://services.healthtech.dtu.dk/service.php?DeepLoc-1.0>) predicted that G_C would be localized to the cell membrane with a 90.5% likelihood, with the residues important for localization corresponding to the transmembrane domain (data not shown). The 11 GPC regions joining to form *EPIC* included three transmembrane domains (GPC-05, GPC-06, and GPC-11) from G_N , NS_M , and G_C , respectively. It was hypothesized that the inclusion of the transmembrane domain from the structural glycoprotein G_C would localize *EPIC* to the cell membrane. Localization prediction by the DeepLoc 1.0 server predicted that *EPIC*

was likely to localize to the cell membrane, with a 78.7% likelihood (**Supplementary Figure 5.6A**). The residues most important for the predicted subcellular localization of *EPIC* (**Supplementary Figure 5.6B**) correspond to the three transmembrane domains included in the construct (**Supplementary Figure 5.6C**). These predictions suggested that inclusion of the transmembrane domains within *EPIC* would localize the antigen to the cell membrane similar to that of the structural glycoprotein G_C during transfection and overexpression of the GPC.

5.3.4 Evaluation of Antigen Expression and Detection with CCHFV Antibodies

5.3.4.1 Recognition of EPIC by Anti-6XHis and Anti-CCHFV Polyclonal Antibodies

EPIC was subcloned into a mammalian expression plasmid behind a Cytomegalovirus (CMV) promoter, designed to yield high levels of constitutive expression of the antigen within transfected mammalian cells. To assess the expression of *EPIC*, the immunofluorescence assay developed using RK13 cells in the previous two chapters was used. Transfected cells were probed with a mAb to the 6X polyhistidine tag, His.H8. Since the epitope tag is on the C-terminus of the protein, it was predicted that cells that are fluorescing when probed with this antibody are expressing the full-length *EPIC* protein. Determining high expression levels via IFA is semi-quantitative, so comparisons were made to transfection with a control plasmid, pCAGGS-GFP, expressing green fluorescent protein (GFP) behind a chicken beta-actin promoter, and the pCAGGS-GPC plasmid, expressing the CCHFV Turkey2004 GPC behind a chicken beta-actin promoter. RK13 cells transfected with the three plasmids were probed with either His.H8 or with hyper-immune mouse ascitic fluid (HMAF) generated against CCHFV strain IbAr10200 (**Figure**

5.2). Fluorescent cells were seen from probing pTWIST-CMV-*EPIC* transfected cells with His.H8, indicating that the full-length multi-epitope antigen could be expressed and detected in mammalian cells. There were similar numbers of fluorescing cells between the His.H8 probed pTWIST-CMV-*EPIC* transfected cells, the HMAF probed pCAGGS-GPC transfected cells, and the pCAGGS-GFP transfected cells, which suggests that the transfection efficiency of the three constructs was similar. The brightness of the staining between the His.H8 probed pTWIST-CMV-*EPIC* transfected cells, and the HMAF probed pCAGGS-GPC transfected cells similar, which suggests there were similar levels of expression of both proteins qualitatively.

When pTWIST-CMV-*EPIC* transfected cells were probed with HMAF, fewer fluorescent cells were present compared to transfected cells probed with His.H8. This suggests that *EPIC* recognition by polyclonal serum raised against CCHFV was limited. Although there was little recognition of *EPIC* by HMAF, the staining pattern of diffuse staining throughout the cell with brighter staining at the edges of the cell was also similar between His.H8 probed pTWIST-CMV-*EPIC* transfected cells and the HMAF probed pCAGGS-GPC transfected cells. The similar staining patterns suggest that *EPIC* may be localized to the cell membrane; however, direct assessment of *EPIC* localization to the cell membrane by conducting the IFA without cell permeabilization was not undertaken.

5.3.4.2 Recognition of *EPIC* by Anti-CCHFV mAbs

Since some pTWIST-CMV-*EPIC* transfected cells were recognized by CCHFV HMAF, mAbs against different CCHFV proteins were used to investigate whether epitopes on NP,

Pre-G_N, GP38 or G_C were being expressed on *EPIC*. Cells transfected with either pTWIST-CMV-*EPIC* or pCAGGS-GPC were probed with His.H8 and HMAF as controls and 16 different CCHFV mAbs (**Table 5.7**). As expected, there were no fluorescent cells detected from probing with the two mAbs targeting the NP, and the remaining 14 mAbs targeting different parts of the GPC produced fluorescent cells in the pCAGGS-GPC transfected cells. pTWIST-CMV-*EPIC* transfected cells probed with either His.H8 or HMAF positive control antibodies produced fluorescent cells. However, the remaining cells probed with the 16 anti-CCHFV mAbs did not produce any detectable fluorescent cells. This experiment was repeated with HEK293T cells to ensure the negative results were not solely due to using RK13 cells, which have not previously been used to express the CCHFV glycoproteins. No detectable fluorescent cells were produced from pTWIST-CMV-*EPIC* transfected HEK293T cells probed with the mAbs.

5.3.5 Tolerability of the DNA Vaccine Candidate in a Mouse Model

This study used C57Bl/6J mice to assess vaccine tolerability and immunogenicity, as this strain of mice has been used for the transient immunosuppression mouse model for assessment of other CCHFV DNA vaccines^{72,77,247}. Mice were separated into two groups: ‘vaccinated’ (N=10) and ‘not vaccinated’ (N=18), and all mice received subcutaneous transponders for unique identification and temperature reading. Vaccinated mice received three doses of the DNA vaccine given 21 days apart starting on Study Day 0. Each dose delivered 25 µg of plasmid in 20 µL of DPBS via intramuscular electroporation (IM-EP) into the anterior tibialis muscle.

Five parameters were assessed daily for vaccine tolerability: clinical score, vaccination limb paralysis, redness at the vaccination site, temperature, and body weight. Mice were visually assessed for vaccination site paralysis and redness (presence or absence) as measures specific to using IM-EP. At no point during the study did any mice receive a clinical score other than healthy or experience paralysis in the vaccination limb. All vaccinated mice exhibited redness at the vaccination site following prime vaccination on Study Day 0 (**Figure 5.3A**). Redness quickly subsided, with 70% having redness at one-day post-prime vaccination, 30% on day 2 post-prime, and only one mouse (10%) having redness after three days post-prime; however, this was determined to be due to a bite wound unrelated to the vaccination. No mice displayed redness at the vaccination site following the second or third vaccinations on study days 21 and 42. Temperature and body weight were measured daily. There were no differences in temperature between the two groups of mice throughout the study (**Figure 5.3B**). Following prime vaccination on Study Day 0, differences in percent change in weight from baseline were tested by unpaired t-test, and significant differences in the mean were seen between the vaccinated and not vaccinated groups on Study Days 1 (***, $p = 0.0004$), 2 (**, $p = 0.0033$), and 6 (*, $p = 0.0153$) (**Figure 5.3C**). All mice gained weight post-vaccination, and the initial difference in percent change in weight by the vaccinated mice did not result in a significant difference in the final weights of the mice between groups (**Figure 5.3D**). These data suggest that vaccination via IM-EP with pTWIST-CMV-EPIC results in a mild reaction after prime vaccination that is localized to the vaccination site and resolves quickly, indicating that the vaccine candidate was well-tolerated by the mice.

5.3.6 Immunogenicity of the DNA vaccine candidate in a mouse model

5.3.6.1 Assessment of Humoral Immunogenicity

Serum was collected from each mouse at 20 days after the first and second doses to measure the presence of *EPIC* and GPC binding antibodies by IFA. Pooled sera collected from vaccinated mice after the second dose was used as a primary antibody during IFA to measure binding antibodies to either *EPIC* or the CCHFV GPC (**Figure 5.4**). No fluorescent cells were detected in either the pTWIST-CMV-*EPIC* or pCAGGS-GPC transfected cells, indicating that the vaccinated mice did not produce antibodies that could recognize either antigen.

One possibility for the lack of immunogenicity of this vaccine candidate is the lack of recognition of human epitopes included in the multi-epitope antigen by the mouse immune system. C57Bl6/J mice are MHC haplotype b, and do not possess the MHC class I H-2L or MHC class II I-E loci, which limits their epitope presentation to only MHC class I H2-K and H-2D and MHC class II I-A loci²⁴⁸. To determine if there were any predicted CTL and HTL epitopes in the GPC that would be recognized by C57Bl6/J mice, the NetCTLpan 1.1 (<https://services.healthtech.dtu.dk/service.php?NetCTLpan-1.1>) and NetMHCII 2.3 (<https://services.healthtech.dtu.dk/service.php?NetMHCII-2.3>) Servers were used to predict epitopes limited to the alleles present in C57Bl6/J mice. Both CTL (**Supplementary Table 5.5**) and HTL (**Supplementary Table 5.6**) epitopes were identified within the GPC that are predicted to be recognized by C57Bl6/J mice. The total number of predicted epitopes (35) was significantly lower than the number of epitopes predicted for human MHC alleles (1093), which was expected due to the much lower

number of alleles used for epitope predictions (10 mouse alleles versus 66 human alleles). All of the predicted mouse epitopes were aligned to the GPC using Clustal Omega (**Supplementary Figure 5.7**) to determine if overlapping epitopes were present with the prediction of epitopes for human alleles. This was quantified and graphed as described previously (**Figure 5.5A**). Alignment and graphing of the predicted mouse CTL and HTL epitopes showed that there were 22 out of the 35 total predicted mouse epitopes (62.9%) epitopes that are predicted to be recognized by C57Bl6/J mice that were included in *EPIC* (**Figure 5.5B** and **Table 5.8**). These results, in addition to the IFA for immunogenicity, suggest that although there are mouse epitopes that are predicted across the GPC and included in *EPIC*, these epitopes did not result in a detectable humoral immune response to either *EPIC* or the GPC.

5.3.6.1 Assessment of Cellular Immunogenicity

The Murine Interferon-gamma (IFN- γ) Single-Color Enzymatic Enzyme-Linked Immunospot (ELISpot) Kit (CTL) was chosen to measure IFN- γ release upon antigen recognition from stimulated T cells. Splenocytes from naïve C57Bl6 mice were stimulated with the polyclonal stimulant Concanavalin A (ConA) at 1X per manufacturer instructions or not stimulated to optimize splenocyte seeding density and the use of fresh versus frozen splenocytes. Stimulation was measured as spot forming units per well, and the total spots from each unstimulated well were subtracted from the stimulated wells for each cell seeding density. Frozen splenocytes did not produce spot counts at the level of fresh splenocytes (**Figure 5.6A**). Near-saturation spot counts (approximately 1,600 spots per

well) were achieved using fresh splenocytes seeded at 250,000 cells per well (**Figure 5.6B**).

Several attempts were made to express and purify *EPIC* using the C-terminal polyhistidine tag to use the purified protein as a stimulant for ELISpot assays however, these attempts were unsuccessful. HEK293T cells were lysed 24 hours post-transfection with pTWIST-CMV-*EPIC*, and the lysates were purified using HisPur™ Nickel-nitrilotriacetic acid (Ni-NTA) resin to positively select for the C-terminal polyhistidine tag. Samples were collected throughout the purification process and assessed for the presence of the polyhistidine tag using a dot blot by probing with His.H8 (**Figure 5.7A**). The signal seen from the transfected lysate was decreased in the supernatant post resin binding dot, which suggests that the polyhistidine residues were binding to the resin and were removed from the supernatant. The signal from the elution fractions was much brighter than the signal from the unpurified transfected cell lysate, which suggested that the purification had enriched the polyhistidine tag in the sample. A decrease in signal from elution fraction 1 to elution fraction 2 suggested that more protein was released from the resin during the first elution step than the second elution step, which was expected.

To assess the purity of the sample, the same samples assessed by dot blot, plus others, were run on a gel and stained with SYPRO Ruby gel protein stain (**Figure 5.7B**). Sample input was standardized by volume rather than protein concentration. The expected molecular weight of *EPIC*, without glycosylation, is 87.4 kDa (Geneious Prime Software), but two regions from the CCHFV MLD, which is known to be highly glycosylated, were included

in *EPIC*, and glycosylation of these regions may increase the molecular weight. Compared to the whole cell lysate, samples that were taken throughout the purification process appeared to have fewer bands, which suggests that some cellular proteins were removed during the purification process. No band was seen at the expected molecular weight of *EPIC* at 87.4 kDa in the stained protein gel. There was one band that ran higher than the 100kDa molecular marker, indicated by an arrow, that was present in the transfected cell lysate (lane 3), but not in the untransfected lysate (lane 2) or supernatant post resin binding (lane 4). It is unknown if this band is the *EPIC* expression product. However, a repeat of this experiment showed the same result, which suggests this could be the correct protein. In the lanes corresponding to the three elution fractions, numerous protein bands were present, and there was not a single thick band, which is characteristic of an overexpressed, purified protein.

It was hypothesized that cellular proteins were binding nonspecifically to the resin, leading to numerous bands in the elution fractions. Whole cell lysates of untransfected HEK293T cells and pTWIST-CMV-*EPIC* or pCAGGS-GPC transfected HEK293T were analyzed by western blot by probing with His.H8 to determine if there were polyhistidine containing proteins in the cell lysate (**Figure 5.8**). There were two bands present in all three samples, indicating that His.H8 recognized cellular proteins. The most prominent band from this western blot, which ran higher than the 55 kDa marker, was found in all three lysates and was found repeatedly in the SYPRO Ruby stained protein gels from samples throughout the purification process, which suggests this protein was binding to the resin, complicating the purification process. In the pTWIST-CMV-*EPIC* transfected HEK293T lysate, there

were two unique bands that were recognized by His.H8; however, both of these bands were very faint. One of the unique bands in the pTWIST-CMV-*EPIC* transfected lysate lane ran slightly above the 100kDa marker, which corresponds to the band seen from the SYPRO Ruby protein gel stain. Together, the western blot and SYPRO Ruby protein gel stain experiments suggested that purification of *EPIC* with this method was not sufficiently efficient to be used.

Another attempt to design ELISA and ELISpot assays explored the use of gamma-irradiated CCHFV-infected whole Vero E6 cell lysates. CCHFV-infected whole cell lysates were available for two strains of CCHFV, Ibar10200, and UG3010, but a preparation using Turkey2004, to be homologous to the vaccine candidate, was not available. R430 Gamma-irradiated CCHFV Ibar10200 Lysate (provided by Dr. Tom Ksiazek) was chosen for evaluation, as this is the prototype strain of CCHFV. Total protein concentration of the lysate was measured using a BCA assay, and the lysate was diluted to 0.1 µg/mL, 0.5 µg/mL, and 1 µg/mL for use as a coating antigen for ELISA. The R430 lysate was probed with three mAbs at three different dilutions each (1:500, 1:1000, and 1:2000), His.H8 (nonspecific binding control), 9D5 (CCHFV NP-specific), and 11E7 (CCHFV G_C specific), or no primary (negative control). Only the 9D5 antibody showed antibody and coating concentration-dependent responses, which suggested that the NP was present in the lysate (**Figure 5.9A**). Signal when probing with the 11E7 mAb was not detectable over His.H8, which suggests that G_C was not recognized in the lysate (**Figure 5.9B**). To assess the presence of CCHFV proteins in the R430 lysate with a more sensitive method, a western blot probing with HMAF was completed (**Figure 5.10**). Whole cell

lysates of untransfected HEK293T cells, and pTWIST-CMV-*EPIC* or pCAGGS-GPC transfected HEK293T cells used in the His.H8 western blot were blotted in addition to 10 µg of the R430 lysate. Only one band was seen in the R430 lysate lane that presented at approximately 55kDa, which corresponds to the NP³¹. The structural glycoproteins G_N and G_C present as bands of approximately at 37 kDa and 75 kDa³¹, respectively, which were not seen in either the pCAGGS-GPC transfected lysate or R430 lysate lanes. There was a single faint band in the pCAGGS-GPC transfected lysate between the 130kDa and 250kDa markers, corresponding to a GPC precursor protein³¹. This blot suggested that CCHFV structural glycoproteins were not detectable in either lysate.

Since the R430 lysate was meant to be used as a stimulant for vaccinated mouse splenocytes, it was important to assess if the lysate produced any nonspecific stimulation in naïve splenocytes. Using the ELISpot parameters described above, fresh splenocytes were stimulated with either 1, 10, or 100 µg/mL R430 lysate, 1X ConA, or were left unstimulated (N=3 wells per condition) (**Figure 5.11**). Stimulation with ConA produced significantly more spot counts ($p = <0.0001$) than stimulation with the R430 lysate when analyzed with an one-way ANOVA with Tukey's Post-Hoc correction for multiple comparisons. Stimulation of naïve splenocytes with the R430 lysate did not result in spot counts above the level of the unstimulated spot counts, suggesting the lysate could be used as an antigen-specific stimulant.

The option of assessing cellular immunogenicity using synthesized overlapping peptides spanning either *EPIC* or the GPC was not explored.

5.4 Discussion

The goal of this chapter was to develop and assess a multi-epitope antigen as a vaccine strategy for CCHFV and improve upon current DNA vaccine candidates that utilize the highly complex CCHFV GPC as the vaccine antigen. The research presented in this chapter provides bioinformatic information for potential targets within the GPC for vaccine development and highlights the complex nature of GPC processing. This underlines the necessity of using the whole GPC or whole proteins of the GPC for CCHFV DNA vaccines. This discussion will cover multiple explanations of the results obtained, and a summary of results that differed from expectations and potential explanations for the differences can be found in **Table 5.9**.

Previous studies have shown that T cell immunogenicity is not evenly distributed across the GPC, and certain regions of the GPC generate stronger recall responses than others^{72,77,79}. In this chapter, *in silico* analyses of CTL and HTL epitopes within the Turkey2004 GPC demonstrate an uneven distribution across the GPC, with certain regions displaying more predicted epitopes than others (Tables 5.1 and 5.2; Figure 5.1; **Supplementary Tables 5.1, 5.2, 5.3 and 5.4; Supplementary Figures 5.1 and 5.2**). These results confirm the published results of splenocyte stimulation with peptide pools spanning the GPC, where splenocytes are not uniformly stimulated across the GPC. Additionally, graphing the predicted T cell epitopes was similar to the results of linear antibody epitope mapping of pooled Turkish sera to peptides generated against the CCHFV strain Turkey-Kelkit06⁸⁹. Together, results from the reactivity of T cells^{77,78}, antibody binding⁸⁹, and prediction of epitopes across the CCHFV GPC (this chapter)²⁴⁰⁻²⁴², provides information

on the regions of the GPC which are predicted to be the most immunogenic and potential targets for vaccine development.

Interestingly, more epitopes were predicted to regions located in the nonstructural proteins than the structural glycoproteins, relative to protein size. This finding is similar to data showing that stimulation with peptides homologous to the vaccine strain generates greater recall responses to nonstructural proteins than the structural glycoproteins, but not with heterologous peptides⁷⁷. It was hypothesized that the selected multi-epitope regions would be more conserved across CCHFV clades than the whole proteins from which the regions originated. MLD is the most genetically diverse protein of the GPC (**Table 5.5**), and this was the only region where both multi-epitope regions demonstrated greater than or equal levels of residue identity and similarity across 50 CCHFV sequences than the whole protein. Regions selected from other GPC proteins had mixed results of either greater or lesser conservation than the whole proteins. Overall, more significant conservation of epitope regions compared to whole proteins was predicted with 6/11 regions, and the remaining 5/11 regions were not more conserved than the whole proteins (**Tables 5.3, 5.4, 5.5, and 5.6; Table 2.1; Supplementary Figure 5.3**). In combination with published data showing variability in immune reactivity between strains^{77,89}, these data suggest that given the widespread distribution of CCHFV, the development of regionally strain-specific vaccines is worth consideration, or that future work should focus on regions with the most significant residue conservation to generate a vaccine candidate that produces heterologous protection across CCHFV clades.

The bioinformatic analyses in this chapter predicted epitopes using the amino acid sequence of the GPC from strain Turkey2004, followed by the evaluation of residue conservation of selected GPC regions across CCHFV clades. The bioinformatic servers predict epitopes based on linear amino acid sequences for protein cleavage and binding of peptides to MHC complexes. The *in silico* analysis is designed to provide information about epitopes that may bind to MHC complexes, however, the complex nature of this biological process is difficult to predict, so it is likely that at least some or many of the predicted epitopes are not immunogenic. Sequence variability can affect the prediction of epitopes, leading to vastly different prediction results. Given the wide range of sequence variability within some of the GPC proteins, epitope predictions could be improved by completing the analyses with multiple CCHFV GPC sequences from diverse strains, then choosing regions based on homologously predicted peptides, rather than assessing conservation after regions were chosen from epitope predictions from a single sequence of GPC.

Recent research in multi-epitope vaccines for CCHFV has been limited to computational studies and the use of bioinformatic servers²⁴⁰⁻²⁴². The work presented here is the first study to evaluate a CCHFV derived multi-epitope antigen *in vitro* and compare the antigen directly to the whole GPC for assessment of antibody binding (**Supplementary Figure 5.4**). Previous attempts at epitope mapping of the GPC have used peptide scan ELISA or microarray approaches^{75,87,89,90}; this work was the first to explore antibody binding of different GPC regions in a single protein rather than peptides. It was hypothesized that using long stretches of the GPC (≥ 36 residues) would maintain some of the secondary

structure of these regions and, therefore conformational antibody binding epitopes within the antigen, making *EPIC* more likely to bind CCHFV antibodies than previous peptide approaches. Expression of the synthesized multi-epitope antigen in a mammalian expression plasmid could be detected using antibodies to the C-terminal polyhistidine tag, indicating that the full-length protein was being expressed; however, few cells were positive when CCHFV polyclonal sera were used to detect the antigen compared to the polyhistidine tag. It is unlikely that the reduction in binding of the HMAF is due to the sequence of *EPIC* being based on the Turkey2004 sequence since the full-length GPC sequence used as a control was also strain Turkey2004. Any CCHFV mAbs could not detect *EPIC*, and this result was seen using both RK13 and HEK293T cells by IFA. Together, the limited staining of *EPIC* with HMAF and the lack of recognition by any CCHFV mAbs suggest that even with the use of long residue length regions of the GPC, omitting large sections of the GPC likely prevented proper processing and folding for the formation of most GPC conformational epitopes. (**Figure 5.2; Table 5.7**). At 853 residues, *EPIC* is a large antigen that includes three transmembrane domains, making antigen processing complex within the cell. Improper protein folding and processing due to the lack of signal peptide in *EPIC*, which was omitted for expression of *EPIC* in the cytoplasm to facilitate proteasomal cleavage, could be a potential explanation of the poor expression of antigens. Future work on development of CCHFV multi-epitope antigens would need to include a signal peptide for protein processing in the ER, similar to the CCHFV GPC.

It was hypothesized that the inclusion of epitopes in *EPIC* recognized by MHC class II molecules would generate HTLs that activate B cells to generate humoral responses since

a multi-epitope vaccine for HTNV, SEOV, and PUUV generated binding and neutralizing antibodies against all three viruses²⁴⁴. Vaccination with the DNA vaccine candidate was well-tolerated in C57Bl/6J mice (**Figure 5.3**), but the vaccine did not induce detectable humoral immunity in this mouse model after two doses (**Figure 5.4**). The regimen for other CCHFV DNA vaccines and the HTNV, SEOV, and PUUV multi-epitope vaccine is three doses, using high-efficiency expression vectors such as pCAGGS^{72,75,77,78,244}, and each dose increases antigen-specific humoral responses. A pCAGGS-GPC plasmid was used in transfection experiments throughout this chapter, but unfortunately was not included for a positive control group in this study. Given the lack of a response following the first two vaccinations, immunogenicity was not assessed following the third dose of pTWIST-CMV-*EPIC*. It would have been interesting to assess immunogenicity after the third dose of this vaccine candidate to rule out the possibility of a humoral response being at a detectable level after an additional dose; however, the immune response would be predicted to be low. Inclusion of a pCAGGS-GPC vaccinated group would have lent much needed information about whether the mice in this study were able to mount humoral responses to CCHFV GPC proteins, or if there were issues with the IM-EP. It is possible that using IFA to detect a humoral response was not a sensitive enough method to detect low levels of binding antibodies induced by vaccination, and that binding antibodies still would not have been detectable at the end of the study using this method. Serum from pCAGGS-GPC vaccinated mice could have been used as a positive control to determine if humoral immune responses could be detected using IFA. Development of a more sensitive detection method, such as using *EPIC* as a binding antigen in ELISA, was not possible due to issues expressing and purifying the protein (**Figure 5.7, 5.8, and 5.10**).

A significant limitation of this study was the inability to assess T cell responses in vaccinated animals since the generation of this antigen was based on T cell epitope prediction, and T cells play an essential role in the survival of humans from severe CCHF infection^{66,85}. Previous studies have used IFN- γ production of splenocytes after antigen stimulation to measure antigen-specific CD8+ CTL reactivity. IFN- γ producing T cells could be quantified from splenocytes of naïve C57Bl/6 mice stimulated with the polyclonal stimulant ConA, with fresh splenocytes seeded at 250,000 cells per well, giving near-saturation spot counts (**Figure 5.6**). These results demonstrated the feasibility of using the Murine IFN- γ Single-Color Enzymatic ELISpot Kit (CTL) to measure cellular immune responses in C57Bl/6 mice. Although *EPIC* is approximately half the size of the GPC, generation of overlapping peptides spanning either *EPIC* or the GPC for use as a stimulant for ELISpots, as in previous studies^{66,77,78}, was not feasible for this study. Instead, generation of antigen-specific reagents to assess cellular responses in pTWIST-CMV-*EPIC* vaccinated mice explored expression and purification of *EPIC* and the use of gamma-irradiated CCHFV-IbAr10200-infected whole Vero E6 cell lysates.

There were multiple attempts to purify *EPIC* using the C-terminal polyhistidine tag to select for the protein out of whole cell lysate, which were unsuccessful. An increase in signal was seen from purification elution fractions compared to whole cell lysate of pTWIST-CMV-*EPIC* transfected HEK293T cells in a His.H8 probed dot blot, which suggested that polyhistidine residues had been enriched within the sample (**Figure 5.7A**), however, when these samples were analyzed by SYPRO Ruby protein gel stain, multiple bands were seen within the elution fractions, indicating the presence of numerous cellular

proteins that had not been removed during purification (**Figure 5.7B**). There was one faint band of interest unique to the pTWIST-CMV-*EPIC* transfected HEK293T cell lysate that was visualized above the 100kDa marker by both SYPRO Ruby protein gel stain and His.H8 western blot that could have been the *EPIC* expression product; however, no further studies were undertaken to confirm if this was the *EPIC* expression product. Together, the His.H8 western blot and SYPRO Ruby protein gel stain suggested that *EPIC* had a low level of expression, which did not make purification of *EPIC* feasible. These results were in contrast to the IFA results, where a bright signal insinuated a high level of expression of the protein within individual cells. These results are also in contrast to the immunogenic HTNV, SEOV, and PUUV multi-epitope vaccine, where the multi-epitope antigen was highly expressed and purified for use in a splenocyte proliferation assay²⁴⁴. A significant limitation throughout these purification attempts was the lack of a plasmid vector control. These studies would have benefitted from the use of a different protein within the pTWIST-CMV vector, such as a 6XHis-tagged GFP, to control for plasmid expression levels. If a different protein within the same pTWIST-CMV vector demonstrated high levels of expression, and could have been purified using the HisPur™ Ni-NTA resin, this would have demonstrated that there were issues with the *EPIC* protein itself. As this control was not available, it is unknown if expression and purification issues are due to the *EPIC* protein, mammalian expression vector, or the purification method.

As an alternative to purifying *EPIC* for assessment of pTWIST-CMV-*EPIC* induced cellular immunity, these studies explored the use of gamma-irradiated CCHFV-IbAr10200-infected whole Vero E6 cell lysates (R430). This option was chosen secondary

to purifying *EPIC* since previous studies have shown that splenocytes from vaccinated animals are less responsive to peptides from heterologous strains of CCHFV⁷⁷. Probing of the R430 lysate with CCHFV mAbs to the NP and G_C by ELISA (**Figure 5.9**), or with HMAF via western blot (**Figure 5.10**), suggested that the NP, but not G_C, was detectable in the lysate. pCAGGS-GPC transfected HEK293T cell lysate was used as a positive control for the HMAF western blot. HEK293T cells are commonly used to generate GPC lysates at 48 hours post-transfection for analysis of G_N and G_C by western blot⁷⁷. There was a faint band in the positive control lane between the 130kDa and 250kDa markers, which may correspond to a GPC precursor protein³¹. The very faint band of a precursor protein suggests that harvesting of the lysates at 24 hours post-transfection, which was chosen from IFA results, may not give enough time for antigen production and protein processing. These results could also be due to low transfection efficiency, which may be an explanation for protein expression issues throughout these studies.

Ultimately, cellular immunogenicity from pTWIST-CMV-*EPIC* vaccinated mice was not assessed, as there was no antigen-specific stimulant available to conduct the ELISpot assays. For assessment of cellular immunogenicity from future CCHFV vaccine candidates, it would be interesting to use GPC-transfected HEK293T cell lysates as a stimulant for ELISpot assays, since these studies suggest that whole cell lysates could be used as an antigen-specific stimulant, since splenocytes from naïve mice did not react to CCHFV-infected Vero E6 lysates (**Figure 5.11**). Perhaps more interesting would be the use of virus-like-particles or purified G_N or G_C as stimulants to be able to compare the

reactivity of splenocytes to whole virus particles, whole proteins, or the current method of peptide pools.

Overall, there are multiple considerations regarding the results of this chapter, and a lack of proper controls throughout the experiments prevents a single explanation for the lack of detectable immunogenicity from pTWIST-CMV-*EPIC* vaccinated C57Bl/6J mice. While humoral immunogenicity was not detected using IFA, it is possible that cellular immunity may have been detectable, had an antigen-specific stimulant been available to complete the ELISpot assays. Issues with antigen expression could be due to antigen size, lack of a signal peptide, plasmic vector choice, or transfection efficiency. Evaluation of this vaccine candidate designed from predictions of human epitopes in a mouse model is a significant limitation of the studies in this chapter and may be another explanation for the lack of immunogenicity. Predictions for epitopes across the GPC recognized by C57Bl6/J mice resulted in a significantly lower number of epitopes compared to predictions for human epitopes. The possibility cannot be ruled out that this vaccine candidate may be immunogenic in a different animal model due to variation in MHC haplotypes and epitope processing, such as the *Cynomolgus macaque* model that is more closely related to humans and has also been used to assess CCHFV DNA vaccines⁷⁸.

In conclusion, the lack of detectable immunogenicity from this vaccine candidate showcases the need to use the whole GPC or whole proteins of the GPC as vaccine antigens until more information is available regarding protective CCHFV epitopes for future development of multi-epitope vaccines.

Table 5.1: Total CTL and HTL predicted epitopes by GPC region.

Total CTL and HTL epitope prediction results from using the NetCTL 1.2 (<https://services.healthtech.dtu.dk/service.php?NetCTL-1.2>) and NetMHCII 2.3 (<https://services.healthtech.dtu.dk/service.php?NetMHCII-2.3>) servers are shown. Epitopes were aligned to the Turkey2004 GPC sequence to determine corresponding GPC region.

Number of Predicted Epitopes					
GPC Region	Type of Epitope				Total
	CTL	HLA-DR	HLA-DQ	HLA-DP	
MLD	19	39	140	11	209 (19.1%)
MLD-GP38*	0	0	0	0	0 (0%)
GP38	41	94	17	25	177 (16.2%)
GP38-G_N*	1	0	0	0	1 (0.1%)
G_N	54	42	10	37	143 (13.1%)
G_N-NS_M*	2	5	5	0	12 (1.1%)
NS_M	40	43	66	14	163 (14.9%)
NS_M-G_C*	1	3	4	0	8 (0.7%)
G_C	98	130	100	52	380 (34.8%)
Total	256	356	342	139	1093 (100%)

*Epitopes located across cleavage sites

Table 5.2: Total CTL and HTL predicted epitopes in each selected multi-epitope region.

The ten regions of the GPC with the greatest number of overlapping epitopes, and an eleventh region containing predicted epitopes in addition to an experimentally demonstrated epitope⁶⁸ were selected and named as Epitope Regions GPC-01 through GPC-11. Shown below is the length in residues of each region, and the number and type of predicted epitopes included in each selected region.

Number of Predicted Epitopes							
Epitope Region	Length	GPC Protein	Type of Epitope				Total
			CTL	HLA-DR	HLA-DQ	HLA-DP	
GPC-01	77	MLD	6	11	62	0	79
GPC-02	40	MLD	4	15	63	0	82
GPC-03	36	GP38	9	19	0	7	35
GPC-04	97	GP38	17	52	14	18	101
GPC-05	100	G _N	32	9	7	35	83
GPC-06	85	NS _M	15	36	45	10	106
GPC-07	63	G _C	11	16	23	0	50
GPC-08	56	G _C	8	2	10	0	20
GPC-09	101	G _C	14	22	16	0	52
GPC-10	58	G _C	11	39	44	0	94
GPC-11	92	G _C	21	43	0	46	110
Total			148	264	284	116	812

Table 5.3: Percent identity of each multi-epitope region between 50 different CCHFV GPC sequences.

Each of the 11 CCHFV Turkey2004 multi-epitope region sequences were compared individually to the same region in 50 selected sequences across all CCHFV clades using William Pearson's *align* program run through the Swiss Institute of Bioinformatics ExPASy Bioinformatics Resource Portal (https://embnet.vital-it.ch/software/LALIGN_form.html). The percentage of amino acid identity between Turkey2004 sequence and the listed sequence is shown.

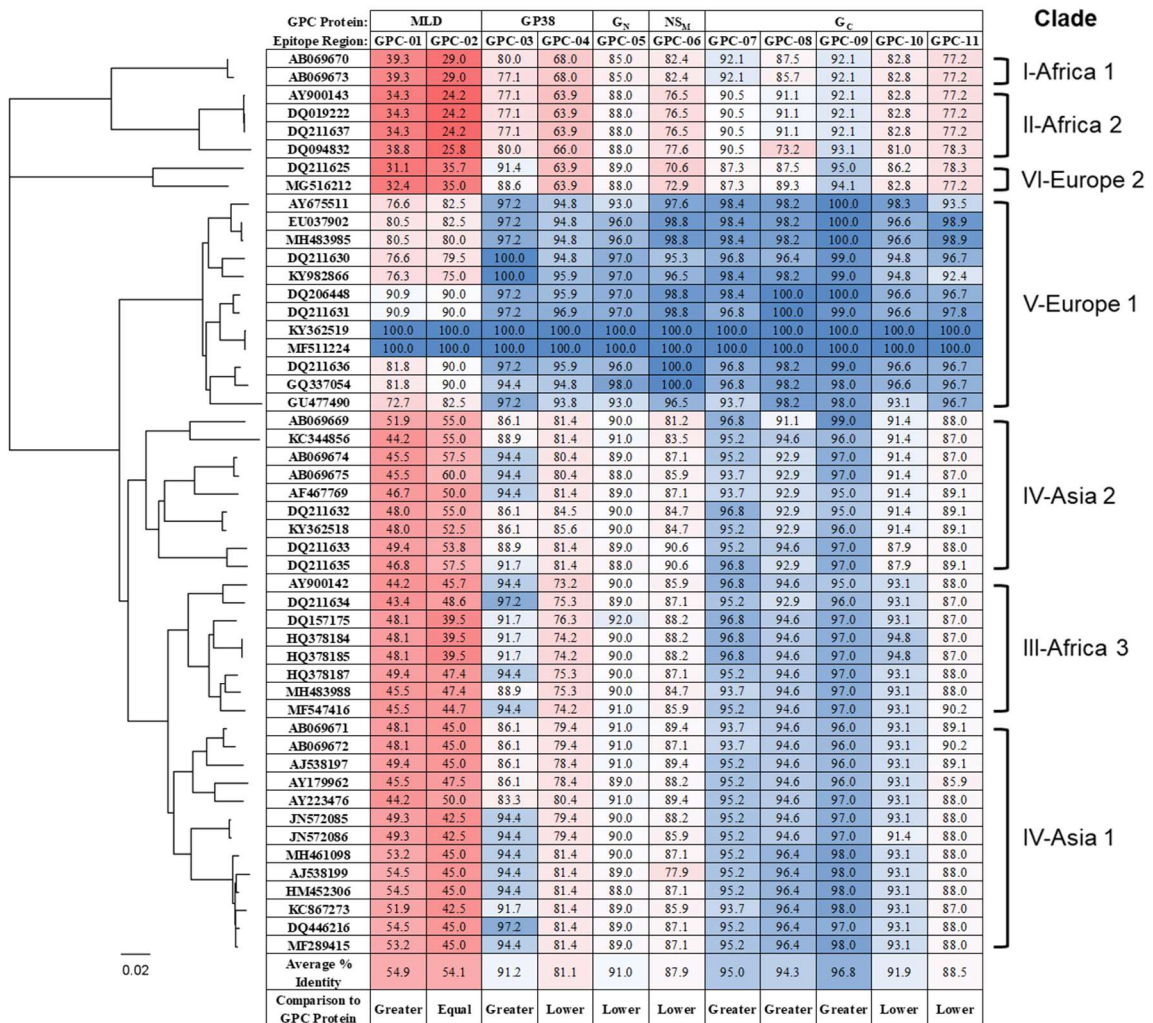


Table 5.4: Percent similarity of each multi-epitope region between 50 different CCHFV GPC sequences.

Each of the 11 CCHFV Turkey2004 multi-epitope region sequences were compared individually to the same region in 50 selected sequences across all CCHFV clades using William Pearson's *align* program run through the Swiss Institute of Bioinformatics ExPASy Bioinformatics Resource Portal (https://embnet.vital-it.ch/software/LALIGN_form.html). The percentage of amino acid similarity between Turkey2004 sequence and the listed sequence is shown.

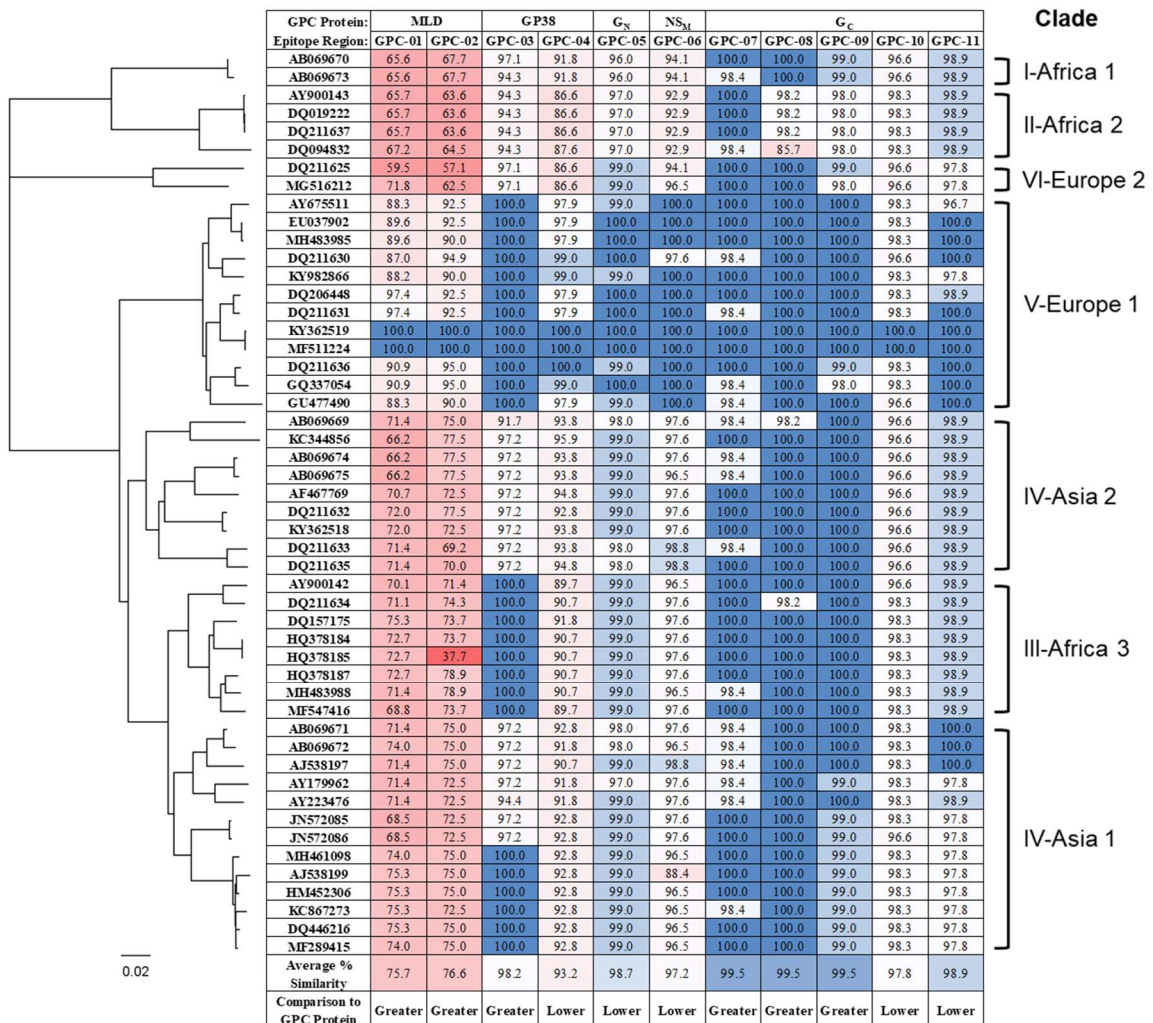


Table 5.5: Percent identity and similarity of each GPC protein between 50 different CCHFV GPC sequences.

Each Turkey2004 GPC protein sequence was compared individually to the same protein sequence in 50 selected sequences across all CCHFV clades using William Pearson's *align* program (https://embnet.vital-it.ch/software/LALIGN_form.html) through the Swiss Institute of Bioinformatics ExPASy Bioinformatics Resource Portal. The percentage of amino acid identity (Id.) and similarity (Sim.) between Turkey2004 sequence and the listed sequence is shown.

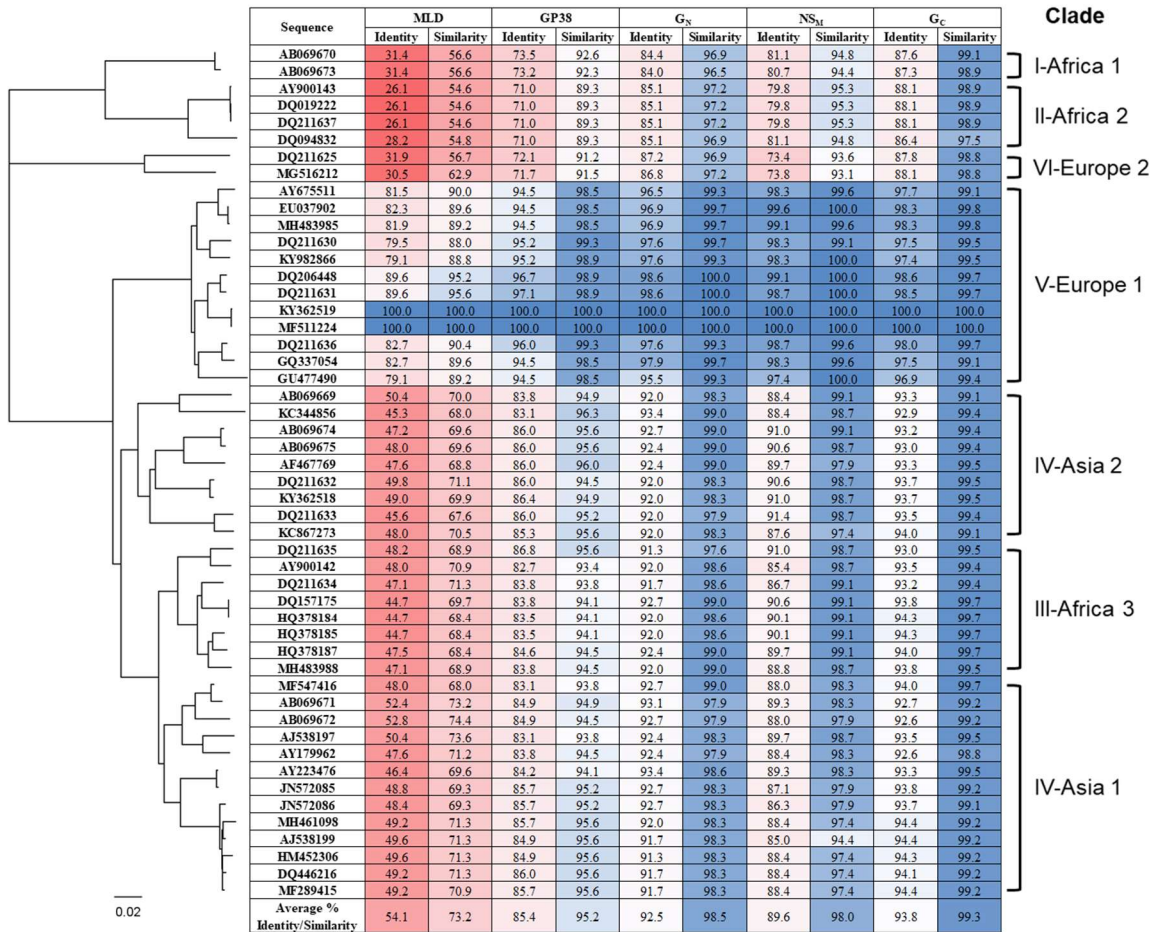


Table 5.6: Summary of residue conservation between GPC proteins and multi-epitope regions.

The average percent identity and similarity of each GPC protein (A) from comparison of the Turkey2004 sequence to 50 selected GPC sequences is shown. The average percent identity and similarity of each epitope region was compared to the average percent identity and similarity, respectfully, of the GPC protein the epitope region originated from (B).

A

GPC Protein	Average % Identity	Average % Similarity
MLD	54.1	73.2
GP38	85.4	95.2
G_N	92.5	98.5
NS_M	89.6	98.0
G_C	93.8	99.3
Total	83.1	92.9

B

Epitope Region	GPC Protein	Average % Identity	Average % Similarity	Comparison to Protein (Id/Sim)
GPC-01	MLD	54.9	75.7	↑/↑
GPC-02	MLD	54.1	76.6	=/↑
GPC-03	GP38	91.2	98.2	↑/↑
GPC-04	GP38	81.1	93.2	↓/↓
GPC-05	G _N	91.0	98.7	↓/↓
GPC-06	NS _M	87.9	97.2	↓/↓
GPC-07	G _C	95.0	99.5	↑/↑
GPC-08	G _C	94.3	99.5	↑/↑
GPC-09	G _C	96.8	99.5	↑/↑
GPC-10	G _C	91.9	97.8	↓/↓
GPC-11	G _C	88.5	98.9	↓/↓
Total	-	84.3	94.1	↑/↑

↑ Greater identity/similarity of epitope region to respective protein

= Equal identity/similarity of epitope region to respective protein

↓ Lesser identity/similarity of epitope region to respective protein

Table 5.7: *EPIC* is not recognized by CCHFV monoclonal antibodies.

The results of an IFA are shown. pTWIST-CMV-*EPIC* transfected RK13 cells had fluorescent cells when probed with His.H8 and HMAF antibodies but had no fluorescent cells when probed with any of the mAbs. The pCAGGS-GPC transfected RK13 cells did not have any fluorescent cells when probed with the polyhistidine epitope tag or nucleoprotein targeting antibodies but did have fluorescent cells when probed with all antibodies targeting the GPC, as expected.

Antibody	GPC Protein Target	GPC Transfected Cells	<i>EPIC</i> Transfected Cells
His.H8	N/A	Negative	Positive
HMAF	All Proteins	Positive	Positive
9D5	NP	Negative	Negative
2B11	NP	Negative	Negative
11F6	Pre-G _N	Positive	Negative
13G8	GP38	Positive	Negative
5A5	GP38	Positive	Negative
8F10	GP38	Positive	Negative
10E11	GP38	Positive	Negative
7F5	GP38	Positive	Negative
6B12	GP38	Positive	Negative
11E7	G _C	Positive	Negative
3E3	G _C	Positive	Negative
1H6	G _C	Positive	Negative
30F7	G _C	Positive	Negative
12A9	G _C	Positive	Negative
13G5	G _C	Positive	Negative
8A1	G _C	Positive	Negative

Table 5.8: Total mouse CTL and HTL predicted epitopes in each selected multi-epitope region.

The results of the alignment of the mouse epitopes to the GPC, and the number and type of predicted epitope included in each of the 11 epitope regions included in the multi-epitope antigen.

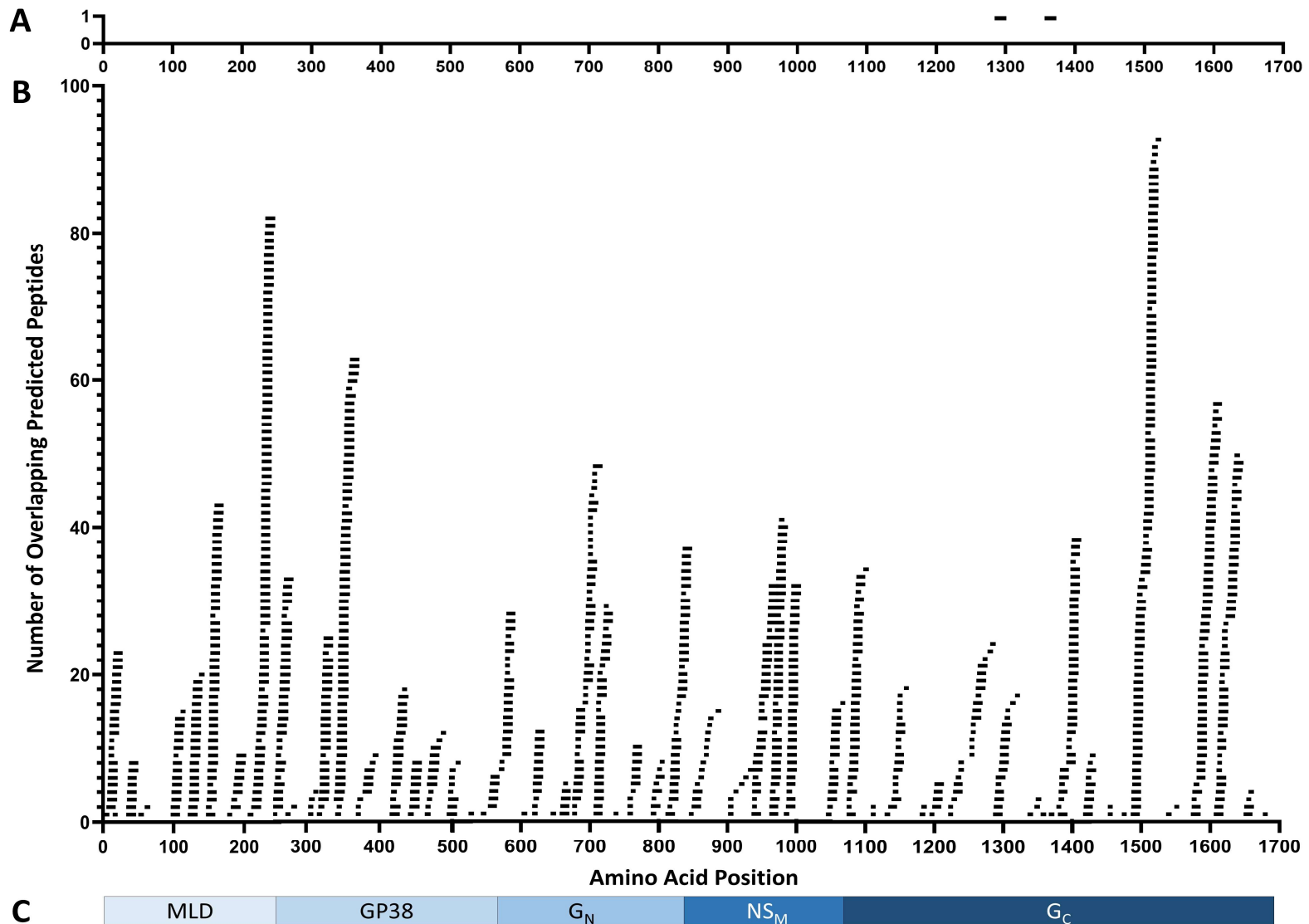
Number of Predicted Mouse Epitopes				
Epitope Region	Type of Epitope			Total
	H2-K	H2-D	I-A	
GPC-01	0	2	5	7
GPC-02	0	1	6	7
GPC-03	0	1	0	1
GPC-04	0	0	0	0
GPC-05	0	0	0	0
GPC-06	0	0	0	0
GPC-07	0	0	4	4
GPC-08	0	0	3	3
GPC-09	0	0	0	0
GPC-10	0	0	0	0
GPC-11	0	0	0	0
Total	0	4	18	22 (62.9%)

Table 5.9: Summary of results that differed from expectations, and potential explanations.

Expected Result	Result Obtained	Potential Explanation(s)
Epitopes predicted by the software are immunogenic	Multi-epitope antigen is not immunogenic	Epitopes were selected through bioinformatic analyses, not experimentally demonstrated immunogenic epitopes. The epitopes predicted by the servers could be non-immunogenic.
Recognition of <i>EPIC</i> by CCHFV HMAF or mAbs	Reduced number of fluorescent cells from probing with HMAF compared to His.H8; no <i>EPIC</i> recognition with mAbs	Likely that only using parts of the GPC led to improper protein folding or secondary structure of the included regions, therefore conformational epitopes were not retained.
High level of <i>EPIC</i> expression and detection of <i>EPIC</i> using western blot	No band at expected size, faint unique band in transfected lysate	Unknown if the lack of detection of <i>EPIC</i> expression product is due to low expression of the plasmid, since there was not a control for a different protein in the same backbone.
Purified <i>EPIC</i> protein for use in ELISA and ELISpot assays	Expression and purification methods not sufficiently efficient for producing purified protein	Low levels of protein expression resulted in nonspecific binding of cellular proteins to purification resin. Did not have a 6XHis tagged protein expression vector control.
Immunogenic vaccine candidate	Serum of vaccinated mice did not recognize <i>EPIC</i> or GPC transfected cells by IFA	IFA is not the most sensitive method for assessment of binding antibody responses. Further, the mouse study lacked a positive control. This missing element could have provided information if the lack of immunogenicity was due to the antigen, plasmid vector, or if there were issues with the electroporation.
ELISpot assay for assessment of cellular immunity	ELISpot assay could not be completed using vaccinated mouse splenocytes	Lack of experience with the assay, and lack of antigen-specific reagent available for use in the assay. ConA worked for stimulation of naïve splenocytes, but the glycoproteins were not detected from the R430 lysate, and <i>EPIC</i> could not be purified for use in the assay.

Figure 5.1: Alignment of all included epitopes to the GPC.

(A) Location of two experimentally demonstrated T cell epitopes aligned to the GPC⁶⁸. (B) Alignment of all predicted epitopes to the GPC, excluding the 21 epitopes predicted across known GPC cleavage sites, for a total of 1072 aligned epitopes. (C) Schematic diagram of the five post-cleavage GPC proteins and 11 regions of the GPC chosen for generation of the multi-epitope antigen.



(A)

Figure 5.2: *EPIC* is expressed in mammalian cells and is detectable with antibodies to the C-terminal polyhistidine tag and polyclonal CCHFV serum.

RK13 cells were fixed and stained 24 hours after transfection with pTWIST-CMV-*EPIC*, pCAGGS-GPC, or pCAGGS-GFP. This figure shows specific detection of *EPIC* with the antibody to the polyhistidine tag, with similar numbers of fluorescing cells compared to the GFP control. Detection of *EPIC* with the CCHFV polyclonal serum shows reduced numbers of fluorescing cells compared to the GPC and GFP controls.

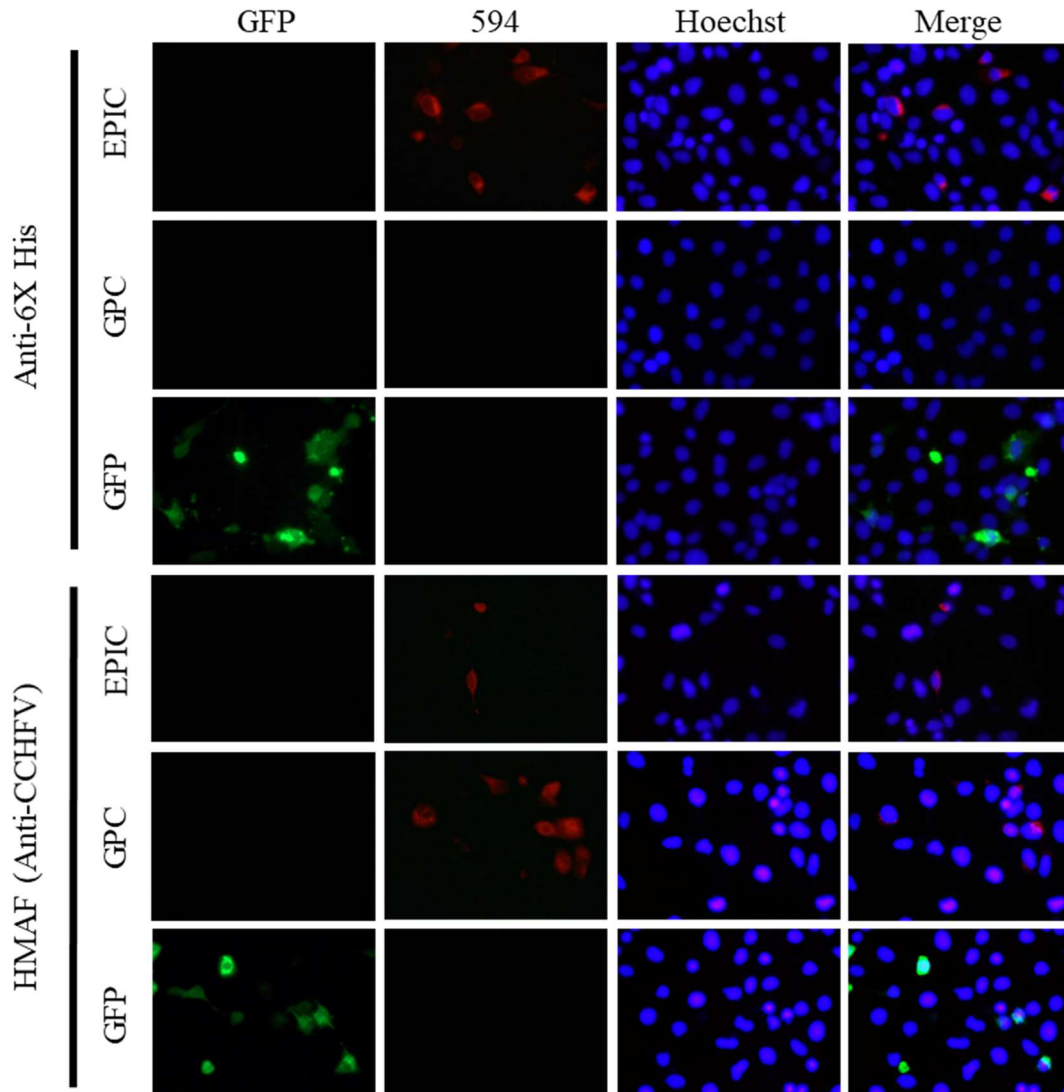
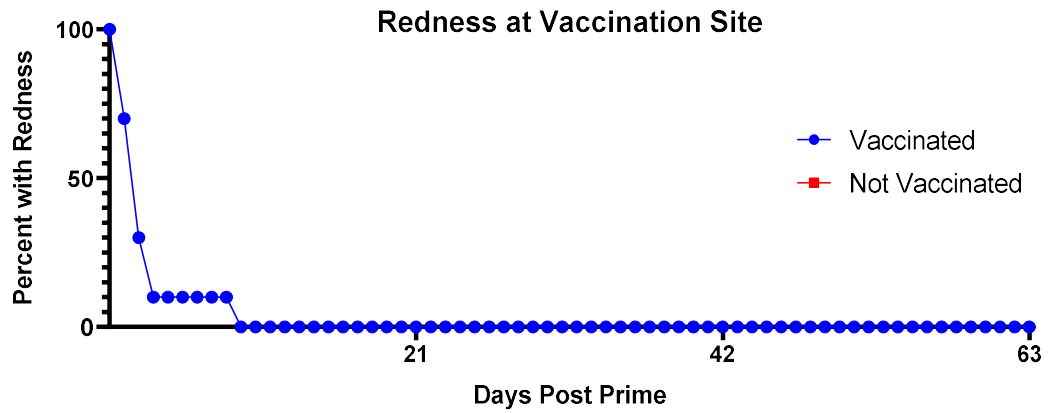


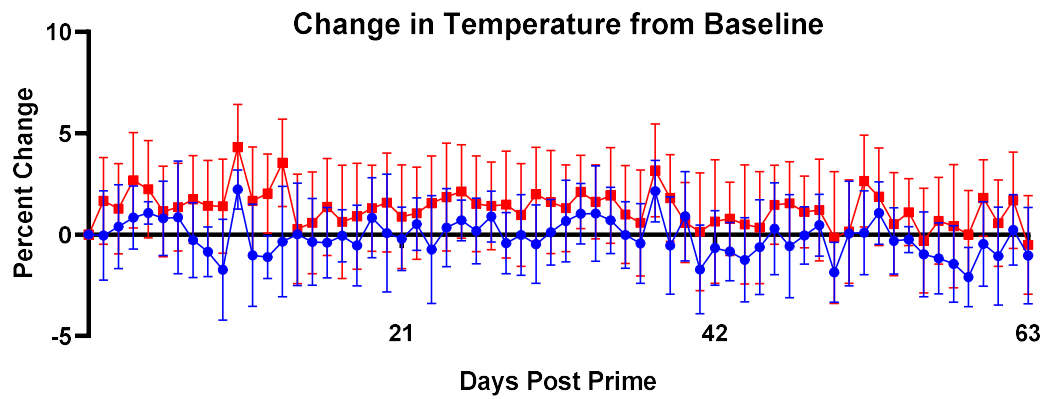
Figure 5.3: EPIC is well-tolerated as a DNA vaccine given via IM-EP.

C57Bl6/J mice were given three DNA plasmid doses at 21-day intervals. Mice were assessed daily for give measures of vaccine tolerability: redness at the vaccination site (A), temperature (B), weight (C and D), paralysis of the vaccination limb, and clinical scores. No mice experienced any paralysis or clinical scores throughout the study (data not shown).

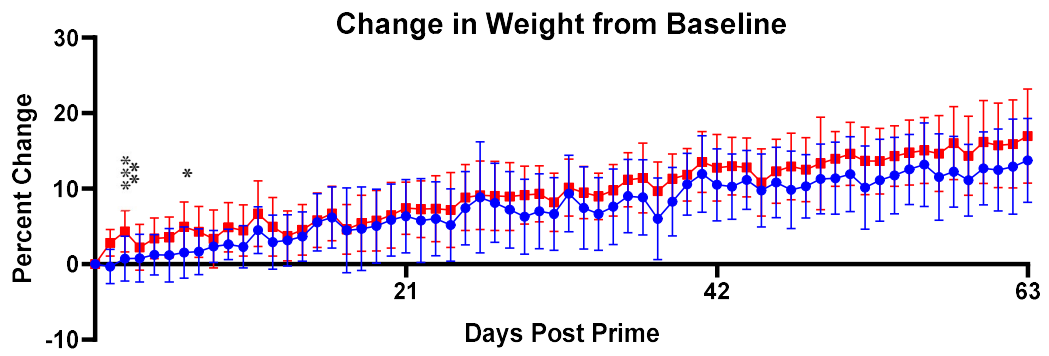
A



B



C



D

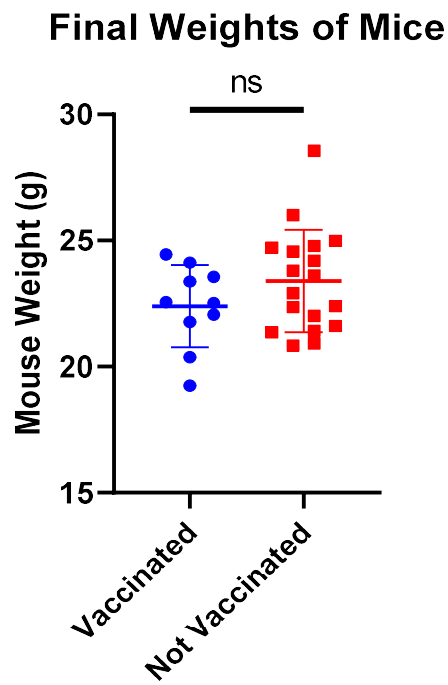


Figure 5.4: Vaccinated mouse serum does not recognize *EPIC* or *GPC* expressed in mammalian cells.

RK13 cells were fixed and stained 24 hours after transfection with pTWIST-CMV-*EPIC* or pCAGGS-*GPC*. This figure shows no fluorescent cells in either transfected cell group from probing with pooled serum from pTWIST-CMV-*EPIC* vaccinated mice.

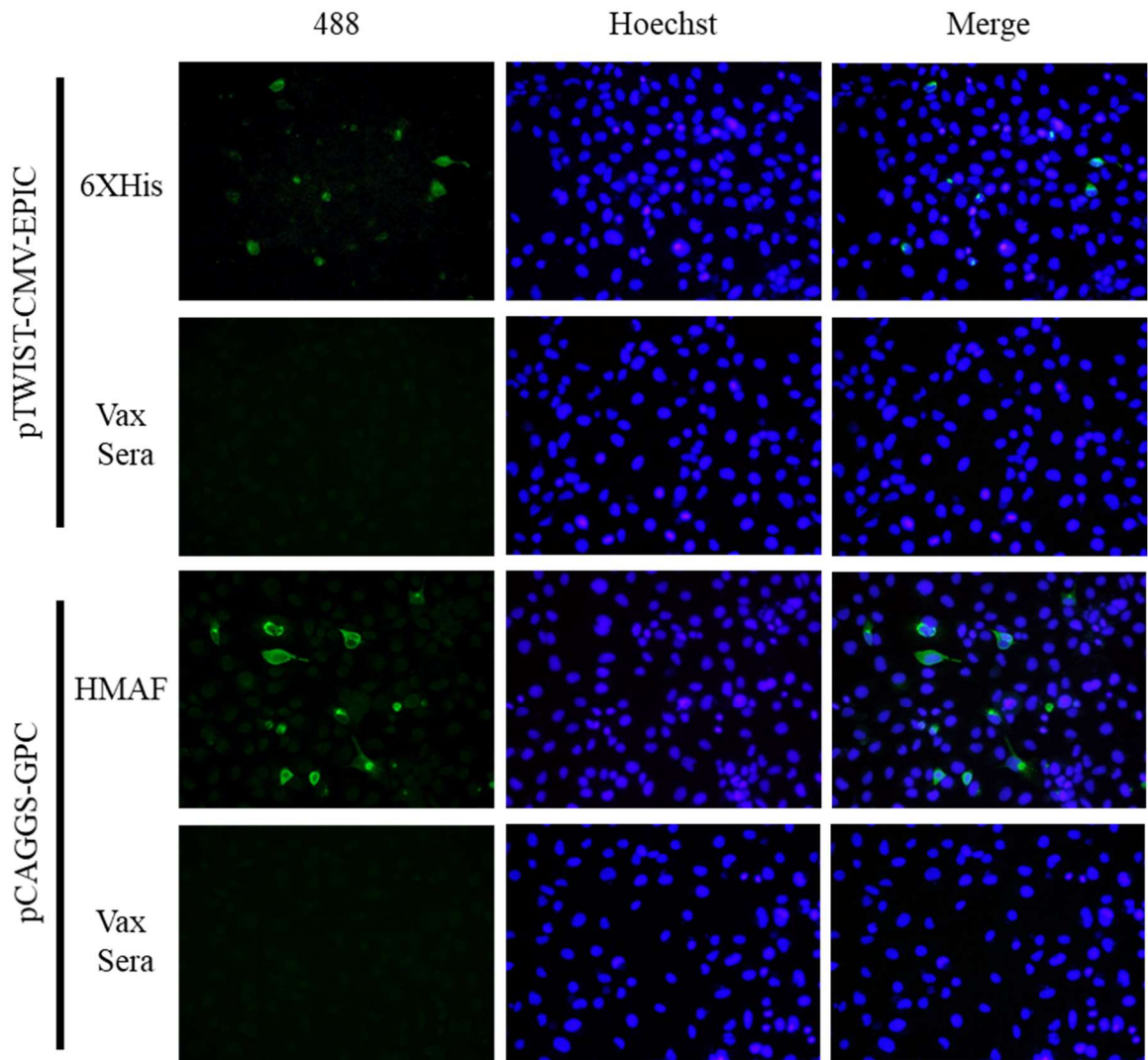


Figure 5.5: Alignment of all mouse epitopes to the GPC.

(A) Alignment of the 35 predicted mouse epitopes to the GPC. (B) Schematic diagram of the five post-cleavage GPC proteins and 11 regions of the GPC chosen for generation of the multi-epitope antigen. The figure shows that regions included in the multi-epitope antigen include some epitopes predicted to bind to the mouse H-2 complex alleles.

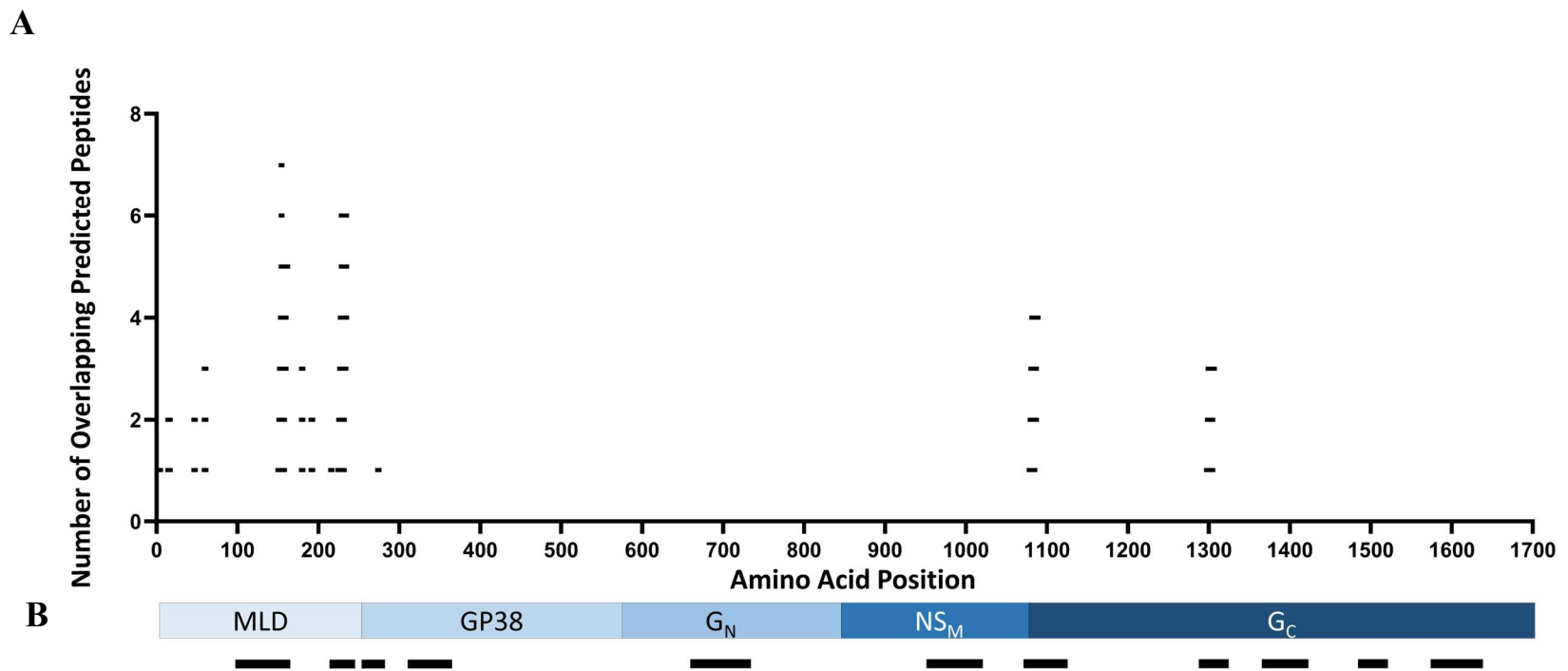


Figure 5.6: IFN- γ + T cells quantified by ELISpot after polyclonal stimulation with ConA.

(A) Fresh or thawed from frozen splenocytes from naïve C57Bl6 mice were stimulated with ConA or unstimulated and assessed for IFN- γ production. Fresh splenocytes had higher levels of IFN- γ production. (B) Near-saturation spot counts with stimulation of ConA (approximately 1600 spots per well) were achieved with seeding of 250,000 fresh splenocytes per well.

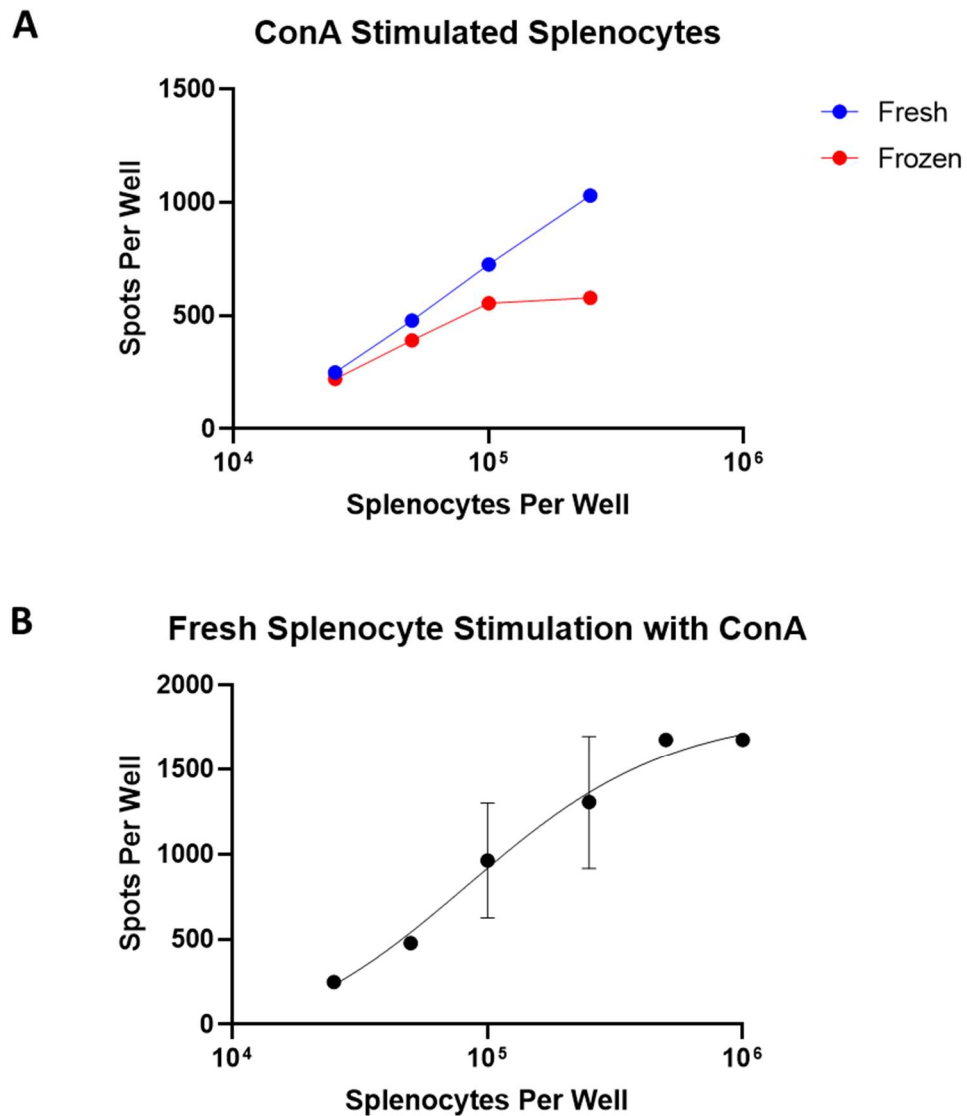


Figure 5.7: HisPur™ Ni-NTA resin purification of EPIC.

(A) Dot blot of samples taken throughout the purification process of *EPIC*. (B) SYPRO Ruby protein gel stain of samples taken throughout the purification process of *EPIC*. (1) Ladder, (2) Untransfected Lysate, (3) Transfected Lysate, (4) Supernatant Post Resin Binding, (5) Wash 1, (6) Wash 2, (7) Elution Fraction 1, (8) Elution Fraction 2, (9) Elution Fraction 3, (10) Bovine Albumin

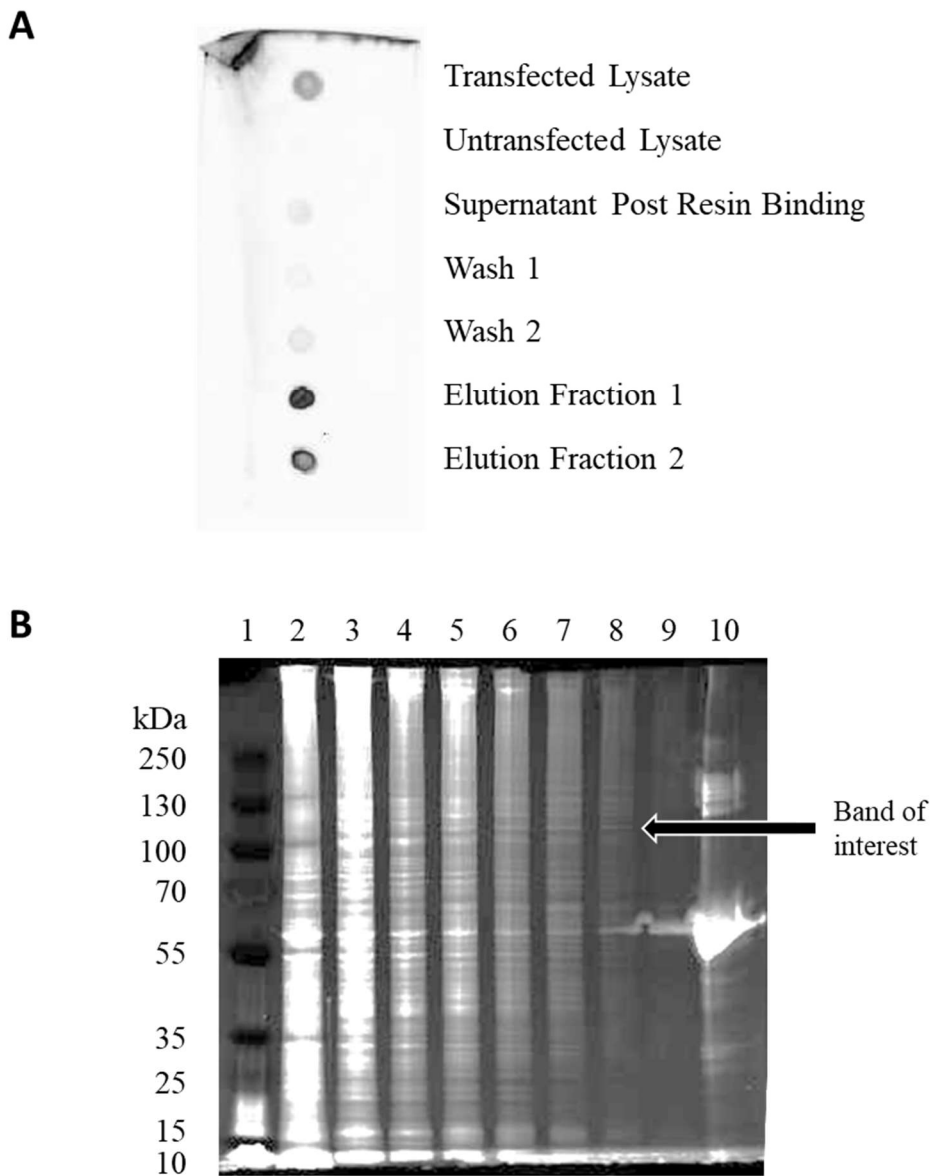


Figure 5.8: His.H8 western blot of HEK293T cell lysates.

Western blot of HEK293T cell lysates probed with His.H8. Two bands corresponding to cellular proteins reacted with the mAb, but there were two faint bands specific to the pTWIST-CMV-*EPIC* lane. The top band, visualized above the 100kDa marker corresponds to the band of interest in Figure 5.7B. (1) Ladder, (2) Untransfected HEK293T cell lysate, (3) pTWIST-CMV-*EPIC* transfected HEK293T cell lysate, (4) pCAGGS-GPC transfected HEK293T cell lysate.

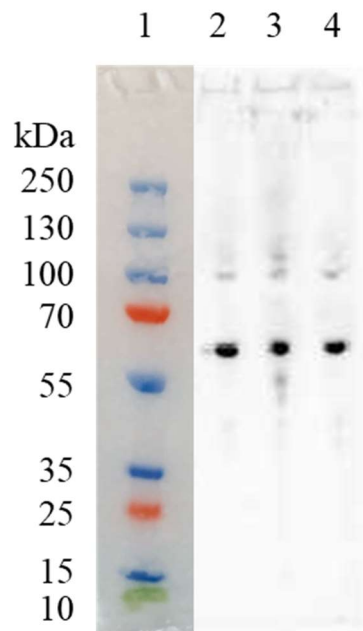


Figure 5.9: The NP, but not Gc, is recognized in R430 lysate by ELISA.

R430 gamma-irradiated CCHFV IbAr10200 cell lysate was used as a protein coat for ELISA at three different concentrations. The lysate was probed with three different dilutions of the mAbs 9D5, 11E7, and His.H8. (A) 9D5 demonstrated antibody and coating concentration-dependent increases in signal. (B) At the lowest mAb dilution, 11E7 did not display any signal above nonspecific background, suggesting the NP, but not GC could be detected in the lysate.

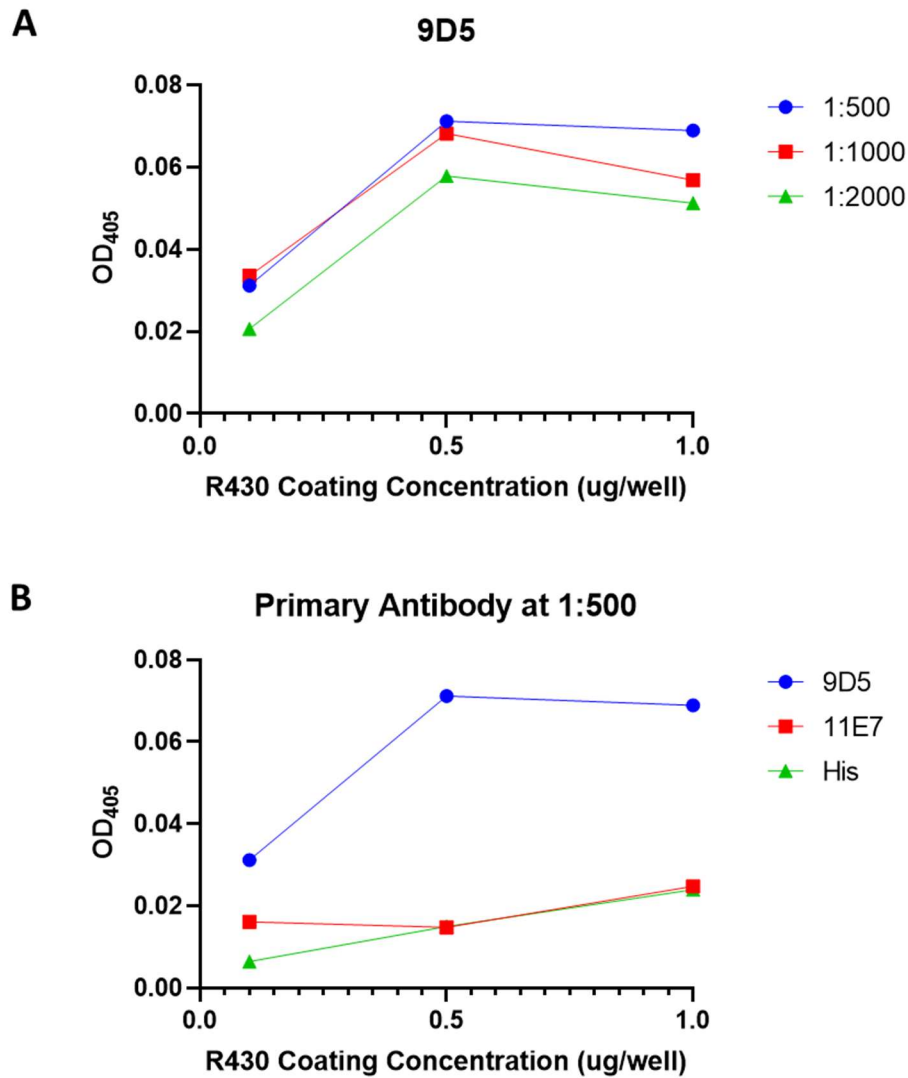


Figure 5.10: CCHFV HMAF western blot of HEK293T cell lysates and R430 lysate.

No bands of approximately 37 kDa and 75 kDa were seen in either the GPC-transfected HEK293T lysate or R430 lysate, which would correspond to the structural glycoproteins G_N and G_C , respectively³¹. The faint band in the pCAGGS-GPC transfected lysate between the 130kDa and 250kDa markers, may correspond to a GPC precursor protein. This blot suggests that the structural glycoproteins were not detectable in either lysate. (1) Ladder, (2) Untransfected HEK293T cell lysate, (3) pTWIST-CMV-*EPIC* transfected HEK293T cell lysate, (4) pCAGGS-GPC transfected HEK293T cell lysate, (5) R430 lysate (10 μ g).

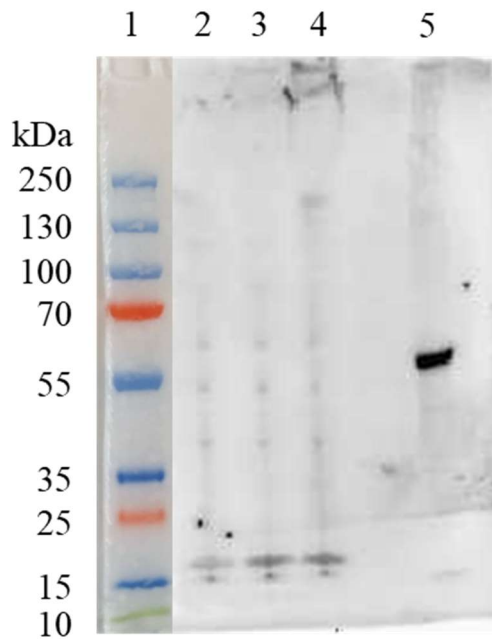
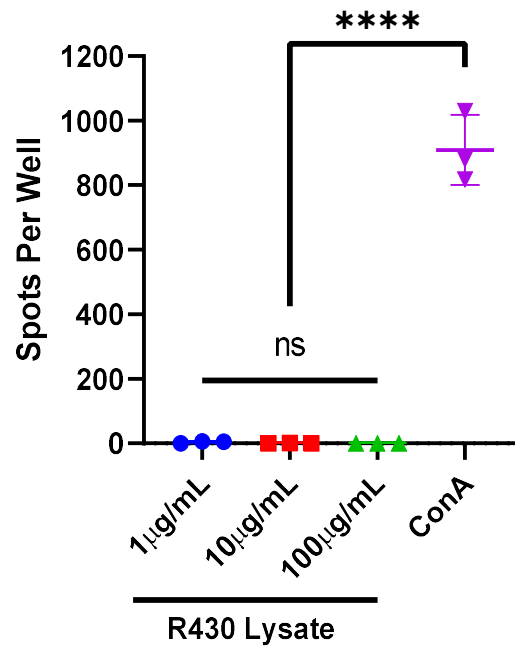


Figure 5.11: Stimulation of naïve splenocytes with R430 lysate does not produce IFN- γ .

Fresh splenocytes of naïve C57B16 mice were stimulated with either 1, 10, or 100 $\mu\text{g/mL}$ R430 lysate, 1X ConA, or were left unstimulated (N=3 wells per condition). Stimulation with the R430 lysate did not produce IFN- γ spot counts above the unstimulated wells. Stimulation with ConA produced significantly more spot counts ($p = <0.0001$) than stimulation with the R430 lysate when analyzed with an ordinary one-way ANOVA with Tukey's Post-Hoc correction for multiple comparisons. This suggests that the R430 lysate could be used as an antigen-specific stimulant for ELISpot assays.



Chapter 6: An *in vitro* Approach to Evaluate the Biological Impact of Subolesin Antisera

6.1 Abstract

This chapter sought to evaluate changes in the metabolic and transcriptomic profiles of the *Ixodes scapularis* embryonic cell line (ISE6) after incubation with Subolesin antisera. It was hypothesized that anti-Subolesin antibodies could enter tick cells to bind cytoplasmic Subolesin, resulting in changes to the metabolism and transcriptome of the cells. Subolesin expression in ISE6 cells was recognized by Subolesin antisera from rabbits or mice immunized with purified *R. microplus* Subolesin protein in adjuvant and pooled sera from mice vaccinated with RABV-Subolesin. ISE6 cells incubated with Subolesin antisera displayed a distinct fluorescent pattern of puncta concentrated near the nucleus, compared to cells probed with the antibodies after fixation and permeabilization or cells incubated with negative control sera. This suggested that antibodies were internalized by the cells and bound Subolesin within the cytosol. Incubation of ISE6 cells with Subolesin antisera did not result in any measurable metabolic changes. RNA-seq analysis of ISE6 cells incubated with rabbit Subolesin antisera revealed five differentially expressed genes in the cells compared to the rabbit mock control, but no differentially expressed genes between mouse mock serum treated cells and mouse Subolesin antiserum treated cells. Ultimately, this chapter provides evidence for the internalization of anti-subolesin antibodies by tick cells, which contributes to a mechanism of action for Subolesin-based anti-tick vaccines. However, the lack of biological impact on ISE6 cell cultures from incubation with Subolesin antisera demonstrates the need for *in vivo* vaccine efficacy evaluation.

6.2 Introduction

Previous chapters of this dissertation have investigated anti-tick vaccines and evaluated immunogenicity, but not efficacy, of the vaccine candidates. Current methods for assessing anti-tick vaccine efficacy can be difficult, time-consuming, and expensive^{249,250}. These methods rely on the use of force-feeding adult ticks serum from vaccinated animals or placing ticks on vaccinated animals to feed, where the impact on the ticks ability to digest and metabolize the blood meal can be evaluated by the reduction of several measures of tick biology, such as attachment, engorgement, molting, fertility, oviposition, and survival^{123,250}. Ticks that have been fed serum from Subolesin vaccinated animals display negative impacts on numerous biological processes such as engorgement, oviposition, and gene expression^{123,140}, but the biological role of this serum has yet to be investigated at the cellular level. Tick cell cultures provide a unique opportunity for evaluating the impact of Subolesin antibodies on tick biological processes.

Various tick species and cell lines have been used to evaluate the role of Subolesin in gene expression^{123,125,127,133,134,136,140,142,251,252}. It is known that silencing Subolesin expression in ISE6 cells results in numerous differentially expressed genes¹²⁵, Subolesin demonstrates auto-regulation and has a role in NF- κ B/Relish mediated gene expression^{123,127}, and differential expression of Subolesin is observed in female ticks which have fed on Subolesin vaccinated cattle¹⁴². The putative mechanism of Subolesin vaccine protection is the interaction of anti-Subolesin antibodies with Subolesin in feeding arthropods. The mechanism for interaction of anti-Subolesin antibodies with Subolesin is unknown. However, it has been hypothesized that the antibodies can enter tick cells to interact with

Subolesin in the cytoplasm^{123,142}, as previous work in the *Ixodes scapularis* embryonic cell line (ISE6) has demonstrated the ability of antibodies to intracellularly bind actin when ISE6 cells were incubated with an anti-actin mAb¹⁴².

Only two studies have assessed the impact of anti-Subolesin antibodies on gene expression. These studies were limited to evaluating the expression of Subolesin only, and demonstrated a significant decrease in Subolesin transcripts following feeding of ticks with Subolesin antiserum or on Subolesin immunized animals^{140,142}. This chapter sought to demonstrate the internalization of anti-Subolesin antibodies by ISE6 tick cells and assess the biological impact of antibody-Subolesin interactions by measuring changes in metabolism and gene expression. The results presented in this chapter show the first work evaluating anti-Subolesin antibody internalization by tick cells and assessment of the biological role of anti-Subolesin antibodies on tick cells.

6.3 Results

6.3.1 Antibodies from *R. microplus* Subolesin Protein in Adjuvant Immunization Recognize *I. scapularis* Subolesin

Previous chapters in this dissertation have focused on using Subolesin from *R. microplus* or *H. marginatum* ticks, which share 91.3% amino acid identity. There is less conservation between these two sequences and the sequence of *I. scapularis* Subolesin. There are 13 residue differences between *R. microplus* and *H. marginatum* (91.3% identity), 56 differences between *R. microplus* and *I. scapularis* (75.3% identity), and 53 differences between *H. marginatum* and *I. scapularis* (77.1% identity) (**Supplementary Figure 6.1**).

To confirm the sequence of Subolesin from the ISE6 cells used within this chapter, total RNA was extracted from ISE6 cells and submitted to the UTMB Next Generation Sequencing (NGS) core facility. cDNA libraries were prepared using random primers, and the libraries were sequenced on the NextSeq550 platform. Reads were aligned to the *I. scapularis* Subolesin reference sequence (Accession # AY652654) to form a consensus sequence, then the open reading frame of the consensus sequence was translated. There were no amino acid differences between the reference sequence and the sequence of Subolesin from the ISE6 cells used throughout these studies.

It was previously shown that rabbit serum generated from immunization with purified *R. microplus* Subolesin protein in adjuvant recognizes Subolesin in ISE6 cells¹⁴⁰. To ensure that the rabbit antiserum used in Chapters 3 and 4 (generated from immunization with purified Subolesin protein in Montanide ISA 50 V2 adjuvant) recognized *I. scapularis* Subolesin, ISE6 cells were probed with either rabbit or mouse Subolesin antiserum after fixation and permeabilization of the cells in an immunofluorescence assay (IFA) (**Figure 6.1**). Every cell appeared to have fluorescent staining when probed with either antiserum, although ISE6 cells probed with the rabbit antiserum appeared brighter than cells probed with mouse antiserum, although this was not quantified. The fluorescent pattern from staining with both mouse and rabbit antiserum was similar to previous results showing both nuclear and diffuse cytoplasmic staining in ISE6 cells¹²³. These results suggested that anti-Subolesin antibodies generated against purified *R. microplus* Subolesin protein recognized the *I. scapularis* Subolesin protein expressed in ISE6 tick cells.

6.3.2 Anti-Subolesin Antibodies Can Enter Nonpermeabilized ISE6 Cells to Bind Subolesin

It was hypothesized that anti-Subolesin antibodies could enter tick cells to bind Subolesin^{123,142}. To evaluate antibody internalization by ISE6 cells, cells were incubated for 24 hours with rabbit or mouse Subolesin antisera. The media containing the anti-Subolesin sera was removed, and cells were washed, fixed, permeabilized, then probed with a fluorescent-conjugated secondary antibody to IgG (**Figure 6.2**). This method allowed for the detection of antibodies that were internalized during the incubation, as the cells were not permeabilized when they were incubated with the antisera. To control for recognition of Subolesin expression by the antisera, cells were probed with the mouse or rabbit antisera after the cells were fixed and permeabilized (**Section 6.3.1, Figure 6.1**). To control for background fluorescence, ISE6 cells were incubated with medium that did not contain mouse or rabbit sera and were probed with the secondary antibody only. However, ISE6 cells were not incubated with negative control (non-Subolesin) mouse or rabbit sera to control for nonspecific antibody binding or internalization. Fluorescent staining appeared to be present in every cell, and the difference in fluorescence intensity between rabbit and mouse antisera was similar to that presented in Figure 6.1 from probing for Subolesin after fixation and permeabilization. The presence of fluorescent cells suggested that the anti-Subolesin antibodies from the mouse and rabbit antisera entered the cells during incubation and that the antibodies could bind to Subolesin within the cell. However, since a non-Subolesin antiserum was not incubated with the cells as a control, nonspecific antibody binding could not be excluded. To ensure that the antibody internalization was

specific to anti-Subolesin antibodies within the sera, additional controls were included in subsequent experiments.

Notably, the fluorescent patterns differed between ISE6 cells incubated pre-fixation with the antisera and ISE6 cells probed with the antisera after fixation (**Figure 6.3**). Cells incubated with antisera pre-fixation appeared to have large fluorescent puncta in the cytoplasm, with these puncta concentrated near the nucleus. Some fluorescent puncta were seen in the ISE6 cells probed with serum post-fixation, however, these puncta were smaller and scattered throughout the cell instead of being concentrated near the nucleus. Primarily, staining of Subolesin in ISE6 cells following fixation and permeabilization showed diffuse fluorescence located throughout the cell, rather than large puncta.

6.3.3 Internalization of Anti-Subolesin Antibodies in ISE6 Cells is Concentration-Dependent

To generate the rabbit anti-Subolesin serum, rabbits received three doses of purified *R. microplus* Subolesin protein in adjuvant (Montanide ISA 50 V2), whereas the mouse anti-Subolesin serum was generated using two doses of the same antigen and adjuvant. When the UTMB anti-Subolesin ELISA was developed, the rabbit anti-Subolesin serum was used as a positive control at a 1:100 dilution. Sera from *R. microplus* purified Subolesin protein in Montanide ISA 50 V2 immunized mice was evaluated at a 1:20 dilution in the ELISA (Chapter 3, **Figure 3.6A**). The mean OD₄₀₅ (\pm standard deviation) of the mouse antiserum at a 1:20 dilution was 3.19 (\pm 0.12) and the mean OD₄₀₅ of the rabbit antisera at the 1:100 dilution was 3.48 (\pm 0.16) (**Supplementary Figure 6.2**). The means of these two groups

were not statistically different by Welch's t-test. This suggested that the anti-Subolesin antibody concentration of the rabbit antiserum was approximately five times greater than the mouse antiserum. Thus, it was hypothesized that the significant difference in brightness from probing ISE6 cells with rabbit or mouse antisera was due to the difference in antibody titers between the sera, and that the internalization of anti-Subolesin antibodies by ISE6 cells would be concentration dependent. Three dilutions of the mouse antiserum were chosen to test this hypothesis. For the IFA results in Figures 6.1 and 6.2, serum was used at a 1:50 dilution, following previous experiments using rabbit antiserum to probe for Subolesin in ISE6 cells by IFA¹²³. Additionally, this was the first dilution of serum used in the anti-Subolesin ELISA (**Figure 4.4**), which gave the maximum signal for calculation of the EC50 titer. The second dilution (1:250) was chosen from the use of this dilution for the anti-Subolesin IFAs in Chapters 3 and 4. Finally, the dilution from the anti-Subolesin ELISA closest to the EC50 (1:17,017), which was 1:12,150, was used (**Figure 4.4**). ISE6 cells were incubated with the three different serum dilutions or with media only (mock) for 24 hours before fixation, permeabilization, and probing with the fluorescent-conjugated secondary antibody (**Figure 6.4**). Similar to previous results, every cell incubated with the 1:50 dilution appeared to have a fluorescent signal. This demonstrated that the internalization of anti-Subolesin antibodies from incubation of the ISE6 cells with mouse antiserum was repeatable. Further, there was a significant decrease in fluorescent signal from the ISE6 cells incubated with the 1:250 dilution of mouse serum, with few cells displaying fluorescence. ISE6 cells incubated with the 1:12,150 dilution of mouse serum only had one or two fluorescent cells in the whole well. The decreasing number of

fluorescent cells with decreasing antibody concentration suggested that the internalization of anti-Subolesin antibodies by the ISE6 cells was concentration dependent.

6.3.4 Starvation of ISE6 Cells Before Incubation with Anti-Subolesin Antibodies Increases Antibody Internalization

Previous studies in mammalian cells have demonstrated an increase of antibody internalization following a period of serum starvation²⁵³. Thus, it was hypothesized that starvation of the ISE6 cells before incubation with anti-Subolesin antibodies would increase antibody internalization. As incubation of ISE6 cells with a 1:250 dilution of mouse serum displayed a clear fluorescent signal in few cells, this dilution was chosen to evaluate whether or not starvation of the tick cells before incubation would increase the number of fluorescent cells. ISE6 cells were incubated in complete medium (referred to as ‘normal’) or Leibovitz's L-15 medium without additives (referred to as ‘starved’) for 24 hours. Complete media containing the 1:250 dilution of mouse serum was added to the cells, and cells were incubated for an additional 24 hours, then fixed and stained as in previous experiments (**Figure 6.5A**). The number of fluorescent cells and nuclei were counted from five fields of view from two independent experiments to quantify the percent of cells that had internalized anti-Subolesin antibodies (**Figure 6.5B**). The mean percentage of fluorescent cells using normal conditions was 4.1%, whereas starvation of cells before incubation with the mouse antiserum resulted in fluorescence of 6.5% of cells. While there was an increase in the percent of fluorescent cells following starvation, this increase was not statistically significant, as tested by an unpaired t-test.

6.3.5 Anti-Subolesin Antibodies from Vaccination with RABV-Subolesin Can Enter ISE6 Cells to Bind Subolesin

The previous results in this chapter have shown that antibodies generated against *R. microplus* Subolesin recognize *I. scapularis* Subolesin. However, the modified Subolesin protein encoded by RABV-Subolesin used the sequence of *H. marginatum*. It was hypothesized that anti-Subolesin antibodies generated by RABV-Subolesin would also recognize *I. scapularis* Subolesin for three reasons: 1) anti-Subolesin antibodies induced by vaccination with RABV-Subolesin recognized *R. microplus* Subolesin in the anti-Subolesin ELISA, 2) antibodies generated by immunization with *R. microplus* Subolesin protein recognized *I. scapularis* Subolesin, and 3) the *H. marginatum* and *I. scapularis* Subolesin sequences have greater homology than the *R. microplus* and *I. scapularis* Subolesin sequences. The signal (Delta Value ~1.4) from the RABV-Subolesin pooled sera at 1:50 in the anti-Subolesin ELISA was the same as the 1:12,150 dilution of the mouse antiserum from protein in adjuvant immunization (**Figure 4.4**). Since there were fluorescent cells present from incubation of ISE6 cells with the 1:12,150 dilution of mouse antiserum, albeit few, there was potential for detecting fluorescent cells using the RABV-Subolesin pooled sera at 1:50. ISE6 cells were starved for 24 hours before incubation with pooled sera from RABV-Subolesin mice, and pooled sera from the RABV-Empty and Saline groups was used to control for nonspecific fluorescence from RABV immunization or mouse serum components, respectively (**Figure 6.6A**). Bright fluorescent background and nonspecific signal were present in ISE6 cells probed with the pooled sera from all three groups. However, the distinct fluorescent pattern of large puncta in the cytoplasm concentrated around the nucleus was only seen in the ISE6 cells incubated with pooled sera

from RABV-Subolesin vaccinated mice (**Figure 6.6B**). This suggested that this fluorescent pattern, as seen in the previous IFA experiments, was specific to Subolesin antisera, and was not from internalization or binding from nonspecific antibodies present from RABV immunization or normal mouse serum components. There were few cells throughout the well with large puncta in the cytoplasm, which was expected from the previous IFA using the 1:12,150 dilution of mouse antiserum. This experiment suggests that serum samples that reacted similarly in the anti-Subolesin ELISA produced similar anti-Subolesin antibody internalization results when incubated with ISE6 cells. Further, humoral responses induced from immunization with a chimeric *H. marginatum* Subolesin-RABV-G protein recognize Subolesin expressed in *I. scapularis* cells.

6.3.6 Incubation of Tick Cells with Anti-Subolesin Antibodies Does Not Impact Cell Metabolism

Evaluation of the Subolesin/Akirin interactome has shown that Subolesin is involved in numerous metabolic processes¹²³. To determine if incubation of ISE6 cells with Subolesin antisera impacted cellular metabolism, the MTT cell proliferation assay was used. ISE6 cells were treated in the same manner as in the IFA experiments, where cells were starved for 24 hours before incubation with anti-Subolesin antibodies diluted in complete media or complete media without antibodies (mock) for 24 hours. Six different groups were assessed using biological triplicates: mouse antiserum from protein in adjuvant immunization at both 1:50 and 1:250 dilutions, rabbit antiserum at a 1:50 dilution, and pooled sera from RABV-Subolesin, RABV-Empty, and Saline groups at a 1:50 dilution (**Figure 6.7**). ISE6 cells incubated in complete media without antibodies (mock) were used to determine the

baseline metabolism of the MTT reagent, and the mean absorbance of these wells was considered 100% metabolism for the experiment. The percent change in absorbance from mock was calculated for each treatment group as a measure of the change in metabolism from treatment with Subolesin antisera or other controls. There were slight differences in the metabolism of ISE6 cells treated with antisera, but none of these differences were statistically different from mock by one-way ANOVA with Tukey's post-hoc correction for multiple comparisons. These results suggested incubation of ISE6 cells with Subolesin antisera does not impact the metabolism of the cells.

6.3.7 Evaluation of Downregulated Genes in Response to Subolesin Knockdown

The results presented within this chapter thus far suggest that anti-Subolesin antibodies can enter ISE6 cells to bind Subolesin in the cytoplasm. It was hypothesized that antibody binding of Subolesin in the cytoplasm might prevent nuclear translocation of Subolesin, therefore impacting gene expression. To test this hypothesis, genes known to be downregulated by the absence of Subolesin were evaluated by qRT-PCR.

Studies by Dr. Jose de la Fuente's laboratory have evaluated the genes most significantly downregulated from silencing Subolesin in ISE6 cells (unpublished results). To determine this, ISE6 cells were left untreated or were incubated with Subolesin dsRNA for three days to silence Subolesin using RNA interference (RNAi). Total RNA was then extracted from the samples and submitted for RNA-seq. Differential gene expression was analyzed between the untreated ISE6 cells and the Subolesin RNAi treated ISE6 cells. The names of the 10 most downregulated genes were provided by Dr. de la Fuente's laboratory. These

RNA-seq results were not confirmed by qRT-PCR. Of the 10 gene names provided, five were chosen for evaluation based on the presence of literature about the encoded protein in ticks, insects, or arthropod cell lines. The five genes chosen were solute carrier organic anion transporter family member 74D (OATP-74D), solute carrier family 2, facilitated glucose transporter member 1 (GLUT-1), solute carrier family 26 member 6 (Slc26a6), phospholipase A and acyltransferase 3 (PLAAT3), and nicotinamide adenine dinucleotide phosphate (NADP)-dependent malic enzyme (Malic) (**Table 6.1**).

Two-step reverse transcription then quantitative polymerase chain reaction (RT-qPCR) was chosen to determine the impact of incubation of tick cells with anti-Subolesin antibodies on the five genes of interest and Subolesin, with β -Actin serving as a reference gene. Primers were designed using Geneious Prime software and Primer3 version 4.1.0 (<https://primer3.ut.ee/>) to amplify a 150 nucleotide (nt) region of each gene (**Table 2.2**). The same size fragment was chosen from each gene to ensure similar PCR reaction efficiency for each primer pair. Primers were designed by the software programs to have melting temperatures (T_m) close to 60°C, which was recommended by the iTaq Universal SYBR Green Supermix protocol. Only one gene (OATP-74D) had two transcription isoforms in GenBank, and a region conserved in both isoforms was targeted for amplification to avoid lack of amplification due to transcript variation.

Preliminary experiments were undertaken to ensure that the primers would amplify the genes of interest from ISE6 cells. Total RNA was extracted from ISE6 cells to prepare cDNA using the SuperScript III First-Strand Synthesis System. Each real-time PCR

followed the recommendations of the iTaq Universal SYBR Green Supermix protocol for reagent and cDNA concentrations and thermal cycling for the Roche Lightcycler. β -Actin amplified with a cycle threshold value (Ct) of 23.25, however, the Ct of the remaining genes was low (27.44 to 32.91). Thus, it was essential to evaluate the abundance of transcripts of the five genes of interest, plus Subolesin, and β -Actin in ISE6 cells. NGS results of the total RNA from the ISE6 cells described at the beginning of the chapter produced 6,099,837 total reads. Bowtie2 was used to align reads to the reference sequence of each gene of interest and obtain the number of reads that aligned to either the whole coding sequence (CDS) or the 150nt PCR fragment (**Table 6.2**). The most reads aligned to β -Actin and Subolesin, with few or no reads mapping to the five genes of interest. There were 92 reads that mapped to the Actin PCR fragment, and seven reads that mapped to the Subolesin PCR fragment. While Subolesin had the second-most aligned reads of the genes of interest, for each read that aligned to the PCR product of Subolesin, there were 13.1-fold more reads that aligned to the PCR product of Actin. This suggested that Subolesin was expressed at a much lower rate than Actin. Of the other five genes of interest, only PLAAT3 had one read that mapped to its PCR product, the remaining genes of interest did not have any reads that mapped to their PCR products. This suggested that the five genes of interest were expressed at a much lower rate than Subolesin and Actin. These results corroborated the low Ct values from the preliminary PCR and suggested that the cDNA concentration needed to be increased to improve the detection of each gene.

To determine real-time PCR reproducibility and optimal cDNA input for each gene, the PCR was repeated using five dilutions of the previously prepared cDNA and a no template

control (NTC). cDNA was used at 1000 ng, 100 ng, 10 ng, 1 ng, and 0.1 ng per reaction for this experiment, with the initial dilution of 1000 ng being 10 times more input than recommended by the kit, to determine the lowest Ct that could be obtained for each gene using this method. Amplification of the β -Actin and Subolesin real-time PCR products were detected with a difference of approximately three cycles between each dilution, as expected for ten-fold dilutions (**Supplementary Figure 6.3A**). This was not achieved with any of the five genes of interest. Although increasing the amount of cDNA for each reaction increased the Ct, the Ct values for each of the five genes of interest remained high. An additional repeat of the PCR using 1000ng of cDNA produced Ct values that were very different to the results of the first experiment for the five genes of interest (**Supplementary Figure 6.3B**). Together, the NGS and real-time PCR results suggested that the five genes shown to be downregulated by Subolesin knockdown are transcribed at low levels in ISE6 cells, and two-step qRT-PCR was unable to be used for statistically significant evaluation of the differential expression of these genes of interest following treatment of ISE6 cells with anti-Subolesin antibodies.

6.3.8 Incubation of Tick Cells with Subolesin Antisera Does Not Impact the Cell Transcriptome

RNA-seq was used to determine the impact on the cell transcriptome from incubating ISE6 cells with Subolesin antisera. Biological triplicates of ISE6 cells were treated with rabbit or mouse Subolesin antisera from protein in adjuvant immunization (purified *R. microphus* Subolesin protein in Montanide ISA 50 V2) at a 1:50 dilution, or with sera from a rabbit or mouse not immunized with Subolesin at a 1:50 dilution (mocks). Mock sera from a

rabbit (anti-West Nile virus envelope protein domain III, kindly provided by Dr. Alan Barrett) or a mouse (Montanide ISA 50 V2 only, Chapter 3) were used to control for the addition of extra sera components in the Subolesin antisera treated wells, instead of using complete media only as in the previous experiments. Triplicate IFAs were conducted in parallel using the same cells and antibody dilutions as the triplicate samples for RNA-seq. All cells were treated as in previous experiments, where cells were starved for 24 hours prior to incubation with sera for 24 hours. ISE6 cells for RNA-seq were lysed with Trizol and samples were stored at -80°C until use. The triplicate IFAs were fixed, stained, and imaged as previously described (**Supplementary Figure 6.4**). Fluorescent signal of the cells was similar to previous experiments, and similar across the three replicates, suggesting reproducibility of the assay and consistency between replicates. Cytosolic puncta were present in cells that were incubated with the rabbit or mouse Subolesin antisera, but not present in cells that were incubated with the mock sera or cells that were probed with the Subolesin antisera after fixation and permeabilization. This was consistent with previous results and provided confidence that the cells treated for the RNA-seq analysis had internalized the anti-Subolesin antibodies. Cells incubated with the rabbit mock serum had unexpected fluorescence that was brightest around the outside of the cell, but this fluorescence did not appear to be localized within cells, and the pattern was distinctly different from Subolesin antiserum treated cells (**Supplementary Figure 6.4A**). Similar bright fluorescence was not seen in cells that were incubated with the mouse mock serum (**Supplementary Figure 6.4B**). This gave further confidence of the specificity of the Subolesin antiserum-Subolesin protein interactions, since the mouse negative control serum was from a mouse immunized with water in Montanide ISA 50 V2, which is the

same adjuvant used for the Subolesin protein in adjuvant immunization used to generate the mouse Subolesin antiserum.

Total RNA was extracted from the treated ISE6 cells and submitted to the UTMB Next Generation Sequencing core facility for RNA-seq. There was an average of approximately 35 million reads per sample that were aligned to the NCBI reference genome assembly for *I. scapularis* (GCA_016920785.2). A counts table of the number of reads per annotated gene (32,436 genes) was provided by the UTMB Next Generation Sequencing core facility. The total number of reads per sample, the number and percent of uniquely mapped reads, the number and percent of reads that were too short to be mapped, and the total number of counts per sample and per group are shown in **Table 6.3**. Two samples, rabbit mock 1 and rabbit mock 2, had a similar number of total reads to the other 10 samples, however, these two samples only had 23.50% and 41.27% of the reads that uniquely mapped to the *I. scapularis* genome assembly, compared to the 79.03% to 80.94% of uniquely mapped reads of the other 10 samples. In the rabbit mock 1 and rabbit mock 2 samples, 72.80% and 52.16% of the reads were too short (<75nt) to be mapped to the genome assembly. This was reflected in the total count of mapped reads per group. The rabbit mock group had an average of 17,498,373 reads per sample that corresponded to annotated genes, whereas the other groups had an average of 20,012,978 to 22,931,191 reads per sample that corresponded to annotated genes. Although the rabbit mock group had less reads that corresponded to annotated genes, this difference was not statistically different from the rabbit Subolesin antiserum treated group by Welch's t-test (**Figure 6.8**).

To evaluate differentially expressed genes between mock samples and Subolesin antisera treated samples, the DESeq2 package in R was used. First, read counts were normalized to take into account the total number of counts per gene, per sample. The normalized read counts were then used for all downstream analyses. Similarities between individual samples were visualized using a principal component analysis (PCA). Ten of the 12 samples clustered together, suggesting a high level of similarity of these samples. Two of the rabbit mock serum treated samples (rabbit mock 1 and rabbit mock 2) showed greater variance from the clustering of the remaining samples, which suggested a difference between these two samples and the remaining 10 (**Figure 6.9A**). The PCA was repeated using only the mouse mock serum treated samples, and rabbit and mouse Subolesin antiserum treated samples (**Figure 6.9B**). This PCA plot showed that the samples in these three groups did not form distinct clusters. Rather, these samples overlapped, which further suggested similarity between the samples.

Statistically significant differences in the normalized read counts between groups was determined using the DESeq2 package, and differentially expressed genes were visualized using volcano plots (**Figure 6.9C and D**). Genes were considered to be differentially expressed between the mock and Subolesin antiserum treated groups, if they had a \log_2 fold change >0.58 and an adjusted p -value <0.1 . Based on these criteria, here were no genes that were considered differentially expressed between the mouse mock serum treated group and the mouse Subolesin antiserum treated group (**Figure 6.9C**). This suggested that treatment of the ISE6 cells with the mouse Subolesin antiserum for 24 hours did not result in any changes to the transcriptome of the cells. There were five genes that were considered

significantly upregulated in the rabbit Subolesin antiserum group compared to the rabbit mock serum treated group (**Figure 6.9D**). The gene that was calculated to be the most upregulated was roundabout homolog 1 (ROBO1), which had a log₂ fold change of 9.43 and an adjusted *p*-value of 4.48×10^{-13} (**Table 6.4**). The remaining four genes that were considered to be upregulated were small subunit ribosomal RNA, tubulin alpha chain-like, tubulin beta chain, and small subunit ribosomal RNA (**Table 6.4**). The statistical significance of the differential expression of these four genes was low, and the adjusted *p*-values ranged from 0.014 to 0.039. These results suggested that the transcriptomic differences between the rabbit mock serum treated group and the rabbit Subolesin antiserum treated group were minimal. Although not biologically relevant, comparisons between the rabbit and mock groups were conducted (**Supplementary Figure 6.5**). These comparisons showed that there were seven differentially expressed genes between the mouse mock serum treated and rabbit mock serum treated ISE6 cells (**Supplementary Table 6.1**). The analysis was conducted in a directional manner, so the genes that were considered statistically different between the groups were upregulated in the mouse mock serum treated group compared to the rabbit mock serum treated group. These upregulated genes were very similar to the upregulated genes between the rabbit mock serum treated and rabbit Subolesin antiserum treated groups, with ROBO1 being the most upregulated followed by genes for tubulin and small subunit ribosomal RNA genes. There were no differentially expressed genes when the rabbit Subolesin antiserum treated group was compared to either the mouse mock serum or mouse Subolesin antiserum treated groups (**Supplementary Figure 6.4**). Together, these results suggested that the differences in gene expression between the rabbit Subolesin antiserum treated group and the rabbit mock

serum treated groups were different from the differentially expressed genes between the two mock groups, although they were similar. In combination with the IFA results showing fluorescence of the rabbit mock serum treated cells, and the variation between the rabbit mock serum treated samples by PCA, it is likely that the differentially expressed genes are present in the rabbit mock serum treated samples instead of being due to impact from the Subolesin antisera treatment. Overall, these results suggest that incubation of ISE6 cells with Subolesin antiserum for 24 hours does not result in major transcriptomic differences in the tick cells.

6.4 Discussion

Current strategies for evaluation of anti-tick vaccine efficacy require the use of live ticks and force-feeding via capillary tubes or placement of ticks on live vaccinated animals. As these methods are difficult, time-consuming, and expensive, this chapter sought to assess the biological impact of anti-Subolesin antibodies on tick cells *in vitro*. The ISE6 cell line was chosen for these studies, as it is the most widely used tick cell line^{254,255} and has previously been used for *in vitro* assessment of Subolesin using RNAi^{123,127,140,256}. As antibodies are the putative mechanism of protection of Subolesin based vaccines, although Subolesin is an intracellular protein and in mammalian cells antibodies are not thought to be able to enter the cells, it was hypothesized that anti-Subolesin antibodies could enter tick cells to prevent the function of Subolesin, therefore leading to measurable changes in metabolism or gene expression of tick cells^{123,142}. The results presented within this chapter suggest that anti-Subolesin antibodies can enter tick cells in a concentration-dependent

manner, but incubation of ISE6 cells with anti-Subolesin antibodies does not impact cell metabolism or gene expression.

Previous chapters in this dissertation have used Subolesin sequences from *R. microplus* or *H. marginatum*, whereas this chapter used *I. scapularis* tick cells. The Subolesin sequences of *R. microplus* and *H. marginatum* have greater homology (91.3%) than either sequence compared to *I. scapularis* (75.3% and 77.1%, respectively) (**Supplementary Figure 6.1**). The consensus sequence of *I. scapularis* Subolesin from the ISE6 cells used in this chapter was obtained using NGS, and there were no amino acid differences between the consensus sequence from the ISE6 cells and the reference sequence. Previously, Dr. Jose de la Fuente's laboratory has demonstrated that serum from rabbits immunized with purified *R. microplus* Subolesin protein recognizes Subolesin expressed in ISE6 cells¹²³. This result was confirmed using the same rabbit serum, in addition to sera from mice immunized with purified *R. microplus* Subolesin protein (**Figure 6.1**). As these sera demonstrated recognition of *I. scapularis* Subolesin, they were used to test the hypothesis that anti-Subolesin antibodies can enter tick cells to bind cytoplasmic Subolesin, as a previous study suggested antibodies can enter tick cells to bind actin¹⁴². ISE6 cells were incubated with anti-Subolesin antibodies before fixation and permeabilization, then probed with a fluorescent-conjugated secondary antibody only to detect antibodies that had been internalized during the incubation. Every cell appeared to have a fluorescent signal, with a distinct fluorescent pattern of large puncta surrounding the nucleus. This pattern differed from ISE6 cells probed with the sera after fixation and permeabilization, where fluorescence was diffuse and located throughout the cell (**Figures 6.1, 6.2, 6.3, and**

Supplementary Figure 6.4). The same fluorescent pattern was seen in ISE6 cells incubated with pooled RABV-Subolesin sera (**Figure 6.6**). Together, these results suggested that the anti-Subolesin antibodies were internalized by the ISE6 cells and that the antibodies were binding Subolesin in the cytoplasm. Unfortunately, a negative control serum from a mouse or rabbit that had not been immunized with Subolesin was not used in the initial experiment, so the possibility of nonspecific internalization or binding could not be excluded and additional IFAs utilizing proper controls were undertaken. In subsequent experiments, four different negative control sera were used to demonstrate that the large fluorescent puncta in the cytoplasm of Subolesin antiserum treated ISE6 cells was specific to Subolesin antibody-Subolesin protein interactions. The same fluorescent pattern was not seen in ISE6 cells that were incubated with sera from Montanide ISA 50 V2 (adjuvant only) immunized mice, RABV-Empty immunized mice, saline immunized mice, or serum from WNV EDIII immunized rabbits.

It is known that tick midgut cells digest blood meal products through endocytosis^{109,257}. Treatment of ISE6 cells with pooled sera from the RABV-Empty group and the rabbit anti-WNV EDIII serum were important controls to exclude the possibility of the large puncta being vacuoles of antibodies ingested through endocytosis. The ELISA results in Chapter 4 showed that there were similar levels of RABV-G binding antibodies in the RABV-Subolesin and RABV-Empty groups. If ISE6 cells were internalizing antibodies via endocytosis for digestion, the same distinct puncta would also be seen in the ISE6 cells incubated with the RABV-Empty pooled sera or rabbit anti-WNV EDIII serum, but this was not the case. Although unlikely, to completely exclude the possibility of antibodies

being internalized by endocytosis and digested, future IFA experiments would need to utilize endosome or lysosome markers in addition to the incubation with the Subolesin antisera and calculate colocalization coefficients of the different fluorophores. Together, these experiments demonstrated that similar antibody internalization and binding of Subolesin in the cytoplasm was achieved when using different samples, despite samples originating from different experiments (three independent experiments at three separate institutions of mouse immunization with protein in adjuvant, rabbit immunization with protein in adjuvant, or mouse immunization with RABV-Subolesin), antigen types (purified Subolesin protein or chimeric Subolesin-RABV-G within RABV), immunization strategies (protein in adjuvant or live recombinant virus), and animal models (mouse or rabbit).

When comparing IFA results of Subolesin antiserum from protein in adjuvant immunization, ISE6 cells appeared brighter when probed with rabbit antiserum compared to mouse antiserum. Both the anti-mouse and anti-rabbit secondary antibodies were conjugated to the same fluorophore, Alexa Fluor™ 488, and were used at the same dilution, so it is unlikely that difference in fluorescence between the IFA results was due to the use of different secondary antibodies. Given that rabbits received three doses of protein in adjuvant, and mice received two doses of the protein in adjuvant, it was hypothesized that the difference in brightness was due to differences in Subolesin-binding antibody titer between the sera (**Supplementary Figure 6.2**). Incubating ISE6 cells with different dilutions of mouse antiserum resulted in different numbers of fluorescent cells, suggesting that the internalization of anti-Subolesin antibodies was concentration dependent (**Figure**

6.4). What was interesting, however, was that rather than seeing a decrease in fluorescence of all cells upon incubation with a greater dilution of serum (1:250), fewer cells were fluorescent, and these few fluorescing cells were brighter than ISE6 cells incubated with the 1:50 serum dilution. This result suggested that there may be variability in antibody internalization by cells within the same culture. As tick cell lines were generated from embryonic tick tissues, ISE6 have the potential to further differentiate in culture²⁵⁵. It is interesting to consider that cells in different stages of the cell cycle, or cells that may have a slightly different phenotype, may internalize anti-Subolesin antibodies at a different rate compared to other cells in the same culture. The possibility of cell type sub-populations within the culture adds additional complexity to the evaluation of the biological impact of anti-Subolesin antibodies *in vitro*.

Ticks are subject to long periods of starvation between blood meals and can tolerate starvation for months²⁵⁴. Upon engorgement, ticks quickly process nutrients from the blood meal²⁵⁷. Similarly, it has been shown that ISE6 cells can survive for multiple days under starvation conditions, although this increases transcription of genes associated with autophagy²⁵⁴. While mammals do not go through periods of starvation like ticks, it has been shown that starvation of various mammalian cell lines before incubation with an antibody targeting an intracellular protein significantly increases antibody internalization²⁵³. Thus, it was hypothesized that starvation of the ISE6 cells before incubation with anti-Subolesin antibodies would increase antibody internalization. Numerous additives are introduced to Leibovitz's L-15 medium to make the complex, complete ISE6 cell media. A previous study has demonstrated that total deprivation of

amino acids from incubation of ISE6 cells in Hanks' Balanced Salt Solution (HBSS) induces expression of autophagy-associated genes in ISE6 cells²⁵⁴. To avoid induction of autophagy, ISE6 cells were "starved" using L-15 medium without the serum, protein, or amino acid additives used to make complete medium for ISE6 cell culture. Starvation of the ISE6 cells resulted in an average of 2.4% more fluorescent cells than non-starved cells (**Figure 6.5**). While this increase in the mean percent of fluorescent cells was not statistically significant between starved and non-starved cells, this could be due to the dilution of serum used. As this experiment only used one dilution of serum, it's possible that this increase could be significant when using a different serum dilution. Quantifying fluorescence brightness between starved and non-starved ISE6 cells incubated with a 1:50 serum dilution could have proved a worthwhile alternative of assessing more uniform antibody internalization since every cell appeared to be fluorescent when non-starved cells were incubated with serum at 1:50. However, this experiment was not undertaken.

As mentioned previously, fluorescent signal from ISE6 cells incubated with the mouse or rabbit Subolesin antiserum displayed fluorescent puncta in the cytoplasm with the puncta concentrated near the nucleus. It was theorized that these puncta were aggregates of antibody-bound Subolesin within the cytosol, and that the accumulation of Subolesin within the cytosol would prevent nuclear translocation of the protein, therefore preventing the function of this transcription co-factor and resulting in measurable changes in the metabolic or gene expression profile of ISE6 cells. Previous studies have demonstrated the utility of the MTT assay for the detection of significant differences in tick cell metabolism after various treatments^{258,259}. An MTT assay was used to assess the metabolic activity of

ISE6 cells after incubation with anti-Subolesin antibodies. With Subolesin's involvement in cellular and metabolic processes¹²³, it was hypothesized that if the anti-Subolesin antibodies were sequestering Subolesin in the cytosol and preventing its function as a transcription co-factor, then there would be a decrease in the metabolism of the ISE6 cells after incubation with the antibodies. ISE6 cells incubated with anti-Subolesin antibodies did not demonstrate any decreases in metabolism compared to mock cells (**Figure 6.7**). In contrast, ISE6 cells incubated with antibodies had slightly increased percent metabolism. As the cells were starved before the incubation with antibodies, it's likely that the slightly increased proliferation was due to the marginally higher serum content of the media in the treated wells compared to the mock wells since this slight increase was also seen in the ISE6 cells treated with the pooled sera from the RABV-Empty and saline groups, which served as nonspecific antibody controls. It is possible that the impact on metabolic processes seen in ticks that have fed on animals immunized with Subolesin is too complex to be replicated in cell culture and cannot be measured with this type of assay. Alternatively, the 1:50 serum dilution may still be too low to completely inhibit the function of Subolesin, rendering metabolic changes below the limit of detection of this assay.

Subolesin plays a role in the gene expression of ticks¹²⁵. Silencing of Subolesin using RNAi resulted in numerous differentially expressed genes in ISE6 cells. Ten genes were identified by Dr. de la Fuente's laboratory as the most significantly downregulated genes in ISE6 cells, and five of these genes were selected for evaluation within these studies (**Table 6.1**). It was hypothesized that binding of Subolesin in the cytoplasm to prevent

nuclear translocation, and the function of Subolesin as a transcription co-factor, would result in downregulation of the five genes of interest, similar to the results from RNAi. These studies sought to use two-step reverse transcription then real-time PCR to evaluate differences in expression of the five genes of interest and Subolesin, with β -actin serving as a reference gene. Ultimately, few NGS reads corresponded to the genes of interest, and amplification of the PCR products had high Ct variability between replicates (**Table 6.2; Supplementary Figure 6.3**). Together, these results suggested that this method was unsuitable for evaluating the downregulation of the five genes of interest after incubation of ISE6 cells with anti-Subolesin antibodies, and a different method was needed to evaluate differential gene expression following treatment of ISE6 cells with Subolesin antisera. Numerous variables may have impeded the reliability of this assay and, therefore, the ability to use this method in these studies. Previous work attempting to assess differentially expressed genes in tick cells have demonstrated difficulties in establishing RT-PCR methods for certain genes²⁵¹. ISE6 cells grow slowly in culture, and it is a taxing process to generate enough cells for experiments and obtain high concentrations of total RNA after RNA extraction. As the genes of interest had few or no reads from NGS of ISE6 cell total RNA, it's possible that the two-step RT-PCR method was not sensitive enough to accurately capture the low numbers of transcripts of these genes from the low cell numbers used in these experiments. The transcript levels of the downregulated genes identified from the RNAi experiments should have been considered when selecting the genes of interest, rather than only selecting genes of interest based on the presence of literature about the protein in ticks, insects, or arthropod cell lines.

Since differential gene expression following Subolesin knockdown by RNAi was evaluated using RNA-seq, this technique was hypothesized to be more suitable than the two-step RT-PCR method for evaluating changes in gene expression following treatment of ISE6 cells with Subolesin antisera. IFAs conducted in parallel showed that the ISE6 cells used for the RNA-seq experiment had similar fluorescent patterns than previous experiments, highlighting the reproducibility of antibody internalization by the cells (**Supplementary Figure 6.4**). The IFAs also showed that cells incubated with the rabbit mock antisera were fluorescent, with a very different pattern than the Subolesin antisera treated ISE6 cells (**Supplementary Figure 6.4A**). Overall, the IFA results gave confidence that the distinct fluorescent puncta were only seen in the Subolesin antiserum treated cells, and that the ISE6 cells submitted for RNA-seq analysis had internalized the anti-Subolesin antibodies.

Two of the rabbit mock serum treated samples had a low percentage of uniquely mapped reads, and the majority of reads were too short to be mapped (**Table 6.3**). Despite the low values of these two samples, there was no statistically significant difference in the mean of total counts per sample between the rabbit mock serum treated group and the rabbit Subolesin antiserum treated group (**Figure 6.8**). The DESeq2 package in R that was used to evaluate differential gene expression between groups normalizes the total counts of reads that aligned to each annotated gene within the *I. scapularis* genome assembly, so the lower number of reads for two of the rabbit samples should not have affected downstream analyses. However, PCA of the normalized RNA-seq results showed that the two samples treated with the rabbit mock antisera that had a low percentage of uniquely mapped reads were more variable than the other 10 samples (**Figure 6.9A**). Also, the third rabbit mock

treated sample that had a similar percentage of uniquely mapped reads as the nine samples from the other three groups clustered with the nine samples. These results suggested that there was a wide range of variability between the three samples in the rabbit mock serum treated group, which may be attributable to issues with the two variable samples during library preparation and/or sequencing.

The DESeq2 package in R was also used to evaluate differentially expressed genes between mock serum treated and Subolesin antiserum treated ISE6 cells. There were no differentially expressed genes between the groups that were treated with mouse mock sera or mouse Subolesin antisera (**Figure 6.9C**). However, there were differentially expressed genes between the rabbit mock serum treated and the rabbit Subolesin antiserum treated groups (**Figure 6.9D** and **Table 6.4**). Although additional comparisons were not biologically relevant due to the biological differences between the rabbit and mouse serum, the remaining sample groups were compared (**Supplementary Figure 6.5** and **Supplementary Table 6.1**). These additional comparisons suggested that there were similar differentially expressed genes between the mouse mock serum treated group and the rabbit mock serum treated group as the rabbit mock serum and rabbit Subolesin antiserum treated groups. In combination with the variability of two of the rabbit mock serum treated samples showing a high percentage of reads that were too short to be mapped, and fluorescence in ISE6 cells in the IFA conducted in parallel, this suggested that the differentially expressed genes may not be a result of Subolesin treatment and may be due to the variability of the two rabbit mock serum treated samples. The DESeq2 package requires replicates for evaluating differentially expressed genes between groups, so the

analysis could not be conducted using only rabbit mock serum treated sample 3, which had a similar percentage of uniquely mapped reads as the samples in other groups, to exclude this possibility.

Given the distinct fluorescent pattern of ISE6 cells that had been incubated with either mouse or rabbit Subolesin antiserum, it was surprising that only five genes were found to be differentially expressed between the rabbit mock serum treated group and the rabbit Subolesin antiserum treated group, and that no genes were differentially expressed between the mouse sera treated groups. However, these results further support the results of the MTT assay, since no changes in metabolic transcripts were seen using RNA-seq. As discussed with the MTT assay, it is possible that the rabbit and mouse Subolesin antisera treatment at 1:50 was too low of a concentration to inhibit the function of Subolesin. It is interesting, however, that the previously discussed IFA experiments appeared to suggest that antibody internalization by the ISE6 cells was concentration dependent, and differentially expressed genes were only seen between the rabbit sera treated groups. Although it is unclear whether or not this was related to the Subolesin antiserum titer, the rabbit Subolesin antiserum was from rabbits immunized three times with purified Subolesin protein in Montanide ISA 50 VS, compared to only two doses of the same protein in adjuvant in the mice. It is also possible that cells could have initially changed the expression of Subolesin to compensate for the antibody-Subolesin aggregates in the cytosol prior to the timepoint of the experiment, so at 24 hours post treatment, changes in the transcriptome were no longer present. It would be interesting to evaluate higher concentrations of antibody treatment at various time points using RNA-seq, to confirm

whether or not anti-Subolesin antibodies have any impact on the ISE6 cell transcriptome. Alternatively, future studies may investigate the impact of Subolesin antisera treatment of ISE6 cells coupled with a stimulant known to impact the innate immune response and Subolesin expression, such as infection with *Anaplasma marginale*^{145,251,260}. It is also likely that the complexities of tick feeding and the interactions of anti-Subolesin antibodies with Subolesin within ticks cannot be modeled in an *in vitro* system, and that the use of tick cell lines is not a suitable alternative to *in vivo* testing of anti-tick vaccines.

In conclusion, the work presented in this chapter suggests that anti-Subolesin antibodies can be internalized by ISE6 cells, and the antibodies appear to bind Subolesin in the cytoplasm, but this did not reduce cellular metabolism or significantly alter the cell transcriptome. These results suggest that *in vivo* methods of feeding ticks on vaccinated animals or using capillary tube feeding are still needed to evaluate the biological impact of anti-Subolesin antibodies on ticks.

Table 6.1: Most significantly downregulated genes in response to Subolesin knockdown in ISE6 cells.

Subolesin transcription was silenced in ISE6 cells using RNAi. Three days after silencing, RNA was harvested from the tick cells for RNA-seq. The table lists five of the most significantly downregulated genes after knockdown of Subolesin by RNAi and the fold change in expression compared to untreated cells. Data were provided by the laboratory of Dr. Jose de la Fuente.

Acronym	Full Gene Name	Accession #	Fold change (log₂)
OATP-74D	Solute carrier organic anion transporter family member 74D	XM_029989177	-2.74744
GLUT-1	Solute carrier family 2, facilitated glucose transporter member 1	XM_029970436	-2.2195
Slc26a6	Solute carrier family 26 member 6	XM_040222974	-2.02095
PLAAT3	Phospholipase A and acyltransferase 3	XM_040208814	-1.67584
Malic	NADP-dependent malic enzyme	XM_042291906	-1.61046

Table 6.2: Number of reads of genes of interest from NGS of ISE6 cells.

Total RNA was extracted from 1.5 million ISE6 cells and submitted for NGS. There were 6,099,837 total reads for this sample. Reads were mapped to either the whole coding sequence (CDS) or the PCR product for each gene of interest.

Gene	Accession	# Reads Mapped (Whole CDS)	# Reads Mapped (PCR Product)
Actin	AF426178	678	92
Subolesin	AY652654	41	7
OATP-74D	XM_029989177	1	0
GLUT-1	XM_029970436	7	0
Slc26a6	XM_040222974	0	0
PLAAT3	XM_040208814	3	1
Malic	XM_042291906	8	0

Table 6.3: Number of reads and read counts per sample and group from RNA-seq.

Sample	Total Number of Reads	Uniquely mapped reads	Reads that were too short to be mapped	Total read counts in count table	Total counts per group (Mean ± SD)
Mouse Mock 1	35687204	35687204 (79.03%)	3237174 (9.07%)	23455049	20,012,978 ± 3,466,526
Mouse Mock 2	24851339	19759206 (79.51%)	2090611 (8.41%)	16522503	
Mouse Mock 3	29870339	23912667 (80.05%)	2462864 (8.25%)	20061384	
Mouse Subolesin 1	31193500	24871773 (79.73%)	2558853 (8.20%)	20841202	22,893,580 ± 2,056,769
Mouse Subolesin 2	37060416	29654639 (80.02%)	2984989 (8.05%)	24954713	
Mouse Subolesin 3	33247204	26910574 (80.94%)	2537202 (7.63%)	22884825	
Rabbit Mock 1	26910574	12096289 (23.50%)	37469682 (72.80%)	10103265	17,498,373 ± 10,130,039
Rabbit Mock 2	39109924	16140559 (41.27%)	20399064 (52.16%)	13347235	
Rabbit Mock 3	43862415	34795632 (79.33%)	2974053 (8.40%)	29044620	
Rabbit Subolesin 1	33020562	26192580 (79.32%)	2864319 (8.67%)	21934043	22,931,191 ± 889,571
Rabbit Subolesin 2	34715195	27661919 (79.68%)	2921726 (8.42%)	23216204	
Rabbit Subolesin 3	35421841	28261234 (79.78%)	2974053 (8.40%)	23643328	

Table 6.4: Differentially expressed genes between the rabbit mock serum treated and rabbit Subolesin antiserum treated ISE6 cells.

Log2 Fold Change	Adjusted <i>p</i>-value	Accession	Gene Name
9.43	4.48E-13	LOC8024969	Roundabout homolog 1 (ROBO1)
5.99	0.014	LOC120847219	Small subunit ribosomal RNA
5.03	0.017	LOC8024345	Tubulin alpha chain-like
1.97	0.030	LOC8026892	Tubulin beta chain
3.17	0.039	LOC120847184	Small subunit ribosomal RNA

Figure 6.1: Antibodies generated by immunization with *R. microplus* Subolesin protein in adjuvant recognize Subolesin in ISE6 cells.

ISE6 cells were fixed, then probed with mouse serum or rabbit serum generated from immunization with purified *R. microplus* Subolesin protein in adjuvant. Subolesin in the ISE6 cells was recognized by both sera. Staining was present throughout the cells, which was expected based on previous studies¹²³.

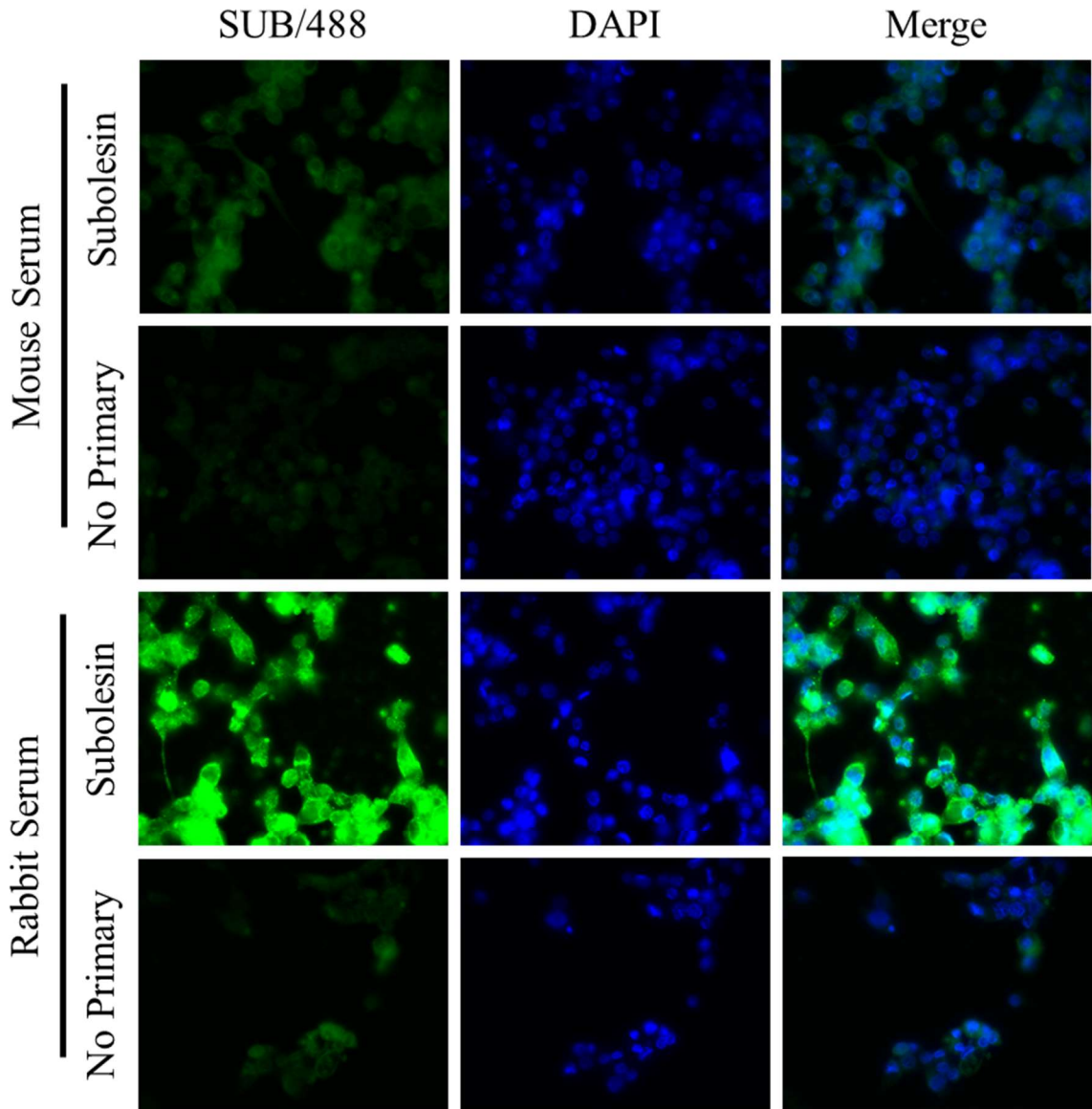


Figure 6.2: Anti-Subolesin antibodies can enter ISE6 cells to bind Subolesin without permeabilization.

ISE6 cells were incubated with mouse serum or rabbit serum generated from immunization with purified *R. microplus* Subolesin protein in adjuvant for 24 hours before fixing and detecting bound IgG with a fluorescent-conjugated secondary antibody.

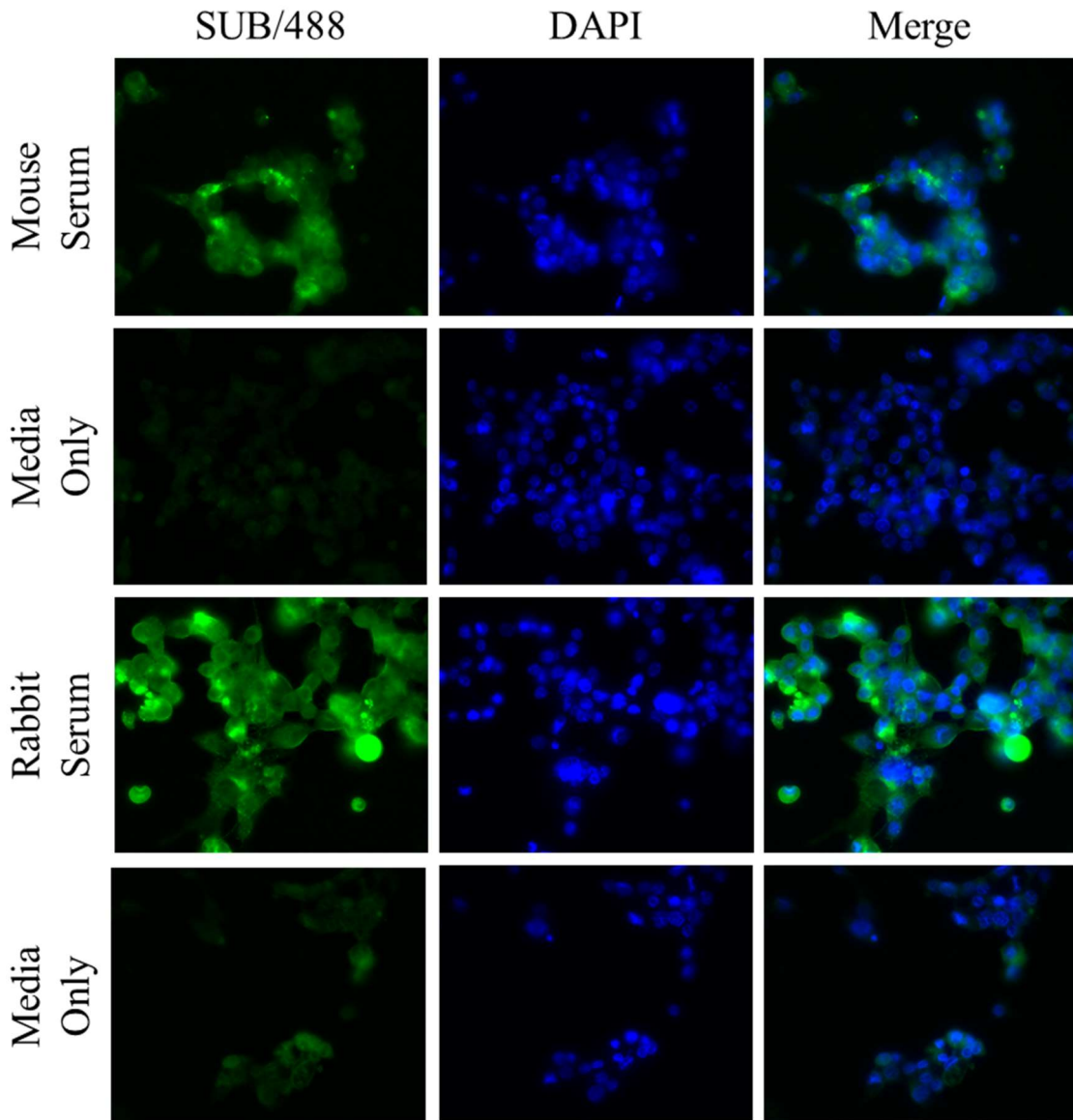


Figure 6.3: Large cytoplasmic puncta are present in ISE6 cells incubated with mouse Subolesin antiserum, but not in ISE6 cells stained post-fixation.

Representative merged images of ISE6 cells incubated with mouse Subolesin antiserum or stained with mouse Subolesin antiserum post-fixation. The yellow box highlights the part of the image that has been enlarged to show the cytoplasmic puncta.

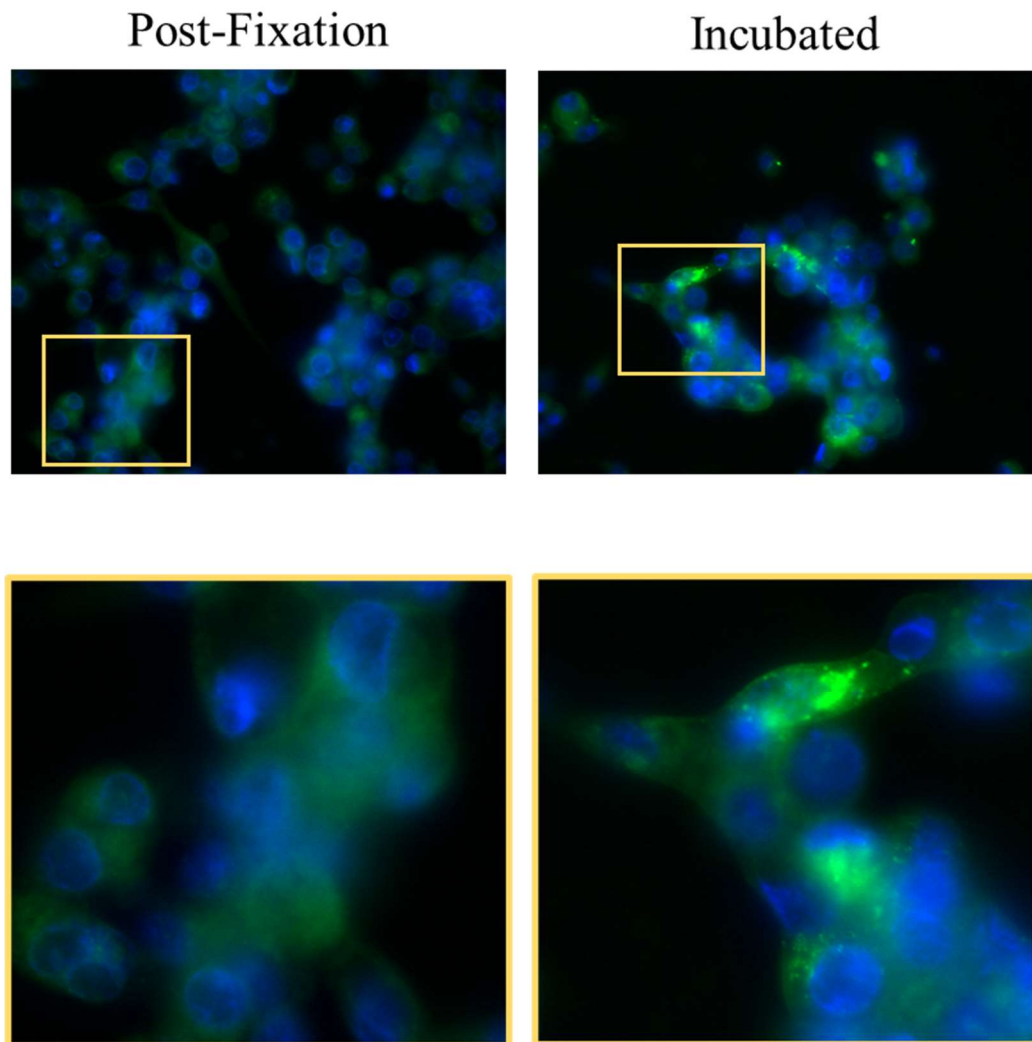


Figure 6.4: Antibody internalization and binding is concentration-dependent.

ISE6 cells were incubated with mouse serum at three dilutions for 24 hours before fixing and detecting bound IgG with a fluorescent-conjugated secondary antibody. Each cell displayed fluorescent staining at the lowest dilution, with a significant reduction in the number of fluorescent cells as the serum was diluted.

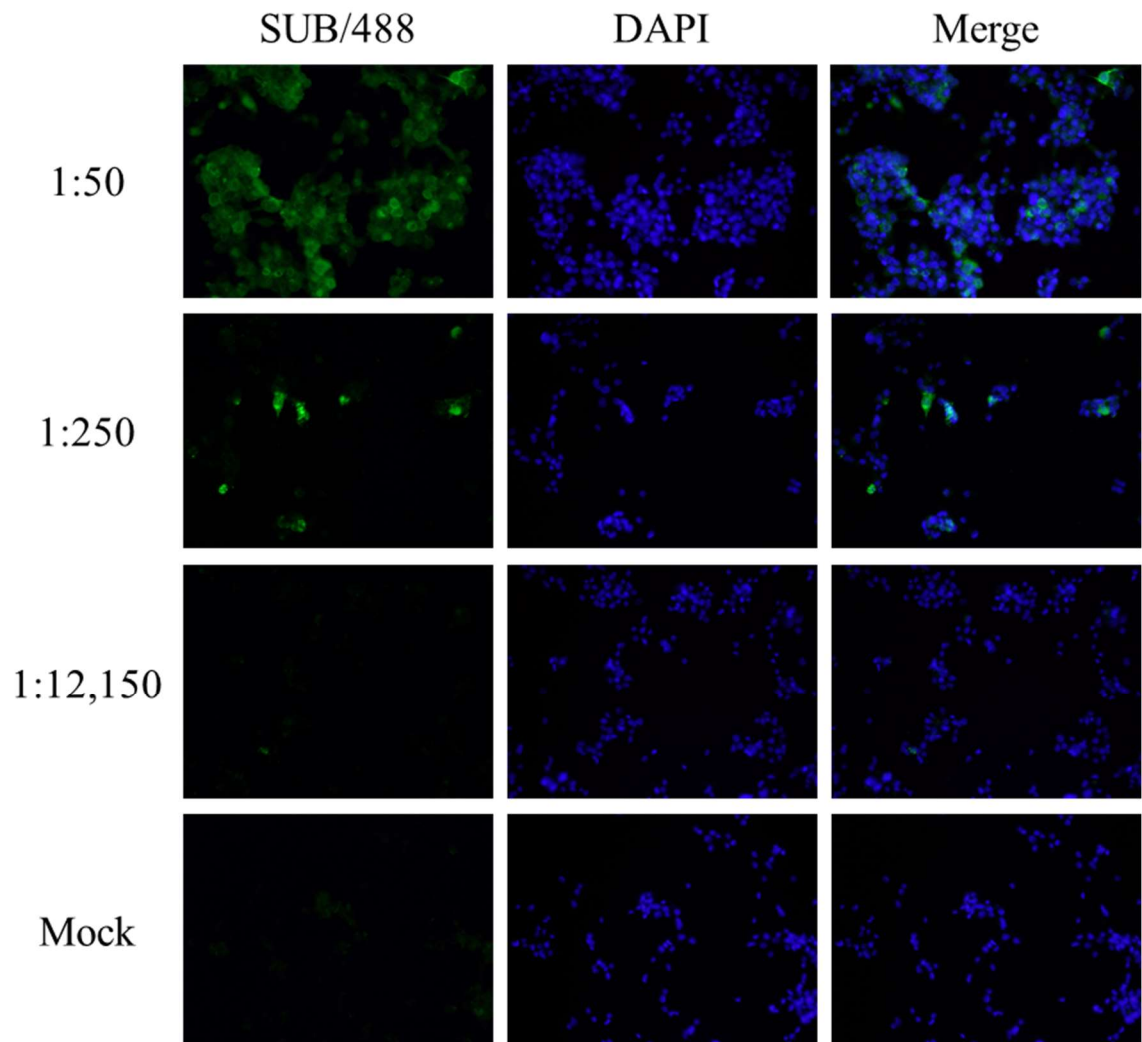
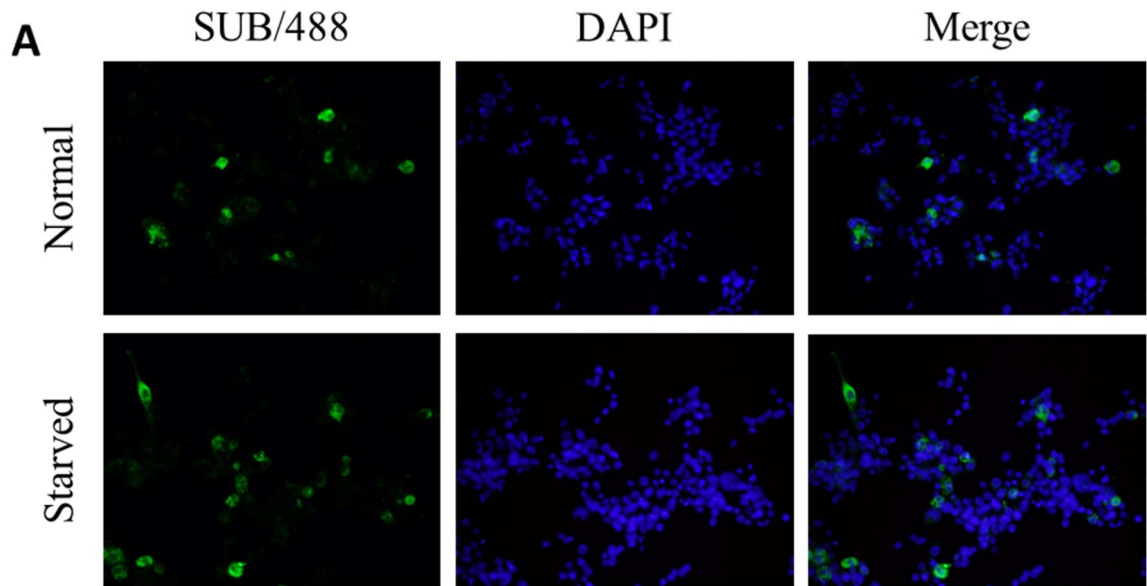


Figure 6.5: Starvation of the tick cells before incubation with anti-Subolesin antibodies increases antibody internalization.

ISE6 cells were incubated for 24 hours with complete media (Normal) or with L-15 without additives (Starved) for 24 hours before incubation with mouse serum at a 1:250 dilution for 24 hours. Cells were then fixed, and bound IgG was detected with a fluorescent-conjugated secondary antibody. (A) Representative IFA images of normal or starved ISE6 cells incubated with anti-Subolesin mouse serum. (B) Quantification of the percent of fluorescent cells from 5 fields of view from two independent experiments for each condition. While there was an increase in the percent of fluorescent cells after starvation, the increase was not statistically significant by unpaired t-test.



B

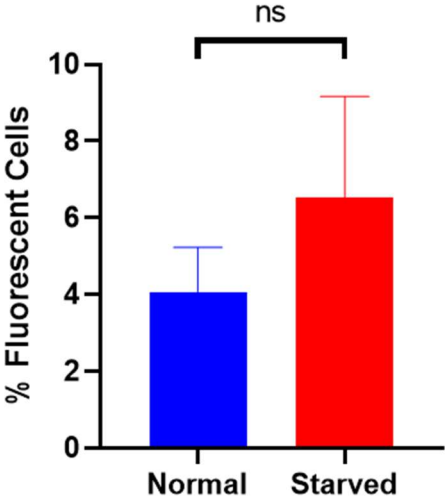
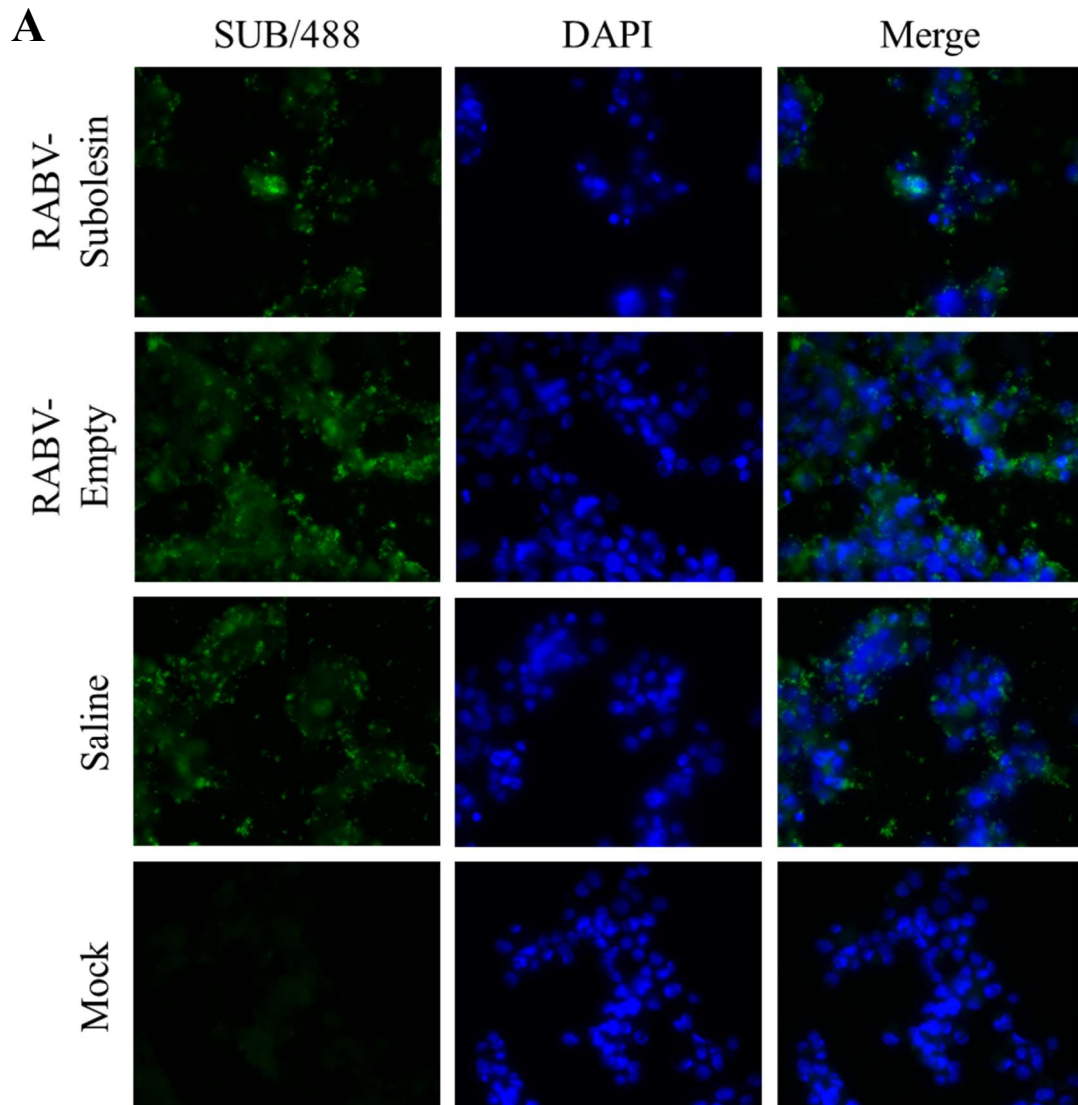


Figure 6.6: Antibodies from RABV-Subolesin immunization can enter ISE6 Tick cells and bind Subolesin.

ISE6 cells were incubated with pooled mouse sera at a 1:50 dilution for 24 hours before fixing and detecting bound IgG with a fluorescent-conjugated secondary antibody (A). Only in the RABV-Subolesin probed ISE6 cells were intracellular puncta visualized (B), as seen with the mouse serum from protein in adjuvant immunization. High staining levels were present in both the RABV-Empty and Saline groups, but the staining pattern lacked the expected intracellular puncta, suggesting that this was nonspecific background staining.



B

RABV-Subolesin

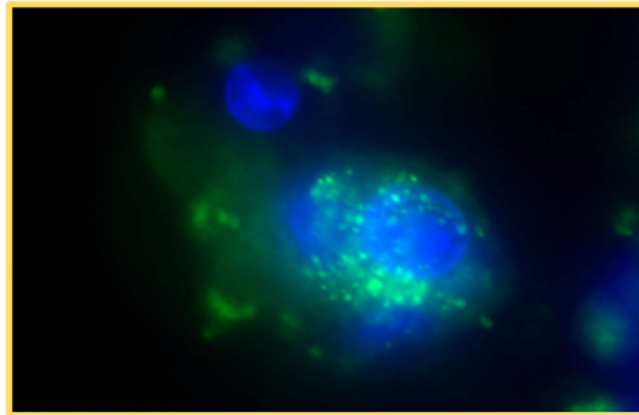
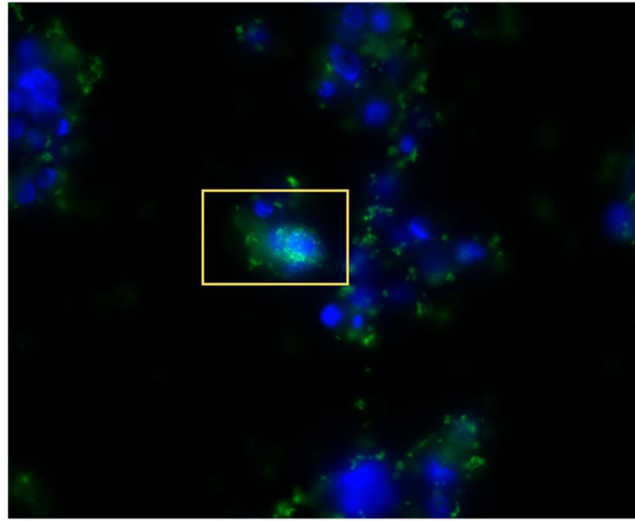


Figure 6.7: Incubation of tick cells with anti-Subolesin antibodies does not reduce cell metabolism.

ISE6 cells were incubated with mock or Subolesin antisera for 24 hours in biological triplicates prior to completion of the MTT assay. The change in percent metabolism was calculated based on the difference in absorbance from mock.

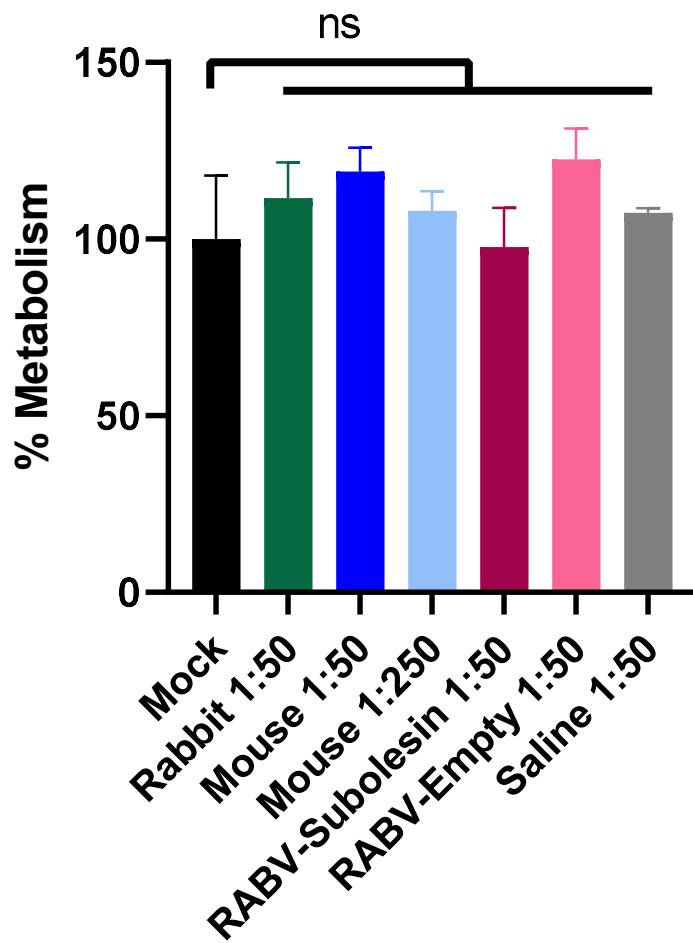


Figure 6.8: Total counts of reads that correspond to annotated genes of the *I. scapularis* genome.

The number of reads (counts) that aligned to each annotated gene of the *I. scapularis* genome were provided in a counts table by the UTMB NGS core facility. The total counts number for each sample were graphed. There were no significant differences between the two mouse sera treated groups or the two rabbit sera treated groups as tested by a Welch's t-test.

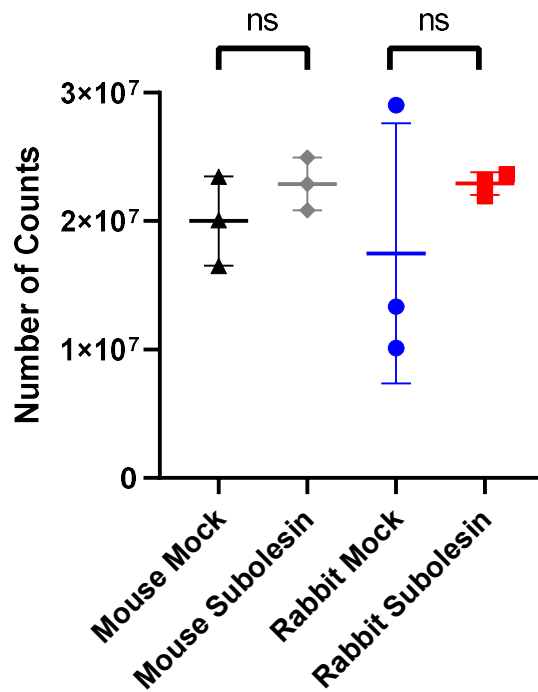
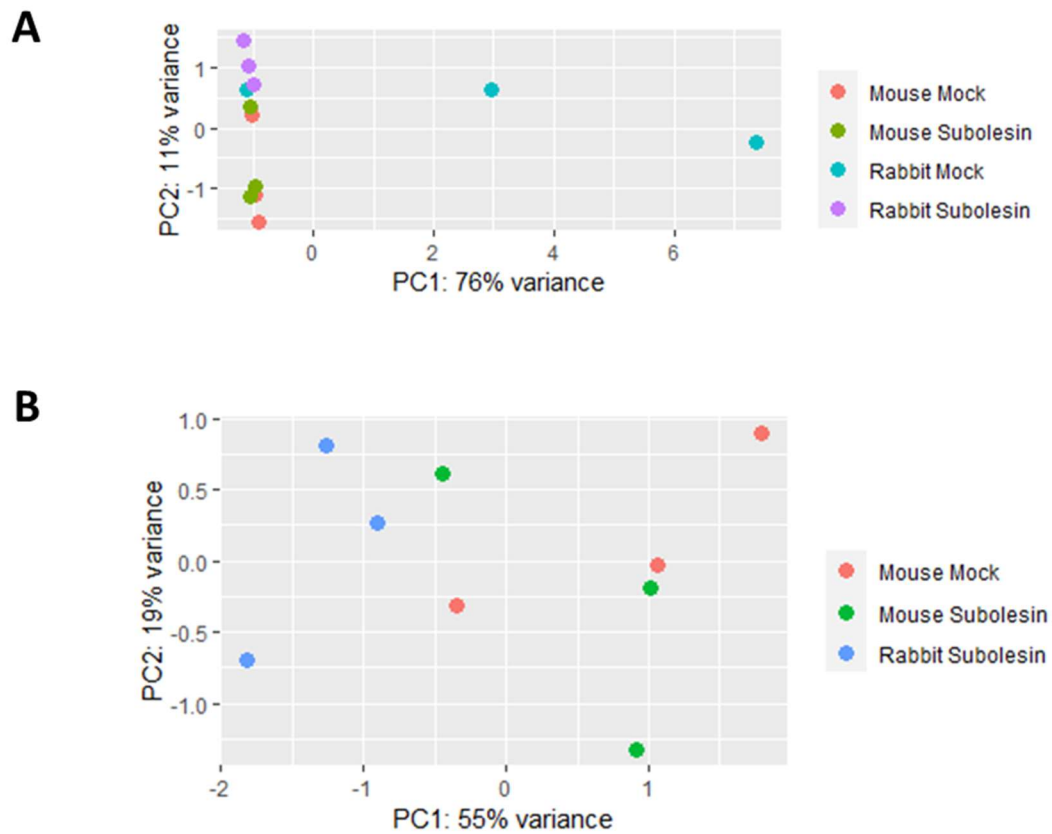


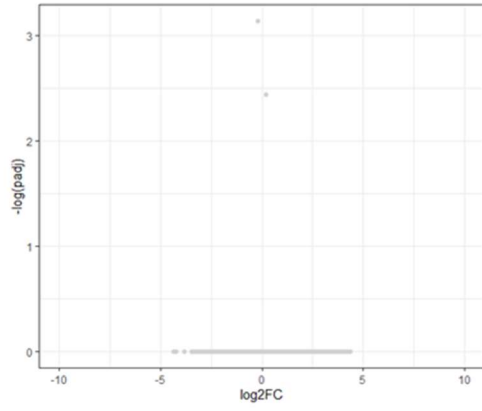
Figure 6.9: Analysis of differentially expressed genes from Subolesin antiserum treated ISE6 cells.

Twelve samples were submitted for RNA-seq analysis (four groups of biological triplicates). (A) Principal component analysis of all samples. (B) Principal component analysis excluding the rabbit mock antiserum samples. (C and D) Volcano plots visualizing differentially expressed genes between groups.



C

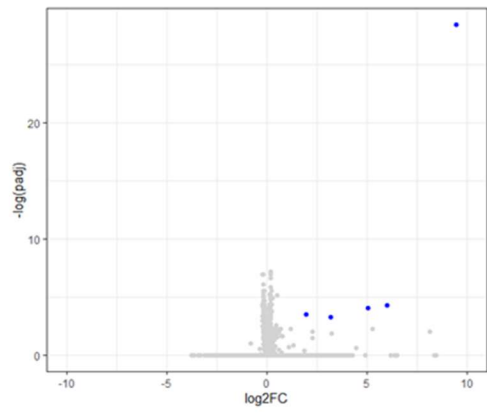
Mouse Subolesin vs Mouse Mock



- Genes Statistically Different Between Groups
- Genes Not Statistically Different Between Groups

D

Rabbit Subolesin vs Rabbit Mock



- Genes Statistically Different Between Groups
- Genes Not Statistically Different Between Groups

Chapter 7: Final Discussion

CCHFV has the most extensive geographic range of the medically significant tick-borne viruses, and it is estimated that three billion people are at risk of infection⁹. The range of the primary vector and reservoir of CCHFV, *Hyalomma* ticks, continues to expand, causing new foci of CCHFV to emerge in several parts of the world^{2,12,13}. CCHFV can infect various animals and circulate cryptically in a tick-vertebrate-tick cycle in nature, and humans are incidental hosts and the only species that develop clinical disease². Due to the potentially severe nature of this hemorrhagic disease in humans, vaccine development has been a focus of CCHFV research for decades. Despite extensive research, no vaccine candidate for CCHFV has advanced to clinical trials⁷³. For these reasons, this dissertation aimed to utilize different vaccine platform technologies to target unique points in the CCHFV transmission cycle in ticks and animal hosts as new strategies for vaccine development for CCHFV. Protecting humans through vaccinating animals and targeting ticks is considered a One Health approach to human health. The overall goal of this dissertation was to develop and evaluate tick and virus targeting vaccine candidates for both the tick vector and vertebrate host interaction points in the CCHFV transmission cycle. Specific goals of the dissertation were to develop novel vaccine candidates for *Hyalomma* ticks and CCHFV, evaluate the immunogenicity of the vaccine candidates, and assess the biological impact of anti-Subolesin antibodies on tick cells.

The concealed tick antigen, Subolesin, and the CCHFV GPC were chosen for developing the tick and virus targeting vaccine candidates, respectively. Previous studies have demonstrated that Subolesin is a highly conserved, immunogenic, and efficacious tick

antigen when used as a protein in adjuvant vaccine formulation¹³⁹. Subolesin is a transcription co-factor of Relish/NF- κ B and plays an essential role in gene expression, tick survival, and completion of the tick life cycle^{123,132–137}. Ticks fed on Subolesin immunized animals display reduced infestation, weight, oviposition, fertility, and infection with bacteria and parasites¹³⁹. The CCHFV GPC encodes a polyprotein that undergoes extensive cleavage and processing to form the structural glycoproteins found as heterodimers on the virion surface^{2,26,28,31,34,39,41}. The GPC has been a popular antigen for CCHFV vaccine development due to the development of binding and neutralizing antibodies to these proteins during natural infections and the complex processing needed to form the mature glycoproteins with proper conformation^{54,73}. Some vaccine candidates encoding the GPC or structural glycoproteins have demonstrated 100% protection from lethal challenge in animal models^{75,77–80,82,84,183}. However, most of these candidates require multiple doses, which is not ideal for people in rural areas at the greatest risk of *Hyalomma* tick bites and infection with CCHFV². Thus, a different strategy for the development of CCHFV vaccines, by targeting the reservoir and vector of the virus, or a different vaccine platform technology for human vaccine development is needed to improve current CCHFV vaccine candidates.

7.1 Vaccine Development to Prevent CCHF

To overcome the size and complex processing of the GPC, it has been hypothesized that a multi-epitope antigen would be an improvement over conventional candidate CCHFV GPC DNA vaccines⁷³. This dissertation shows the first work to evaluate a multi-epitope antigen-based DNA vaccine for CCHFV beyond *in silico* analyses.

Bioinformatic analyses of the GPC revealed numerous T cell epitopes that were predicted to be immunogenic. The overall pattern of the predicted epitopes was similar to previous reports of reactivity to GPC of serum samples collected from CCHFV patients after clinical disease⁸⁹. Epitope prediction and serum reactivity patterns have the strongest responses within the nonstructural proteins, which is also seen in T cell recall responses of GPC-vaccinated animals^{77,78,89}. In addition, recent studies have demonstrated the importance of one of the nonstructural proteins, GP38, as a vaccine antigen and target of protective antibody responses^{77,88}. Together, these results suggest that regions of the GPC other than the structural glycoproteins should be evaluated for inclusion in rational vaccine development.

This dissertation shows the first work evaluating a multi-epitope antigen for CCHFV beyond *in silico* analyses. Regrettably, these studies had many limitations, primarily regarding a lack of controls or available reagents. The multi-epitope antigen developed in these studies, referred to as *EPIC*, was synthesized and subcloned into a different mammalian expression vector than the full-length GPC control plasmid. The transfection efficiency of both plasmids was low in RK13 and HEK293T cells, and future studies should devote time to optimizing transfection to increase the efficiency. Low levels of *EPIC* expression that prevented the purification of the protein for use in ELISA and ELISpot assays may be due to low transfection efficiency or a poor choice of mammalian expression plasmid. While there was some reactivity with CCHFV antiserum in *EPIC* transfected cells, *EPIC* was not recognized by any of the CCHFV mAbs used. The GPC control

plasmid was used in these studies, so the possibility of impeded recognition of the mAbs due to differences in the epitopes of CCHFV strain (IbAr10200 mAbs versus Turkey2004 *EPIC* and GPC) could be excluded. A signal peptide was not included within the multi-epitope antigen. Since the GPC is extensively processed through the secretory pathway^{25,31-39}, future multi-epitope antigens for CCHFV may need to include a signal peptide to target the antigen to the ER for post-translational modifications such as glycosylation³¹. Although large regions of the GPC were included within *EPIC*, conformational epitopes may not be retained since the processing of *EPIC* was different from the GPC, preventing mAb recognition.

Immunization of C57Bl6 mice did not induce detectable antibody responses to either *EPIC* or the GPC. The most significant limitations of these studies were the inability to assess T cell responses in vaccinated animals and the lack of inclusion of the GPC control group in the animal studies. The lack of immunogenicity of this vaccine candidate could be due to the plasmid backbone choice, lack of signal peptide, issues with immunization, or the presence of cellular immunity, rather than humoral immunity, that could not be detected. None of these possibilities can be excluded due to the lack of appropriate controls in the study or the inability to evaluate T cell responses. It will be important for future studies to conduct direct comparisons of multi-epitope antigens and the full-length GPC using the same plasmid backbone and to utilize methods that have already been demonstrated for evaluating cellular immunity to candidate CCHFV vaccines, such as pooled peptides for ELISpot assays.

Overall, future work on multi-epitope vaccines for CCHFV would benefit from mapping protective epitopes across the GPC or NP rather than relying on bioinformatic software to predict immunogenic epitopes.

7.2 Development of Anti-Tick Vaccines

Hyalomma marginatum are primarily two host ticks. Upon feeding on a small mammal, the larva will stay on the same host while molting to the nymph instar, take another blood meal, and then drop off their first host to molt into an adult. Adult ticks will then find a large mammal to take another blood meal. Immature and adult stages of *H. marginatum* have distinct host preferences⁹⁸, and these vector-host interactions can be targeted for developing anti-tick vaccines. As an anti-tick vaccine antigen, Subolesin has demonstrated efficacy against both immature and adult stages of a variety of tick species (**Table 1.3**). Previously, only one study has evaluated Subolesin as a viral-vectored vaccine candidate (VACV)¹⁴⁶. The work in Chapters 3 and 4 demonstrates the use of Subolesin within two different viral-vectored vaccine candidates for the preferred hosts of immature and adult *H. marginatum* ticks, respectively.

In Chapter 3, Subolesin was encoded within wtMYXV to target the most preferred hosts of immature *H. marginatum* ticks: small mammals such as rabbits⁹⁸. The recombinant virus, vMyx-GFP-Subolesin, was successfully rescued but was not an immunogenic vaccine candidate in mice. The most likely explanation for the lack of detectable immunogenicity in vaccinated mice is the lack of detection of the Subolesin protein expressed from the viral vector. Studies in this chapter were initially hindered by the lack

of Subolesin antiserum that was not cross-reactive with MYXV, which prevented evaluation of the expression of Subolesin from vMyx-GFP-Subolesin before the immunogenicity study. It will be important for future studies to have appropriate reagents for evaluating the expression of Subolesin from viral-vectored vaccine candidates before *in vivo* studies.

It was surprising that expression of Subolesin was not detected from wtMYXV since the previous study utilizing a viral vector (VACV) for Subolesin demonstrated high levels of Subolesin expression and was immunogenic in mice¹⁴⁶. Subolesin was encoded behind a synthetic early/late VACV promoter, so the protein should have been expressed quickly after infection of cells with the recombinant virus and continue to be expressed throughout infection. However, the expression of Subolesin was only evaluated at 24 hours post-infection, so the possibility of Subolesin expression and degradation before this time point cannot be excluded. While the previous study also utilized a poxviral vector for Subolesin, there are a few important differences between VACV and MYXV as vaccine vectors. First, VACV is permissive in various hosts, whereas wtMYXV is only permissive in rabbits¹⁶⁰. Numerous immunomodulatory genes encoded within wtMYXV are involved in the strict host-restriction of the virus, including proteins known to downregulate members of the NF- κ B pathway^{155,158}, which may impact Subolesin expression. Subolesin appeared to localize to the nucleus of RK13 cells that had been transfected with a mammalian expression plasmid encoding Subolesin. Since Subolesin is involved in innate immune responses as a transcription co-factor, and transfection is known to trigger innate immune responses²²⁷, it would be interesting for future studies to evaluate whether or not Subolesin can interact

with the mammalian NF- κ B pathway and whether or not interactions could be prevented by ablation of the nuclear localization signals of Subolesin. The strain of VACV used in the previous study is vRB12, which lacks the F13L gene. F13L encodes the VP37 outer envelope protein, and deletion of this gene renders the virus unable to produce EEV particles, attenuating the virus^{261,262}. The use of an attenuated strain of VACV, which lacks the strict host-restriction of wtMYXV, may explain the expression and immunogenicity of Subolesin from the VACV vector compared to the wtMYXV vector used in these studies.

The choice of MYXV as a viral vector for Subolesin offered many advantages for downstream applications. Since Leporidae are the most preferred host of immature *Hyalomma* ticks, and MYXV is only permissive in Leporidae, this virus could act to target these hosts specifically in the wild. Many studies have evaluated gene deletions that result in attenuated MYXV, and studies of attenuated field isolates have demonstrated that attenuated strains of MYXV are more transmissible by mechanical vectors due to the longer survival time of affected hosts¹⁵⁷. Unfortunately, these studies did not evaluate attenuated MYXV viruses as a viral vector. Previous studies using MYXV as a viral vector in sheep and cats used attenuated MYXV viruses that lacked various virulence genes. Thus, an attenuated strain of MYXV, possibly lacking NF- κ B immunomodulatory genes, may be an ideal choice for wildlife vaccination of rabbits against ticks. This should be explored in future studies utilizing rabbits to evaluate immunogenicity instead of mice as in these studies.

In Chapter 4, a chimeric Subolesin-RABV-G protein was encoded within an attenuated RABV vector. This vaccine candidate was developed to target cattle, the most preferred hosts of adult *H. marginatum* ticks⁹⁸. This chimeric antigen was shown to be incorporated within the virion of the recombinant virus, RABV-Subolesin. Previous work with a Subolesin chimeric antigen demonstrated that incorporating the chimeric antigen within bacterial membranes enhanced the immunogenicity to Subolesin when given as a protein in adjuvant vaccine^{153,263}. In contrast to this previous work, a single dose of live RABV-Subolesin did not result in humoral immune responses that were greater than two doses of purified Subolesin protein in adjuvant. However, a comparison of the immunogenicity of the RABV-Subolesin vaccine candidate and the protein in adjuvant formulation should be undertaken with care. While the sera from these two vaccine candidates were evaluated in the same ELISA, the sera were generated in different mouse species that are known to have different immunological biases (C57Bl/6J [RABV-Subolesin immunized], and BALB/c [Subolesin protein in Montanide ISA 50 V2 immunized] mice are immunologically biased for Th1- and Th2-type responses, respectively²³⁸). Other studies have shown that inactivated RABV with chimeric antigens incorporated within the virion induces stronger immune responses than the vaccine candidate given as a live preparation^{178,179}. Future studies should evaluate the immunogenicity of RABV-Subolesin given as an inactivated virus in adjuvant and include a group of Subolesin protein in Montanide ISA 50 V2 immunized mice within the same study for direct comparison of immunogenicity of the vaccine candidates. Further, it will be necessary for future studies to feed ticks on immunized animals to evaluate the efficacy of the vaccine candidates.

Results from Chapters 3 and 4 suggest that the viral vector, vaccine preparation, and generation of a chimeric Subolesin antigen are key considerations for developing an anti-tick vaccine. Future work should combine available knowledge of wildlife vaccination against RABV with that known for arthropod vectors. Wildlife vaccination against RABV in the United States uses the licensed vaccine RABORAL V-RG, which is an attenuated, recombinant VACV expressing the RABV G²⁶⁴. This vaccine is licensed in the European Union and the United States of America, has been widely distributed within oral baits since 1987, and has an extensive safety, immunogenicity, and efficacy profile²⁶⁴. Baits for distributing this vaccine to wildlife can be modified to target different animals. Subolesin has already been shown to be immunogenic when expressed from an attenuated, recombinant VACV when given orally¹⁴⁶. However, this vaccine resulted in only a 52% decrease in tick infestation on vaccinated mice¹⁴⁶. Clearly, better vaccine efficacy is needed. It would be interesting for future studies to utilize the Subolesin-RABV-G chimeric antigen within a recombinant VACV vector and evaluate the immunogenicity and efficacy of this candidate through different administrations. Ideally, a single anti-tick vaccine candidate would be developed that could be given through various routes for both domestic livestock and wildlife populations. Developing this anti-tick vaccine candidate would be a significant step toward reducing *H. marginatum* populations and, subsequently, the transmission of CCHFV.

7.3 Understanding the Mechanism of Action of Anti-Tick Vaccines

Studies in Chapter 6 helped clarify part of the mechanism of antibody-Subolesin interactions by showing that antibodies can enter ISE6 cells and bind Subolesin within the

cytoplasm. Further work is needed to understand the biological impact of these antibody-Subolesin interactions, as the current studies were unable to identify metabolic changes in the tick cells from incubation of the cells with Subolesin antisera at the single time point tested. Five genes were differentially expressed between the rabbit mock serum treated group and the rabbit Subolesin antiserum treated group. However, it is likely that these genes are not differentially expressed due to Subolesin antiserum treatment; rather, likely due to the variability of two of the rabbit mock serum treated samples. There are several explanations for the lack of biological impact seen using an embryonic tick cell line, including differences in cell culture, which is generated from a tick egg cluster, compared to the complexities of tick feeding in the whole organism, the dilution of Subolesin antisera used, and the single time point evaluated. Subolesin antisera were used at a 1:50 dilution to treat the ISE6 cells. If the fluorescent puncta visualized by IFA around the nucleus of Subolesin antiserum treated cells were aggregates of Subolesin antibodies and protein, it is possible that the antibody dilution was too low to inhibit Subolesin function. As ticks concentrate their bloodmeal, immunoglobulins cross the midgut membrane to enter the hemocoel. The serum is not diluted during this process, so future studies should explore the use of Subolesin antisera without dilution, which may need to be preabsorbed to prevent non-specific reactivity. For evaluation of the next steps in the mechanism of Subolesin antisera-Subolesin protein interactions, studies should be undertaken to determine whether antibody binding of Subolesin inhibits nuclear translocation or inhibits interaction with known Subolesin binding partners. As the interactome of Subolesin has not been fully elucidated, more research is needed in this area before these experiments will be possible.

Overall, future studies should evaluate higher concentrations of Subolesin antiserum, multiple time points after treatment, and conduct the studies in parallel to force-feeding of the same antisera to ticks. In addition, it would be interesting for future studies to evaluate transcriptomic changes in tick tissues following ingestion of Subolesin antisera compared to transcriptomic differences in tick cell cultures. These studies would provide insight into the role of Subolesin at both the single-cell and whole-organism levels.

7.4 Conclusion

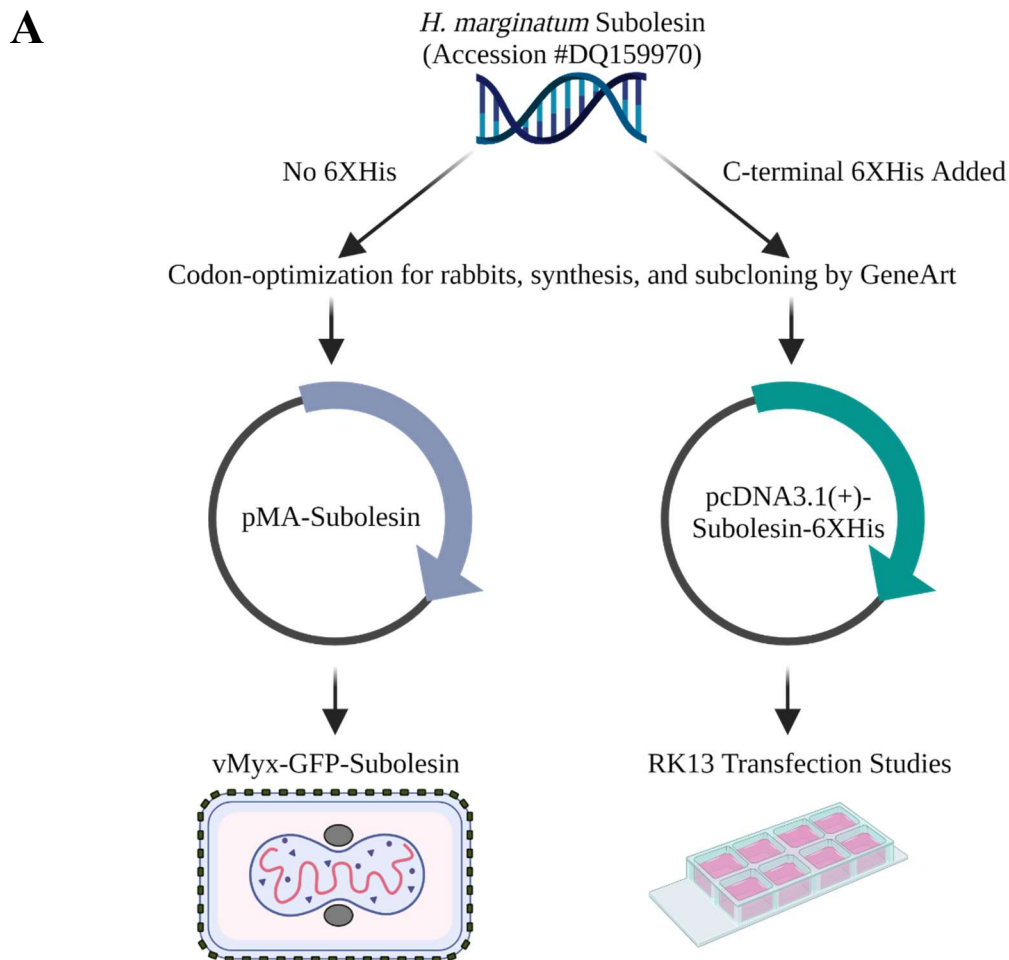
This dissertation has provided evidence for the development of vaccine candidates targeting unique vector-host interaction points of the CCHFV transmission cycle. These studies used two types of platform vaccine technology, viral-vectored vaccines and DNA vaccines, to develop three vaccine candidates. In theory, platform vaccine technology offers an advantage for rapidly generating new vaccine candidates using methods that have already been demonstrated to generate immunogenic vaccine candidates. As the studies in this dissertation show, antigens that are immunogenic using one type of vaccine technology, such as Subolesin when it is used as a purified protein in various adjuvants, are not necessarily immunogenic using other platform technologies. To properly utilize platform vaccine technologies, a robust understanding of the basic biology of the antigen of interest is necessary. Further work needs to be done to understand the function of Subolesin in ticks and tick cells, and to determine the immunogenic and protective regions of the CCHFV GPC. In closing, this dissertation has evaluated three different vaccine development strategies that provide information for future tick and CCHFV vaccine development research.

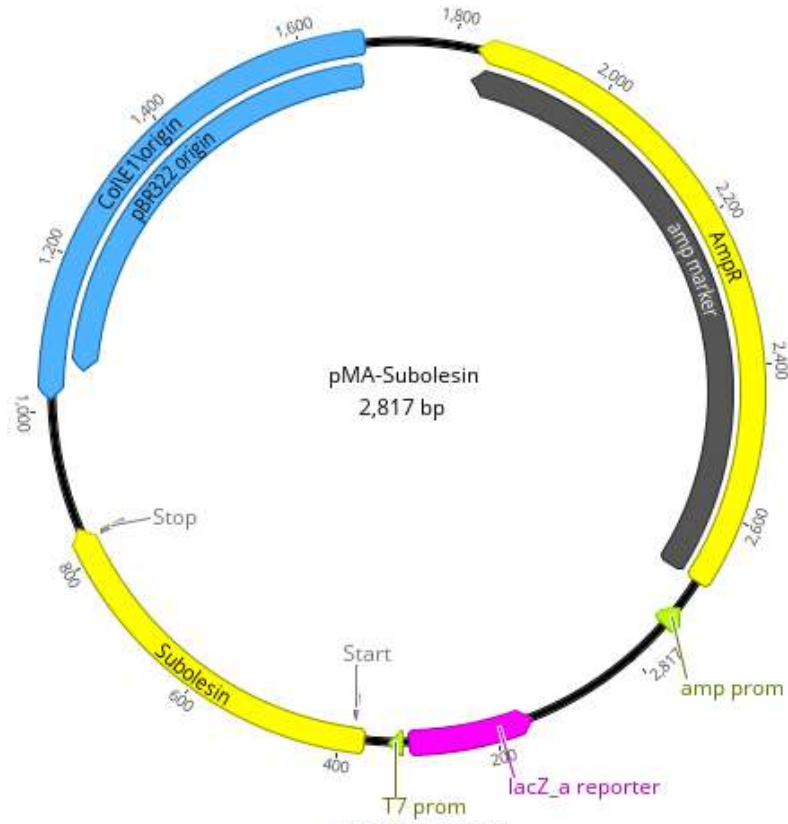
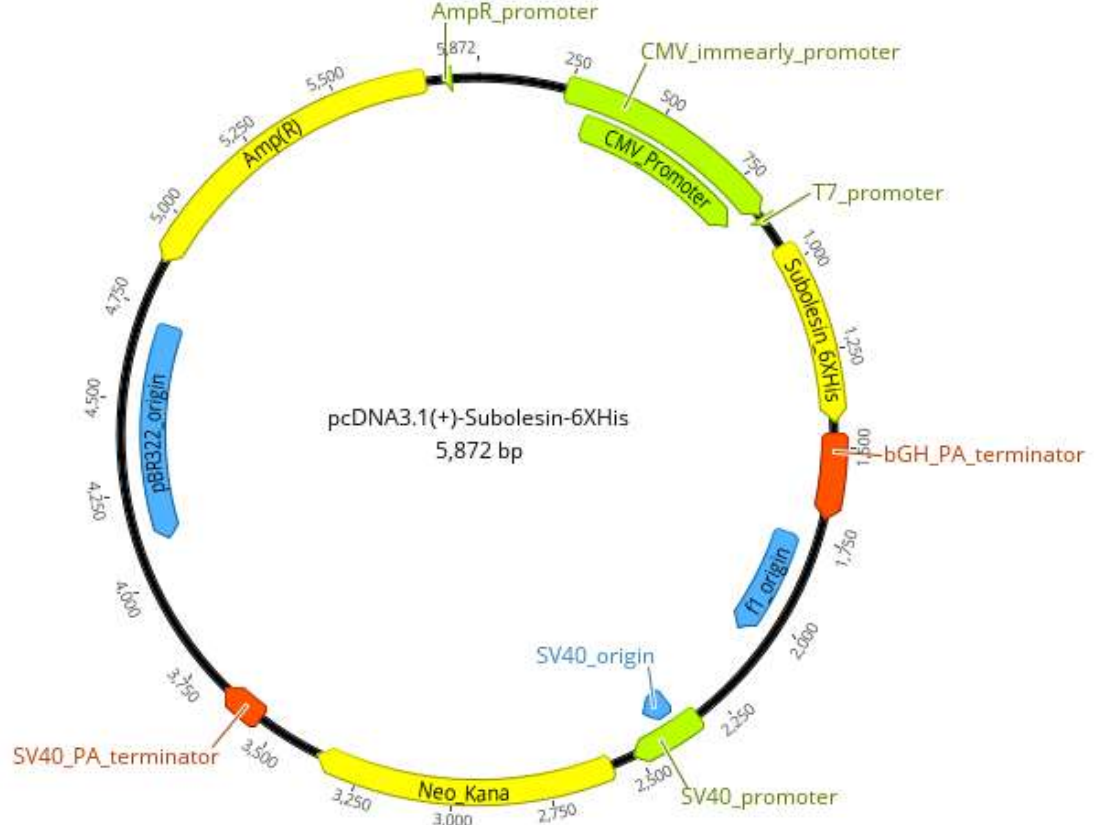
Appendix A

Supplementary Figures for Chapter 3

Supplementary Figure 3.1: Overview of Subolesin plasmid generation, plasmid uses, and plasmid maps of pMA-Subolesin and pcDNA3.1(+)-Subolesin-6XHis.

(A) Subolesin was codon-optimized for rabbits and synthesized with or without a C-terminal polyhistidine tag. The two different Subolesin genes were subcloned into a basic plasmid for use in rescuing the recombinant virus vMyx-GFP-Subolesin (pMA-Subolesin), or into a mammalian expression plasmid for use in RK13 transfection studies (pcDNA3.1(+)-Subolesin-6XHis). Plasmid maps with labels and nucleotide numbers for each region (B) pMA-Subolesin and (C) pcDNA3.1(+)-Subolesin-6XHis. Schematic diagram and plasmid maps generated with BioRender.com and Geneious Prime software.



B**C**

Supplementary Figure 3.2: Nucleotide differences between tick and rabbit codon-optimized Subolesin.

Nucleotide differences between *H. marginatum* Subolesin (Accession # DQ159970) and the *Oryctolagus cuniculus* codon-optimized Subolesin sequences of pMA-Subolesin and pcDNA3.1(+)-Subolesin-6XHis by Thermo Fisher GeneArt for synthesis. Alignment and figure made with Geneious Prime software.

```

                10      20      30      40      50      60
Consensus      AUGGCCUGCG CCACACUGAA GCGVACCCAC GAUUGGGGAUC CUCUGCACAG UCCUAACGGC
DQ159970       .....U.... .A...U.A.. ..A..A... ..C..... .C..... ..G..U...
pcDNA3.1(+)-Subolesin-6XHis .....          .A.G.....          C.....
pMA-Subolesin  .....          ..C.....          .....TC.....A

                70      80      90      100     110     120
Consensus      CGAUCBCCUA AAAGACGCCG CUGCAUGCCU CUGUCUCCAC CAGCUCCUCC AACAAAGGGCC
DQ159970       ....G..A.. .G.....GA. G..U....C U...C.... ..A..... ..C.....U
pcDNA3.1(+)-Subolesin-6XHis A...T....          .....
pMA-Subolesin  ..CAGC....          .....

                130     140     150     160     170     180
Consensus      CACCAGAUGA ACCCAUCUCC AUUCGGCGAG GUGCCACCUA AGAUGACCUC HGAGGAAUUC
DQ159970       .....U.....G.. C.....A..A ....G..C. ....U.. A.....G..A
pcDNA3.1(+)-Subolesin-6XHis .....          .....          ..... T.....
pMA-Subolesin  .....          .....          .....AG C..A.....

                190     200     210     220     230     240
Consensus      GCCGCCAACA UCCGCGAGGA AAUGAGAAGG CUGCAGCGCC GCAAGCAGCU GUGUUUCCAG
DQ159970       ..A..... .U..... G...C..C.. ..A..A..G. ....C.....
pcDNA3.1(+)-Subolesin-6XHis .....          .A.....          ..... T...
pMA-Subolesin  .....          .....          .....A .A..... ..C.....

                250     260     270     280     290     300
Consensus      GGCACCGAUC CUGAGUCBCA GCAGACCUCU GGACUCGUGU CUCCAGUCGC AAGAGAUACAG
DQ159970       ..G..A..C. .A..A..G.. .....GAG. ..C..CU... .G..U..C.. UC...C...
pcDNA3.1(+)-Subolesin-6XHis .....          .AGC...          .....
pMA-Subolesin  .....          .T...          .....

                310     320     330     340     350     360
Consensus      CCHCUGUUCA CCUUUCGCCA GGUCGGACUG AUCUGCGAGC GCAUGAUGAA GGAACGAGAG
DQ159970       ..A..... ..C..... ..G..C..C ..U....A. .G..... ..G.....
pcDNA3.1(+)-Subolesin-6XHis ..T.....          .....          ..... A.....
pMA-Subolesin  ..C.....          .....          .....          .....C...

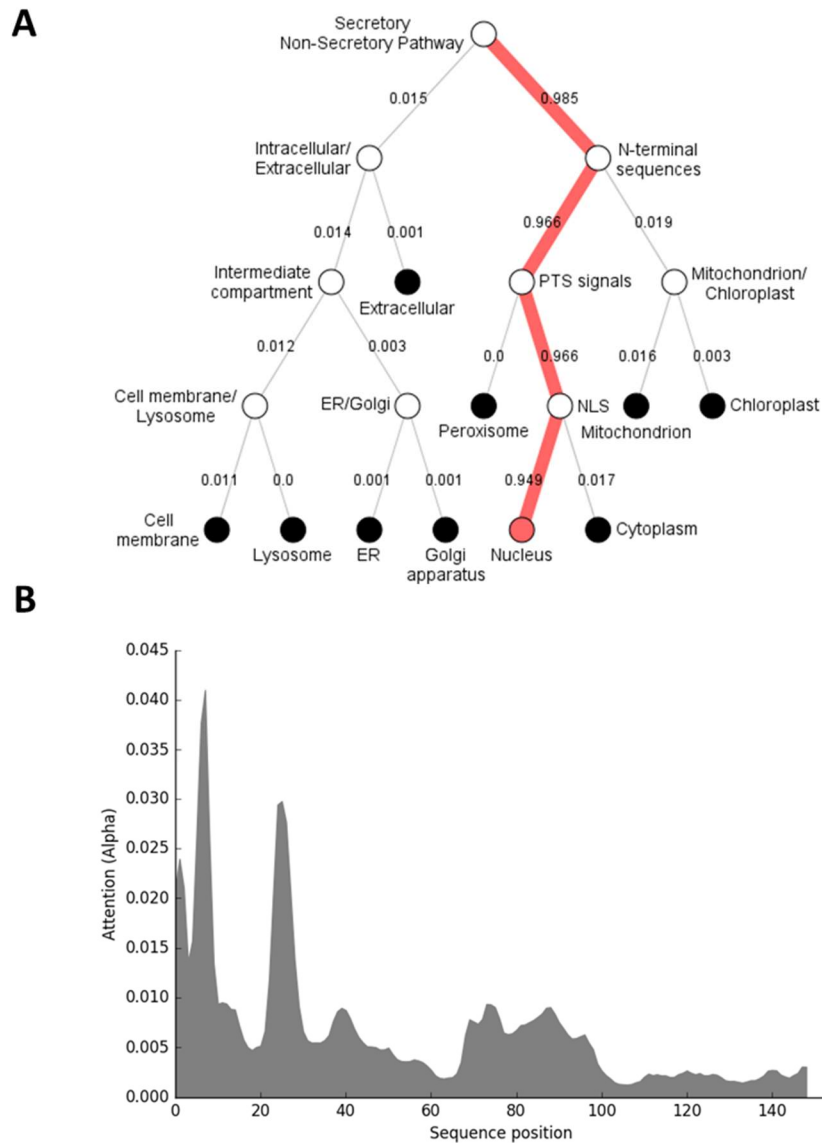
                370     380     390     400     410     420
Consensus      AGCCAGAUGC GCGAGGAGUA CGACCACGUG CUGUCUACCA AACUGGCCGG GCAGUACGAC
DQ159970       .....A. .G..... U....U... ..U..... .G..U..A.. A.....
pcDNA3.1(+)-Subolesin-6XHis .....          .A.....          .....
pMA-Subolesin  .....          .A..... ..T..... ..AGC.....

                430     440     450     460
Consensus      ACCUUCGUGA AGUUCACCUA CGACCAGYRM CACCACCAUC ACCACUGA
DQ159970       ..A..U..C. ....U..G.. .....A--- -----
pcDNA3.1(+)-Subolesin-6XHis .....          .....CAC .....
pMA-Subolesin  .....          .....TGA -----

```

Supplementary Figure 3.3: Outputs of Subolesin localization prediction and residues important for localization.

Results of the submission of the *Hyalomma marginatum* Subolesin sequence to the DeepLoc 1.0 Server for prediction of subcellular localization. (A) Hierarchical tree output showing the most likely localization of the antigen with numbers representing percent likelihood. (B) Graph of the importance of each residue for localization. The two peaks correspond to the nuclear localization signals.



Supplementary Figure 3.4: Homology of Subolesin between *Rhipicephalus microplus* and *Hyalomma marginatum*.

The amino acid sequence of Subolesin from *Rhipicephalus microplus* (Accession # ABA62330) and *Hyalomma marginatum* (Accession # DQ159970). Alignment and figure made with Geneious Prime software.

```

Consensus  MACATLKRTHDWDPLHSPXGRSPKRRRCMPLSPPXPTRAHQXBPSPPFGXVPPKXTSEEI   60
ABA62330   .....S.....--.....ID.....D....L.....   58
DQ159970   .....N.....AP.....MN.....E....M.....   60

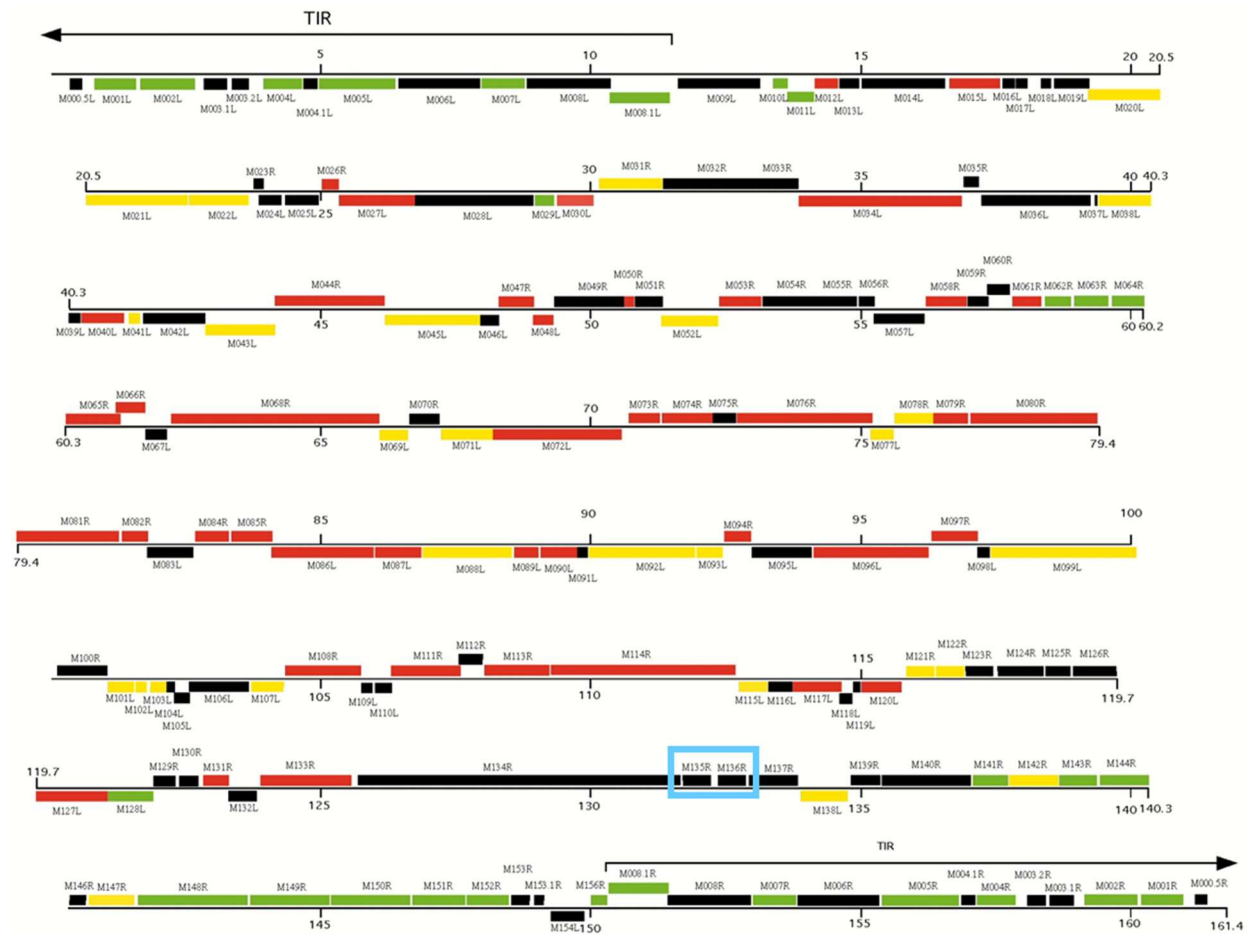
Consensus  AANIREEMRRLQRRKQLCFQGXDPESQXTSGLXSPVXRDQPLFTFRQVGLICERMMKERE   120
ABA62330   .....R....H...S...H.....   118
DQ159970   .....T....Q...L...R.....   120

Consensus  SXIREEYDHVLSTKLAXQYDTFVKFTYDQ*   150
ABA62330   .K.....E.....-   147
DQ159970   .Q.....G.....   150

```

Supplementary Figure 3.5: Schematic diagram of wtMYXV genome.

Schematic diagram of the myxoma virus genome¹⁵⁹. The blue box highlights the M135R and M136R genes and intergenic region (ITR) where genes are inserted. Used with permission from Elsevier Publishing Group, 2018; License: 5237901470214.



Supplementary Figure 3.6: Sequence of vMyx-GFP-Subolesin.

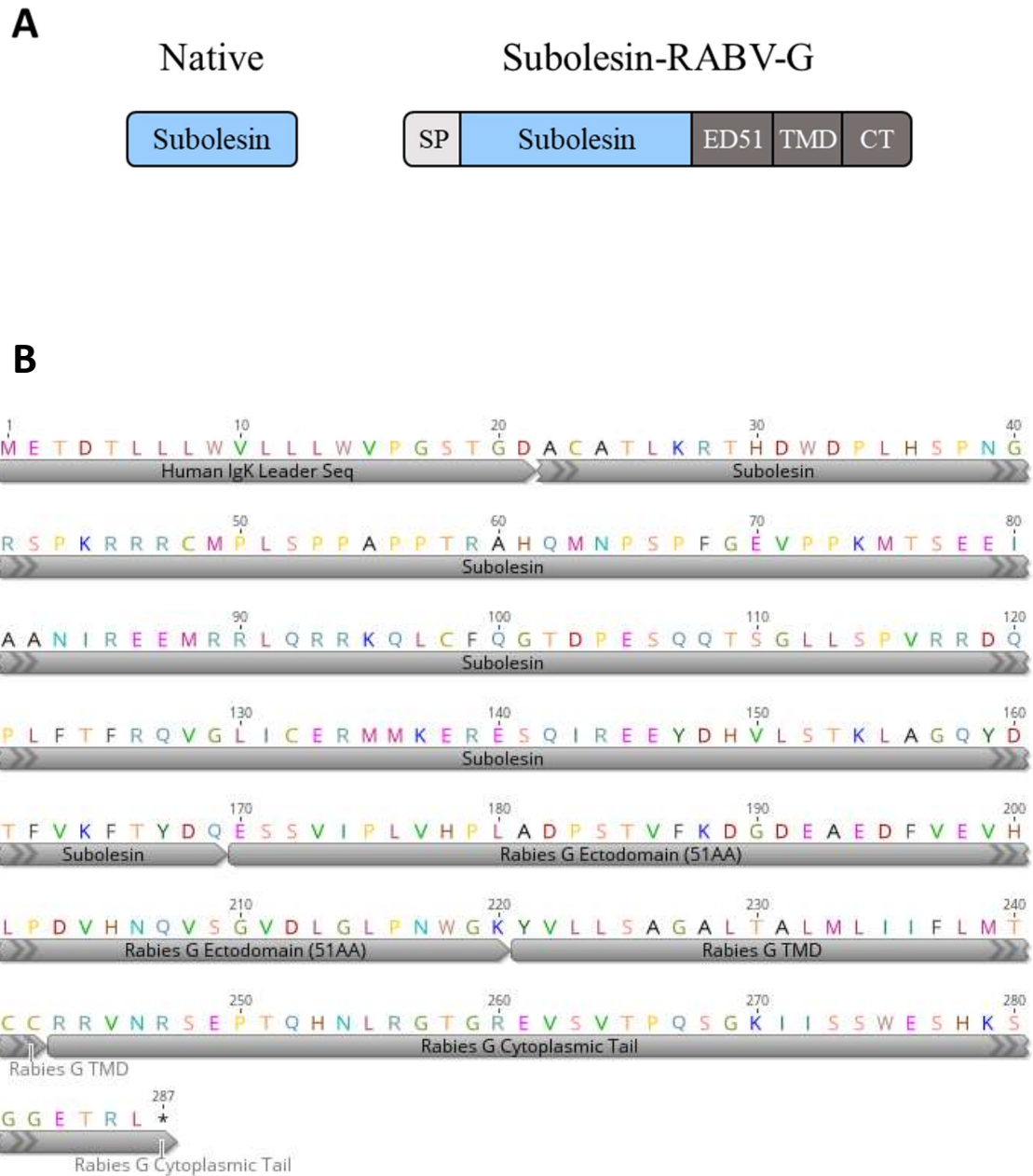
Nucleotide sequence of the insertion of Subolesin and EmGFP between the M135R-M136R genes. Sequence was confirmed with Sanger sequencing at the UTMB molecular genomics core. Alignment of reads and figure made with Geneious Prime Software.



Appendix B:
Supplementary Figures for Chapter 4

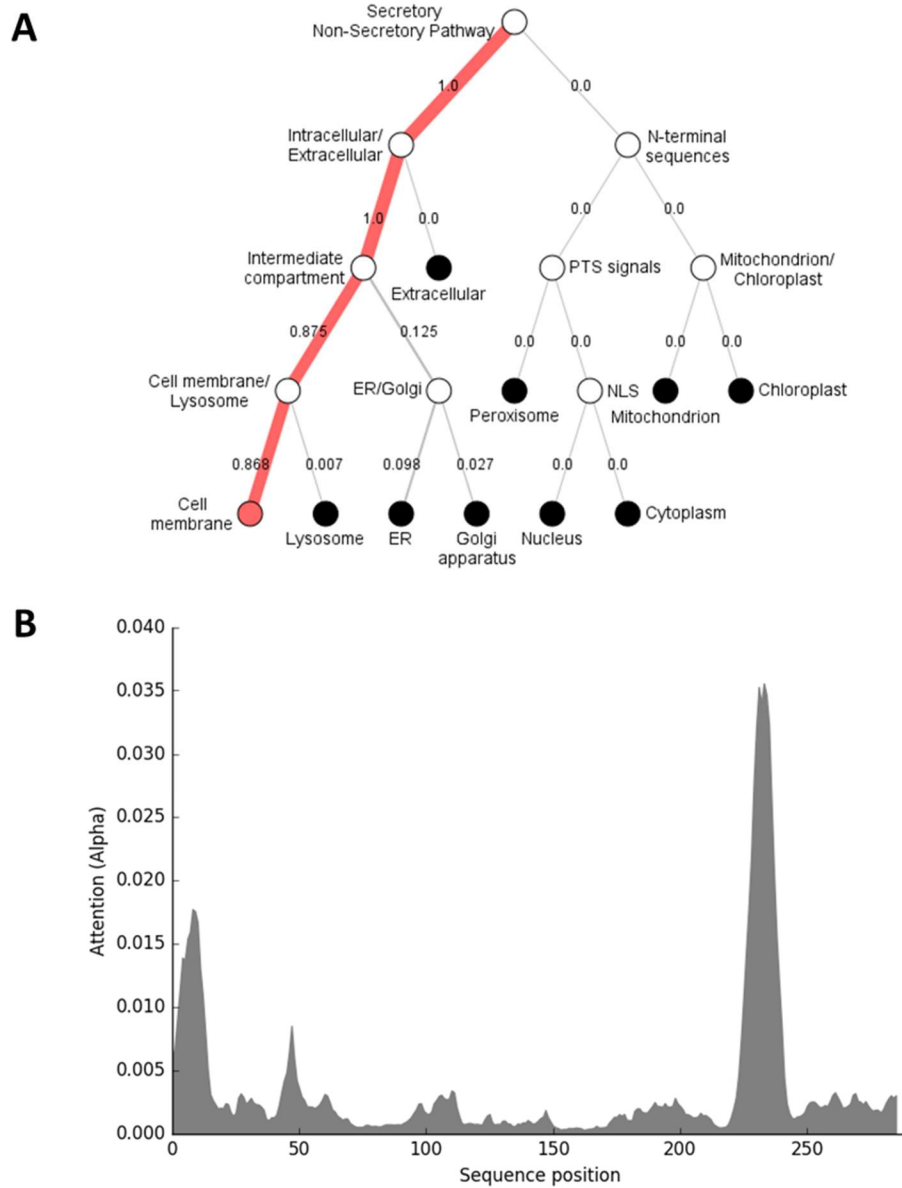
Supplementary Figure 4.1: Modification of the Subolesin antigen.

(A) Schematic diagram of the native form of Subolesin and the modifications made to generate the Subolesin-RABV-G chimeric protein. (B) The amino acid sequence of the Subolesin-RABV-G protein with annotations. Figure made with Geneious Prime software.



Supplementary Figure 4.2: Outputs of Subolesin-RABV-G localization prediction and residues important for localization.

Results of the Subolesin-RABV-G sequence submission to the DeepLoc 1.0 Server for subcellular localization prediction. (A) Hierarchical tree output shows the antigen's most likely localization with numbers representing percent likelihood. (B) Graph of the importance of each residue for localization. The peak corresponds to the RABV G TMD.



Supplementary Figure 4.3: Nucleotide differences between tick and mammalian codon-optimized Subolesin.

(A) Alignment of Subolesin sequences from *H. marginatum* Subolesin (Accession # DQ159970), the rabbit codon-optimized (-CO) Subolesin sequence of pcDNA3.1(+) Subolesin-6XHis, the cattle codon-optimized Subolesin sequence of pCAGGS-Subolesin-RABV-G, and the mouse codon-optimized Subolesin sequence. The N-terminal methionine and C-terminal modifications (6XHis or RABV-G) are removed to only consider nucleotide differences of Subolesin. (B) Summary of the number of nucleotide differences and percent identity between two given sequences. Alignment and percent identity calculations made using Geneious Prime software.

A

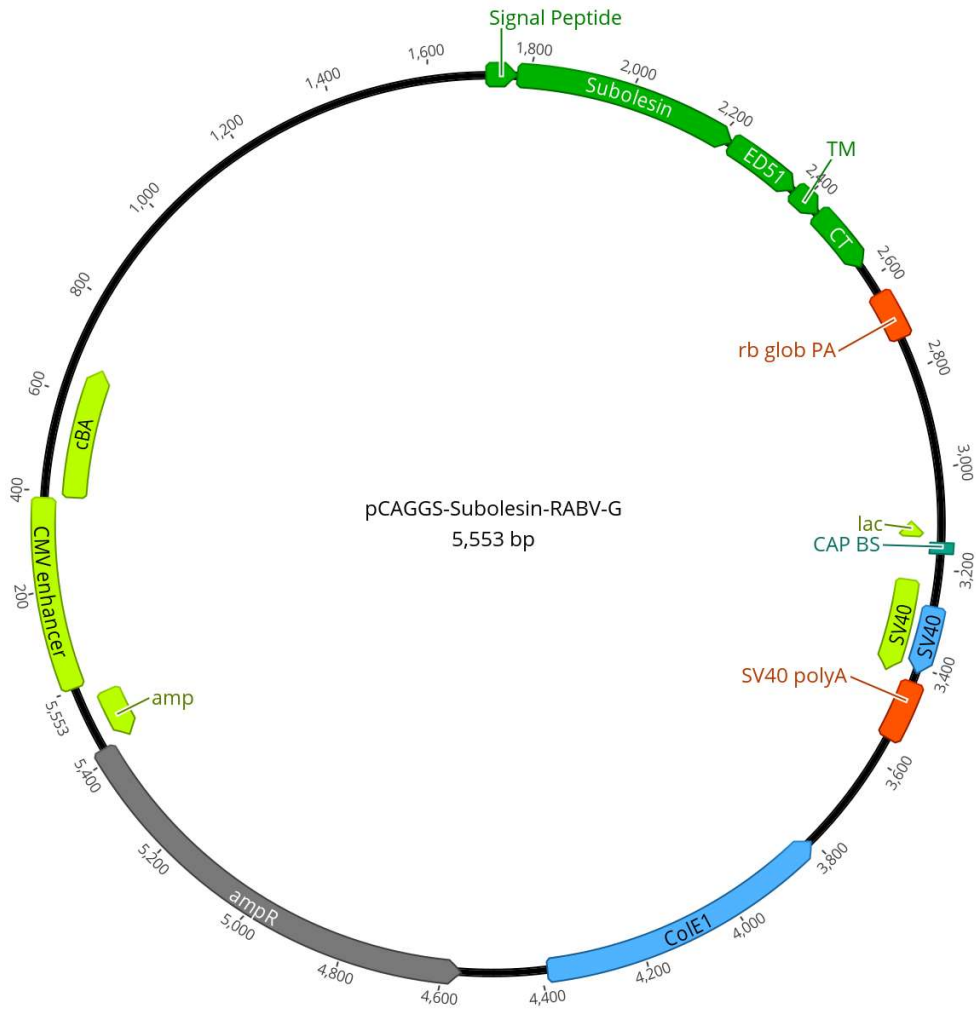
	10	20	30	40	50	60
Consensus	GCTTGCGCCA	CAYTGAARCG	MACACAYGAC	TGGGAYCCCC	TGCACWSYCC	AAATGGNCGC
H.marginatumA.	..U.A..G..	A.....C...U....AGU..	G.....C..A
Cattle-CO	..A..T....	.CC....AA.	A.....T...C....AGC..G...
Rabbit-CO	..C.....	..C....G..	C..C..C..TT..T.TCT..	T..C..A...
Mouse-COTT....A.	C.....T...C....	.T...TCC..T..G
	70	80	90	100	110	120
Consensus	AGCCCTAARA	GRCGCMGGTG	YATGCCTYTG	TCYCCACCWG	CACCTCCAAC	NMGGGCYCAC
H.marginatum	UCG..A..G.	.A..GA....	U.....CU..	..C.....A.CA....	U....
Cattle-COC..GC	.G...C....	C.....T..	..C.....T.	.C..G.....	GC.A..C...
Rabbit-COA.	.A...C.C..	C.....C..	..T.....A.	.T.....AA....	C...
Mouse-COA.	.G..AA.A..	T.....AC.C	..T.....T.C..	TC....T...
	130	140	150	160	170	180
Consensus	CAGATGAAYC	CMTCTCCATT	CGGAGAAGTG	CCACCYAAGA	TGACTTCMGA	AGAAATAGCT
H.marginatumU.	.A..G..C..G..C....A..	G..G.....A
Cattle-COC.	.C.....T..	T.....	..C..C..A.A..A..T...
Rabbit-COC.	.A.....	...C..G...T....CAGC..C..C
Mouse-CO	..A.....T.	.C..C.....	...G.....TT....C..
	190	200	210	220	230	240
Consensus	GCCAACATCC	GCGAGGARAT	GMGACGGCTG	CARMGGMGAA	AGCAGCTGTG	TTTCCAGGGC
H.marginatumU.G..	.C.....A	..AC..C.C.C..G
Cattle-COA.....G..	.A.G..A...	..GA..A...
Rabbit-COA..	.A..A....	..GC.CA...C.....
Mouse-CO	..A.....A.	...A..A..	.C.C.....T	..AA.AC.G.	...A.....	...T.....
	250	260	270	280	290	300
Consensus	ACTGAYCCAG	ARTCTCAGCA	GACCAGTGGT	CTSCTGWSTC	CAGTNCNMG	RGAYCAGCCN
H.marginatum	..A..C....	.A..G.....	...G.....C	..CU..UCG.	.U..C..UC.	A..C.....A
Cattle-COT....	.A..C.....C...	..C..AAG..	.G..AA.GC.	G..C.....G
Rabbit-CO	..C..T..T.	.G.....	...TC...A	..G..TC..G..AA.	A..T.....C
Mouse-COC..C.	.G.....	T.G..TAG..T..CA.	G..T..A..T
	310	320	330	340	350	360
Consensus	CTGTTCACCT	TYCGCCARGT	GGGCCTSATC	TGYGARCGCA	TGATGAAGGA	ACGCGAGWSC
H.marginatumC.....G..C..U	..C..A..G.G..A..	AG.
Cattle-CO	..C.....A.	.C..G..A..C...	..T..G....A.G...	TCT
Rabbit-COT.....G..	C..A..G...	..C..G....AG.
Mouse-CO	T.....	.TA.A..A..	T.....G..A	..T..A..A.A..TC.
	370	380	390	400	410	420
Consensus	CARATMCGNG	AAGAGTAYGA	TCACGTGCTG	AGYACCAAGC	TKGCAGGGCA	GTAYGACACC
H.marginatum	..G..A..G.	.G.....U..	C..U.....U	UCU.....	.U.....A..	...C.....A
Cattle-CO	..A..A..T.C..C.....	.G.....C..	...T.....
Rabbit-CO	..G..C..C.C..C.....A.	.G..C.....	...C.....
Mouse-CO	..A..C..A.T..A...	..T..A....	.T..T.....	...T..T..T
	430	440				
Consensus	TTTGTCAAGT	TYACCTAYGA	YCAA			
H.marginatumU..G..C..	C...			
Cattle-COC.....T..	T...			
Rabbit-CO	..C..G....	.C.....C..	C..G			
Mouse-COT.....T..	T...			

B

	Tick	Rabbit-CO	Cattle-CO	Mouse-CO
Tick	100.0%	94/444 (78.8%)	104/444 (76.6%)	110/444 (75.2%)
Rabbit-CO	-	100.0%	107/444 (75.9%)	112/444 (74.8%)
Cattle-CO	-	-	100.0%	99/444 (77.7%)
Mouse-CO	-	-	-	100.0%

Supplementary Figure 4.4: Plasmid map of pCAGGS-Subolesin-RABV-G.

Plasmid map with labels and nucleotide numbers for each region.



Appendix C:
Supplementary Tables and Figures for Chapter 5

Supplementary Table 5.1: CTL epitopes identified in the CCHFV Turkey2004 GPC sequence.

The total output of the NetCTL 1.2 Server (<https://services.healthtech.dtu.dk/service.php?NetCTL-1.2>) used to predict the binding of 9-mer CTL peptides to 12 MHC class I supertypes (A1, A2, A3, A24, A26, B7, B8, B27, B39, B44, B58, and B62). Predicted peptides were selected based on a combined score of >1.0 given from the prediction of MHC class I binding, proteasomal C terminal cleavage, and TAP transport efficiency to yield 70% sensitivity and 98.5% specificity of CTL ligand prediction accuracy.

Supertype	Name	Sequence	Score
A1	A1_1	TAEIHDDNY	1.9266
	A1_2	STDNTNSTT	1.7988
	A1_3	CIFCKALFY	1.5758
	A1_4	SIMDLSQMY	1.4893
	A1_5	FTDHMFVKW	1.396
	A1_6	ASLACTGCY	1.3523
	A1_7	EMHDLNCSY	1.2775
	A1_8	ETDYTKTFH	1.2588
	A1_9	GTDSTFKAF	1.2342
	A1_10	TLLVCFILY	1.0886
	A1_11	FLWFSSFGY	1.0794
	A1_12	SWDGCDDLY	1.0659
	A1_13	MGDWPSCTY	1.0582
	A1_14	LVDSVSDSF	1.0447
	A1_15	MTSPAQSIL	1.0205
A2	A2_1	LLVCFILYL	1.413
	A2_2	KLNDRCILV	1.3746
	A2_3	FLKDNLIDL	1.2186
	A2_4	RMAIYICRM	1.0065
	A2_5	FLWFSSFGY	1.015
	A2_6	ALFYSLIII	1.0926
	A2_7	LLVLLTVSL	1.0809
	A2_8	LLTVSLSPV	1.1768
	A2_9	FTSICLFML	1.082

	A2_10	FMLGSILFI	1.4982
	A2_11	MLGSILFIV	1.3773
	A2_12	SILFIVSCL	1.0465
	A2_13	ILFIVSCLV	1.0702
	A2_14	CILTLTICV	1.03
	A2_15	FLDSIVKGM	1.1548
	A2_16	NLGPVTITL	1.0738
	A2_17	KLPPEITL	1.2808
	A2_18	KLQSCTHGI	1.3103
	A2_19	KASCWLESV	1.1531
	A2_20	ILLFLAPFV	1.1697
	A2_21	LLFLAPFVL	1.0439
	A2_22	FVLLVLFFM	1.0223
A3	A3_1	SLLSVSSLK	1.7477
	A3_2	GLFKYRHLK	1.7011
	A3_3	VLFFMFGWK	1.6262
	A3_4	KIAELFSTK	1.5871
	A3_5	RVNGHLIHK	1.5799
	A3_6	QMYSVPFEY	1.5557
	A3_7	CIFCKALFY	1.4842
	A3_8	VLSASTVCK	1.4728
	A3_9	KTFHFHSKR	1.4701
	A3_10	ILYLQLLGR	1.4634
	A3_11	ILTLSQGLK	1.4438
	A3_12	GTYKIVIDK	1.4366
	A3_13	LTLSQLKK	1.4266
	A3_14	TINRVKSFK	1.4153
	A3_15	GTFIPGTYK	1.3981
	A3_16	QLHLSICKK	1.3966
	A3_17	HTLESSTIK	1.3751
	A3_18	KLPTVEPFK	1.359
	A3_19	TLLVCFILY	1.3564
	A3_20	RIIERLNNK	1.3195
	A3_21	AINVQSTFK	1.3169
	A3_22	LSNCHAVIK	1.2799
	A3_23	SLCFYIVEK	1.2794
	A3_24	IIIGTLGKK	1.2782
	A3_25	HQLHLSICK	1.2776
	A3_26	RIAETPGPK	1.2717
	A3_27	FLWFSGFY	1.2599
	A3_28	LIIGTLGK	1.2096
	A3_29	ASTSLTARK	1.1625
	A3_30	CTSSTCLHK	1.1151

	A3_31	RTRGLFKYR	1.1011
	A3_32	RLGSELGCY	1.0681
	A3_33	PLFLDSIVK	1.0322
	A3_34	ILVTNCVIK	1.0182
A24	A24_1	GYFNEVLQF	1.6606
	A24_2	MYS PVFEYL	1.5807
	A24_3	YYGKILKLL	1.5752
	A24_4	PFVLLVLF	1.4786
	A24_5	LFMLGSILF	1.4544
	A24_6	SWLIVLLVL	1.3866
	A24_7	YFAKGFLSI	1.3367
	A24_8	VLLVLFMF	1.3175
	A24_9	AMPKTSLCF	1.2854
	A24_10	KYYGKILKL	1.2713
	A24_11	TTMAFLFWF	1.2512
	A24_12	TFIPGTYKI	1.2155
	A24_13	CWLESVKSF	1.1503
	A24_14	SFGYVITCI	1.1393
	A24_15	FFQKRIEF	1.1132
	A24_16	EYIKTEAIV	1.1045
	A24_17	FWFSFGYVI	1.0968
	A24_18	NFFIGILLF	1.0943
	A24_19	TFVICILTL	1.054
A26	A26_1	YTINRVKSF	2.2813
	A26_2	SIMDLSQMY	1.9742
	A26_3	EMHDLNCSY	1.9411
	A26_4	STFKAFSAM	1.6702
	A26_5	ETYQTREGF	1.5844
	A26_6	EKVEETELY	1.5017
	A26_7	SLIEAGTRF	1.4958
	A26_8	EFFVTGEGY	1.3478
	A26_9	FLFWFSFGY	1.341
	A26_10	FVLLVLFM	1.3409
	A26_11	SIVKGMKNL	1.3002
	A26_12	ETSSQHSAM	1.2978
	A26_13	CSIGSINGF	1.2279
	A26_14	GIPGDLQVY	1.1999
	A26_15	EIITLHPKV	1.1893
	A26_16	TTMAFLFWF	1.1733
	A26_17	EGFTSICLF	1.1316
	A26_18	TLSQGLKKY	1.1285
	A26_19	PTVEPFKSY	1.0474
	A26_20	NCSYNICPY	1.0299

B7	B7_1	YPRSSTSGL	1.7711
	B7_2	SPAQSILPM	1.7011
	B7_3	TPGPKTTSL	1.6729
	B7_4	HPRTTMAFL	1.6224
	B7_5	MPTNITHTL	1.6201
	B7_6	APVGHGKTI	1.5777
	B7_7	IPWIVRKLL	1.5619
	B7_8	VPLLGRMAI	1.5388
	B7_9	RPTYGAGEI	1.5174
	B7_10	HPARLLSV	1.5014
	B7_11	KPTVSTANI	1.4925
	B7_12	TPRQSESSA	1.4918
	B7_13	TPSPMTSPA	1.4488
	B7_14	RPATTATST	1.4082
	B7_15	IPKGTGDIL	1.3329
	B7_16	CPYCRHCSA	1.2963
	B7_17	TPVKCRQGF	1.2779
	B7_18	EPHFNTSWM	1.2335
	B7_19	SAMSRTPTL	1.2281
	B7_20	TVSTANIAL	1.1668
	B7_21	EVRKGQSVL	1.1397
	B7_22	SPSTPPTPQ	1.1268
	B7_23	IPGTYKIVI	0.102
	B7_24	KPLVSTTPP	1.0587
	B7_25	KASTGSRKL	1.051
	B7_26	TIEASRRAL	1.0063
	B7_27	EPRNIQQKL	1.0006
B8	B8_1	FFQKRIEEF	2.0254
	B8_2	ILKLLHLTL	2.0242
	B8_3	FVKWKVEYI	1.7426
	B8_4	YPRSSTSGL	1.672
	B8_5	FCKALFYSL	1.6204
	B8_6	FGYVITCIF	1.3681
	B8_7	VPLLGRMAI	1.2987
	B8_8	HPRTTMAFL	1.2943
	B8_9	EVRKGQSVL	1.2658
	B8_10	EALVLRKPL	1.1437
	B8_11	YTINRVKSF	1.1279
	B8_12	ELKPQTCTI	1.0797
	B8_13	WLIVLLVLL	1.069
	B8_14	IPWIVRKLL	1.0073
B27	B27_1	KRMCFRATI	1.8495
	B27_2	RRTRGLFKY	1.7894

	B27_3	GRMAIYICR	1.7504
	B27_4	FRATIEASR	1.6319
	B27_5	RRALLIRSI	1.6235
	B27_6	KRSSWLIVL	1.5368
	B27_7	GRSESIMKL	1.4646
	B27_8	GRGHVKLSR	1.3386
	B27_9	IRSIINTTF	1.2654
	B27_10	ERIPWIVRK	1.2626
	B27_11	RQYKTEIKI	1.2359
	B27_12	VRKGQSVLR	1.1331
	B27_13	ERLNNKKGK	1.121
	B27_14	RKTGSNVML	1.1178
	B27_15	HQLHLSICK	1.088
	B27_16	FMFGWKILF	1.0721
	B27_17	QRLGSELGC	1.0665
B39	B39_1	HREIEINVL	2.4852
	B39_2	NHAAFVNLL	2.2036
	B39_3	YGAGEITVL	1.9092
	B39_4	IHVDEPDEL	1.7566
	B39_5	IHPARSL	1.6556
	B39_6	NHPRTTMAF	1.5644
	B39_7	IEAGTRFNL	1.5123
	B39_8	KRSSWLIVL	1.415
	B39_9	FFYGLKNML	1.3252
	B39_10	SADREIHQL	1.3118
	B39_11	FSAMPKTSL	1.2929
	B39_12	GRSESIMKL	1.2765
	B39_13	RKTGSNVML	1.1503
	B39_14	TEAIVCVEL	1.1422
	B39_15	FMFGWKILF	1.0672
	B39_16	QEGRGHVKL	1.0398
	B39_17	VSESTGVAL	1.0164
	B39_18	HNHAAFVNL	1.0096
B44	B44_1	LEVEIILT	2.0677
	B44_2	REIEINVLL	2.0432
	B44_3	EETELYLNL	1.7598
	B44_4	IEAGTRFNL	1.7553
	B44_5	GEGYFNEVL	1.7496
	B44_6	NEVLQFKTL	1.7154
	B44_7	REGFTSICL	1.6973
	B44_8	QEGRGHVKL	1.6604
	B44_9	LEFGTDSTF	1.6046
	B44_10	IEHRGNKIL	1.5719

	B44_11	GEITVLVEV	1.5501
	B44_12	KEKVEETEL	1.4756
	B44_13	TEAIVCVEL	1.4217
	B44_14	VEDASESKL	1.3561
	B44_15	LEEDTEGLL	1.3176
	B44_16	IETDYTKTF	1.2829
	B44_17	LEQPQSILI	1.2699
	B44_18	VEEGFFDLM	1.2467
	B44_19	NEDDTQKCL	1.101
	B44_20	SEEPGDDCI	1.0855
	B44_21	IEASRRALL	1.0016
	B44_22	REVRKGQSV	1.0016
B58	B58_1	STANIALSW	1.8884
	B58_2	RTTMAFLFW	1.6517
	B58_3	TSLSIEAPW	1.6396
	B58_4	MAFLWFWSF	1.6115
	B58_5	FTDHMFVKW	1.531
	B58_6	RNWRCNPTW	1.5216
	B58_7	LVLFFMFGW	1.4947
	B58_8	TTMAFLFWF	1.4474
	B58_9	RSSTSGLQL	1.4393
	B58_10	GAINVQSTF	1.3733
	B58_11	SSTCLHKEW	1.3449
	B58_12	QMYSVPFEY	1.3228
	B58_13	CSIGSINGF	1.3072
	B58_14	FGYVITCIF	1.2625
	B58_15	HFNTSWMSW	1.2342
	B58_16	LSQMYSVPF	1.2187
	B58_17	SGDRQVEEW	1.1984
	B58_18	RSSWLIVLL	1.198
	B58_19	FLWFWSFGY	1.1598
	B58_20	LSASTVCKL	1.1579
	B58_21	RMAIYICRM	1.1318
	B58_22	FGWKILFCF	1.1078
	B58_23	YLNLERIPW	1.0882
	B58_24	SLIEAGTRF	1.0382
	B58_25	KSHVCDYSL	1.0175
B62	B62_1	QMYSVPFEY	1.5112
	B62_2	FMFGWKILF	1.4565
	B62_3	YTINRVKSF	1.4419
	B62_4	FLWFWSFGY	1.4399
	B62_5	EMHDLNCSY	1.3557
	B62_6	SIMDLSQMY	1.3389

B62_7	SLIEAGTRF	1.3274
B62_8	AMPKTSLCF	1.2655
B62_9	ASLACTGCY	1.2262
B62_10	FLSIDSGYF	1.2105
B62_11	FQKRIEEFF	1.18
B62_12	MAFLWFWSF	1.1783
B62_13	LQFKTLSTL	1.1767
B62_14	VTQHNHAAF	1.1687
B62_15	SLTARKLEF	1.1283
B62_16	FEIESHKCY	1.1126
B62_17	LSQMYSVPF	1.1023
B62_18	LEFGTDSTF	1.0637
B62_19	GAINVQSTF	1.0475
B62_20	YCSLFCCPY	1.0449
B62_21	LFMLGSILF	1.029
B62_22	TLSQGLKKY	1.0277
B62_23	CSIGSINGF	1.0188

Supplementary Table 5.2: HTL epitopes of HLA locus DR identified in the CCHFV Turkey2004 GPC sequence.

The total output of the NetMHCII 2.3 Server (<https://services.healthtech.dtu.dk/service.php?NetMHCII-2.3>) used to predict the binding of 15-mer HTL peptides to 25 HLA-DR alleles. Predicted peptides were selected if they met the criteria of (1) a strong binder threshold of <2.00%-rank to a set of 1,000,000 random natural peptides and (2) a predicted IC50 value <50 nM.

Allele	Name	Sequence	Affinity (nM)	% Rank
B1_0101	DR_1	AQSILPMSAAPTAIQ	5.1	0.6
	DR_2	KSFFYGLKNMLGSVF	5.8	0.9
	DR_3	QSILPMSAAPTAIQN	5.8	0.9
	DR_4	PAQSILPMSAAPTAI	5.9	0.9
	DR_5	FILYLQLLGRGGAHG	5.9	0.9
	DR_6	CFILYLQLLGRGGAH	6.3	1.1
	DR_7	VKSFFYGLKNMLGSV	6.4	1.1
	DR_8	ILYLQLLGRGGAHGQ	6.7	1.2
	DR_9	SFFYGLKNMLGSVFG	7	1.4
	DR_10	SILPMSAAPTAIQNI	7.8	1.7
	DR_11	VCFILYLQLLGRGGA	7.9	1.7
	DR_12	SVKSFFYGLKNMLGS	8	1.8
	DR_13	SPAQSILPMSAAPTA	8.4	1.9
B1_0103	None that meet affinity criteria			
B1_0301	DR_14	TYKIVIDKKNKLNDR	11.3	0.25
	DR_15	GTYKIVIDKKNKLND	13.1	0.4
	DR_16	YKIVIDKKNKLNDRC	13.3	0.4
	DR_17	PGTYKIVIDKKNKLN	14.7	0.4
	DR_18	FRATIEASRRALLIR	15.1	0.5
	DR_19	RATIEASRRALLIRS	15.8	0.5
	DR_20	KIVIDKKNKLNDRCI	19.8	0.7
	DR_21	CFRATIEASRRALLI	21.5	0.8
	DR_22	IPGTYKIVIDKKNKL	26	1
	DR_23	ATIEASRRALLIRSI	26.8	1.1
	DR_24	SNVMLAVCKRMCFRA	28.8	1.1
	DR_25	DYSLDTDGPPVRLPHI	31.5	1.3
	DR_26	NVMLAVCKRMCFRAT	31.8	1.3
	DR_27	CDYSLDTDGPPVRLPH	33.4	1.4

	DR_28	GSNVMLAVCKRMCFR	33.5	1.4
	DR_29	MCFRATIEASRRALL	34.1	1.4
	DR_30	RKPLFLDSIVKGMKN	41	1.8
	DR_31	VCDYSLDTDGPVRLP	41.6	1.8
	DR_32	YSLDTDGPVRLPHIY	43.4	1.9
B1_0401	DR_33	EVLQFKTLSTLSPTE	13.1	0.17
	DR_34	VLQFKTLSTLSPTEP	14.3	0.25
	DR_35	NEVLQFKTLSTLSPT	14.4	0.25
	DR_36	LQFKTLSTLSPTEPS	15.7	0.3
	DR_37	FNEVLQFKTLSTLSP	21.1	0.5
	DR_38	QFKTLSTLSPTEPSH	22	0.6
	DR_39	QSTFKPTVSTANIAL	24.7	0.7
	DR_40	STFKPTVSTANIALS	26.4	0.8
	DR_41	VQSTFKPTVSTANIA	26.4	0.8
	DR_42	NVQSTFKPTVSTANI	35.9	1.3
	DR_43	TFKPTVSTANIALSW	38.9	1.5
	DR_44	SVSSLKTATTPTPTS	41	1.6
	DR_45	AKGFLSIDSGYFSAK	44.6	1.8
	DR_46	VSSLKTATTPTPTSP	45.8	1.9
B1_0402	None that meet affinity criteria			
B1_0403	None that meet affinity criteria			
B1_0404	DR_47	SIVKGMKNLLNSTSL	12	0.2
	DR_48	DSIVKGMKNLLNSTS	13.3	0.3
	DR_49	IVKGMKNLLNSTSLE	14.6	0.4
	DR_50	RSLLSVSSLKTATTP	17.4	0.5
	DR_51	ARLLSVSSLKTATT	17.9	0.6
	DR_52	AQSILPMSAAPTAIQ	19.6	0.7
	DR_53	LDSIVKGMKNLLNST	20.1	0.7
	DR_54	QSILPMSAAPTAIQN	20.8	0.8
	DR_55	SLLSVSSLKTATTPT	21.3	0.8
	DR_56	PARLLSVSSLKTAT	22.6	0.9
	DR_57	KSFFYGLKNMLGSVF	23	1
	DR_58	PAQSILPMSAAPTAI	23.2	1
	DR_59	SFFYGLKNMLGSVFG	24	1
	DR_60	RMAIYICRMSNHPR	24.2	1.1
	DR_61	LLSVSSLKTATTPTP	24.3	1.1
	DR_62	GRMAIYICRMSNHPR	24.6	1.1
	DR_63	FLDSIVKGMKNLLNS	26.2	1.2
	DR_64	VKGMKNLLNSTSLET	27.4	1.3
DR_65	LSVSSLKTATTPTPT	27.7	1.4	
DR_66	KGMKNLLNSTSLETS	28	1.4	
DR_67	MAIYICRMSNHPRTT	28.6	1.4	
DR_68	TLTICVVSTSAVEME	30.5	1.6	

	DR_69	SPAQSILPMSAAPT	32.4	1.8
	DR_70	DPDVVAASTSLTARK	32.5	1.8
	DR_71	LTICVVSTSAVEMEN	32.6	1.8
	DR_72	PDVVAASTSLTARKL	32.6	1.8
	DR_73	VKSFFYGLKNMLGSV	33.2	1.9
	DR_74	NEVLQFKTLSTLSPT	33.3	1.9
	DR_75	HPARSLLSVSSLKTA	33.6	1.9
B1_0405	DR_76	YFAKGFLSIDSGYFS	19.4	0.4
	DR_77	FAKGFLSIDSGYFSA	22	0.5
	DR_78	SYFAKGFLSIDSGYF	23.7	0.6
	DR_79	AKGFLSIDSGYFSAK	28.7	0.9
	DR_80	KGFLSIDSGYFSAKC	34.7	1.3
	DR_81	EVLQFKTLSTLSPTE	35.5	1.3
	DR_82	NEVLQFKTLSTLSPT	36	1.3
	DR_83	FNEVLQFKTLSTLSP	37.6	1.4
	DR_84	VLQFKTLSTLSPTEP	39.4	1.5
	DR_85	KWKVEYIKTEAIVCV	40.6	1.6
	DR_86	WKVEYIKTEAIVCVE	44.5	1.9
B1_0701	DR_87	ELGTYINRVKSFKL	4	0.12
	DR_88	LGCYTINRVKSFKLC	4.1	0.12
	DR_89	GTYINRVKSFKLCE	4.6	0.17
	DR_90	CYTINRVKSFKLCEN	5.1	0.25
	DR_91	YTINRVKSFKLCENS	5.3	0.25
	DR_92	TINRVKSFKLCENSA	7.1	0.5
	DR_93	VRKLLQVSESTGVAL	7.2	0.5
	DR_94	TDYTKTFHFHSKRVT	7.4	0.6
	DR_95	RKLLQVSESTGVALK	7.8	0.6
	DR_96	ETDYTKTFHFHSKRV	8.1	0.7
	DR_97	DYTKTFHFHSKRVTA	9	0.8
	DR_98	KLLQVSESTGVALKR	9.8	0.9
	DR_99	YTKTFHFHSKRVTAH	10.2	1
	DR_100	IVRKLLQVSESTGVA	10.5	1
	DR_101	WIVRKLLQVSESTGV	11.4	1.2
DR_102	VEPFKSYFAKGFLSI	12.4	1.4	
DR_103	FYSLIIIGTLGKKFK	13.4	1.5	
DR_104	LLQVSESTGVALKRS	13.8	1.6	
DR_105	TKTFHFHSKRVTAHG	13.9	1.6	
DR_106	LFYSLIIIGTLGKKF	13.9	1.6	
DR_107	TVEPFKSYFAKGFLS	14	1.7	
DR_108	PTVEPFKSYFAKGFL	14.6	1.7	
DR_109	EPFKSYFAKGFLSID	14.9	1.8	
DR_110	YSLIIIGTLGKKFKQ	15.5	1.9	
DR_111	INRVKSFKLCENSAT	15.6	1.9	

B1_0801	DR_112	RRTRGLFKYRHLKDD	25.5	0.4
	DR_113	RTRGLFKYRHLKDDE	28	0.5
	DR_114	CRTRGLFKYRHLKD	28.3	0.6
	DR_115	TRGLFKYRHLKDDEE	29	0.6
	DR_116	KTFHFHSKRVTAHGD	29.8	0.6
	DR_117	TFHFHSKRVTAHGDT	30	0.6
	DR_118	TKTFHFHSKRVTAHG	31.7	0.7
	DR_119	LFCFKCCRTRGLFK	32.3	0.7
	DR_120	ILFCFKCCRTRGLF	33	0.8
	DR_121	YTKTFHFHSKRVTAH	34.8	0.9
	DR_122	CCRTRGLFKYRHLK	35.4	0.9
	DR_123	FCFKCCRTRGLFKY	35.9	0.9
	DR_124	FKCCRTRGLFKYRH	36.3	1
	DR_125	CFKCCRTRGLFKYR	39.5	1.1
	DR_126	RGLFKYRHLKDDEET	39.7	1.2
	DR_127	KCCRTRGLFKYRHL	40.9	1.2
	DR_128	FHFHSKRVTAHGDTP	43.5	1.4
	DR_129	SNVMLAVCKRMCFRA	45	1.5
	DR_130	KILFCFKCCRTRGL	45.4	1.5
	DR_131	NVMLAVCKRMCFRAT	45.5	1.5
DR_132	GSNVMLAVCKRMCFR	47.4	1.6	
DR_133	DYTKTFHFHSKRVTA	47.5	1.6	
B1_0802	None that meet affinity criteria			
B1_0901	DR_134	DSTFKAFSAMPKTSL	11.5	0.25
	DR_135	STFKAFSAMPKTS LC	12	0.3
	DR_136	PAQSILPMSAAPT AI	13.5	0.4
	DR_137	TDSTFKAFSAMPK TS	13.6	0.4
	DR_138	AQSILPMSAAPT AIQ	13.9	0.4
	DR_139	TFKAFSAMPKTS LCF	15.8	0.6
	DR_140	SPAQSILPMSAAPT A	16.1	0.6
	DR_141	GRGHVKLSRGSEV VL	16.1	0.6
	DR_142	RGHVKLSRGSEV VLD	16.9	0.7
	DR_143	GTDSTFKAFSAMPK T	17.6	0.7
	DR_144	QSILPMSAAPT AIQN	18	0.7
	DR_145	GHVKLSRGSEV VLDV	21.1	1
	DR_146	STGVALKRSSWLIV L	21.6	1
	DR_147	TGVALKRSSWLIV LL	22.2	1.1
	DR_148	TVSTANIALSWSSIE	22.6	1.1
	DR_149	GVALKRSSWLIV LLV	23.5	1.2
	DR_150	VSTANIALSWSSIEH	23.6	1.2
	DR_151	EGRGHVKLSRGSEV V	23.9	1.2
	DR_152	STANIALSWSSIEHR	25.2	1.3
	DR_153	SILPMSAAPT AIQNI	25.6	1.4

	DR_154	ESTGVALKRSSWLIV	26.6	1.5
	DR_155	TANIALSWSSIEHRG	26.8	1.5
	DR_156	TSPAQSILPMSAAPT	27.8	1.6
	DR_157	FGTDSTFKAFSAMPK	29.8	1.8
	DR_158	VALKRSSWLIVLLVL	30.1	1.8
	DR_159	FKAFSAMPKTSLCFY	30.9	1.9
B1_1001	DR_160	STFKAFSAMPKTSLC	3	0.01
	DR_161	DSTFKAFSAMPKTSL	3.1	0.01
	DR_162	TFKAFSAMPKTSLCF	3.2	0.02
	DR_163	TDSTFKAFSAMPKTS	3.5	0.03
	DR_164	GTDSTFKAFSAMPKT	4	0.05
	DR_165	FGTDSTFKAFSAMPK	5.9	0.2
	DR_166	FKAFSAMPKTSLCFY	6.8	0.4
	DR_167	LQFKTLSTLSPTEPS	6.8	0.4
	DR_168	VLQFKTLSTLSPTEP	7	0.4
	DR_169	QFKTLSTLSPTEPSH	7.1	0.4
	DR_170	EVLQFKTLSTLSPTE	7.1	0.4
	DR_171	NEVLQFKTLSTLSPTE	8.2	0.6
	DR_172	KSFFYGLKNMLGVSF	11.1	1.1
	DR_173	FNEVLQFKTLSTLSP	12.1	1.3
	DR_174	SFFYGLKNMLGVSFVG	12.2	1.3
	DR_175	VKSFFYGLKNMLGVS	13.1	1.5
	DR_176	FFYGLKNMLGVSFGN	13.4	1.6
B1_1101	DR_177	DYTKTFHFHFSKRVT	6.1	0.3
	DR_178	YTKTFHFHFSKRVT	6.6	0.4
	DR_179	TDYTKTFHFHFSKRVT	7	0.4
	DR_180	FKAFSAMPKTSLCFY	7.6	0.5
	DR_181	TFKAFSAMPKTSLCF	7.9	0.5
	DR_182	TKTFHFHFSKRVT	8.5	0.6
	DR_183	STFKAFSAMPKTSLC	8.7	0.6
	DR_184	KTFHFHFSKRVT	9.2	0.7
	DR_185	ETDYTKTFHFHFSKRVT	10	0.8
	DR_186	KAFSAMPKTSLCFY	10	0.8
	DR_187	QLHLSICKKRKTGSN	10.4	0.8
	DR_188	HQLHLSICKKRKTGS	11.2	0.9
	DR_189	DSTFKAFSAMPKTSL	11.4	1
	DR_190	LHLSICKKRKTGSN	11.8	1
	DR_191	LYLQLLGRGGAHGQS	12.9	1.2
	DR_192	ILYLQLLGRGGAHGQ	13.1	1.2
	DR_193	KSFFYGLKNMLGVSF	13.6	1.2
DR_194	KKYYGKILKLLHRTL	14	1.3	
DR_195	FILYLQLLGRGGAHG	14.3	1.3	
DR_196	IHQHLSICKKRKTG	14.5	1.4	

	DR_197	VKSFFYGLKNMLGSV	14.5	1.4
	DR_198	IETDYTKTFHFHSKR	15	1.4
	DR_199	LKKYYGKILKLLHLT	15.4	1.5
	DR_200	KYYGKILKLLHLTLE	16	1.5
	DR_201	GYKRIIERLNNKKGK	16.2	1.6
	DR_202	ELYLNLERIPWIVRK	17.2	1.7
	DR_203	SFFYGLKNMLGSVFG	17.6	1.8
	DR_204	SVKSFFYGLKNMLGS	17.9	1.8
	DR_205	CFILYLQLLGRGGAH	17.9	1.8
	DR_206	TGYKRIIERLNNKKG	18.2	1.8
B1_1201	DR_207	AKASCWLESVKSFFY	34.6	0.6
	DR_208	KASCWLESVKSFFYG	44.7	1
	DR_209	ASCWLESVKSFFYGL	47.8	1.1
	DR_210	TVSIMDLSQMYSVPF	49.6	1.2
B1_1301	DR_211	LIIGTLGKKFKQYR	4.9	0.7
	DR_212	IIIGTLGKKFKQYRE	5.2	0.8
	DR_213	IILTLSQGLKKYYGK	5.4	0.9
	DR_214	LGCYTINRVKSFKLC	5.8	1
	DR_215	ILTLSQGLKKYYGKI	5.8	1
	DR_216	EIILTLSQGLKKYYG	5.9	1
	DR_217	VEIILTLSQGLKKYY	6.5	1.2
	DR_218	ELGCYTINRVKSFKL	6.6	1.2
	DR_219	CFKCCRTRGLFKYR	6.7	1.3
	DR_220	FKCCRTRGLFKYRH	6.8	1.3
	DR_221	SLIIGTLGKKFKQY	7	1.4
	DR_222	RALLIRSIINTTFVI	7.1	1.4
	DR_223	ALLIRSIINTTFVIC	7.3	1.5
	DR_224	RRALLIRSIINTTFV	7.4	1.5
	DR_225	LTLSQGLKKYYGKIL	7.5	1.5
	DR_226	FCFKCCRTRGLFKY	7.6	1.6
	DR_227	CCRTRGLFKYRHLK	8.1	1.7
	DR_228	HQLHLSICKKRKTGS	8.1	1.8
DR_229	QLHLSICKKRKTGSN	8.5	1.9	
DR_230	GCYTINRVKSFKLCE	8.6	1.9	
B1_1302	DR_231	GRGHVKLSRGSEVVL	5.5	0.8
	DR_232	RGHVKLSRGSEVVLD	5.7	0.9
	DR_233	LPQIAVNLSNCHAVI	5.9	0.9
	DR_234	GHVKLSRGSEVVLDV	6.3	1
	DR_235	PQIAVNLSNCHAVIK	6.6	1.1
	DR_236	LLPQIAVNLSNCHAV	7.4	1.3
	DR_237	EGRGHVKLSRGSEVV	7.7	1.4
	DR_238	HVKLSRGSEVVLDVC	8.5	1.6
	DR_239	QIAVNLSNCHAVIKS	9.8	1.9

B1_1501	DR_240	PTVEPFKSYFAKGFL	5.6	0.12
	DR_241	LPTVEPFKSYFAKGF	6.1	0.17
	DR_242	KLPTVEPFKSYFAKG	6.9	0.25
	DR_243	TVEPFKSYFAKGFLS	7.2	0.25
	DR_244	AKLPTVEPFKSYFAK	7.7	0.3
	DR_245	CYTINRVKSFKLCEN	9.3	0.5
	DR_246	GCYTINRVKSFKLCE	9.5	0.5
	DR_247	YTINRVKSFKLCENS	10.2	0.5
	DR_248	LGCYTINRVKSFKLC	10.2	0.5
	DR_249	SQGLKKYYGKILKLL	12.2	0.7
	DR_250	QGLKKYYGKILKLLH	12.8	0.8
	DR_251	YFNEVLQFKTLSTLS	12.9	0.8
	DR_252	FNEVLQFKTLSTLSP	13	0.8
	DR_253	TINRVKSFKLCENSA	13.4	0.9
	DR_254	NEVLQFKTLSTLSPT	13.8	0.9
	DR_255	HAKLPTVEPFKSYFA	14	0.9
	DR_256	LSQGLKKYYGKILKL	14.1	0.9
	DR_257	ELGCYTINRVKSFKL	15	1
	DR_258	VEPFKSYFAKGFLSI	15.2	1
	DR_259	GYFNEVLQFKTLSTL	15.4	1
	DR_260	GLKKYYGKILKLLHL	15.6	1.1
	DR_261	CSYNICPYCASRLTS	20	1.5
	DR_262	TLSQGLKKYYGKILK	20	1.5
	DR_263	SYNICPYCASRLTSD	21.2	1.7
	DR_264	NCSYNICPYCASRLT	23.6	1.9
	B1_1602	DR_265	DSTFKAFSAMPKTSL	19.9
DR_266		AKGFLSIDSGYFSAK	21.6	0.6
DR_267		STFKAFSAMPKTSLC	22.2	0.6
DR_268		FAKGFLSIDSGYFSA	22.5	0.7
DR_269		YFAKGFLSIDSGYFS	25	0.8
DR_270		TFKAFSAMPKTSLCF	25.2	0.8
DR_271		HAAFVNLLNIETDYT	28.1	1
DR_272		SYFAKGFLSIDSGYF	28.2	1
DR_273		NHAAFVNLLNIETDY	28.6	1
DR_274		TDSTFKAFSAMPKTS	30	1.1
DR_275		KSFFYGLKNMLGSVF	31	1.1
DR_276		VEPFKSYFAKGFLSI	31.5	1.2
DR_277		HNHAAFVNLLNIETD	31.9	1.2
DR_278		FKAFSAMPKTSLCFY	32.6	1.2
DR_279		VKSFFYGLKNMLGSV	34.1	1.3
DR_280		QHNHAAFVNLLNIET	34.9	1.4
DR_281		TVEPFKSYFAKGFLS	35.9	1.4
DR_282		ARLLSVSSLKTATT	36.3	1.5

	DR_283	KGFLSIDSGYFSAKC	36.5	1.5
	DR_284	PTVEPFKSYFAKGFL	38	1.6
	DR_285	GTDSTFKAFSAMPKT	39.9	1.7
	DR_286	SVKSFFYGLKNMLGS	40.7	1.8
	DR_287	PARLLSVSSLKTAT	41.7	1.8
B3_0101	DR_288	ARKLEFGTDSTFKAF	10.3	0.5
	DR_289	RKLEFGTDSTFKAFS	10.4	0.5
	DR_290	KLEFGTDSTFKAFSA	10.9	0.5
	DR_291	FAKGFLSIDSGYFSA	13.5	0.7
	DR_292	AKGFLSIDSGYFSAK	14.4	0.8
	DR_293	KGFLSIDSGYFSAKC	16.3	0.9
	DR_294	LEFGTDSTFKAFSAM	17.1	0.9
	DR_295	YFAKGFLSIDSGYFS	18.3	1
	DR_296	HVCDYSLDTDGPVRL	21	1.2
	DR_297	TARKLEFGTDSTFKA	21.2	1.2
	DR_298	VCDYSLDTDGPVRLP	23.3	1.3
	DR_299	GFLSIDSGYFSAKCY	27.1	1.6
	DR_300	CDYSLDTDGPVRLPH	32.8	1.9
	B3_0202	None that meet % rank criteria		
B3_0301	DR_301	GDKITICNGSTIVDQ	4.4	0.5
	DR_302	PGDKITICNGSTIVD	4.5	0.5
	DR_303	DKITICNGSTIVDQR	4.6	0.5
	DR_304	GPGDKITICNGSTIV	5	0.6
	DR_305	KITICNGSTIVDQRL	5.5	0.8
	DR_306	LTLTICVVSTSAVEM	6.4	1.1
	DR_307	ILTLTICVVSTSAVE	6.6	1.2
	DR_308	CILTLTICVVSTSAV	6.7	1.2
	DR_309	LGPVTITLSEPRNIQ	6.9	1.3
	DR_310	GPVTITLSEPRNIQQ	7	1.3
	DR_311	TLTICVVSTSAVEME	7.3	1.5
	DR_312	NLGPVTITLSEPRNI	7.3	1.5
	DR_313	PVTITLSEPRNIQQK	7.6	1.6
	DR_314	ALLIRSIINTTFVIC	7.8	1.7
	DR_315	PQIAVNLSNCHAVIK	8	1.8
	DR_316	RALLIRSIINTTFVI	8	1.8
	DR_317	LPQIAVNLSNCHAVI	8	1.8
	DR_318	LLIRSIINTTFVICI	8.2	1.9
	DR_319	LLVLLTVSLSPVQSA	8.3	1.9
B4_0101	DR_320	RRALLIRSIINTTFV	21	0.6
	DR_321	SRRALLIRSIINTTF	23.4	0.8
	DR_322	IEINVLLPQIAVNLS	25.7	0.9
	DR_323	YGKILKLLHLTLEED	29.9	1.2
	DR_324	YYGKILKLLHLTLEE	30.7	1.3

	DR_325	RALLIRSIINTTFVI	32.1	1.4
	DR_326	FDLMHVQKVLSASTV	32.6	1.4
	DR_327	EINVLLPQIAVNLSN	33.2	1.4
	DR_328	HREIEINVLLPQIAV	33.4	1.4
	DR_329	ASRRALLIRSIINTT	33.4	1.4
	DR_330	KYYGKILKLLHLTLE	33.9	1.5
	DR_331	REIEINVLLPQIAVN	35.5	1.6
	DR_332	FFDLMHVQKVLSAST	36.9	1.7
	DR_333	GKILKLLHLTLEEDT	37.7	1.7
	DR_334	LRKPLFLDSIVKGMK	38.3	1.8
	DR_335	KKYYGKILKLLHRTL	38.8	1.8
	DR_336	VLRKPLFLDSIVKGM	39.3	1.8
	DR_337	EIEINVLLPQIAVNL	40	1.9
	DR_338	EHREIEINVLLPQIA	40	1.9
B4_0103	DR_339	CRRTRGLFKYRHLKD	9.7	1.7
	DR_340	CCRTRGLFKYRHLK	9.8	1.8
	DR_341	RRTRGLFKYRHLKDD	10	1.8
	DR_342	NVMLAVCKRMCFRAT	10.4	1.9
B5_0101	DR_343	STFKAFSAMPKTS LC	4.1	0.25
	DR_344	DSTFKAFSAMPKTS L	4.2	0.25
	DR_345	TFKAFSAMPKTS LCF	4.8	0.4
	DR_346	TDSTFKAFSAMPKTS	5.1	0.4
	DR_347	GTDSTFKAFSAMPKT	6.3	0.7
	DR_348	FKAFSAMPKTS LCFY	8.1	1
	DR_349	GREVRKGQSVLRQYK	9.3	1.2
	DR_350	RMCFRATIEASRRAL	10	1.4
	DR_351	FGTDSTFKAFSAMPK	10.1	1.4
	DR_352	AKGFLSIDS GYFSAK	11.1	1.6
	DR_353	REVRKGQSVLRQYKT	11.6	1.7
	DR_354	KGREVRKGQSVLRQY	12	1.8
	DR_355	MCFRATIEASRRALL	12.1	1.8
	DR_356	VEIILTLSQGLKKYY	12.3	1.8

Supplementary Table 5.3: HTL epitopes of HLA locus DQ identified in the CCHFV Turkey2004 GPC sequence.

The total output of the NetMHCII 2.3 Server (<https://services.healthtech.dtu.dk/service.php?NetMHCII-2.3>) used to predict the binding of 15-mer HTL peptides to 20 HLA-DQ alleles. Predicted peptides were selected if they met the criteria of (1) a strong binder threshold of <2.00%-rank to a set of 1,000,000 random natural peptides and (2) a predicted IC50 value <50 nM.

Allele	Name	Sequence	Affinity (nM)	% Rank
A10101- B10501	DQ_1	HPKVEEGFFDLMHVQ	19.8	0.25
	DQ_2	LHPKVEEGFFDLMHV	21.2	0.25
	DQ_3	KVEEGFFDLMHVQKV	23.2	0.3
	DQ_4	PKVEEGFFDLMHVQK	23.2	0.3
	DQ_5	VEEGFFDLMHVQKVL	42.6	0.8
A10102- B10501	DQ_6	QSILPMSAAPTAIQN	4.3	0.03
	DQ_7	AQSILPMSAAPTAIQ	4.4	0.04
	DQ_8	SILPMSAAPTAIQNI	4.7	0.05
	DQ_9	PAQSILPMSAAPTAI	4.7	0.05
	DQ_10	SPAQSILPMSAAPTA	5.6	0.12
	DQ_11	ILPMSAAPTAIQNIH	5.6	0.12
	DQ_12	ALLIRSIINTTFVIC	5.7	0.15
	DQ_13	LLVLLTVSLSPVQSA	5.8	0.15
	DQ_14	SLLSVSSLKTATTPT	6	0.17
	DQ_15	LVLLTVSLSPVQSAP	6.1	0.2
	DQ_16	RLLSVSSLKTATTP	6.1	0.2
	DQ_17	RALLIRSIINTTFVI	6.1	0.2
	DQ_18	LLSVSSLKTATTPTP	6.2	0.2
	DQ_19	RRALLIRSIINTTFV	6.4	0.25
	DQ_20	VLLVLLTVSLSPVQS	6.4	0.25
	DQ_21	ARLLSVSSLKTATT	6.6	0.25
	DQ_22	LLIRSIINTTFVICI	6.7	0.3
	DQ_23	LTLTICVVSTSAVEM	6.9	0.3
	DQ_24	VLLTVSLSPVQSAPV	6.9	0.3
	DQ_25	TLTICVVSTSAVEME	7.1	0.4
	DQ_26	SRRALLIRSIINTTF	7.1	0.4
	DQ_27	PDVVAASTSLTARKL	7.3	0.4
	DQ_28	LLTVSLSPVQSAPVG	7.4	0.4

	DQ_29	LSVSSLKTATTPTPT	7.5	0.5
	DQ_30	LTICVVSTSAVEMEN	7.6	0.5
	DQ_31	PARSLLSVSSLKTAT	7.7	0.5
	DQ_32	DPDVVAASTSLTARK	7.7	0.5
	DQ_33	IVLLVLLTVSLSPVQ	7.7	0.5
	DQ_34	ILTLTICVVSTSAVE	7.9	0.5
	DQ_35	CILTLTICVVSTSAV	8.3	0.6
	DQ_36	SDPDVVAASTSLTAR	8.5	0.7
	DQ_37	ICILTLTICVVSTSA	8.6	0.7
	DQ_38	DVVAASTSLTARKLE	9	0.8
	DQ_39	LIVLLVLLTVSLSPV	9.4	0.9
	DQ_40	TSPAQSILPMSAAPT	10	1.1
	DQ_41	LIRSIINTTFVICIL	10.7	1.3
	DQ_42	HPARSLLSVSSLKTA	10.7	1.3
	DQ_43	KGMKNLLNSTSLETS	10.7	1.3
	DQ_44	SSDPDVVAASTSLTA	10.8	1.3
	DQ_45	LTVSLSPVQSAPVGH	11	1.4
	DQ_46	SIVKGMKNLLNSTSL	11.5	1.5
	DQ_47	VKGMKNLLNSTSLET	11.5	1.5
	DQ_48	EINVLLPQIAVNLSN	11.5	1.5
	DQ_49	ASRRALLIRSIINTT	11.6	1.5
	DQ_50	IVKGMKNLLNSTSLE	11.7	1.6
	DQ_51	GMKNLLNSTSLETSL	11.7	1.6
	DQ_52	IEINVLLPQIAVNLS	11.9	1.6
	DQ_53	SVSSLKTATTPTPTS	11.9	1.6
	DQ_54	DLMHVQKVLASTVC	12.5	1.8
	DQ_55	INVLLPQIAVNLSNC	12.8	1.9
A10102- B10502	None that meet affinity criteria			
A10102- B10602	DQ_56	KKRKTGSNVMLAVCK	20.1	0.1
	DQ_57	KRKTGSNVMLAVCKR	22.3	0.15
	DQ_58	CKKRKTGSNVMLAVC	22.4	0.15
	DQ_59	ICKKRKTGSNVMLAV	29.4	0.25
	DQ_60	RKTGSNVMLAVCKRM	32.3	0.4
A10103- B10603	DQ_61	LTLTICVVSTSAVEM	41.4	0.02
	DQ_62	TLTICVVSTSAVEME	44.6	0.03
A10104- B10503	None that meet affinity criteria			
A10201- B10202	None that meet affinity criteria			
A10201- B10301	DQ_63	PDVVAASTSLTARKL	3.2	0.2
	DQ_64	DVVAASTSLTARKLE	3.3	0.25
	DQ_65	DPDVVAASTSLTARK	3.4	0.25

DQ_66	TICVVSTSAVEMENL	3.5	0.3
DQ_67	TLTICVVSTSAVEME	3.6	0.3
DQ_68	LTICVVSTSAVEMEN	3.6	0.3
DQ_69	SDPDVVAASTSLTAR	3.6	0.3
DQ_70	VVAASTSLTARKLEF	3.7	0.4
DQ_71	ICVVSTSAVEMENLP	3.8	0.4
DQ_72	LTLTICVVSTSAVEM	4.2	0.5
DQ_73	QSILPMSAAPTAIQN	4.7	0.6
DQ_74	SILPMSAAPTAIQNI	4.7	0.6
DQ_75	SSDPDVVAASTSLTA	4.8	0.6
DQ_76	CVVSTSAVEMENLPA	4.8	0.6
DQ_77	AQSILPMSAAPTAIQ	4.8	0.6
DQ_78	ERPATTATSTPSTDN	5.5	0.8
DQ_79	PERPATTATSTPSTD	5.5	0.8
DQ_80	ILTLTICVVSTSAVE	5.6	0.8
DQ_81	RPATTATSTPSTDNT	5.7	0.8
DQ_82	ILPMSAAPTAIQNIH	6.1	0.9
DQ_83	STFKPTVSTANIALS	6.2	1
DQ_84	TFKPTVSTANIALSW	6.2	1
DQ_85	NNPTSTISTSPSSSP	6.3	1
DQ_86	NPTSTISTSPSSSPS	6.3	1
DQ_87	PATTATSTPSTDNTN	6.3	1
DQ_88	TPERPATTATSTPST	6.3	1
DQ_89	FKPTVSTANIALSWS	6.4	1
DQ_90	PAQSILPMSAAPTAI	6.5	1
DQ_91	PTSTISTSPSSSPST	6.6	1.1
DQ_92	HNGTNTTTAPGTSQS	6.6	1.1
DQ_93	NGTNTTTAPGTSQSH	6.8	1.1
DQ_94	VAASTSLTARKLEFG	6.8	1.1
DQ_95	KPTVSTANIALSWSS	6.9	1.1
DQ_96	TSTISTSPSSSPSTP	7	1.1
DQ_97	GTNTTTAPGTSQSHK	7.2	1.2
DQ_98	DNNPTSTISTSPSSS	7.6	1.3
DQ_99	LPMSAAPTAIQNIHP	8	1.4
DQ_100	PTVSTANIALSWSSI	8	1.4
DQ_101	TNTTTAPGTSQSHKP	8	1.4
DQ_102	QSTFKPTVSTANIAL	8.1	1.4
DQ_103	SLLSVSSLKTATTPT	8.7	1.5
DQ_104	ATTATSTPSTDNTNS	8.7	1.6
DQ_105	STISTSPSSSPSTPP	8.9	1.6
DQ_106	EHNGTNTTTAPGTSQ	8.9	1.6
DQ_107	LLSVSSLKTATTPTP	9	1.6
DQ_108	RSLLSVSSLKTATTTP	9.3	1.7

	DQ_109	ATPERPATTATSTPS	9.6	1.8
	DQ_110	VLLTVSLSPVQSAPV	9.6	1.8
	DQ_111	LVLLTVSLSPVQSAP	9.7	1.8
	DQ_112	LSVSSLKTATTPTPT	9.7	1.8
	DQ_113	ARSLLSVSSLKTATT	10.1	1.9
	DQ_114	LLTVSLSPVQSAPVG	10.4	1.9
A10201- B10303	DQ_115	PAQSILPMSAAPTAI	8.2	0.02
	DQ_116	AQSILPMSAAPTAIQ	8.6	0.02
	DQ_117	SPAQSILPMSAAPTA	9.2	0.03
	DQ_118	TSPAQSILPMSAAPT	10	0.04
	DQ_119	QSILPMSAAPTAIQN	10.3	0.05
	DQ_120	SILPMSAAPTAIQNI	12.3	0.09
	DQ_121	MTSPAQSILPMSAAP	13.1	0.12
	DQ_122	NNPTSTISTSPSSSP	15.5	0.2
	DQ_123	NPTSTISTSPSSSPS	15.6	0.2
	DQ_124	DNNPTSTISTSPSSS	16.1	0.25
	DQ_125	PTSTISTSPSSSPST	16.4	0.25
	DQ_126	ILPMSAAPTAIQNIH	17.2	0.25
	DQ_127	LTLTICVVSTSAVEM	17.6	0.3
	DQ_128	PMTSPAQSILPMSAA	17.7	0.3
	DQ_129	TLTICVVSTSAVEME	17.9	0.3
	DQ_130	SPMTSPAQSILPMSA	18.8	0.4
	DQ_131	TSTISTSPSSSPSTP	19	0.4
	DQ_132	LTICVVSTSAVEMEN	19.7	0.4
	DQ_133	SSDPDVVAASTSLTA	20	0.4
	DQ_134	TPERPATTATSTPST	20.5	0.4
	DQ_135	PERPATTATSTPSTD	20.5	0.4
	DQ_136	SDPDVVAASTSLTAR	20.5	0.4
	DQ_137	ILTLTICVVSTSAVE	21.2	0.5
	DQ_138	TICVVSTSAVEMENL	21.3	0.5
	DQ_139	DPDVVAASTSLTARK	21.4	0.5
	DQ_140	PDVVAASTSLTARKL	21.6	0.5
	DQ_141	ERPATTATSTPSTDN	22.2	0.5
	DQ_142	PTTSPMTSPAQSIL	23.2	0.5
	DQ_143	TTPSPMTSPAQSILP	23.2	0.5
	DQ_144	LLTVSLSPVQSAPVG	23.5	0.6
	DQ_145	RPATTATSTPSTDNT	24.1	0.6
	DQ_146	TPSPMTSPAQSILPM	24.9	0.6
	DQ_147	LTVSLSPVQSAPVGH	25.2	0.6
	DQ_148	VLLTVSLSPVQSAPV	25.2	0.6
	DQ_149	NDNNPTSTISTSPSS	25.3	0.7
	DQ_150	KSSDPDVVAASTSLT	25.4	0.7
	DQ_151	LPMSAAPTAIQNIHP	25.8	0.7

DQ_152	DVVAASTSLTARKLE	26	0.7
DQ_153	STISTSPSSSPSTPP	26.1	0.7
DQ_154	PSPMTSPAQSILPMS	27.1	0.8
DQ_155	LVLLTVSLSPVQSAP	27.6	0.8
DQ_156	PATTATSTPSTDNTN	28.2	0.8
DQ_157	ATPERPATTATSTPS	28.3	0.8
DQ_158	STFKPTVSTANIALS	28.4	0.8
DQ_159	QPTTPSPMTSPAQSI	28.5	0.8
DQ_160	LLVLLTVSLSPVQSA	30	0.9
DQ_161	QSTFKPTVSTANIAL	30.1	0.9
DQ_162	ICVVSTSAVEMENLP	30.3	0.9
DQ_163	VSSLKTATTPTPTSP	31.6	1
DQ_164	TVSLSPVQSAPVGHG	32.2	1
DQ_165	SSLKTATTPTPTSPG	33	1.1
DQ_166	AQPTTPSPMTSPAQS	34.1	1.1
DQ_167	VLLVLLTVSLSPVQS	34.5	1.1
DQ_168	VVAASTSLTARKLEF	34.7	1.1
DQ_169	CILTLTICVVSTSAV	34.7	1.1
DQ_170	LMHVQKVLSASTVCK	35.9	1.2
DQ_171	TFKPTVSTANIALSW	35.9	1.2
DQ_172	RTPTLHTTTQVSTES	36.1	1.2
DQ_173	TPTLHTTTQVSTEST	36.2	1.2
DQ_174	SLLSVSSLKTATTPT	37.3	1.3
DQ_175	KPTVSTANIALSWSS	37.4	1.3
DQ_176	TDSTFKAFSAMPKTS	37.8	1.4
DQ_177	PTVSTANIALSWSSI	37.8	1.4
DQ_178	PTLHTTTQVSTESTN	38.1	1.4
DQ_179	MHVQKVLSASTVCKL	38.1	1.4
DQ_180	FKPTVSTANIALSWS	38.2	1.4
DQ_181	HNGTNTTTAPGTSQS	38.9	1.4
DQ_182	SVSSLKTATTPTPTS	39	1.4
DQ_183	RLLSVSSLKTATTP	39.2	1.4
DQ_184	ARLLSVSSLKTATT	39.2	1.4
DQ_185	DLMHVQKVLSASTVC	39.5	1.5
DQ_186	PARLLSVSSLKTAT	39.9	1.5
DQ_187	DSTFKAFSAMPKTSL	40.2	1.5
DQ_188	SLKTATTPTPTSPGE	40.8	1.5
DQ_189	ATTATSTPSTDNTNS	40.9	1.5
DQ_190	SRTPTLHTTTQVSTE	41.3	1.6
DQ_191	HPARLLSVSSLKTA	42.5	1.6
DQ_192	NGTNTTTAPGTSQSH	43	1.7
DQ_193	LSVSSLKTATTPTPT	43	1.7
DQ_194	PMSAAPTAIQNIHPS	43.1	1.7

	DQ_195	HHPARSLLSVSSLKT	43.3	1.7
	DQ_196	LLSVSSLKTATTPTP	43.5	1.7
	DQ_197	EHNGTNTTTAPGTSQ	43.9	1.7
	DQ_198	MSRTPTLHTTTQVST	44.6	1.8
	DQ_199	HVQKVLASTVCKLQ	44.8	1.8
	DQ_200	MNDNNPTSTISTSPS	44.9	1.8
	DQ_201	SAQPTTSPMTSPAQ	45	1.8
	DQ_202	SSAQPTTSPMTSPA	45.5	1.8
	DQ_203	TISTSPSSSPSTPPT	46.4	1.9
	DQ_204	IHHPARSLLSVSSLK	46.5	1.9
	DQ_205	CVVSTSAVEMENLPA	46.8	1.9
	DQ_206	TLHTTTQVSTESTNH	46.9	1.9
	DQ_207	ESSAQPTTSPMTSP	47.1	1.9
A10201- B10402	DQ_208	VAASTSLTARKLEFG	8.2	0.04
	DQ_209	VVAASTSLTARKLEF	8.2	0.04
	DQ_210	AASTSLTARKLEFGT	9	0.05
	DQ_211	DVVAASTSLTARKLE	9.5	0.05
	DQ_212	TDSTFKAFSAMPKTS	10.9	0.07
	DQ_213	DSTFKAFSAMPKTSL	11.3	0.08
	DQ_214	GTDSTFKAFSAMPKT	11.7	0.08
	DQ_215	FGTDSTFKAFSAMPK	11.8	0.08
	DQ_216	ASTSLTARKLEFGTD	13.1	0.12
	DQ_217	EFGTDSTFKAFSAMP	13.1	0.12
	DQ_218	STFKAFSAMPKTSLC	13.9	0.12
	DQ_219	INVQSTFKPTVSTAN	23.1	0.4
	DQ_220	STSLTARKLEFGTDS	23.5	0.4
	DQ_221	VQSTFKPTVSTANIA	24.3	0.4
	DQ_222	LEFGTDSTFKAFSAMP	24.5	0.4
	DQ_223	AINVQSTFKPTVSTA	26.4	0.4
	DQ_224	PAQSILPMSAAPTAI	26.7	0.5
	DQ_225	AQSILPMSAAPTAIQ	27.3	0.5
	DQ_226	QSTFKPTVSTANIAL	27.3	0.5
	DQ_227	TIEASRRALLIRSII	28.2	0.5
	DQ_228	SPAQSILPMSAAPTA	32.9	0.6
	DQ_229	GKTIETYQTREGFTS	33	0.6
	DQ_230	IEASRRALLIRSIIN	34	0.7
	DQ_231	QSILPMSAAPTAIQN	35.1	0.7
	DQ_232	EASRRALLIRSIINT	35.5	0.7
	DQ_233	RSLLSVSSLKTATTP	36.2	0.7
	DQ_234	HGKTIETYQTREGFT	36.4	0.7
DQ_235	PDVVAASTSLTARKL	37.2	0.8	
DQ_236	SLLSVSSLKTATTPT	37.3	0.8	
DQ_237	ASRRALLIRSIINTT	37.8	0.8	

	DQ_238	KTIETYQTREGFTSI	38.7	0.8
	DQ_239	GAINVQSTFKPTVST	38.8	0.8
	DQ_240	ARSLLSVSSLKTATT	41.6	0.9
	DQ_241	YTKTFHFHSKRVTAH	43.9	0.9
	DQ_242	PTSTISTSPSSSPST	43.9	0.9
	DQ_243	NPTSTISTSPSSSPS	47.7	1.1
	DQ_244	NNPTSTISTSPSSSP	47.9	1.1
	DQ_245	HSAMSRPTLHTTTQ	49.6	1.1
A10301- B10301	DQ_246	PTWCWGVGTGCTCCG	34	0.6
	DQ_247	TWCWGVGTGCTCCGV	34.4	0.6
	DQ_248	NPTWCWGVGTGCTCC	38.4	0.7
	DQ_249	CNPTWCWGVGTGCTC	47.9	1
A10301- B10302	None that meet affinity criteria			
A10303- B10402	None that meet affinity criteria			
A10401- B10402	None that meet affinity criteria			
A10501- B10201	None that meet affinity criteria			
A10501- B10301	DQ_250	LKARPTYGAGEITVL	33.6	1
	DQ_251	KARPTYGAGEITVLV	33.6	1
	DQ_252	ARPTYGAGEITVLVE	34.1	1
	DQ_253	RPTYGAGEITVLVEV	36.7	1.1
	DQ_254	PTYGAGEITVLVEVA	43.5	1.5
	DQ_255	EAGTRFNLGPVTITL	44.1	1.5
	DQ_256	AGTRFNLGPVTITLS	44.5	1.5
	DQ_257	GTRFNLGPVTITLSE	47.4	1.7
	DQ_258	DLKARPTYGAGEITV	47.6	1.7
	DQ_259	DPDVVAASTSLTARK	49.1	1.8
	DQ_260	PTVSTANIALSWSSI	49.6	1.8
	DQ_261	PDVVAASTSLTARKL	49.8	1.8
	A10501- B10302	DQ_262	AQSILPMSAAPTAIQ	25.8
DQ_263		SILPMSAAPTAIQNI	26.4	0.01
DQ_264		QSILPMSAAPTAIQN	26.4	0.01
DQ_265		PAQSILPMSAAPTAI	29.3	0.01
DQ_266		SPAQSILPMSAAPTA	33.8	0.01
DQ_267		ILPMSAAPTAIQNIH	38.8	0.01
DQ_268		TSPAQSILPMSAAPT	45.2	0.03
DQ_269		TLTICVVVSTSAVEME	48.5	0.04
A10501- B10303	DQ_270	PAQSILPMSAAPTAI	17.1	0.01
	DQ_271	AQSILPMSAAPTAIQ	17.7	0.01
	DQ_272	QSILPMSAAPTAIQN	19.3	0.01

	DQ_273	SILPMSAAPTAIQNI	22.8	0.01
	DQ_274	SPAQSILPMSAAPTA	24	0.01
	DQ_275	ILPMSAAPTAIQNIH	26.1	0.02
	DQ_276	TSPAQSILPMSAAPT	27.5	0.03
	DQ_277	LPMSAAPTAIQNIHP	29.2	0.04
	DQ_278	PMTSPAQSILPMSAA	30.7	0.05
	DQ_279	MTSPAQSILPMSAAP	32.4	0.07
	DQ_280	SPMTSPAQSILPMSA	38.9	0.15
	DQ_281	PMSAAPTAIQNIHPS	40.2	0.17
	DQ_282	QPTTSPMTSPAQSI	41	0.2
	DQ_283	PTTSPMTSPAQSIL	46.3	0.3
	DQ_284	NNPTSTISTSPSSSP	49.6	0.4
	DQ_285	SDPDVVAASLTAR	49.9	0.4
A10501- B10402	DQ_286	DSTFKAFSAMPKTSL	9.8	0.15
	DQ_287	STFKAFSAMPKTS LC	9.9	0.15
	DQ_288	TDSTFKAFSAMPKTS	10.7	0.17
	DQ_289	GTDSTFKAFSAMPKT	12.2	0.25
	DQ_290	GRMAIYICRMSNHPR	13.9	0.3
	DQ_291	LGRMAIYICRMSNHP	14	0.3
	DQ_292	FGTDSTFKAFSAMPK	14.6	0.4
	DQ_293	LLGRMAIYICRMSNH	14.6	0.4
	DQ_294	PLLGRMAIYICRMSN	15.9	0.4
	DQ_295	TKTFHFHFSKRVT AHG	18.9	0.6
	DQ_296	YTKTFHFHFSKRVT AH	20.4	0.7
	DQ_297	KTFHFHFSKRVT AHGD	20.5	0.7
	DQ_298	VPLLGRMAIYICRMS	21.1	0.7
	DQ_299	TVEPFKSYFAKGFLS	21.3	0.7
	DQ_300	PTVEPFKSYFAKGFL	21.3	0.7
	DQ_301	EASRRALLIRSIINT	22.1	0.8
	DQ_302	ASRRALLIRSIINTT	22.3	0.8
	DQ_303	LPTVEPFKSYFAKGF	24	0.9
	DQ_304	RMAIYICRMSNHPR T	24.4	0.9
	DQ_305	NLERIPWIVRKL LQV	25.2	1
	DQ_306	IEASRRALLIRSI IN	25.3	1
	DQ_307	SGYFSAKCYPR SSTS	25.4	1
	DQ_308	DSGYFSAKCYPR SST	25.4	1
	DQ_309	DYTKTFHFHFSKR VTA	25.6	1
	DQ_310	LERIPWIVRKL LQVS	25.8	1
	DQ_311	TIEASRRALLIR SII	26.1	1
	DQ_312	IDSGYFSAKCYPR SS	26.5	1
	DQ_313	LNLERIPWIVRKL LQ	27	1.1
	DQ_314	VEPFKSYFAKGFL SI	27.3	1.1
	DQ_315	TFKAFSAMPKTS LCF	28.7	12

	DQ_316	AQSILPMSAAPTAIQ	29	1.2
	DQ_317	LCPYEALVLRKPLFL	29.8	1.2
	DQ_318	PAQSILPMSAAPTAI	30	1.3
	DQ_319	QSILPMSAAPTAIQN	30.2	1.3
	DQ_320	TFHFHFSKRVTAHGDT	30.2	1.3
	DQ_321	SIDSGYFSAKCYPRS	30.3	1.3
	DQ_322	INVTQHPARIAETPG	31.1	1.3
	DQ_323	CLCPYEALVLRKPLF	31.2	1.3
	DQ_324	CPYEALVLRKPLFLD	31.5	1.4
	DQ_325	YLNLERIPWIVRKLL	32.4	1.4
	DQ_326	LINVTQHPARIAETP	33.8	1.5
	DQ_327	ECLCPYEALVLRKPL	34.1	1.5
	DQ_328	EPFKSYFAKGFLSID	34.7	1.6
	DQ_329	YNICPYCASRLTSDG	34.9	1.6
	DQ_330	SYNICPYCASRLTSD	36.2	1.6
	DQ_331	ATIEASRRALLIRSI	36.7	1.7
	DQ_332	SPAQSILPMSAAPTA	37	1.7
	DQ_333	NVTQHPARIAETPGP	37.4	1.7
	DQ_334	ERIPWIVRKLLQVSE	37.7	1.7
	DQ_335	MAIYICRMSNHPRTT	38.8	1.8
	DQ_336	CSYNICPYCASRLTS	38.9	1.8
	DQ_337	QLINVTQHPARIAET	39.2	1.8
	DQ_338	KLPTVEPFKSYFAKG	40.2	1.9
A10601- B10402	DQ_339	YTKTFHFHFSKRVTAH	28.9	0.1
	DQ_340	TKTFHFHFSKRVTAHG	30.2	0.12
	DQ_341	KTFHFHFSKRVTAHGD	36.1	0.15
	DQ_342	DYTKTFHFHFSKRVT	39.7	0.2

Supplementary Table 5.4: HTL epitopes of HLA locus DP identified in the CCHFV Turkey2004 GPC sequence.

The total output of the NetMHCII 2.3 Server (<https://services.healthtech.dtu.dk/service.php?NetMHCII-2.3>) used to predict the binding of 15-mer HTL peptides to 9 HLA-DP alleles. Predicted peptides were selected if they met the criteria of (1) a strong binder threshold of <2.00%-rank to a set of 1,000,000 random natural peptides and (2) a predicted IC50 value <50 nM.

Allele	Name	Sequence	Affinity (nM)	% Rank
A10103-B10301	DP_1	RMCFRATIEASRRAL	22.5	0.4
	DP_2	KRMCFRATIEASRRA	23.4	0.4
	DP_3	EASRRALLIRSIINT	26.1	0.4
	DP_4	ASRRALLIRSIINTT	26.4	0.4
	DP_5	MCFRATIEASRRALL	27	0.5
	DP_6	IEASRRALLIRSIIN	27.6	0.5
	DP_7	CFRATIEASRRALLI	30.9	0.5
	DP_8	CKRMCFRATIEASRR	32.1	0.6
	DP_9	TIEASRRALLIRSII	32.7	0.6
	DP_10	ATIEASRRALLIRSI	49.1	0.9
A10103-B10401	DP_11	KNMLGSVFGNFFIGI	16.4	0.6
	DP_12	EPFKSYFAKGFLSID	16.7	0.6
	DP_13	NMLGSVFGNFFIGIL	17.6	0.6
	DP_14	PFKSYFAKGFLSIDS	17.7	0.6
	DP_15	FKSYFAKGFLSIDSG	19.5	0.7
	DP_16	GLKNMLGSVFGNFFI	19.6	0.7
	DP_17	LKNMLGSVFGNFFIG	20.3	0.7
	DP_18	MLGSVFGNFFIGILL	20.4	0.8
	DP_19	VEPFKSYFAKGFLSI	21.2	0.8
	DP_20	YGLKNMLGSVFGNFF	21.2	0.8
	DP_21	MDLSQMYSPPVFEYLS	21.5	0.8
	DP_22	IMDLSQMYSPPVFEYL	24.1	1
	DP_23	TCIFCKALFYSLIII	24.2	1
	DP_24	ITCIFCKALFYSLII	25.7	1
	DP_25	DLSQMYSPPVFEYLSG	25.9	1.1
	DP_26	CIFCKALFYSLIIIG	26	1.1
	DP_27	LGSVFGNFFIGILLF	26.6	1.1
	DP_28	LSQMYSPPVFEYLSGD	28.6	1.2

	DP_29	KSYFAKGFLSIDSGY	28.7	1.2
	DP_30	VITCIFCKALFYSLI	28.8	1.2
	DP_31	FYGLKNMLGSVFGNF	29.4	1.2
	DP_32	TGVALKRSSWLIVLL	33.9	1.5
	DP_33	GSVFGNFFIGILLFL	34.2	1.5
	DP_34	GVALKRSSWLIVLLV	34.8	1.5
	DP_35	IFCKALFYSLIIGT	37.7	1.7
	DP_36	VALKRSSWLIVLLVL	40	1.8
	DP_37	STGVALKRSSWLIVL	42.4	1.9
	DP_38	SQMYSPVFEYLSGDR	42.6	1.9
A10103- B10402	None that meet affinity criteria			
	DP_39	LFLAPFVLLVLFFMF	3	0.2
	DP_40	LLFLAPFVLLVLFFM	3.2	0.25
	DP_41	FLAPFVLLVLFFMFG	3.3	0.3
	DP_42	LAPFVLLVLFFMFGW	3.3	0.3
	DP_43	GILLFLAPFVLLVLF	3.3	0.4
	DP_44	ILLFLAPFVLLVLFF	3.4	0.4
	DP_45	PFVLLVLFFMFGWKI	3.5	0.4
	DP_46	APFVLLVLFFMFGWK	3.5	0.4
	DP_47	IGILLFLAPFVLLVL	3.6	0.4
	DP_48	FVLLVLFFMFGWKIL	3.6	0.5
	DP_49	FIGILLFLAPFVLLV	3.8	0.5
	DP_50	FFIGILLFLAPFVLL	3.9	0.6
	DP_51	VLLVLFFMFGWKILF	3.9	0.6
	DP_52	NFFIGILLFLAPFVL	4.1	0.7
	DP_53	ITCIFCKALFYSLII	4.3	0.7
	DP_54	VFGNFFIGILLFLAP	4.4	0.8
	DP_55	VITCIFCKALFYSLI	4.4	0.8
	DP_56	TCIFCKALFYSLIII	4.5	0.8
	DP_57	FGNFFIGILLFLAPF	4.5	0.8
	DP_58	LLVLFFMFGWKILFC	4.5	0.8
	DP_59	LVLFFMFGWKILFCF	4.7	0.9
	DP_60	CIFCKALFYSLIIG	4.8	1
	DP_61	GNFFIGILLFLAPFV	4.9	1
	DP_62	SVFGNFFIGILLFLA	5	1.1
	DP_63	YVITCIFCKALFYSL	5.3	1.2
	DP_64	LLVCFILYLQLLGRG	5.3	1.2
	DP_65	LVCFILYLQLLGRGG	5.4	1.2
	DP_66	TLLVCFILYLQLLGR	5.4	1.2
	DP_67	HTLLVCFILYLQLLG	5.5	1.3
	DP_68	VLFFMFGWKILFCFK	6	1.5
	DP_69	THTLLVCFILYLQLL	6	1.5
A10103- B10601				

	DP_70	MAFLWFWSFGYVITC	6.5	1.7
	DP_71	IFCKALFYSLIIGT	6.5	1.7
	DP_72	GSVFGNFFIGILLFL	6.5	1.7
	DP_73	TMAFLWFWSFGYVIT	6.6	1.7
	DP_74	ITHTLLVCFILYLQL	6.8	1.9
	DP_75	FLWFWSFGYVITCIF	6.8	1.9
	DP_76	TTMAFLWFWSFGYVI	6.9	1.9
	DP_77	GYVITCIFCKALFYS	7	1.9
A10201- B10101	DP_78	PFKSYFAKGFLSIDS	28.1	0.25
	DP_79	EPFKSYFAKGFLSID	28.9	0.25
	DP_80	FKSYFAKGFLSIDSG	32.1	0.4
	DP_81	VEPFKSYFAKGFLSI	34.7	0.4
	DP_82	KEKVEETELYLNLER	46.8	0.8
A10201- B10501	None that meet affinity criteria			
A10201- B11401	None that meet affinity criteria			
A10301- B10402	DP_83	LKKYYGKILKLLHLT	15.2	0.3
	DP_84	PFKSYFAKGFLSIDS	18.1	0.4
	DP_85	GLKKYYGKILKLLHL	18.4	0.4
	DP_86	KKYYGKILKLLHLT	19.2	0.5
	DP_87	FKSYFAKGFLSIDSG	19.2	0.5
	DP_88	EPFKSYFAKGFLSID	21.6	0.6
	DP_89	QGLKKYYGKILKLLH	22.8	0.7
	DP_90	KYYGKILKLLHLTLE	25.6	0.8
	DP_91	KSYFAKGFLSIDSGY	27.5	0.9
	DP_92	QQHFLKDNLIDLGCP	28.1	1
	DP_93	VEPFKSYFAKGFLSI	31.4	1.2
	DP_94	GQQHFLKDNLIDLGC	32.4	1.2
	DP_95	SQGLKKYYGKILKLL	33.1	1.3
	DP_96	YYGKILKLLHLTLEE	36.1	1.5
	DP_97	QHFLKDNLIDLGCPH	36.5	1.5
	DP_98	GGQQHFLKDNLIDLG	38.1	1.6
	DP_99	ESKLLTVSIMDLSQM	40.7	1.8
	DP_100	KVEETELYLNLERIP	41.6	1.9
A10103- B10201	DP_101	TMAFLWFWSFGYVIT	7.2	0.02
	DP_102	TTMAFLWFWSFGYVI	7.6	0.03
	DP_103	MAFLWFWSFGYVITC	8.4	0.04
	DP_104	AFLWFWSFGYVITCI	9.2	0.05
	DP_105	RTTMAFLWFWSFGYV	9.3	0.06
	DP_106	LVLFFMFGWKILFCF	10.4	0.09
	DP_107	VLLVLFFMFGWKILF	10.4	0.09
	DP_108	LLVLFFMFGWKILFC	10.5	0.09

	DP_109	VLFFMFGWKILFCFK	12.5	0.17
	DP_110	FVLLVLFFMFGWKIL	13	0.2
	DP_111	GSVFGNFFIGILLFL	14.9	0.3
	DP_112	FLWFWSFGYVITCIF	15.2	0.3
	DP_113	PRTTMAFLFWFSFGY	15.7	0.4
	DP_114	TCIFCKALFYSLIII	16.4	0.4
	DP_115	LGSVFGNFFIGILLF	17.1	0.5
	DP_116	ITCIFCKALFYSLII	17.2	0.5
	DP_117	VEPFKSYFAKGFLSI	18.3	0.5
	DP_118	SVFGNFFIGILLFLA	18.7	0.6
	DP_119	VITCIFCKALFYSLI	19	0.6
	DP_120	TLLVCFILYLQLLGR	19.2	0.6
	DP_121	HTLLVCFILYLQLLG	19.3	0.6
	DP_122	CIFCKALFYSLIIIG	20	0.7
	DP_123	EPFKSYFAKGFLSID	20.2	0.7
	DP_124	LFFMFGWKILFCFKC	21	0.7
	DP_125	NMLGSVFGNFFIGIL	21.5	0.8
	DP_126	THTLLVCFILYLQLL	21.8	0.8
	DP_127	LLVCFILYLQLLGRG	22	0.8
	DP_128	MLGSVFGNFFIGILL	22	0.8
	DP_129	YVITCIFCKALFYSL	23	0.9
	DP_130	PFKSYFAKGFLSIDS	24.1	0.9
	DP_131	VFGNFFIGILLFLAP	27.1	1.2
	DP_132	HPRTTMAFLFWFSFG	27.1	1.2
	DP_133	FKSYFAKGFLSIDSG	28.1	1.2
	DP_134	LFWFWSFGYVITCIFIC	28.2	1.2
	DP_135	LVCFILYLQLLGRGG	28.3	1.2
	DP_136	IFCKALFYSLIIIGT	28.5	1.3
	DP_137	KNMLGSVFGNFFIGI	28.6	1.3
	DP_138	PFVLLVLFFMFGWKI	32.7	1.6
	DP_139	FGNFFIGILLFLAPF	36.5	1.9

Supplementary Table 5.5: Mouse CTL epitopes identified in the CCHFV

Turkey2004 GPC sequence.

The total output of the NetCTLpan 1.1 Server (<https://services.healthtech.dtu.dk/service.php?NetCTLpan-1.1>) used to predict the binding of 9-mer peptides to 5 mouse H-2 class I alleles (Db, Dd, Kb, Kd, and Kk). Predicted peptides were selected based on a percent rank < 1.0 which are considered strong binding peptides by the program.

Allele	Name	Sequence	% Rank
Db	Db_1	TTPPHTLES	0.3
	Db_2	ETSSQHSAM	0.3
	Db_3	VCFILYLQL	0.4
	Db_4	RSLLSVSSL	0.4
	Db_5	PTLHTTTQV	0.8
	Db_6	APGTSQSHK	0.8
Dd	Dd_1	TTPPHTLES	0.01
	Dd_2	ETSSQHSAM	0.01
	Dd_3	VCFILYLQL	0.05
	Dd_4	RSLLSVSSL	0.05
	Dd_5	PTLHTTTQV	0.05
	Dd_6	APGTSQSHK	0.05
	Dd_7	SAQPTTSP	0.4
	Dd_8	MPTNITHTL	0.8
	Dd_9	GKILKLLHL	0.8
Kb	None that meet % Rank criteria		
Kd	Kd_1	TTPPHTLES	0.8
	Kd_2	ETSSQHSAM	0.8
Kk	None that meet % Rank criteria		

Supplementary Table 5.6: Mouse HTL epitopes identified in the CCHFV Turkey2004 GPC sequence.

The total output of the NetMHCII 2.3 Server (<https://services.healthtech.dtu.dk/service.php?NetMHCII-2.3>) used to predict the binding of 15-mer HTL peptides to 5 mouse H-2 class II alleles. Predicted peptides were selected if they met the criteria of (1) a strong binder threshold of <2.00%-rank to a set of 1,000,000 random natural peptides and (2) a predicted IC50 value <50 nM.

Allele	Name	Sequence	Affinity (nM)	% Rank
IAb	IAb_1	VQSTFKPTVSTANIA	29.4	0.04
	IAb_2	NVQSTFKPTVSTANI	32.2	0.05
	IAb_3	QSTFKPTVSTANIAL	32.5	0.05
	IAb_4	INVQSTFKPTVSTAN	32.8	0.05
	IAb_5	AQSILPMSAAPTAIQ	48.4	0.12
IAd	IAd_1	PARSLLSVSSLKTAT	22.6	0.03
	IAd_2	ARSLLSVSSLKTATT	22.7	0.03
	IAd_3	HPARSLLSVSSLKTA	25.5	0.05
	IAd_4	RSLLSVSSLKTATTP	26.4	0.05
	IAd_5	SPAQSILPMSAAPTA	28.8	0.06
	IAd_6	PAQSILPMSAAPTAI	31.4	0.08
	IAd_7	TSPAQSILPMSAAPT	32.8	0.08
	IAd_8	HHPARSLLSVSSLKT	33.1	0.08
	IAd_9	AQSILPMSAAPTAIQ	33.6	0.09
	IAd_10	MTSPAQSILPMSAAP	40.2	0.12
	IAd_11	DLMHVQKVLASTVC	42.9	0.15
	IAd_12	FDMHVQKVLASTV	43.6	0.15
	IAd_13	LMHVQKVLASTVCK	49.7	0.20
IAk	None that meet affinity criteria			
IAs	None that meet affinity criteria			
IAu	None that meet affinity criteria			

Supplementary Figure 5.1: Alignment of all predicted CTL and HTL epitopes to the CCHFV Turkey2004 GPC.

All 1093 predicted epitopes are shown aligned to the GPC. The five individual proteins post-cleavage are shown using different text highlights in the following order:

MLDGP38GNNSMGc. Epitopes excluded from consideration due to location across known

GPC cleavage sites are shown in Gray Text.

GPC	MPTNITHTL LLVCFILYLQLLGRGGAHGQSNATEHNGTNTTTAPGTSQSHKPLVSTTPPHT	60
B7_5	MPTNITHTL-----	9
DP_74	----ITHTLVCFILYLQL-----	15
DP_69	----THTLLVCFILYLQLL-----	15
DP_126	----THTLLVCFILYLQLL-----	15
DP_121	----HTLLVCFILYLQLLG-----	15
DP_67	----HTLLVCFILYLQLLG-----	15
DP_120	----TLLVCFILYLQLLGR-----	15
DP_66	----TLLVCFILYLQLLGR-----	15
A1_10	----TLLVCFILY-----	9
A3_19	----TLLVCFILY-----	9
A2_1	----LLVCFILYL-----	9
DP_127	----LLVCFILYLQLLGRG-----	15
DP_64	----LLVCFILYLQLLGRG-----	15
DP_65	----LVCFILYLQLLGRGG-----	15
DP_135	----LVCFILYLQLLGRGG-----	15
DR_11	----VCFILYLQLLGRGGA-----	15
DR_6	----CFILYLQLLGRGGAH-----	15
DR_205	----CFILYLQLLGRGGAH-----	15
DR_5	----FILYLQLLGRGGAHG-----	15
DR_195	----FILYLQLLGRGGAHG-----	15
DR_8	----ILYLQLLGRGGAHGQ-----	15
DR_192	----ILYLQLLGRGGAHGQ-----	15
A3_10	----ILYLQLLGR-----	9
DR_191	----LYLQLLGRGGAHGQS-----	15
DQ_197	-----EHNGTNTTTAPGTSQ-----	15
DQ_106	-----EHNGTNTTTAPGTSQ-----	15
DQ_92	-----HNGTNTTTAPGTSQS-----	15
DQ_181	-----HNGTNTTTAPGTSQS-----	15
DQ_93	-----NGTNTTTAPGTSQSH-----	15
DQ_192	-----NGTNTTTAPGTSQSH-----	15
DQ_97	-----GTNTTTAPGTSQSHK-----	15
DQ_101	-----TNTTTAPGTSQSHKP-----	15
B7_24	-----KPLVSTTP-----	9
A3_17	-----HT-----	2

GPC	LESSTIKHTTPTSETEGSGETTPPPNTTQGPSPEATPERPATTATSTPSTDNTNSTTQM	120
A3_17	LESSTIK-----	9
DQ_157	-----ATPERPATTATSTPS-----	15
DQ_109	-----ATPERPATTATSTPS-----	15
DQ_88	-----TPERPATTATSTPST-----	15
DQ_134	-----TPERPATTATSTPST-----	15
DQ_135	-----PERPATTATSTPSTD-----	15

DQ_79	-----PERPATTATSTPSTD-----	15
DQ_78	-----ERPATTATSTPSTDN-----	15
DQ_141	-----ERPATTATSTPSTDN-----	15
B7_14	-----RPATTATST-----	9
DQ_81	-----RPATTATSTPSTDNT-----	15
DQ_145	-----RPATTATSTPSTDNT-----	15
DQ_156	-----PATTATSTPSTDNTN-----	15
DQ_87	-----PATTATSTPSTDNTN-----	15
DQ_104	-----ATTATSTPSTDNTNS-----	15
DQ_189	-----ATTATSTPSTDNTNS-----	15
A1_2	-----STDNTNSTT-----	9
DQ_200	-----M-----	1

GPC	NDNNPTSTISTSPSSSPSTPPTPQGIHHPARSLLSVSSLKTATPTPTSPGEISSETSSQ	180
DQ_200	NDNNPTSTISTSPS-----	15
DQ_149	NDNNPTSTISTSPSS-----	15
DQ_98	-DNNPTSTISTSPSS-----	15
DQ_124	-DNNPTSTISTSPSS-----	15
DQ_122	--NNPTSTISTSPSSP-----	15
DQ_244	--NNPTSTISTSPSSP-----	15
DQ_284	--NNPTSTISTSPSSP-----	15
DQ_85	--NNPTSTISTSPSSP-----	15
DQ_243	---NPTSTISTSPSSPS-----	15
DQ_86	---NPTSTISTSPSSPS-----	15
DQ_123	---NPTSTISTSPSSPS-----	15
DQ_242	----PTSTISTSPSSPST-----	15
DQ_91	----PTSTISTSPSSPST-----	15
DQ_125	----PTSTISTSPSSPST-----	15
DQ_96	----TSTISTSPSSPSTP-----	15
DQ_131	----TSTISTSPSSPSTP-----	15
DQ_105	----STISTSPSSPSTPP-----	15
DQ_153	----STISTSPSSPSTPP-----	15
DQ_203	----TISTSPSSPSTPPT-----	15
B7_22	-----SPSTPPTPQ-----	9
DQ_204	-----IHHPARSLLSVSSLK-----	15
B39_5	-----IHHPARSLL-----	9
DQ_195	-----HHPARSLLSVSSLKT-----	15
DQ_191	-----HPARSLLSVSSLKTA-----	15
B7_10	-----HPARSLLSV-----	9
DQ_42	-----HPARSLLSVSSLKTA-----	15
DR_75	-----HPARSLLSVSSLKTA-----	15
DR_56	-----PARSLLSVSSLKTAT-----	15
DQ_31	-----PARSLLSVSSLKTAT-----	15
DR_287	-----PARSLLSVSSLKTAT-----	15
DQ_186	-----PARSLLSVSSLKTAT-----	15
DQ_184	-----ARSLLSVSSLKTATT-----	15
DR_282	-----ARSLLSVSSLKTATT-----	15
DR_51	-----ARSLLSVSSLKTATT-----	15
DQ_21	-----ARSLLSVSSLKTATT-----	15
DQ_113	-----ARSLLSVSSLKTATT-----	15
DQ_240	-----ARSLLSVSSLKTATT-----	15
DR_50	-----RSLLSVSSLKTATTP-----	15
DQ_16	-----RSLLSVSSLKTATTP-----	15
DQ_183	-----RSLLSVSSLKTATTP-----	15
DQ_108	-----RSLLSVSSLKTATTP-----	15
DQ_233	-----RSLLSVSSLKTATTP-----	15
DQ_236	-----SLLSVSSLKTATTP-----	15
DQ_174	-----SLLSVSSLKTATTP-----	15
DR_55	-----SLLSVSSLKTATTP-----	15
DQ_14	-----SLLSVSSLKTATTP-----	15
DQ_103	-----SLLSVSSLKTATTP-----	15
A3_1	-----SLLSVSSLK-----	9

DR_61	-----LLSVSSLKTATTPTP-----	15
DQ_107	-----LLSVSSLKTATTPTP-----	15
DQ_196	-----LLSVSSLKTATTPTP-----	15
DQ_18	-----LLSVSSLKTATTPTP-----	15
DQ_112	-----LSVSSLKTATTPPT-----	15
DQ_193	-----LSVSSLKTATTPPT-----	15
DR_65	-----LSVSSLKTATTPPT-----	15
DQ_29	-----LSVSSLKTATTPPT-----	15
DR_44	-----SVSSLKTATTPPTS-----	15
DQ_53	-----SVSSLKTATTPPTS-----	15
DQ_182	-----SVSSLKTATTPPTS-----	15
DR_46	-----VSSLKTATTPPTSP-----	15
DQ_163	-----VSSLKTATTPPTSP-----	15
DQ_165	-----SSLKTATTPPTSPG-----	15
DQ_188	-----SLKTATTPPTSPGE-----	15
A26_12	-----ETSSQ-----	5

GPC	HSAMSRTPTLHTTTQVSTESTNHSTPRQSESSAQPTTPSPMTSPAQSILPMSAAPTAIQN	240
A26_12	HSAM-----	9
DQ_245	HSAMSRTPTLHTTTQ-----	15
B7_19	-SAMSRTPTL-----	9
DQ_198	---MSRTPTLHTTTQVST-----	15
DQ_190	----SRTPTLHTTTQVSTE-----	15
DQ_172	----RTPTLHTTTQVSTES-----	15
DQ_173	-----TPTLHTTTQVSTEST-----	15
DQ_178	-----PTLHTTTQVSTESTN-----	15
DQ_206	-----TLHTTTQVSTESTNH-----	15
B7_12	-----TPRQSESSA-----	9
DQ_207	-----ESSAQPTTPSPMTSP-----	15
DQ_202	-----SSAQPTTPSPMTSPA-----	15
DQ_201	-----SAQPTTPSPMTSPAQ-----	15
DQ_166	-----AQPTTPSPMTSPAQS-----	15
DQ_159	-----QPTTPSPMTSPAQSI-----	15
DQ_282	-----QPTTPSPMTSPAQSI-----	15
DQ_283	-----PTTPSPMTSPAQSIL-----	15
DQ_142	-----PTTPSPMTSPAQSIL-----	15
DQ_143	-----TTPSPMTSPAQSILP-----	15
B7_13	-----TPSPMTSPA-----	9
DQ_146	-----TPSPMTSPAQSILPM-----	15
DQ_154	-----PSPMTSPAQSILPMS-----	15
DQ_130	-----SPMTSPAQSILPMSA-----	15
DQ_280	-----SPMTSPAQSILPMSA-----	15
DQ_128	-----PMTSPAQSILPMSAA-----	15
DQ_278	-----PMTSPAQSILPMSAA-----	15
A1_15	-----MTSPAQSIL-----	9
DQ_121	-----MTSPAQSILPMSAAP-----	15
DQ_279	-----MTSPAQSILPMSAAP-----	15
DQ_40	-----TSPAQSILPMSAAPT-----	15
DR_156	-----TSPAQSILPMSAAPT-----	15
DQ_118	-----TSPAQSILPMSAAPT-----	15
DQ_276	-----TSPAQSILPMSAAPT-----	15
DQ_268	-----TSPAQSILPMSAAPT-----	15
B7_2	-----SPAQSILPM-----	9
DQ_117	-----SPAQSILPMSAAPTA-----	15
DQ_10	-----SPAQSILPMSAAPTA-----	15
DR_13	-----SPAQSILPMSAAPTA-----	15
DR_69	-----SPAQSILPMSAAPTA-----	15
DR_140	-----SPAQSILPMSAAPTA-----	15
DQ_228	-----SPAQSILPMSAAPTA-----	15
DQ_274	-----SPAQSILPMSAAPTA-----	15
DQ_266	-----SPAQSILPMSAAPTA-----	15

DQ_332	-----SPAQSILPMSAAPTA---	15
DQ_318	-----PAQSILPMSAAPTAI--	15
DQ_265	-----PAQSILPMSAAPTAI--	15
DQ_224	-----PAQSILPMSAAPTAI--	15
DQ_115	-----PAQSILPMSAAPTAI--	15
DQ_270	-----PAQSILPMSAAPTAI--	15
DR_4	-----PAQSILPMSAAPTAI--	15
DR_58	-----PAQSILPMSAAPTAI--	15
DR_136	-----PAQSILPMSAAPTAI--	15
DQ_9	-----PAQSILPMSAAPTAI--	15
DQ_90	-----PAQSILPMSAAPTAI--	15
DR_1	-----AQSILPMSAAPTAIQ-	15
DR_52	-----AQSILPMSAAPTAIQ-	15
DR_138	-----AQSILPMSAAPTAIQ-	15
DQ_225	-----AQSILPMSAAPTAIQ-	15
DQ_271	-----AQSILPMSAAPTAIQ-	15
DQ_316	-----AQSILPMSAAPTAIQ-	15
DQ_262	-----AQSILPMSAAPTAIQ-	15
DQ_77	-----AQSILPMSAAPTAIQ-	15
DQ_7	-----AQSILPMSAAPTAIQ-	15
DQ_116	-----AQSILPMSAAPTAIQ-	15
DQ_73	-----QSILPMSAAPTAIQN	15
DQ_6	-----QSILPMSAAPTAIQN	15
DQ_272	-----QSILPMSAAPTAIQN	15
DQ_264	-----QSILPMSAAPTAIQN	15
DQ_319	-----QSILPMSAAPTAIQN	15
DR_3	-----QSILPMSAAPTAIQN	15
DR_54	-----QSILPMSAAPTAIQN	15
DR_144	-----QSILPMSAAPTAIQN	15
DQ_119	-----QSILPMSAAPTAIQN	15
DQ_231	-----QSILPMSAAPTAIQN	15
DR_153	-----SILPMSAAPTAIQN	14
DR_10	-----SILPMSAAPTAIQN	14
DQ_8	-----SILPMSAAPTAIQN	14
DQ_120	-----SILPMSAAPTAIQN	14
DQ_273	-----SILPMSAAPTAIQN	14
DQ_263	-----SILPMSAAPTAIQN	14
DQ_74	-----SILPMSAAPTAIQN	14
DQ_275	-----ILPMSAAPTAIQN	13
DQ_267	-----ILPMSAAPTAIQN	13
DQ_11	-----ILPMSAAPTAIQN	13
DQ_82	-----ILPMSAAPTAIQN	13
DQ_126	-----ILPMSAAPTAIQN	13
DQ_99	-----LPMSAAPTAIQN	12
DQ_151	-----LPMSAAPTAIQN	12
DQ_277	-----LPMSAAPTAIQN	12
DQ_194	-----PMSAAPTAIQN	11
DQ_281	-----PMSAAPTAIQN	11

GPC	IHPSPTNRSKRNLEVEIILTLSQGLKYYGKILKLLHLTLEDETEGLEWCKRNLGSSCD	300
DQ_263	I-----	15
DR_10	I-----	15
DR_153	I-----	15
DQ_8	I-----	15
DQ_74	I-----	15
DQ_120	I-----	15
DQ_273	I-----	15
DQ_267	IH-----	15
DQ_11	IH-----	15
DQ_82	IH-----	15
DQ_275	IH-----	15
DQ_126	IH-----	15

DQ_99	IHP-----	15
DQ_277	IHP-----	15
DQ_151	IHP-----	15
DQ_194	IHPS-----	15
DQ_281	IHPS-----	15
B44_1	-----LEVEIILTTL-----	9
DR_217	-----VEIILTLSQGLKYY-----	15
DR_356	-----VEIILTLSQGLKYY-----	15
DR_216	-----EILTLSQGLKYYG-----	15
DR_213	-----IILTLSQGLKYYGK-----	15
A3_11	-----ILTLSQGLK-----	9
DR_215	-----ILTLSQGLKYYGKI-----	15
DR_225	-----LTLSQGLKYYGKIL-----	15
A3_13	-----LTLSQGLKK-----	9
A26_18	-----TLSQGLKKY-----	9
B62_22	-----TLSQGLKKY-----	9
DR_262	-----TLSQGLKYYGKIILK-----	15
DR_256	-----LSQGLKYYGKIILKL-----	15
DR_249	-----SQGLKYYGKIILKLL-----	15
DP_95	-----SQGLKYYGKIILKLL-----	15
DP_89	-----QGLKYYGKIILKLLH-----	15
DR_250	-----QGLKYYGKIILKLLH-----	15
DP_85	-----GLKYYGKIILKLLHL-----	15
DR_260	-----GLKYYGKIILKLLHL-----	15
DP_83	-----LKKYYGKIILKLLHLT-----	15
DR_199	-----LKKYYGKIILKLLHLT-----	15
DR_194	-----KKYYGKIILKLLHLTL-----	15
DR_335	-----KKYYGKIILKLLHLTL-----	15
DP_86	-----KKYYGKIILKLLHLTL-----	15
DR_200	-----KYYGKIILKLLHLTLE-----	15
DR_330	-----KYYGKIILKLLHLTLE-----	15
DP_90	-----KYYGKIILKLLHLTLE-----	15
A24_10	-----KYYGKIILKL-----	9
A24_3	-----YYGKIILKLL-----	9
DP_96	-----YYGKIILKLLHLTLEE-----	15
DR_324	-----YYGKIILKLLHLTLEE-----	15
DR_323	-----YGKIILKLLHLTLEED-----	15
DR_333	-----GKIILKLLHLTLEEDT-----	15
B8_2	-----ILKLLHLTL-----	9
B44_15	-----LEEDTEGLL-----	9
GPC	DDFFQKRIEEFFVTGEGYFNEVLQFKTLSTLSPTESHAKLPTVEPFKSYFAGFLSIDS	360
A24_15	---FFQKRIEEF-----	9
B8_1	---FFQKRIEEF-----	9
B62_11	---FQKRIEEFF-----	9
A26_8	---EFFVTGEGY-----	9
B44_5	---GEGYFNEVL-----	9
A24_1	---GYFNEVLQF-----	9
DR_259	---GYFNEVLQFKTLSTL-----	15
DR_251	---YFNEVLQFKTLSTLS-----	15
DR_252	---FNEVLQFKTLSTLSP-----	15
DR_37	---FNEVLQFKTLSTLSP-----	15
DR_83	---FNEVLQFKTLSTLSP-----	15
DR_173	---FNEVLQFKTLSTLSP-----	15
B44_6	---NEVLQFKTL-----	9
DR_254	---NEVLQFKTLSTLSPT-----	15
DR_82	---NEVLQFKTLSTLSPT-----	15
DR_74	---NEVLQFKTLSTLSPT-----	15
DR_35	---NEVLQFKTLSTLSPT-----	15
DR_171	---NEVLQFKTLSTLSPT-----	15
DR_170	---EVLQFKTLSTLSPTE-----	15
DR_33	---EVLQFKTLSTLSPTE-----	15
DR_81	---EVLQFKTLSTLSPTE-----	15

DR_168	-----VLQFKTLSTLSPTPE-----	15
DR_84	-----VLQFKTLSTLSPTPE-----	15
DR_34	-----VLQFKTLSTLSPTPE-----	15
DR_36	-----LQFKTLSTLSPTEPS-----	15
DR_167	-----LQFKTLSTLSPTEPS-----	15
B62_13	-----LQFKTLSTL-----	9
DR_38	-----QFKTLSTLSPTEPSH-----	15
DR_169	-----QFKTLSTLSPTEPSH-----	15
A3_18	-----KLPTVEPFK-----	9
A26_19	-----PTVEPFKSY-----	9
DR_255	-----HAKLPTVEPFKSYFA-----	15
DR_244	-----AKLPTVEPFKSYFAK-----	15
DQ_338	-----KLPTVEPFKSYFAKG-----	15
DR_242	-----KLPTVEPFKSYFAKG-----	15
DR_241	-----LPTVEPFKSYFAKGF-----	15
DQ_303	-----LPTVEPFKSYFAKGF-----	15
DR_108	-----PTVEPFKSYFAKGFL-----	15
DQ_300	-----PTVEPFKSYFAKGFL-----	15
DR_240	-----PTVEPFKSYFAKGFL-----	15
DR_284	-----PTVEPFKSYFAKGFL-----	15
DR_243	-----TVEPFKSYFAKGFLS-----	15
DQ_299	-----TVEPFKSYFAKGFLS-----	15
DR_107	-----TVEPFKSYFAKGFLS-----	15
DR_281	-----TVEPFKSYFAKGFLS-----	15
DR_276	-----VEPFKSYFAKGFLSI-----	15
DR_102	-----VEPFKSYFAKGFLSI-----	15
DP_117	-----VEPFKSYFAKGFLSI-----	15
DP_81	-----VEPFKSYFAKGFLSI-----	15
DP_93	-----VEPFKSYFAKGFLSI-----	15
DP_19	-----VEPFKSYFAKGFLSI-----	15
DR_258	-----VEPFKSYFAKGFLSI-----	15
DQ_314	-----VEPFKSYFAKGFLSI-----	15
DQ_328	-----EPFKSYFAKGFLSID-----	15
DP_88	-----EPFKSYFAKGFLSID-----	15
DP_12	-----EPFKSYFAKGFLSID-----	15
DR_109	-----EPFKSYFAKGFLSID-----	15
DP_123	-----EPFKSYFAKGFLSID-----	15
DP_79	-----EPFKSYFAKGFLSID-----	15
DP_78	-----PFKSYFAKGFLSIDS-----	15
DP_14	-----PFKSYFAKGFLSIDS-----	15
DP_130	-----PFKSYFAKGFLSIDS-----	15
DP_84	-----PFKSYFAKGFLSIDS-----	15
DP_15	-----FKSYFAKGFLSIDS-----	14
DP_87	-----FKSYFAKGFLSIDS-----	14
DP_80	-----FKSYFAKGFLSIDS-----	14
DP_133	-----FKSYFAKGFLSIDS-----	14
DP_29	-----KSYFAKGFLSIDS-----	13
DP_91	-----KSYFAKGFLSIDS-----	13
DR_78	-----SYFAKGFLSIDS-----	12
DR_272	-----SYFAKGFLSIDS-----	12
A24_7	-----YFAKGFLSI-----	9
DR_76	-----YFAKGFLSIDS-----	11
DR_269	-----YFAKGFLSIDS-----	11
DR_295	-----YFAKGFLSIDS-----	11
DR_291	-----FAKGFLSIDS-----	10
DR_268	-----FAKGFLSIDS-----	10
DR_77	-----FAKGFLSIDS-----	10
DR_266	-----AKGFLSIDS-----	9
DR_352	-----AKGFLSIDS-----	9
DR_292	-----AKGFLSIDS-----	9
DR_45	-----AKGFLSIDS-----	9
DR_79	-----AKGFLSIDS-----	9
DR_283	-----KGFLSIDS-----	8

DR_80	-----KGFLSIDS	8
DR_293	-----KGFLSIDS	8
DR_299	-----GFLSIDS	7
B62_10	-----FLSIDS	6
DQ_321	-----SIDS	4
DQ_312	-----IDS	3
DQ_308	-----DS	2
DQ_307	-----S	1

GPC	GYFSAKCYPRSSTSGLQLINVTQHPARIAETPGPKTTSLKTINCINLRASVFKHEHREIEI	420
DP_87	G-----	15
DP_80	G-----	15
DP_133	G-----	15
DP_15	G-----	15
DP_29	GY-----	15
DP_91	GY-----	15
B62_10	GYF-----	9
DR_272	GYF-----	15
DR_78	GYF-----	15
DR_76	GYFS-----	15
DR_295	GYFS-----	15
DR_269	GYFS-----	15
DR_268	GYFSA-----	15
DR_77	GYFSA-----	15
DR_291	GYFSA-----	15
DR_352	GYFSAK-----	15
DR_45	GYFSAK-----	15
DR_292	GYFSAK-----	15
DR_266	GYFSAK-----	15
DR_79	GYFSAK-----	15
DR_80	GYFSAKC-----	15
DR_293	GYFSAKC-----	15
DR_283	GYFSAKC-----	15
DR_299	GYFSAKCY-----	15
DQ_321	GYFSAKCYPRS-----	15
DQ_312	GYFSAKCYPRSS-----	15
DQ_308	GYFSAKCYPRSST-----	15
DQ_307	GYFSAKCYPRSSTS-----	15
B7_1	-----YPRSSTSGL-----	9
B8_4	-----YPRSSTSGL-----	9
B58_9	-----RSSTSGLQL-----	9
DQ_337	-----QLINVTQHPARIAET-----	15
DQ_326	-----LINVTQHPARIAETP-----	15
DQ_322	-----INVTQHPARIAETPG-----	15
DQ_333	-----NVTQHPARIAETPGP-----	15
A3_26	-----RIAETPGPK-----	9
B7_3	-----TPGPKTTSL-----	9
DR_338	-----EHREIEI-----	7
DR_328	-----HREIEI-----	6
B39_1	-----HREIEI-----	6
B44_2	-----REIEI-----	5
DR_331	-----REIEI-----	5
DR_337	-----EIEI-----	4
DR_322	-----IEI-----	3
DQ_52	-----IEI-----	3
DQ_48	-----EI-----	2
DR_327	-----EI-----	2
DQ_55	-----I-----	1

GPC	NVLLPQIAVNLNSNCHAVIKSHVCDYSLDLDGVPVRLPHIYHEGTFIPGTYKIVIDKKNKLN	480
-----	---	-----

B39_1	NVL-----	9
B44_2	NVLL-----	9
DR_338	NVLLPQIA-----	15
DR_337	NVLLPQIAVNL-----	15
DR_331	NVLLPQIAVN-----	15
DR_328	NVLLPQIAV-----	15
DR_327	NVLLPQIAVNLSN-----	15
DR_322	NVLLPQIAVNLS-----	15
DQ_55	NVLLPQIAVNLSNC-----	15
DQ_52	NVLLPQIAVNLS-----	15
DQ_48	NVLLPQIAVNLSN-----	15
DR_236	--LLPQIAVNLSNCHAV-----	15
DR_233	---LPQIAVNLSNCHAVI-----	15
DR_317	---LPQIAVNLSNCHAVI-----	15
DR_235	----PQIAVNLSNCHAVIK-----	15
DR_315	----PQIAVNLSNCHAVIK-----	15
DR_239	-----QIAVNLSNCHAVIKS-----	15
A3_22	-----LSNCHAVIK-----	9
B58_25	-----KSHVCDYSL-----	9
DR_296	-----HVCDSLDTDGPVRL-----	15
DR_298	-----VCDYSLDTDGPVRLP-----	15
DR_31	-----VCDYSLDTDGPVRLP-----	15
DR_27	-----CDYSLDTDGPVRLPH-----	15
DR_300	-----CDYSLDTDGPVRLPH-----	15
DR_25	-----DYSLDTDGPVRLPHI-----	15
DR_32	-----YSLDTDGPVRLPHIY-----	15
A3_15	-----GTFIPGTYK-----	9
A24_12	-----TFIPGTYKI-----	9
B7_23	-----IPGTYKIVI-----	9
A3_12	-----GTYKIVIDK-----	9
DR_22	-----IPGTYKIVIDKKNKL-----	15
DR_17	-----PGTYKIVIDKKNKLN-----	15
DR_15	-----GTYKIVIDKKNKLN-----	14
DR_14	-----TYKIVIDKKNKLN-----	13
DR_16	-----YKIVIDKKNKLN-----	12
DR_20	-----KIVIDKKNKLN-----	11
A2_2	-----KLN-----	3

GPC	DRCILVTNCVIKGREVRKQSVLRQYKTEIKIGKASTGSRKLLSEEPGDDCISRTQLLRT	540
DR_15	D-----	15
DR_14	DR-----	15
DR_16	DRC-----	15
DR_20	DRCI-----	15
A2_2	DRCILV-----	9
A3_34	---ILVTNCVIK-----	9
DR_354	-----KGREVRKQSVLRQY-----	15
DR_349	-----GREVRKQSVLRQYK-----	15
DR_353	-----REVRKQSVLRQYKT-----	15
B44_22	-----REVRKQSV-----	9
B7_21	-----EVRKQSVL-----	9
B8_9	-----EVRKQSVL-----	9
B27_12	-----VRKQSVLR-----	9
B27_11	-----RQYKTEIKI-----	9
B7_25	-----KASTGSRKL-----	9
B44_20	-----SEEPGDDCI-----	9

GPC	ETAETHDDNYGGPGDKITICNGSTIVDQRLGSELGCTINRVKSFKLCENSATGKTCEID	600
A1_1	-TAETHDDNY-----	9
DR_304	-----GPGDKITICNGSTIV-----	15
DR_302	-----PGDKITICNGSTIVD-----	15
DR_301	-----GDKITICNGSTIVDQ-----	15

DR_303	-----DKITICNGSTIVDQR-----	15
DR_305	-----KITICNGSTIVDQRL-----	15
B27_17	-----QRLGSELGC-----	9
A3_32	-----RLGSELGCY-----	9
DR_87	-----ELGCVTINRVKSFKL-----	15
DR_218	-----ELGCVTINRVKSFKL-----	15
DR_257	-----ELGCVTINRVKSFKL-----	15
DR_88	-----LGCYTINRVKSFKLC-----	15
DR_214	-----LGCYTINRVKSFKLC-----	15
DR_248	-----LGCYTINRVKSFKLC-----	15
DR_246	-----GCVTINRVKSFKLCE-----	15
DR_89	-----GCVTINRVKSFKLCE-----	15
DR_230	-----GCVTINRVKSFKLCE-----	15
DR_90	-----CVTINRVKSFKLCEN-----	15
DR_245	-----CVTINRVKSFKLCEN-----	15
A26_1	-----YTINRVKSF-----	9
B8_11	-----YTINRVKSF-----	9
B62_3	-----YTINRVKSF-----	9
DR_91	-----YTINRVKSFKLCENS-----	15
DR_247	-----YTINRVKSFKLCENS-----	15
A3_14	-----TINRVKSFK-----	9
DR_253	-----TINRVKSFKLCENSA-----	15
DR_92	-----TINRVKSFKLCENSA-----	15
DR_111	-----INRVKSFKLCENSAT-----	15

GPC	STPVKCRQGFCLKITQEGRGHVKLSRGSEVVLVDCSSCEVMIPKGTGDILVDCSGGQQH	660
B7_17	-TPVKCRQGF-----	9
B39_16	-----QEGRGHVKL-----	9
B44_8	-----QEGRGHVKL-----	9
B27_8	-----GRGHVKLSR-----	9
DR_151	-----EGRGHVKLSRGSEVV-----	15
DR_237	-----EGRGHVKLSRGSEVV-----	15
DR_231	-----GRGHVKLSRGSEVVL-----	15
DR_141	-----GRGHVKLSRGSEVVL-----	15
DR_142	-----RGHVKLSRGSEVVL-----	15
DR_232	-----RGHVKLSRGSEVVL-----	15
DR_145	-----GHVKLSRGSEVVL-----	15
DR_234	-----GHVKLSRGSEVVL-----	15
DR_238	-----HVKLSRGSEVVL-----	15
B7_15	-----IPKGTGDIL-----	9
DP_98	-----GGQQH-----	5
DP_94	-----GQQH-----	4
DP_92	-----QQH-----	3
DP_97	-----QH-----	2

GPC	FLKDNLIDLGCPhVPLLGRMAIYICRMSNHPRRTMAFLWFSGYVITCIFCKALFYSLI	720
A2_3	FLKDNLIDL-----	9
DP_98	FLKDNLIDL-----	15
DP_94	FLKDNLIDL-----	15
DP_92	FLKDNLIDL-----	15
DP_97	FLKDNLIDL-----	15
B7_8	-----VPLLGRMAI-----	9
B8_7	-----VPLLGRMAI-----	9
DQ_298	-----VPLLGRMAIYICRMS-----	15
DQ_294	-----PLLGRMAIYICRMS-----	15
DQ_293	-----LLGRMAIYICRMSNH-----	15
DQ_291	-----LGRMAIYICRMSNH-----	15
DQ_290	-----GRMAIYICRMSNH-----	15
B27_3	-----GRMAIYICR-----	9
DR_62	-----GRMAIYICRMSNH-----	15
A2_4	-----RMAIYICRM-----	9

B58_21	-----RMAIYICRM-----	9
DR_60	-----RMAIYICRMSNHPRT-----	15
DQ_304	-----RMAIYICRMSNHPRT-----	15
DR_67	-----MAIYICRMSNHPRTT-----	15
DQ_335	-----MAIYICRMSNHPRTT-----	15
B39_6	-----NHPRTTMAF-----	9
B7_4	-----HPRTTMAFL-----	9
B8_8	-----HPRTTMAFL-----	9
DP_132	-----HPRTTMAFLWFWSFG-----	15
DP_113	-----PRTTMAFLWFWSFGY-----	15
DP_105	-----RTTMAFLWFWSFGYV-----	15
B58_2	-----RTTMAFLFW-----	9
A24_11	-----TTMAFLFWF-----	9
A26_16	-----TTMAFLFWF-----	9
B58_8	-----TTMAFLFWF-----	9
DP_76	-----TTMAFLWFWSFGYVI-----	15
DP_102	-----TTMAFLWFWSFGYVI-----	15
DP_101	-----TMAFLWFWSFGYVIT-----	15
DP_73	-----TMAFLWFWSFGYVIT-----	15
B58_4	-----MAFLWFWSF-----	9
B62_12	-----MAFLWFWSF-----	9
DP_70	-----MAFLWFWSFGYVITC-----	15
DP_103	-----MAFLWFWSFGYVITC-----	15
DP_104	-----AFLWFWSFGYVITCI-----	15
DP_112	-----FLWFWSFGYVITCIF-----	15
A1_11	-----FLWFWSFGY-----	9
A2_5	-----FLWFWSFGY-----	9
A3_27	-----FLWFWSFGY-----	9
A26_9	-----FLWFWSFGY-----	9
B58_19	-----FLWFWSFGY-----	9
B62_4	-----FLWFWSFGY-----	9
DP_75	-----FLWFWSFGYVITCIF-----	15
DP_134	-----LWFWSFGYVITCIFC-----	15
A24_17	-----FWFSFGYVI-----	9
A24_14	-----SGYVITCI-----	9
B58_14	-----FGYVITCIF-----	9
B8_6	-----FGYVITCIF-----	9
DP_77	-----GYVITCIFCKALFYS-----	15
DP_63	-----YVITCIFCKALFYSL-----	15
DP_129	-----YVITCIFCKALFYSL-----	15
DP_30	-----VITCIFCKALFYSLI-----	15
DP_55	-----VITCIFCKALFYSLI-----	15
DP_119	-----VITCIFCKALFYSLI-----	15
DP_116	-----ITCIFCKALFYSLI-----	14
DP_53	-----ITCIFCKALFYSLI-----	14
DP_24	-----ITCIFCKALFYSLI-----	14
DP_56	-----TCIFCKALFYSLI-----	13
DP_23	-----TCIFCKALFYSLI-----	13
DP_114	-----TCIFCKALFYSLI-----	13
DP_60	-----CIFCKALFYSLI-----	12
DP_26	-----CIFCKALFYSLI-----	12
DP_122	-----CIFCKALFYSLI-----	12
A3_7	-----CIFCKALFY-----	9
A1_3	-----CIFCKALFY-----	9
DP_35	-----IFCKALFYSLI-----	11
DP_136	-----IFCKALFYSLI-----	11
DP_71	-----IFCKALFYSLI-----	11
B8_5	-----FCKALFYSL-----	9
A2_6	-----ALFYSLI-----	7
DR_106	-----LFYSLI-----	6
DR_103	-----FYSLI-----	5
DR_110	-----YSLI-----	4
DR_221	-----SLI-----	3

A3_28	-----LI	2
DR_211	-----LI	2
DR_212	-----I	1
GPC	IIGTLGKKFKQYRELKPQTCTICETAPVNAIDAEMHDLNCSYNICPYCASRLTSDGLARH	780
DP_53	I-----	15
DP_24	I-----	15
DP_116	I-----	15
DP_23	II-----	15
DP_56	II-----	15
DP_114	II-----	15
A2_6	II-----	9
DP_26	IIG-----	15
DP_122	IIG-----	15
DP_60	IIG-----	15
DP_35	IIGT-----	15
DP_71	IIGT-----	15
DP_136	IIGT-----	15
A3_28	IIGTLGK-----	9
A3_24	IIGTLGKK-----	9
DR_106	IIGTLGKKF-----	15
DR_103	IIGTLGKKFK-----	15
DR_110	IIGTLGKKFKQ-----	15
DR_221	IIGTLGKKFKQY-----	15
DR_211	IIGTLGKKFKQYR-----	15
DR_212	IIGTLGKKFKQYRE-----	15
B8_12	-----ELKPQTCTI-----	9
A1_7	-----EMHDLNCSY-----	9
A26_3	-----EMHDLNCSY-----	9
B62_5	-----EMHDLNCSY-----	9
A26_20	-----NCSYNICPY-----	9
DR_264	-----NCSYNICPYCASRLT-----	15
DR_261	-----CSYNICPYCASRLTS-----	15
DQ_336	-----CSYNICPYCASRLTS-----	15
DR_263	-----SYNICPYCASRLTSD-----	15
DQ_330	-----SYNICPYCASRLTSD-----	15
DQ_329	-----YNICPYCASRLTSDG-----	15
GPC	VPQCPKRKEKVEETELYLNLERIPWIVRKLLQVSESTGVALKRSSWLIVLLVLLTVSLSP	840
B44_12	-----KEKVEETEL-----	9
DP_82	-----KEKVEETELYLNLER-----	15
A26_6	-----EKVEETELY-----	9
DP_100	-----KVEETELYLNLERIP-----	15
B44_3	-----EETELYLNL-----	9
DR_202	-----ELYLNLERIPWIVRK-----	15
B58_23	-----YLNLERIPW-----	9
DQ_325	-----YLNLERIPWIVRKLL-----	15
DQ_313	-----LNLERIPWIVRKLLQ-----	15
DQ_305	-----NLERIPWIVRKLLQV-----	15
DQ_310	-----LERIPWIVRKLLQVS-----	15
B27_10	-----ERIPWIVRK-----	9
DQ_334	-----ERIPWIVRKLLQVSE-----	15
B7_7	-----IPWIVRKLL-----	9
B8_14	-----IPWIVRKLL-----	9
DR_101	-----WIVRKLLQVSESTGV-----	15
DR_100	-----IVRKLLQVSESTGVA-----	15
DR_93	-----VRKLLQVSESTGVAL-----	15
DR_95	-----RKLLQVSESTGVALK-----	15
DR_98	-----KLLQVSESTGVALKR-----	15
DR_104	-----LLQVSESTGVALKRS-----	15
B39_17	-----VSESTGVAL-----	9

DR_154	-----ESTGVALKRSSWLIV-----	15
DR_146	-----STGVALKRSSWLIVL-----	15
DP_37	-----STGVALKRSSWLIVL-----	15
DP_32	-----TGVALKRSSWLIVLL-----	15
DR_147	-----TGVALKRSSWLIVLL-----	15
DP_34	-----GVALKRSSWLIVLLV-----	15
DR_149	-----GVALKRSSWLIVLLV-----	15
DP_36	-----VALKRSSWLIVLLVL-----	15
DR_158	-----VALKRSSWLIVLLVL-----	15
B27_6	-----KRSSWLIVL-----	9
B39_8	-----KRSSWLIVL-----	9
B58_18	-----RSSWLIVLL-----	9
A24_6	-----SWLIVLLVL-----	9
B8_13	-----WLIVLLVL-----	9
DQ_39	-----LIVLLVLLTVSLSP	14
DQ_33	-----IVLLVLLTVSLSP	13
DQ_20	-----VLLVLLTVSLSP	12
DQ_167	-----VLLVLLTVSLSP	12
A2_7	-----LLVLLTVSL--	9
DQ_160	-----LLVLLTVSLSP	11
DR_319	-----LLVLLTVSLSP	11
DQ_13	-----LLVLLTVSLSP	11
DQ_15	-----LVLLTVSLSP	10
DQ_155	-----LVLLTVSLSP	10
DQ_111	-----IVLLTVSLSP	10
DQ_110	-----VLLTVSLSP	9
DQ_148	-----VLLTVSLSP	9
DQ_24	-----VLLTVSLSP	9
A2_8	-----LLTVSLSP	8
DQ_28	-----LLTVSLSP	8
DQ_114	-----LLTVSLSP	8
DQ_144	-----LLTVSLSP	8
DQ_45	-----LTVSLSP	7
DQ_147	-----LTVSLSP	7
DQ_164	-----TVSLSP	6

GPC	VQSAPVGHGKTIETYQTREGFTSICLFMLGSILFIVSCLVKGLVDSVSDSFFPGLSVCKT	900
A2_8	V-----	9
DQ_39	V-----	15
DQ_33	VQ-----	15
DQ_167	VQS-----	15
DQ_20	VQS-----	15
DQ_13	VQSA-----	15
DR_319	VQSA-----	15
DQ_160	VQSA-----	15
DQ_111	VQSAP-----	15
DQ_155	VQSAP-----	15
DQ_15	VQSAP-----	15
DQ_110	VQSAPV-----	15
DQ_148	VQSAPV-----	15
DQ_24	VQSAPV-----	15
DQ_28	VQSAPVG-----	15
DQ_144	VQSAPVG-----	15
DQ_114	VQSAPVG-----	15
DQ_45	VQSAPVGH-----	15
DQ_147	VQSAPVGH-----	15
DQ_164	VQSAPVGHG-----	15
B7_6	---APVGHGKTI---	9
DQ_234	-----HGKTIETYQTREGFT-----	15
DQ_229	-----GKTIETYQTREGFTS-----	15
DQ_238	-----KTIETYQTREGFTSI-----	15
A26_5	-----ETYQTREGF-----	9

B44_7	-----REGFTSICL-----	9
A26_17	-----EGFTSICLF-----	9
A2_9	-----FTSICLFML-----	9
A24_5	-----LFMLGSILF-----	9
B62_21	-----LFMLGSILF-----	9
A2_10	-----FMLGSILFI-----	9
A2_11	-----MLGSILFIV-----	9
A2_12	-----SILFIVSCL-----	9
A2_13	-----ILFIVSCLV-----	9
A1_14	-----LVDSVSDSF-----	9

GPC	CSIGSINGFEIESHKCYCSLFCPCPYCRHCSADREIHQLHLSICKKRKTGSNVMLAVCKRM	960
B58_13	CSIGSINGF-----	9
B62_23	CSIGSINGF-----	9
A26_13	CSIGSINGF-----	9
B62_16	-----FEIESHKCY-----	9
B62_20	-----YCSLFCPCPY-----	9
B7_16	-----CPYCRHCSA-----	9
B39_10	-----SADREIHQL-----	9
DR_196	-----IHQLHLSICKKRKTG-----	15
A3_25	-----HQLHLSICK-----	9
B27_15	-----HQLHLSICK-----	9
DR_228	-----HQLHLSICKKRKTGS-----	15
DR_188	-----HQLHLSICKKRKTGS-----	15
A3_16	-----QLHLSICKK-----	9
DR_187	-----QLHLSICKKRKTGSN-----	15
DR_229	-----QLHLSICKKRKTGSN-----	15
DR_190	-----LHLSICKKRKTGSNV-----	15
DQ_59	-----ICKKRKTGSNVMLAV-----	15
DQ_58	-----CKKRKTGSNVMLAVC-----	15
DQ_56	-----KKRKTGSNVMLAVCK-----	15
DQ_57	-----KRKTGSNVMLAVCKR-----	15
B27_14	-----RKTGSNVML-----	9
B39_13	-----RKTGSNVML-----	9
DQ_60	-----RKTGSNVMLAVCKRM-----	15
DR_132	-----GSNVMLAVCKRM-----	12
DR_28	-----GSNVMLAVCKRM-----	12
DR_24	-----SNVMLAVCKRM-----	11
DR_129	-----SNVMLAVCKRM-----	11
DR_26	-----NVMLAVCKRM-----	10
DR_342	-----NVMLAVCKRM-----	10
DR_131	-----NVMLAVCKRM-----	10
DP_8	-----CKRM-----	4
B27_1	-----KRM-----	3
DP_2	-----KRM-----	3
DR_350	-----RM-----	2
DP_1	-----RM-----	2
DR_29	-----M-----	1
DR_355	-----M-----	1
DP_5	-----M-----	1

GPC	CFRATIEASRRALLIRSIINTTFVICILTLTICVSTSAVEMENLPAGTWEREEDLTNFC	1020
DR_28	CFR-----	15
DR_132	CFR-----	15
DR_24	CFRA-----	15
DR_129	CFRA-----	15
DR_342	CFRAT-----	15
DR_26	CFRAT-----	15
DR_131	CFRAT-----	15
B27_1	CFRATI-----	9
DP_8	CFRATIEASRR-----	15

DP_2	CFRATIEASRR-----	15
DR_350	CFRATIEASRRAL-----	15
DP_1	CFRATIEASRRAL-----	15
DR_29	CFRATIEASRRALL-----	15
DR_355	CFRATIEASRRALL-----	15
DP_5	CFRATIEASRRALL-----	15
DP_7	CFRATIEASRRALLI-----	15
DR_21	CFRATIEASRRALLI-----	15
B27_4	-FRATIEASR-----	9
DR_18	-FRATIEASRRALLIR-----	15
DR_19	--RATIEASRRALLIRS-----	15
DR_23	---ATIEASRRALLIRSI-----	15
DQ_331	---ATIEASRRALLIRSI-----	15
DP_10	---ATIEASRRALLIRSI-----	15
DP_9	----TIEASRRALLIRSII-----	15
DQ_311	----TIEASRRALLIRSII-----	15
DQ_227	----TIEASRRALLIRSII-----	15
B7_26	----TIEASRRAL-----	9
DQ_230	----IEASRRALLIRSIIN-----	15
DP_6	----IEASRRALLIRSIIN-----	15
DQ_306	----IEASRRALLIRSIIN-----	15
B44_21	----IEASRRALL-----	9
DQ_301	----EASRRALLIRSIINT-----	15
DQ_232	----EASRRALLIRSIINT-----	15
DP_3	----EASRRALLIRSIINT-----	15
DQ_302	----ASRRALLIRSIINTT-----	15
DP_4	----ASRRALLIRSIINTT-----	15
DQ_237	----ASRRALLIRSIINTT-----	15
DQ_49	----ASRRALLIRSIINTT-----	15
DR_329	----ASRRALLIRSIINTT-----	15
DQ_26	-----SRRALLIRSIINTTF-----	15
DR_321	-----SRRALLIRSIINTTF-----	15
DR_320	-----RRALLIRSIINTTFV-----	15
B27_5	-----RRALLIRSI-----	9
DR_224	-----RRALLIRSIINTTFV-----	15
DQ_19	-----RRALLIRSIINTTFV-----	15
DQ_17	-----RALLIRSIINTTFVI-----	15
DR_222	-----RALLIRSIINTTFVI-----	15
DR_325	-----RALLIRSIINTTFVI-----	15
DR_316	-----RALLIRSIINTTFVI-----	15
DR_314	-----ALLIRSIINTTFVIC-----	15
DQ_12	-----ALLIRSIINTTFVIC-----	15
DR_223	-----ALLIRSIINTTFVIC-----	15
DQ_22	-----LLIRSIINTTFVICI-----	15
DR_318	-----LLIRSIINTTFVICI-----	15
DQ_41	-----LIRSIINTTFVICIL-----	15
B27_9	-----IRSIINTTF-----	9
A24_19	-----TFVICILTL-----	9
DQ_37	-----ICILTLTICVVSTSA-----	15
DQ_35	-----CILTTLTICVVSTSAV-----	15
A2_14	-----CILTTLTICV-----	9
DQ_169	-----CILTTLTICVVSTSAV-----	15
DR_308	-----CILTTLTICVVSTSAV-----	15
DR_307	-----ILTTLTICVVSTSAVE-----	15
DQ_80	-----ILTTLTICVVSTSAVE-----	15
DQ_137	-----ILTTLTICVVSTSAVE-----	15
DQ_34	-----ILTTLTICVVSTSAVE-----	15
DQ_127	-----LTLTICVVSTSAVEM-----	15
DR_306	-----LTLTICVVSTSAVEM-----	15
DQ_23	-----LTLTICVVSTSAVEM-----	15
DQ_61	-----LTLTICVVSTSAVEM-----	15
DQ_72	-----LTLTICVVSTSAVEM-----	15
DR_68	-----TLTICVVSTSAVEME-----	15

DR_311	-----TLTICVVSTSAVEME-----	15
DQ_67	-----TLTICVVSTSAVEME-----	15
DQ_25	-----TLTICVVSTSAVEME-----	15
DQ_129	-----TLTICVVSTSAVEME-----	15
DQ_269	-----TLTICVVSTSAVEME-----	15
DQ_62	-----TLTICVVSTSAVEME-----	15
DQ_30	-----LTICVVSTSAVEMEN-----	15
DQ_68	-----LTICVVSTSAVEMEN-----	15
DQ_132	-----LTICVVSTSAVEMEN-----	15
DR_71	-----LTICVVSTSAVEMEN-----	15
DQ_66	-----TICVVSTSAVEMENL-----	15
DQ_138	-----TICVVSTSAVEMENL-----	15
DQ_71	-----ICVVSTSAVEMENLP-----	15
DQ_162	-----ICVVSTSAVEMENLP-----	15
DQ_76	-----CVVSTSAVEMENLPA-----	15
DQ_205	-----CVVSTSAVEMENLPA-----	15
GPC	HQECQVTETECLCPYEALVLRKPLFLDSIVKGMKNLLNSTSLETSLSIEAPWGAINVQST	1080
DQ_327	-----ECLCPYEALVLRKPL-----	15
DQ_323	-----CLCPYEALVLRKPLF-----	15
DQ_317	-----LCPYEALVLRKPLFL-----	15
DQ_324	-----CPYEALVLRKPLFLD-----	15
B8_10	-----EALVLRKPL-----	9
DR_336	-----VLRKPLFLDSIVKGM-----	15
DR_30	-----RKPLFLDSIVKGMKN-----	15
DR_334	-----LRKPLFLDSIVKGMK-----	15
A3_33	-----PLFLDSIVK-----	9
A2_15	-----FLDSIVKGM-----	9
DR_63	-----FLDSIVKGMKNLLNS-----	15
DR_53	-----LDSIVKGMKNLLNST-----	15
DR_48	-----DSIVKGMKNLLNSTS-----	15
DR_47	-----SIVKGMKNLLNSTSL-----	15
DQ_46	-----SIVKGMKNLLNSTSL-----	15
A26_11	-----SIVKGMKNL-----	9
DR_49	-----IVKGMKNLLNSTSLE-----	15
DQ_50	-----IVKGMKNLLNSTSLE-----	15
DQ_47	-----VKGMKNLLNSTSLET-----	15
DR_64	-----VKGMKNLLNSTSLET-----	15
DQ_43	-----KGMKNLLNSTSLETS-----	15
DR_66	-----KGMKNLLNSTSLETS-----	15
DQ_51	-----GMKNLLNSTSLETSL-----	15
B58_3	-----TSLSIEAPW-----	9
DQ_239	-----GAINVQST-----	8
B58_10	-----GAINVQST-----	8
B62_19	-----GAINVQST-----	8
DQ_223	-----AINVQST-----	7
A3_21	-----AINVQST-----	7
DQ_219	-----INVQST-----	6
DR_42	-----NVQST-----	5
DQ_221	-----VQST-----	4
DR_41	-----VQST-----	4
DR_39	-----QST-----	3
DQ_226	-----QST-----	3
DQ_102	-----QST-----	3
DQ_161	-----QST-----	3
DQ_158	-----ST-----	2
DR_40	-----ST-----	2
DQ_83	-----ST-----	2
DQ_84	-----T-----	1
DQ_171	-----T-----	1
DR_43	-----T-----	1

GPC	FKPTVSTANIALSWSSIEHRGNKILVTGRSESIMKLEERTGVSWDLGVEDASESKLLTVS	1140
B58_10	F-----	9
B62_19	F-----	9
A3_21	FK-----	9
DQ_239	FKPTVST-----	15
DQ_223	FKPTVSTA-----	15
DQ_219	FKPTVSTAN-----	15
DR_42	FKPTVSTANI-----	15
DR_41	FKPTVSTANIA-----	15
DQ_221	FKPTVSTANIA-----	15
DQ_102	FKPTVSTANIAL-----	15
DR_39	FKPTVSTANIAL-----	15
DQ_226	FKPTVSTANIAL-----	15
DQ_161	FKPTVSTANIAL-----	15
DQ_158	FKPTVSTANIALS-----	15
DQ_83	FKPTVSTANIALS-----	15
DR_40	FKPTVSTANIALS-----	15
DR_43	FKPTVSTANIALSW-----	15
DQ_84	FKPTVSTANIALSW-----	15
DQ_171	FKPTVSTANIALSW-----	15
DQ_180	FKPTVSTANIALSWS-----	15
DQ_89	FKPTVSTANIALSWS-----	15
B7_11	-KPTVSTANI-----	9
DQ_95	-KPTVSTANIALSWSS-----	15
DQ_175	-KPTVSTANIALSWSS-----	15
DQ_260	--PTVSTANIALSWSSI-----	15
DQ_100	--PTVSTANIALSWSSI-----	15
DQ_177	--PTVSTANIALSWSSI-----	15
DR_148	---TVSTANIALSWSSIE-----	15
B7_20	---TVSTANIAL-----	9
DR_150	----VSTANIALSWSSIEH-----	15
B58_1	----STANIALSW-----	9
DR_152	----STANIALSWSSIEHR-----	15
DR_155	-----TANIALSWSSIEHRG-----	15
B44_10	-----IEHRGNKIL-----	9
B27_7	-----GRSESIMKL-----	9
B39_12	-----GRSESIMKL-----	9
B44_14	-----VEDASESKL-----	9
DP_99	-----ESKLLTVS-----	8
DR_210	-----TVS-----	3
A1_4	-----S-----	1
A26_2	-----S-----	1
B62_6	-----S-----	1

GPC	IMDLSQMYSPVFEYLSGDRQVEEWPKATCTGDCPERCGCTSSSTCLHKWPHSRNWRNRCNPT	1200
DP_99	IMDLSQM-----	15
A1_4	IMDLSQMY-----	9
A26_2	IMDLSQMY-----	9
B62_6	IMDLSQMY-----	9
DR_210	IMDLSQMYSPVF-----	15
DP_22	IMDLSQMYSPVFEYL-----	15
DP_21	-MDLSQMYSPVFEYLS-----	15
DP_25	--DLSQMYSPVFEYLSG-----	15
B62_17	---LSQMYSPVF-----	9
B58_16	---LSQMYSPVF-----	9
DP_28	---LSQMYSPVFEYLSGD-----	15
DP_38	---SQMYSPVFEYLSGDR-----	15
B62_1	----QMYSPVFEY-----	9
B58_12	----QMYSPVFEY-----	9
A3_6	----QMYSPVFEY-----	9
A24_2	-----MYPVFEYL-----	9

B58_17	-----SGDRQVEEW-----	9
A3_30	-----CTSSTCLHK-----	9
B58_11	-----SSTCLHKEW-----	9
B58_6	-----RNWRCNPT	8
DQ_249	-----CNPT	4
DQ_248	-----NPT	3
DQ_247	-----T	1
DQ_246	-----PT	2
GPC	WCWGVGTGCTCCGVDVKDLFTDHFVKKVVEYIKTEAIVCVELTSQERQCSLIEAGTRFN	1260
B58_6	W-----	9
DQ_249	WCWGVGTGCTC-----	15
DQ_248	WCWGVGTGCTCC-----	15
DQ_246	WCWGVGTGCTCCG-----	15
DQ_247	WCWGVGTGCTCCGV-----	15
B58_5	-----FTDHFVKKW-----	9
A1_5	-----FTDHFVKKW-----	9
B8_3	-----FVKWKVEYI-----	9
DR_85	-----KWKVEYIKTEAIVCV-----	15
DR_86	-----WKVEYIKTEAIVC-----	15
A24_16	-----EYIKTEAIV-----	9
B39_14	-----TEAIVCVEL-----	9
B44_13	-----TEAIVCVEL-----	9
B58_24	-----SLIEAGTRF-----	9
B62_7	-----SLIEAGTRF-----	9
A26_7	-----SLIEAGTRF-----	9
B39_7	-----IEAGTRFN	8
B44_4	-----IEAGTRFN	8
DQ_255	-----EAGTRFN	7
DQ_256	-----AGTRFN	6
DQ_257	-----GTRFN	5
A2_16	-----N	1
DR_312	-----N	1
GPC	LGPVTITLSEPRNIQQKLPPEIITLHPKVEEGFFDLMHVQKVLASTVCKLQSCTHGIPG	1320
B44_4	L-----	9
B39_7	L-----	9
DQ_255	LGPVTITL-----	15
A2_16	LGPVTITL-----	9
DQ_256	LGPVTITLS-----	15
DQ_257	LGPVTITLSE-----	15
DR_312	LGPVTITLSEPRNI-----	15
DR_309	LGPVTITLSEPRNIQ-----	15
DR_310	-GPVTITLSEPRNIQQ-----	15
DR_313	--PVTITLSEPRNIQQK-----	15
B7_27	-----EPRNIQQKL-----	9
A2_17	-----KLPPEIITL-----	9
A26_15	-----EIIITLHPKV-----	9
DQ_2	-----LHPKVEEGFFDLMHV-----	15
DQ_1	-----HPKVEEGFFDLMHVQ-----	15
DQ_4	-----PKVEEGFFDLMHVQK-----	15
DQ_3	-----KVEEGFFDLMHVQKV-----	15
B44_18	-----VEEGFFDLM-----	9
DQ_5	-----VEEGFFDLMHVQKVL-----	15
DR_332	-----FFDLMHVQKVLAST-----	15
DR_326	-----FDLMHVQKVLASTV-----	15
DQ_54	-----DLMHVQKVLASTVC-----	15
DQ_185	-----DLMHVQKVLASTVC-----	15
DQ_170	-----LMHVQKVLASTVCK-----	15
DQ_179	-----MHVQKVLASTVCKL-----	15

DQ_199	-----HVQKVLASTVCKLQ-----	15
A3_8	-----VLSASTVCK-----	9
B58_20	-----LSASTVCKL-----	9
A2_18	-----KLSQCTHGI--	9
A26_14	-----GIPG	4

GPC	DLQVYHIGNLLKGRVNGHLIHKIEPHFNTSWMMSWDGCDLDYCNMGDWPSCTYTGVTQH	1380
A26_14	DLQVY-----	9
A3_5	-----RVNGHLIHK-----	9
B7_18	-----EPHFNTSWM-----	9
B58_15	-----HFNTSWMMSW-----	9
A1_12	-----SWDGCDDY-----	9
A1_13	-----MGDWPSCTY-----	9
B62_14	-----VTQH	4
DR_280	-----QH	2
B39_18	-----H	1
DR_277	-----H	1

GPC	NHAAFVLLNIETDYTKTFHFHFSKRVTAHGDTPQLDLKARPTYGAGEITVLVEVADMELH	1440
B62_14	NHAAF-----	9
B39_18	NHAAFVNL-----	9
DR_280	NHAAFVLLNIET-----	15
DR_277	NHAAFVLLNIETD-----	15
B39_2	NHAAFVLL-----	9
DR_273	NHAAFVLLNIETDY-----	15
DR_271	-HAAFVLLNIETDYT-----	15
DR_198	-----IETDYTKTFHFHFSKR-----	15
DR_185	-----ETDYTKTFHFHFSKRV-----	15
B44_16	-----IETDYTKTF-----	9
A1_8	-----ETDYTKTFH-----	9
DR_96	-----ETDYTKTFHFHFSKRV-----	15
DR_94	-----TDYTKTFHFHFSKRVT-----	15
DR_179	-----TDYTKTFHFHFSKRVT-----	15
DR_97	-----DYTKTFHFHFSKRVT-----	15
DR_133	-----DYTKTFHFHFSKRVT-----	15
DQ_309	-----DYTKTFHFHFSKRVT-----	15
DR_177	-----DYTKTFHFHFSKRVT-----	15
DQ_342	-----DYTKTFHFHFSKRVT-----	15
DR_178	-----YTKTFHFHFSKRVTAH-----	15
DR_99	-----YTKTFHFHFSKRVTAH-----	15
DQ_241	-----YTKTFHFHFSKRVTAH-----	15
DQ_339	-----YTKTFHFHFSKRVTAH-----	15
DR_121	-----YTKTFHFHFSKRVTAH-----	15
DQ_296	-----YTKTFHFHFSKRVTAH-----	15
DQ_295	-----TKTFHFHFSKRVTAHG-----	15
DR_118	-----TKTFHFHFSKRVTAHG-----	15
DR_105	-----TKTFHFHFSKRVTAHG-----	15
DR_182	-----TKTFHFHFSKRVTAHG-----	15
DQ_340	-----TKTFHFHFSKRVTAHG-----	15
DR_116	-----KTFHFHFSKRVTAHGD-----	15
DQ_341	-----KTFHFHFSKRVTAHGD-----	15
DR_184	-----KTFHFHFSKRVTAHGD-----	15
DQ_297	-----KTFHFHFSKRVTAHGD-----	15
A3_9	-----KTFHFHFSKR-----	9
DQ_320	-----TFHFHFSKRVTAHGDT-----	15
DR_117	-----TFHFHFSKRVTAHGDT-----	15
DR_128	-----FHFHFSKRVTAHGDT-----	15
DQ_258	-----DLKARPTYGAGEITV-----	15
DQ_250	-----LKARPTYGAGEITVL-----	15
DQ_251	-----KARPTYGAGEITVLV-----	15
DQ_252	-----ARPTYGAGEITVLVE-----	15

DQ_253	-----RPTYGAGEITVLVEV-----	15
B7_9	-----RPTYGAGEI-----	9
DQ_254	-----PTYGAGEITVLVEVA-----	15
B39_3	-----YGAGEITVL-----	9
B44_11	-----GEITVLVEV-----	9

GPC	TKKVEISGLKFASLACTGCYACSSGISCKVRIHVDEPDELTVHVKSSDPDVVAASTSLTA	1500
B62_9	-----ASLACTGCY-----	9
A1_6	-----ASLACTGCY-----	9
B39_4	-----IHVDEPDEL-----	9
DQ_150	-----KSSDPDVVAASTSLT-----	15
DQ_75	-----SSDPDVVAASTSLTA-----	15
DQ_44	-----SSDPDVVAASTSLTA-----	15
DQ_133	-----SSDPDVVAASTSLTA-----	15
DQ_136	-----SDPDVVAASTSLTA-----	14
DQ_285	-----SDPDVVAASTSLTA-----	14
DQ_36	-----SDPDVVAASTSLTA-----	14
DQ_69	-----SDPDVVAASTSLTA-----	14
DQ_65	-----DPDVVAASTSLTA-----	13
DQ_32	-----DPDVVAASTSLTA-----	13
DR_70	-----DPDVVAASTSLTA-----	13
DQ_139	-----DPDVVAASTSLTA-----	13
DQ_259	-----DPDVVAASTSLTA-----	13
DQ_140	-----PDVVAASTSLTA-----	12
DQ_63	-----PDVVAASTSLTA-----	12
DQ_261	-----PDVVAASTSLTA-----	12
DR_72	-----PDVVAASTSLTA-----	12
DQ_27	-----PDVVAASTSLTA-----	12
DQ_235	-----PDVVAASTSLTA-----	12
DQ_38	-----DVVAASTSLTA-----	11
DQ_211	-----DVVAASTSLTA-----	11
DQ_152	-----DVVAASTSLTA-----	11
DQ_64	-----DVVAASTSLTA-----	11
DQ_70	-----VVAASTSLTA-----	10
DQ_168	-----VVAASTSLTA-----	10
DQ_209	-----VVAASTSLTA-----	10
DQ_94	-----VAASTSLTA-----	9
DQ_208	-----VAASTSLTA-----	9
DQ_210	-----AASTSLTA-----	8
DQ_216	-----ASTSLTA-----	7
A3_29	-----ASTSLTA-----	7
DQ_220	-----STSLTA-----	6
B62_15	-----SLTA-----	4
DR_297	-----TA-----	2
DR_288	-----A-----	1

GPC	RKLEFGTDSTFKAFSAMPKTSLCFYIVEKEYCKSCNEDDTQKCLDTKLEQSQSILIEHKG	1560
DQ_285	R-----	15
DQ_36	R-----	15
DQ_69	R-----	15
DQ_136	R-----	15
DQ_259	RK-----	15
A3_29	RK-----	9
DQ_32	RK-----	15
DQ_65	RK-----	15
DR_70	RK-----	15
DQ_139	RK-----	15
DQ_235	RKL-----	15
DQ_63	RKL-----	15
DR_72	RKL-----	15
DQ_27	RKL-----	15

DQ_140	RKL-----	15
DQ_261	RKL-----	15
DQ_64	RKLE-----	15
DQ_152	RKLE-----	15
DQ_211	RKLE-----	15
DQ_38	RKLE-----	15
DQ_70	RKLEF-----	15
DQ_168	RKLEF-----	15
B62_15	RKLEF-----	9
DQ_209	RKLEF-----	15
DQ_208	RKLEFG-----	15
DQ_94	RKLEFG-----	15
DQ_210	RKLEFGT-----	15
DQ_216	RKLEFGTD-----	15
DQ_220	RKLEFGTDS-----	15
DR_297	RKLEFGTDSTFKA-----	15
DR_288	RKLEFGTDSTFKAF-----	15
DR_289	RKLEFGTDSTFKAFS-----	15
DR_290	-KLEFGTDSTFKAFSA-----	15
B44_9	--LEFGTDSTF-----	9
B62_18	--LEFGTDSTF-----	9
DR_294	--LEFGTDSTFKAFSAM-----	15
DQ_222	--LEFGTDSTFKAFSAM-----	15
DQ_217	---EFGTDSTFKAFSAMP-----	15
DQ_215	---FGTDSTFKAFSAMPK-----	15
DR_351	---FGTDSTFKAFSAMPK-----	15
DQ_292	---FGTDSTFKAFSAMPK-----	15
DR_157	---FGTDSTFKAFSAMPK-----	15
DR_165	---FGTDSTFKAFSAMPK-----	15
DQ_214	----GTDSTFKAFSAMPKT-----	15
DR_164	----GTDSTFKAFSAMPKT-----	15
DR_143	----GTDSTFKAFSAMPKT-----	15
DQ_289	----GTDSTFKAFSAMPKT-----	15
DR_347	----GTDSTFKAFSAMPKT-----	15
A1_9	----GTDSTFKAF-----	9
DR_285	----GTDSTFKAFSAMPKT-----	15
DR_274	-----TDSTFKAFSAMPKTS-----	15
DR_346	-----TDSTFKAFSAMPKTS-----	15
DQ_288	-----TDSTFKAFSAMPKTS-----	15
DR_137	-----TDSTFKAFSAMPKTS-----	15
DR_163	-----TDSTFKAFSAMPKTS-----	15
DQ_176	-----TDSTFKAFSAMPKTS-----	15
DQ_212	-----TDSTFKAFSAMPKTS-----	15
DR_134	-----DSTFKAFSAMPKTSL-----	15
DR_189	-----DSTFKAFSAMPKTSL-----	15
DQ_286	-----DSTFKAFSAMPKTSL-----	15
DR_344	-----DSTFKAFSAMPKTSL-----	15
DR_161	-----DSTFKAFSAMPKTSL-----	15
DQ_213	-----DSTFKAFSAMPKTSL-----	15
DR_265	-----DSTFKAFSAMPKTSL-----	15
DQ_187	-----DSTFKAFSAMPKTSL-----	15
A26_4	-----STFKAFSAM-----	9
DQ_218	-----STFKAFSAMPKTSLC-----	15
DR_160	-----STFKAFSAMPKTSLC-----	15
DR_183	-----STFKAFSAMPKTSLC-----	15
DR_343	-----STFKAFSAMPKTSLC-----	15
DQ_287	-----STFKAFSAMPKTSLC-----	15
DR_135	-----STFKAFSAMPKTSLC-----	15
DR_267	-----STFKAFSAMPKTSLC-----	15
DR_181	-----TFKAFSAMPKTSLCF-----	15
DR_162	-----TFKAFSAMPKTSLCF-----	15
DR_270	-----TFKAFSAMPKTSLCF-----	15
DR_345	-----TFKAFSAMPKTSLCF-----	15

DQ_315	-----TFKAFSAMPKTSLCF-----	15
DR_139	-----TFKAFSAMPKTSLCF-----	15
DR_180	-----FKAFSAMPKTSLCFY-----	15
DR_166	-----FKAFSAMPKTSLCFY-----	15
DR_159	-----FKAFSAMPKTSLCFY-----	15
DR_278	-----FKAFSAMPKTSLCFY-----	15
DR_348	-----FKAFSAMPKTSLCFY-----	15
DR_186	-----KAFSAMPKTSLCFYI-----	15
B39_11	-----FSAMPKTSL-----	9
A24_9	-----AMPKTSLCF-----	9
B62_8	-----AMPKTSLCF-----	9
A3_23	-----SLCFYIVEK-----	9
B44_19	-----NEDDTQKCL-----	9
B44_17	-----LEQPQSILI-----	9

GPC	TIIGKQNDTCTAKASCWLESVKSFYGLKNMLGSVFGNFFIGILLFLAPFVLLVLFMFG	1620
DR_207	-----AKASCWLESVKSFY-----	15
DR_208	-----KASCWLESVKSFY-----	15
A2_19	-----KASCWLESV-----	9
DR_209	-----ASCWLESVKSFYGL-----	15
A24_13	-----CWLESVKS-----	9
DR_12	-----SVKSFFYGLKNMLGS-----	15
DR_204	-----SVKSFFYGLKNMLGS-----	15
DR_286	-----SVKSFFYGLKNMLGS-----	15
DR_175	-----VKSFFYGLKNMLGSV-----	15
DR_279	-----VKSFFYGLKNMLGSV-----	15
DR_197	-----VKSFFYGLKNMLGSV-----	15
DR_73	-----VKSFFYGLKNMLGSV-----	15
DR_7	-----VKSFFYGLKNMLGSV-----	15
DR_2	-----KSFFYGLKNMLGSVF-----	15
DR_193	-----KSFFYGLKNMLGSVF-----	15
DR_172	-----KSFFYGLKNMLGSVF-----	15
DR_275	-----KSFFYGLKNMLGSVF-----	15
DR_57	-----KSFFYGLKNMLGSVF-----	15
DR_9	-----SFFYGLKNMLGSVFG-----	15
DR_59	-----SFFYGLKNMLGSVFG-----	15
DR_203	-----SFFYGLKNMLGSVFG-----	15
DR_174	-----SFFYGLKNMLGSVFG-----	15
B39_9	-----FFYGLKNML-----	9
DR_176	-----FFYGLKNMLGSVFGN-----	15
DP_31	-----FYGLKNMLGSVFGNF-----	15
DP_20	-----YGLKNMLGSVFGNFF-----	15
DP_16	-----GLKNMLGSVFGNFFI-----	15
DP_17	-----LKNMLGSVFGNFFIG-----	15
DP_11	-----KNMLGSVFGNFFIGI-----	15
DP_137	-----KNMLGSVFGNFFIGI-----	15
DP_13	-----NMLGSVFGNFFIGIL-----	15
DP_125	-----NMLGSVFGNFFIGIL-----	15
DP_18	-----MLGSVFGNFFIGILL-----	15
DP_128	-----MLGSVFGNFFIGILL-----	15
DP_27	-----LGSVFGNFFIGILLF-----	15
DP_115	-----LGSVFGNFFIGILLF-----	15
DP_33	-----GSVFGNFFIGILLFL-----	15
DP_111	-----GSVFGNFFIGILLFL-----	15
DP_72	-----GSVFGNFFIGILLFL-----	15
DP_118	-----SVFGNFFIGILLFLA-----	15
DP_62	-----SVFGNFFIGILLFLA-----	15
DP_54	-----VFGNFFIGILLFLAP-----	15
DP_131	-----VFGNFFIGILLFLAP-----	15
DP_57	-----FGNFFIGILLFLAPF-----	15
DP_139	-----FGNFFIGILLFLAPF-----	15
DP_61	-----GNFFIGILLFLAPFV-----	15

A24_18	-----NFFIGILLF-----	9
DP_52	-----NFFIGILLFLAPFVL-----	15
DP_50	-----FFIGILLFLAPFVLL-----	15
DP_49	-----FIGILLFLAPFVLLV-----	15
DP_47	-----IGILLFLAPFVLLVL-----	15
DP_43	-----GILLFLAPFVLLVLF-----	15
A2_20	-----ILLFLAPFV-----	9
DP_44	-----ILLFLAPFVLLVLF-----	15
A2_21	-----LLFLAPFVL-----	9
DP_40	-----LLFLAPFVLLVLF-----	15
DP_39	-----LFLAPFVLLVLF-----	15
DP_41	-----FLAPFVLLVLF-----	15
DP_42	-----LAPFVLLVLF-----	14
DP_46	-----APFVLLVLF-----	13
DP_138	-----PFVLLVLF-----	12
DP_45	-----PFVLLVLF-----	12
A24_4	-----PFVLLVLF-----	9
A26_10	-----FVLLVLF-----	9
A2_22	-----FVLLVLF-----	9
DP_110	-----FVLLVLF-----	11
DP_48	-----FVLLVLF-----	11
A24_8	-----VLLVLF-----	9
DP_51	-----VLLVLF-----	10
DP_107	-----VLLVLF-----	10
DP_58	-----LLVLF-----	9
DP_108	-----LLVLF-----	9
DP_59	-----LVLF-----	8
DP_106	-----LVLF-----	8
B58_7	-----LVLF-----	8
A3_3	-----VLF-----	7
DP_68	-----VLF-----	7
DP_109	-----VLF-----	7
DP_124	-----LFF-----	6
B27_16	-----FMFG-----	4
B39_15	-----FMFG-----	4
B62_2	-----FMFG-----	4
B58_22	-----FG-----	2

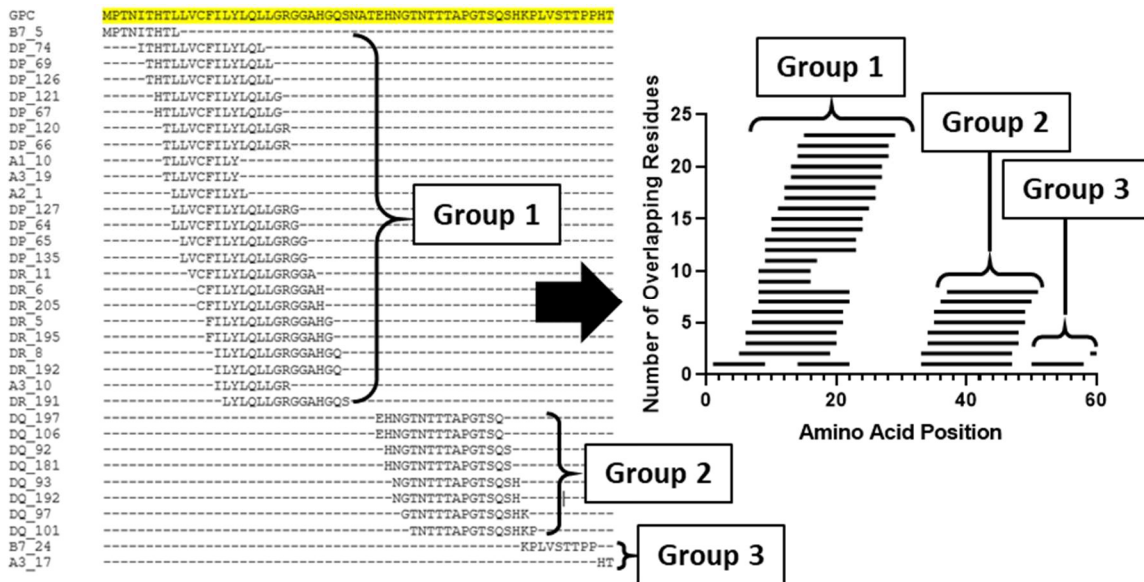
GPC	WKILFCFKCCRRTRGLFKYRHLKDDEETGYKRIERLNNKKGKNRLLDGERLADRKIAEL	1680
B58_7	W-----	9
DP_42	W-----	15
A3_3	WK-----	9
DP_46	WK-----	15
DP_45	WKI-----	15
DP_138	WKI-----	15
DP_48	WKIL-----	15
DP_110	WKIL-----	15
B27_16	WKILF-----	9
B39_15	WKILF-----	9
DP_51	WKILF-----	15
DP_107	WKILF-----	15
B62_2	WKILF-----	9
DP_58	WKILFC-----	15
DP_108	WKILFC-----	15
DP_106	WKILFCF-----	15
B58_22	WKILFCF-----	9
DP_59	WKILFCF-----	15
DP_68	WKILFCFK-----	15
DP_109	WKILFCFK-----	15
DP_124	WKILFCFKC-----	15
DR_130	-KILFCFKCCRRTRGL-----	15
DR_120	--ILFCFKCCRRTRGLF-----	15

DR_119	---LFCFKCCRRTRGLFK-----	15
DR_226	---FCFKCCRRTRGLFKY-----	15
DR_123	---FCFKCCRRTRGLFKY-----	15
DR_219	----CFKCCRRTRGLFKYR-----	15
DR_125	----CFKCCRRTRGLFKYR-----	15
DR_124	----FKCCRRTRGLFKYRH-----	15
DR_220	----FKCCRRTRGLFKYRH-----	15
DR_127	-----KCCRRTRGLFKYRHL-----	15
DR_122	-----CCRTRGLFKYRHLK-----	15
DR_227	-----CCRTRGLFKYRHLK-----	15
DR_340	-----CCRTRGLFKYRHLK-----	15
DR_339	-----CRRTRGLFKYRHLKD-----	15
DR_114	-----CRRTRGLFKYRHLKD-----	15
B27_2	-----RRTRGLFKY-----	9
DR_341	-----RRTRGLFKYRHLKDD-----	15
DR_112	-----RRTRGLFKYRHLKDD-----	15
A3_31	-----RTRGLFKYR-----	9
DR_113	-----RTRGLFKYRHLKDDE-----	15
DR_115	-----TRGLFKYRHLKDDEE-----	15
DR_126	-----RGLFKYRHLKDDEET-----	15
A3_2	-----GLFKYRHLK-----	9
DR_206	-----TGKRIIERLNNKKG-----	15
DR_201	-----GYKRIIERLNNKKGK-----	15
A3_20	-----RIIERLNNK-----	9
B27_13	-----ERLNNKKGK-----	9
A3_4	-----KIAEL-----	5

GPC	FSTKTHIG*	1688
A3_4	FSTK-----	9

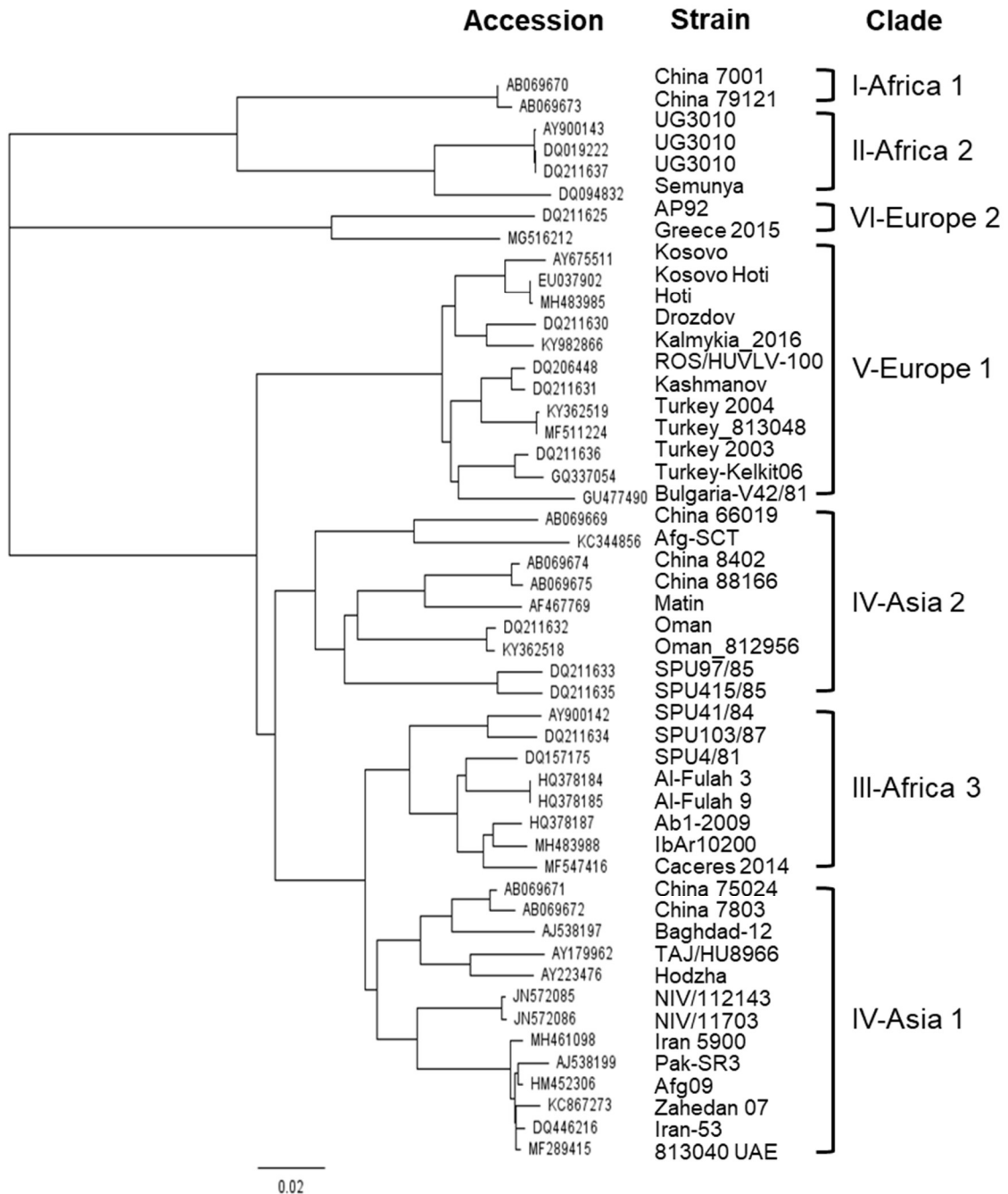
Figure 5.2: Method of graphing overlapping epitopes.

The first 60 residues of the CCHFV GPC are shown with all epitopes aligned to this region. Multiple epitopes that include the same residue are referred to as overlapping epitopes and were grouped based on shared residues. The number of epitopes that overlap a set of residues were quantified and graphed as seen on the right.



Supplementary Figure 5.3: Geneious Tree Builder output of 50 GPC sequences.

Phylogenetic tree of the 50 GPC translation sequences selected for the conservation analysis. Assignment of clades is based on previous publications^{2,50}. Produced with Geneious Prime Software using default settings.



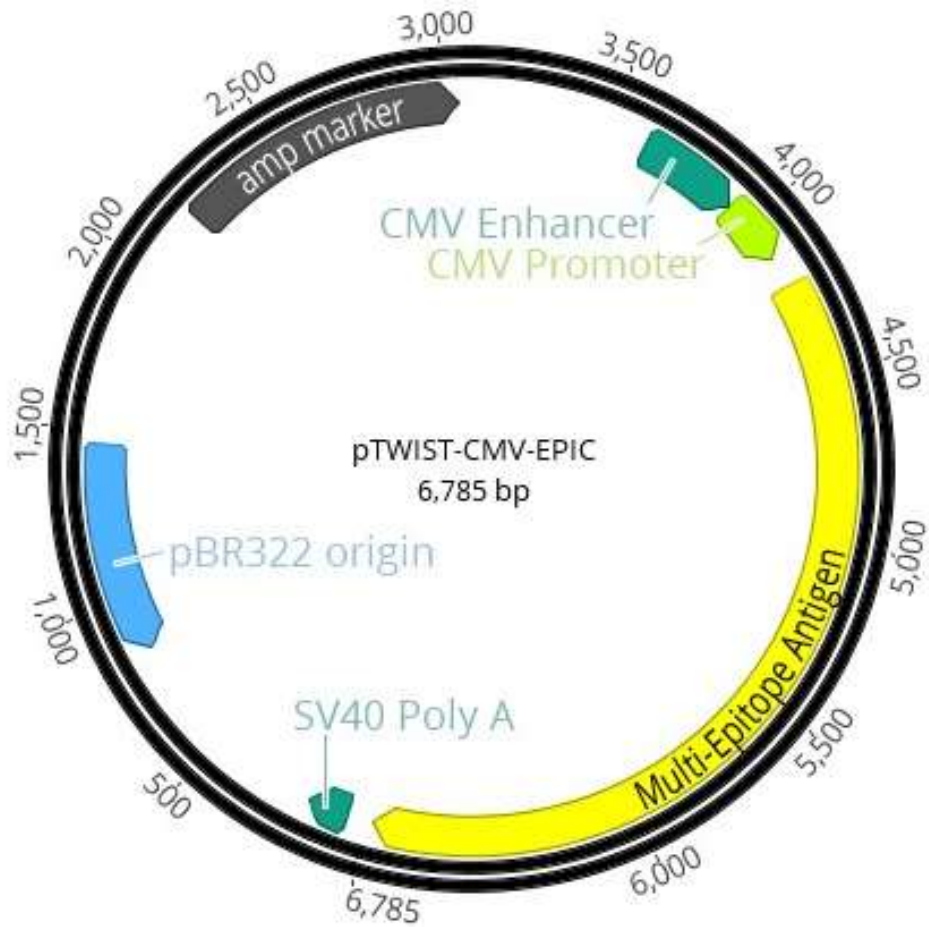
Supplementary Figure 5.4: Amino acid sequence of *EPIC*.

Annotated sequence of *EPIC* within the mammalian expression plasmid pTWIST-CMV-*EPIC*. Figure made with Geneious Prime Software.



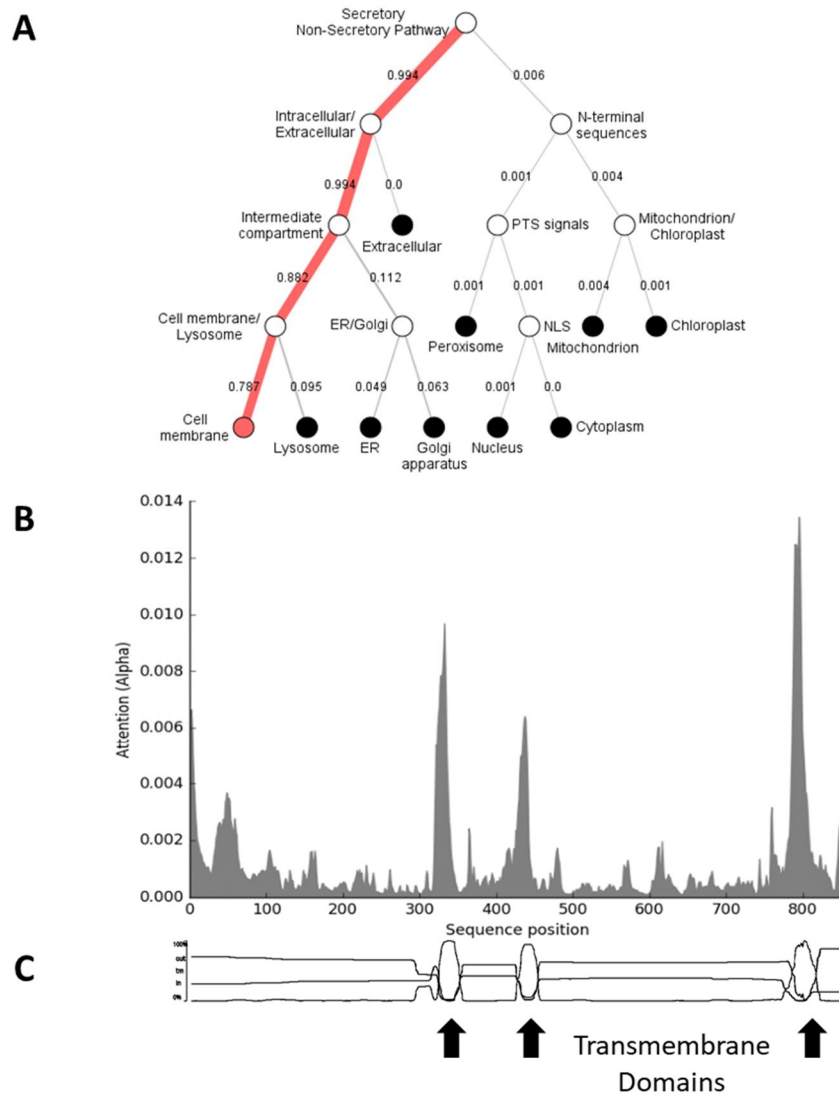
Supplementary Figure 5.5: pTWIST-CMV-EPIC DNA plasmid map.

The plasmid map of the synthesized construct is shown with nucleotide numbers.



Supplementary Figure 5.6: Outputs of multi-epitope antigen localization prediction and residues important for localization.

Results of the submission of the multi-epitope antigen sequence to the DeepLoc 1.0 Server (<https://services.healthtech.dtu.dk/service.php?DeepLoc-1.0>) for prediction of subcellular localization. (A) Hierarchical tree output showing the most likely localization of the antigen with numbers representing percent likelihood. (B) Graph of the importance of each residue for localization. (C) The three peaks highlighted by arrows correspond to the three transmembrane domains (Geneious Prime software).



Supplementary Figure 5.7: Alignment of all predicted mouse CTL and HTL epitopes to the CCHFV Turkey2004 GPC.

The 35 predicted mouse epitopes are shown aligned to the GPC. The five individual proteins post-cleavage are shown using different text highlights in the following order:

MLDGP38GNNSMGc.

GPC	MPTNITHLLVCFILYLQLLGRGGAHQSNATEHNGTNTTTAPGTSQSHKPLVSTTPPHT	60
Dd_8	MPTNITHTL-----	9
Dd_3	-----VCFILYLQL-----	9
Db_3	-----VCFILYLQL-----	9
Dd_6	-----APGTSQSHK-----	9
Db_6	-----APGTSQSHK-----	9
Db_1	-----TTPPHT	6
Dd_1	-----TTPPHT	6
Kd_1	-----TTPPHT	6
GPC	LESSTIKHTTPTSETEGSGETTPPPNTTQGPSPEATPERPATTATSTPSTDNTNSTTQM	120
Db_1	LES-----	9
Dd_1	LES-----	9
Kd_1	LES-----	9
GPC	NDNNPTSTISTSPSSSPSTPPTPQGIHHPARLLSVSSLKTATTPTTSPGEISSETSSQ	180
IAd_8	-----HHPARLLSVSSLKT-----	15
IAd_3	-----HPARLLSVSSLKTA-----	15
IAd_1	-----PARLLSVSSLKTAT-----	15
IAd_2	-----ARLLSVSSLKTATT-----	15
IAd_4	-----RLLSVSSLKTATTP-----	15
Dd_4	-----RLLSVSSL-----	9
Db_4	-----RLLSVSSL-----	9
Kd_2	-----ETSSQ	5
Dd_2	-----ETSSQ	5
Db_2	-----ETSSQ	5
GPC	HSAMSRTPTLHTTTQVSTESTNHSTPRQSESSAQPTTSPMTSPAQSILPMSAAPTAIQN	240
Kd_2	HSAM-----	9
Dd_2	HSAM-----	9
Db_2	HSAM-----	9
Dd_5	-----PTLHTTTQV-----	9
Db_5	-----PTLHTTTQV-----	9
Dd_7	-----SAQPTTSP-----	9
IAd_10	-----MTSPAQSILPMSAAP-----	15
IAd_7	-----TSPAQSILPMSAAPT-----	15
IAd_5	-----SPAQSILPMSAAPTA-----	15
IAd_6	-----PAQSILPMSAAPTAI-----	15
IAd_9	-----AQSILPMSAAPTAIQ-----	15
IAb_5	-----AQSILPMSAAPTAIQ-----	15
GPC	IHPSPTNRSKRNLEVEIILTLSQLKYYGKILKLLHLLTLEEDTEGLLEWCKRNLGSSCD	300
Dd_9	-----GKILKLLHL-----	9
GPC	DDFFQKRIEFFVTGEGYFNEVLQFKTLSTLSPTPEPSHAKLPTVEPFKSYFAKGFLSIDS	360
GPC	GYFSAKCYPRSSSTSGLQLINVTQHPARIAETPGPKTTSCLKTINCINLRASVFKEHREIEI	420

GPC	NVLLPQIAVNLSNCHAVIKSHVCDYSLD TDGPVRLPHIYHEGTFIPGTYKIVIDKKNKLN	480
GPC	DRCILVTNCVIKGREVRKQSVLRQYKTEIKIGKASTGSRKLLSEEPGDDCISRTQLLRT	540
GPC	ETAIEHDDNYGGPGDKITICNGSTIVDQRLGSELGCYTINRVKSFKLCENSATGKTCEID	600
GPC	STPVKCRQGFCLKITQEGRGHVKLSRGSEVLDVCDSSCEVMI PKGTGDILVDCSGGQQH	660
GPC	FLKDNLIDLGC PHVPLLGRMAIYICRMSNHPRTTMAFLWFWSFGYVITCIFCKALFYSLI	720
GPC	IIGTLGKKFKQYRELKPQTCTICETAPVNAIDAEMHDLNCSYNICPYCASRLTSDGLARH	780
GPC	VPQCPKRKEKVEETEYLNLERIPWIVRKLQVSESTGVALKRSSWLIVLLVLLTVSLSP	840
GPC	VQSAPVGHGKTIETYQTREGFTSICLFMLGSILFIVSCLVKGLVDSVSDSFFPGLSVCKT	900
GPC	CSIGSINGFEIESHKCYCSLFCCPYCRHCSADREIHQLHLSICKKRKTGSNVMLAVCKRM	960
GPC	CFRATIEASRRALLIRSIINTTFVICILTITICVSTSAVEMENLPAGTWEREEDLTNFC	1020
GPC	HQECQVTEETECLCPYEALVLRKPLFLDSIVKGMKNLLNSTSLETSLSIEAPWGAINVQST	1080
IAb_4	-----INVQST	6
IAb_2	-----NVQST	5
IAb_1	-----VQST	4
IAb_3	-----QST	3
GPC	FKPTVSTANIALSWSSIEHRGNKILVTGRSESIMKLEERTGVSWDLGVEDASESKLLTVS	1140
IAb_4	FKPTVSTAN-----	15
IAb_2	FKPTVSTANI-----	15
IAb_1	FKPTVSTANIA-----	15
IAb_3	FKPTVSTANIAL-----	15
GPC	IMDLSQMYSVPFEYLSGDRQVEEWPKATCTGDCPERCGCTSSSTCLHKWPHSRNWRCNPT	1200
GPC	WCWVGVTGCTCCGVDVKDLFTDHMFVKWVEYIKTEAIVCVELTSQERQCSLIEAGTRFN	1260
GPC	LGPVTITLSEPRNIQQKLPPEIITLHPKVEEGFFDLMHVQKVL SASTVCKLQ SCTHGIPG	1320
IAd_12	-----FDMHVQKVL SASTV-----	15
IAd_11	-----DLMHVQKVL SASTVC-----	15
IAd_13	-----LMHVQKVL SASTVCK-----	15
GPC	DLQVYHIGNLLKGDRVNGHLIHKIEPHFNTS WMSWDGCDLDYCNMGDWPSCTYTGVTQH	1380
GPC	NHAAFVNLLNIE TDYTKTFHFHFSKRVT AHGDT PQDLKARPTYGAGEITV LVEVADMELH	1440
GPC	TKKVEISGLKFASLACTGCIYACSSGISCKVRIHVDEPDELTVHVKSSDPDVVAASTSLTA	1500
GPC	RKLEFGTDSTFKAFSAMPKTS LCFYIVEKEYCKSCNEDDTQKCLDTKLEQPQSILIEHKG	1560
GPC	TIIGQNDTCTAKASCWLESVKSFFYGLKNM LGSVFGNFFIGILLFLAPFVLLV LFFMFG	1620
GPC	WKILFCFKCCRRTRGLFKYRHLKDDEETGYKRI IERLNNKKGKNRLLDGERLADRKIAEL	1680
GPC	FSTKTHIG* 1688	

Appendix D:
Supplementary Tables and Figures for Chapter 6

Supplementary Table 6.1: Differentially expressed genes between ISE6 cells treated with mouse mock and rabbit mock sera.

Log2 Fold Change	Adjusted <i>p</i>-value	Accession	Gene Name
9.28	7.11E-12	LOC8024969	Roundabout homolog 1 (ROBO1)
8.42	5.00E-05	LOC8052898	Tubulin alpha 1-C chain
6.33	0.004	LOC120847219	Small subunit ribosomal RNA
5.11	0.016	LOC8024345	Tubulin alpha chain-like
3.00	0.077	LOC120847184	Small subunit ribosomal RNA
2.41	0.0817	LOC115318740	Forkhead box protein C1-like
1.87	0.054	LOC8026892	Tubulin beta chain

Supplementary Figure 6.1: Homology of Subolesin between *Rhipicephalus microplus*, *Hyalomma marginatum*, and *Ixodes scapularis*.

The amino acid sequence of Subolesin from *Rhipicephalus microplus* (Accession # ABA62330), *Hyalomma marginatum* (Accession # DQ159970), and *Ixodes scapularis* (Accession # AY652654). There are 13 residue differences between *R. microplus* and *H. marginatum*, 56 differences between *R. microplus* and *I. scapularis*, and 53 differences between *H. marginatum* and *I. scapularis*. (A) Percent identity table between the three sequences. (B) Alignment of the three sequences. Alignment and percent identity calculations were completed using Geneious Prime software.

A

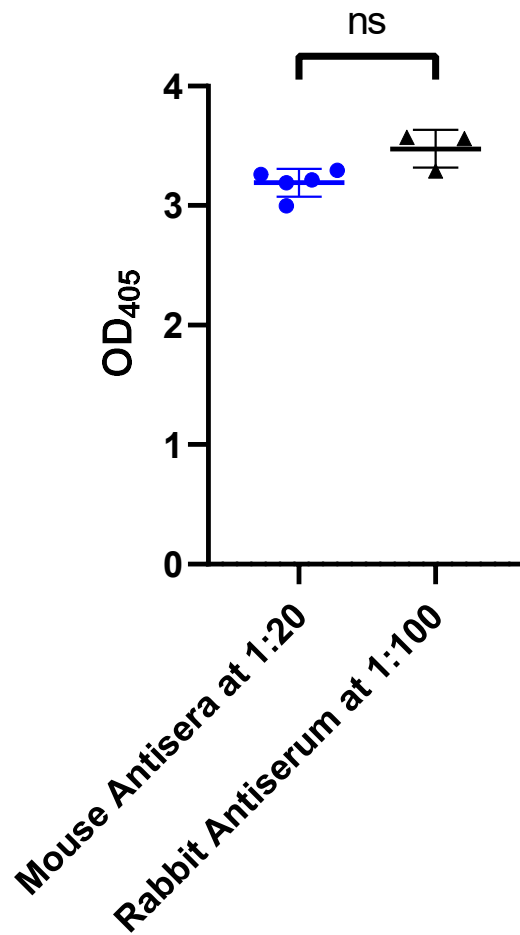
	<i>I. scapularis</i>	<i>H. marginatum</i>	<i>R. microplus</i>
<i>I. scapularis</i>	100.0	77.1	75.3
<i>H. marginatum</i>	-	100.0	91.3
<i>R. microplus</i>	-	-	100.0

B

Consensus	MACATLKRTHDWDPLHSPNGRSPKRRRCMPLSP---PXPPTRAHQINPSPFGEVPPKLTS	57
AY652654VTQAAT.....	60
DQ159970---.A.....M.....M..	57
ABA62330S.....---.---.....D.....D.....	55
Consensus	EEIAANIREEMRRLQRRKQLCFQGXD-----PESQXTSGLLSPVRRD	99
AY652654SSPLESGSPSATPPAADCGPAS.TGLSPG.....	120
DQ159970T.-----.....Q.....	99
ABA62330R.-----.....H.....S...H..	97
Consensus	QPLFTFRQVGLICERMKERESQIREEYDHLVSTKLAEQYDTFVKFTYDQIQKRFEGATP	159
AY652654D.....A.....	180
DQ159970G.....-----	159
ABA62330K.....-----	157
Consensus	SYLS*	164
AY652654	185
DQ159970	-----	149
ABA62330	-----	147

Supplementary Figure 6.2: Comparison of mouse antisera and rabbit antiserum anti-Subolesin ELISA results.

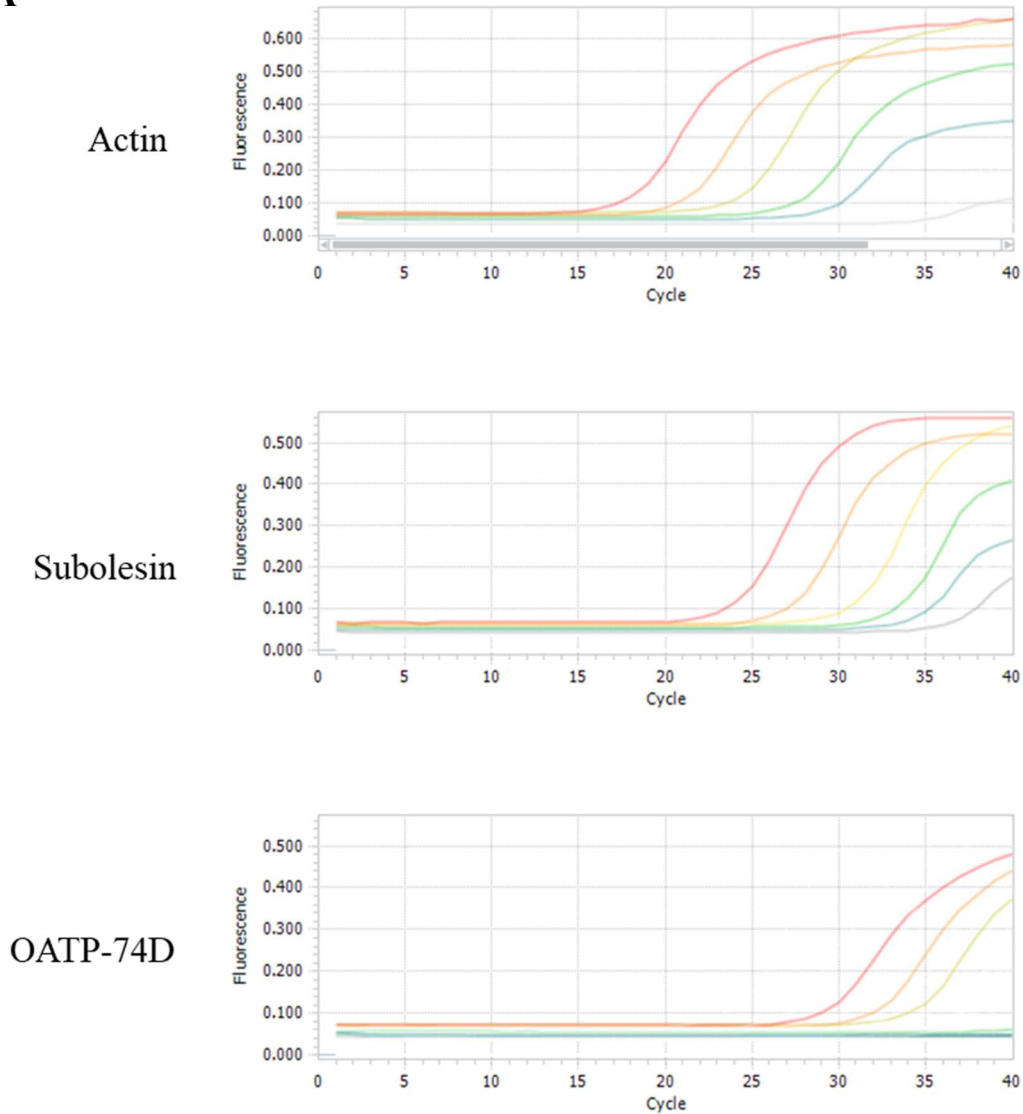
Bacterially expressed purified *R. microplus* Subolesin protein was used as a protein coat for an anti-Subolesin ELISA. Sera collected from BALB/cJ mice immunized with purified *R. microplus* Subolesin in adjuvant was diluted at 1:20 and from rabbits immunized with purified *R. microplus* Subolesin in adjuvant was diluted at 1:100 for use in the anti-Subolesin ELISA. The means of the two groups was not statistically different as tested by Welch's t-test.



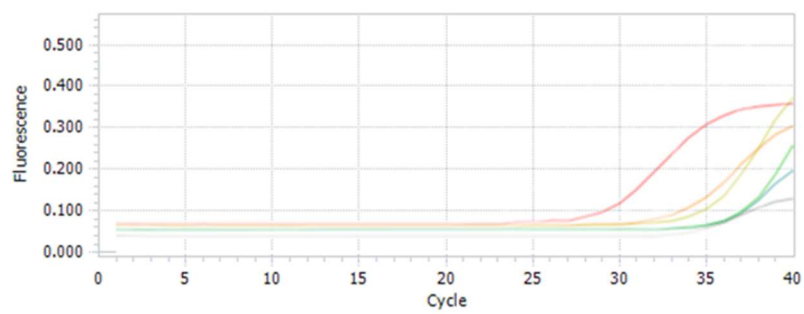
Supplementary Figure 6.3: Amplification curves and cycle threshold values from qRT-PCR experiments.

(A) Amplification curves of 10-fold serial dilutions of ISE6 cDNA. Each color represents a different cDNA concentration per reaction, red (1000ng), orange (100ng), yellow (10ng), green (1ng), blue (0.1ng), or gray (0ng, no template control). (B) Cycle threshold values for two independent experiments using 1000ng of cDNA per reaction or no template controls for each gene of interest.

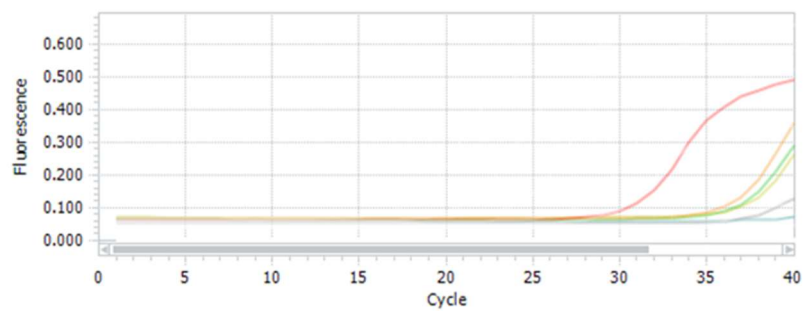
A



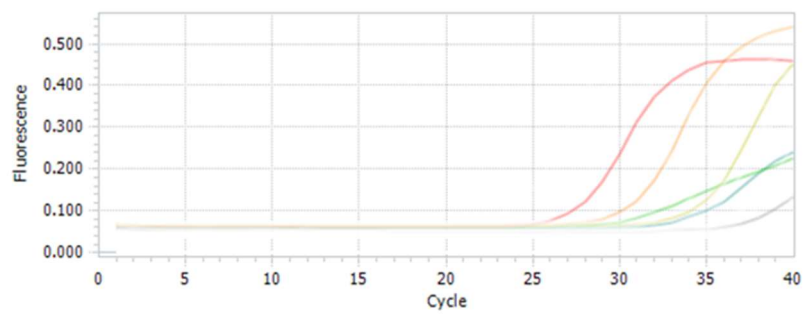
GLUT-1



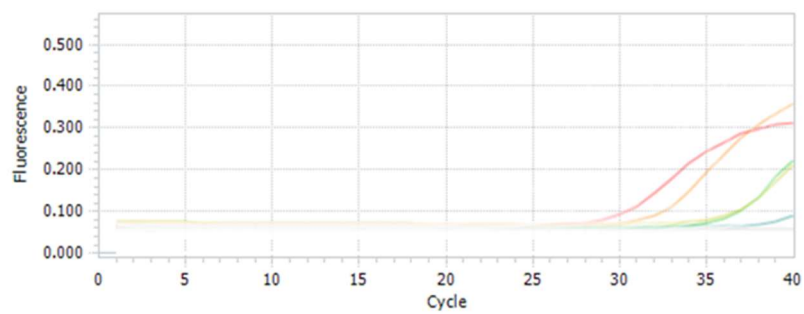
Slc26a6



PLAAT3



Malic

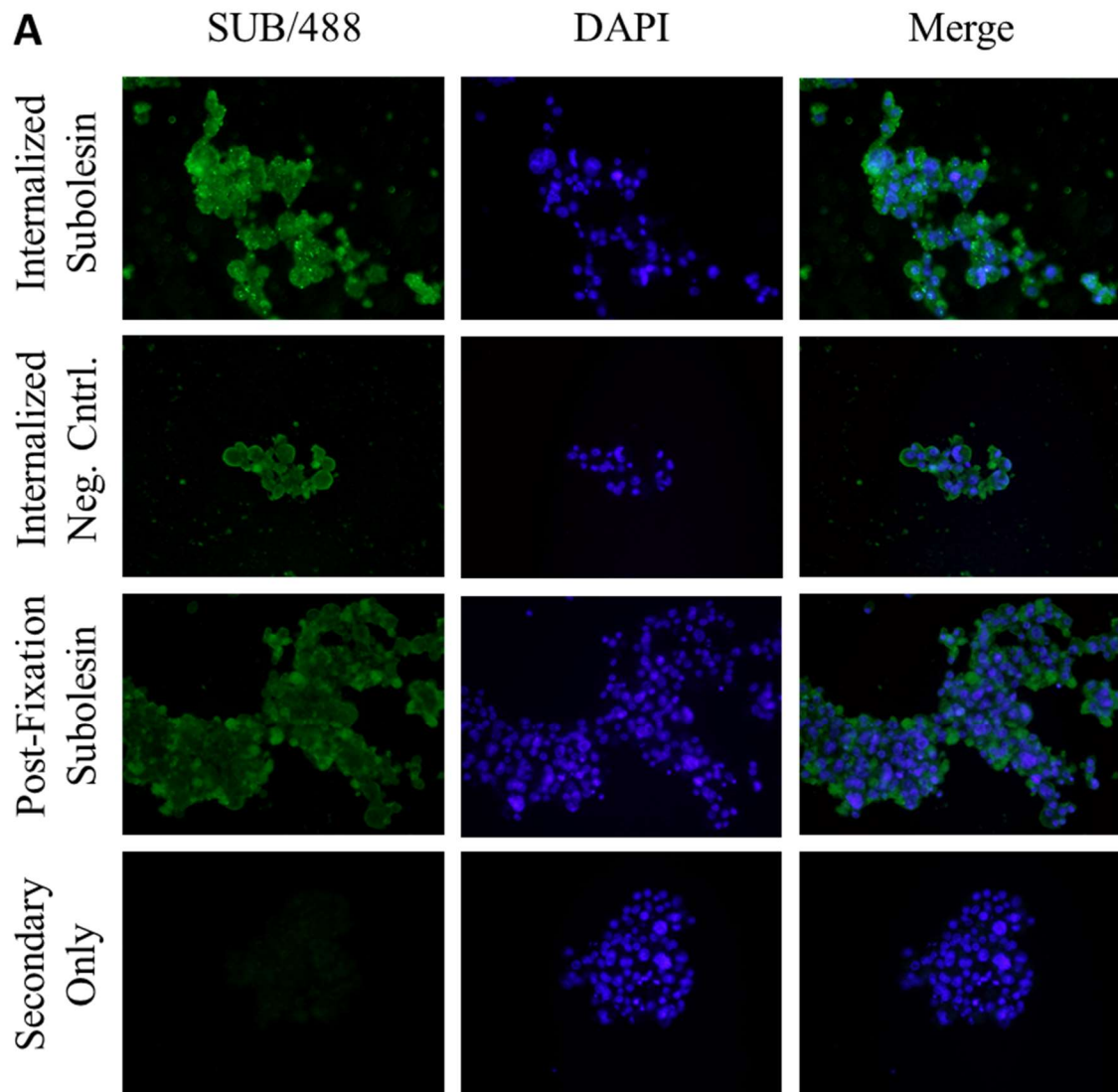


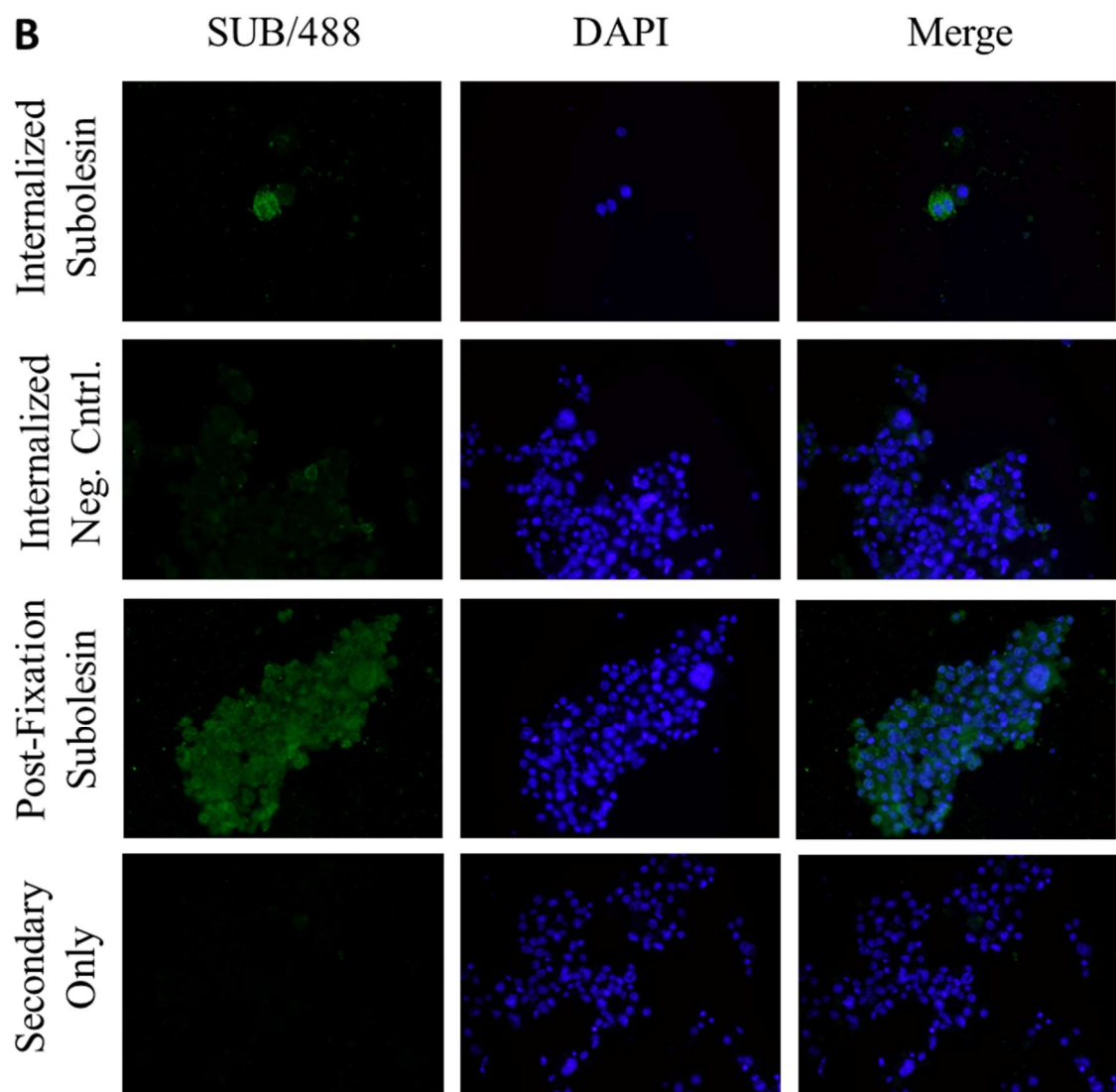
B

Ct Values from qRT-PCR			
cDNA		No template control	
Rep 1	Rep 2	Rep 1	Rep 2
15.77	17.61	32.05	32.31
21.83	23.56	34.86	37.42
28.71	31.79	37.91	-
24.48	27.78	33.69	33.97
31.56	36.63	38.7	36.36
28.93	29.39	32.39	37.33
26.47	30.25	37.51	38.21

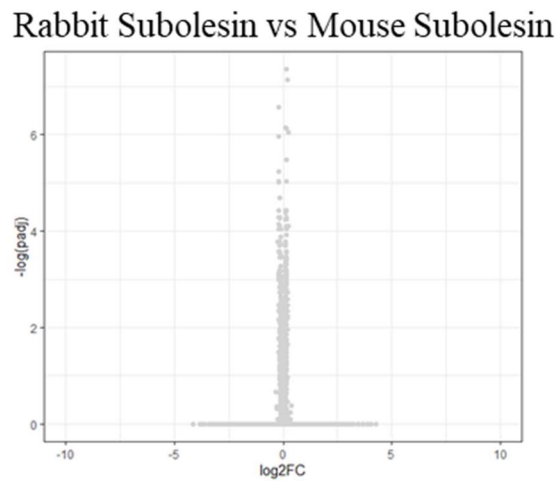
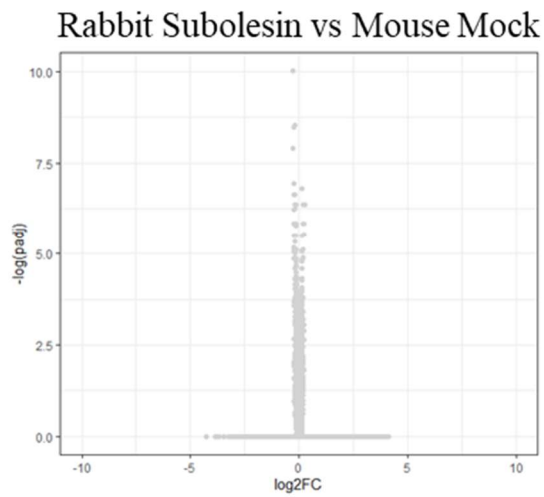
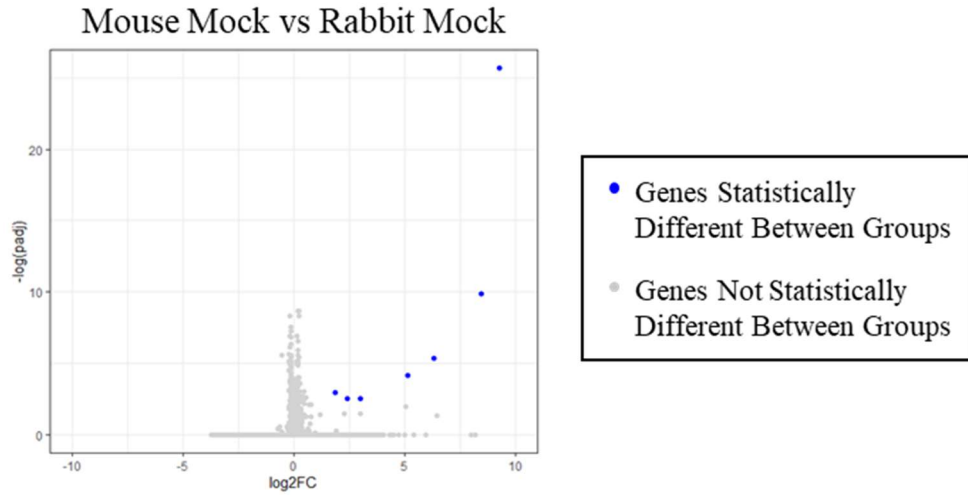
Supplementary Figure 6.4: IFA of ISE6 cells treated with anti-Subolesin antibodies in parallel to the cells treated for RNA-seq.

ISE6 cells were incubated with Subolesin or mock antiserum for 24 hours in biological triplicates. (A) Representative images of each condition using rabbit serum. (B) Representative images of each condition using mouse serum.





Supplementary Figure 6.5: Analysis of differentially expressed genes between rabbit and mouse sera treated groups.



REFERENCES

1. Hoogstraal, H. The epidemiology of tick-borne Crimean-Congo hemorrhagic fever in Asia, Europe, and Africa. *J. Med. Entomol.* **15**, 307–417 (1979).
2. Bente, D. A. *et al.* Crimean-Congo hemorrhagic fever: History, epidemiology, pathogenesis, clinical syndrome and genetic diversity. *Antiviral Res.* **100**, 159–189 (2013).
3. Whitehouse, C. A. Crimean–Congo hemorrhagic fever. *Antiviral Res.* **64**, 145–160 (2004).
4. Chumakov, M. P. A Short Review Of Investigation Of The Virus Of Crimean Hemorrhagic Fever. *Endem. viral Infect.* 193–196 (1965).
5. Simpson, D. I. *et al.* Congo virus: a hitherto undescribed virus occurring in Africa. I. Human isolations--clinical notes. *East Afr. Med. J.* **44**, 86–92 (1967).
6. Woodall, J. ., Williams, M. C. . & Simpson, D. I. Congo virus: a hitherto undescribed virus occurring in Africa. II. Identification studies - PubMed. *East Afr. Med. J.* **44**, 93–98 (1967).
7. Ergönül, Ö. Crimean-Congo haemorrhagic fever. *Lancet Infect. Dis.* **6**, 203–214 (2006).
8. WHO. Crimean-Congo haemorrhagic fever. Available at: https://www.who.int/health-topics/crimean-congo-haemorrhagic-fever/#tab=tab_1. (Accessed: 5th June 2022)
9. Factsheet about Crimean-Congo haemorrhagic fever. *European Centre for Disease Prevention and Control* Available at: <https://www.ecdc.europa.eu/en/crimean-congo-haemorrhagic-fever/facts/factsheet>.
10. NIH/NIAID. NIAID Emerging Infectious Diseases/Pathogens | NIH: National Institute of Allergy and Infectious Diseases. 1 (2017).
11. WHO. *WHO CCHF R&D Roadmap Meeting*. (2018).
12. Spengler, J. R. & Bente, D. A. Crimean-congo hemorrhagic fever in Spain-New arrival or silent resident? *N. Engl. J. Med.* **377**, (2017).

13. Jameson, L. J., Morgan, P. J., Medlock, J. M., Watola, G. & Vaux, A. G. C. Importation of *Hyalomma marginatum*, vector of Crimean-Congo haemorrhagic fever virus, into the United Kingdom by migratory birds. *Ticks Tick. Borne. Dis.* **3**, 95–99 (2012).
14. Gargili, A. *et al.* The role of ticks in the maintenance and transmission of Crimean-Congo hemorrhagic fever virus: A review of published field and laboratory studies. *Antiviral Res.* **144**, (2017).
15. Estrada-Peña, A. & De La Fuente, J. The ecology of ticks and epidemiology of tick-borne viral diseases. *Antiviral Res.* **108**, 104–128 (2014).
16. Estrada-Peña, A., Ayllón, N. & de la Fuente, J. Impact of climate trends on tick-borne pathogen transmission. *Frontiers in Physiology* (2012). doi:10.3389/fphys.2012.00064
17. Estrada-Peña, A., Ruiz-Fons, F., Acevedo, P., Gortazar, C. & De la Fuente, J. Factors driving the circulation and possible expansion of Crimean-Congo haemorrhagic fever virus in the western Palearctic. *J. Appl. Microbiol.* **114**, 278–286 (2013).
18. Estrada-Peña, A., Sánchez, N. & Estrada-Sánchez, A. An assessment of the distribution and spread of the tick *Hyalomma marginatum* in the western Palearctic under different climate scenarios. *Vector Borne Zoonotic Dis.* **12**, 758–768 (2012).
19. Kampen, H., Poltz, W., Hartelt, K., Wölfel, R. & Faulde, M. Detection of a questing *Hyalomma marginatum marginatum* adult female (Acari, Ixodidae) in southern Germany. *Exp. Appl. Acarol.* **43**, 227–231 (2007).
20. Gale, P. *et al.* Impact of climate change on risk of incursion of Crimean-Congo haemorrhagic fever virus in livestock in Europe through migratory birds. *J. Appl. Microbiol.* **112**, 246–257 (2012).
21. Negrodo, A. *et al.* Autochthonous Crimean–Congo Hemorrhagic Fever in Spain. *N. Engl. J. Med.* **377**, 154–161 (2017).
22. Cajimat, M. N. B. *et al.* Genomic Characterization of Crimean-Congo Hemorrhagic Fever Virus in *Hyalomma* Tick from Spain, 2014. *Vector Borne Zoonotic Dis.* **17**, 714–719 (2017).

23. Palomar, A. M. *et al.* Crimean-Congo Hemorrhagic Fever Virus in Ticks from Migratory Birds, Morocco. *Emerg. Infect. Dis.* **19**, 260 (2013).
24. Adams, M. J. *et al.* Changes to taxonomy and the International Code of Virus Classification and Nomenclature ratified by the International Committee on Taxonomy of Viruses (2017). *Arch. Virol.* **162**, (2017).
25. Lasecka, L. & Baron, M. D. The molecular biology of nairoviruses, an emerging group of tick-borne arboviruses. *Arch. Virol.* **159**, 1249 (2014).
26. Walter, C. T. & Barr, J. N. Recent advances in the molecular and cellular biology of bunyaviruses. *J. Gen. Virol.* **92**, 2467–2484 (2011).
27. Jeeva, S. *et al.* Crimean-Congo hemorrhagic fever virus nucleocapsid protein harbors distinct RNA-binding sites in the stalk and head domains. *J. Biol. Chem.* **294**, 5023–5037 (2019).
28. Wichgers Schreur, P. J., Kormelink, R. & Kortekaas, J. Genome packaging of the Bunyavirales. *Curr. Opin. Virol.* **33**, 151–155 (2018).
29. Barnwal, B., Karlberg, H., Mirazimi, A. & Tan, Y. J. The Non-structural Protein of Crimean-Congo Hemorrhagic Fever Virus Disrupts the Mitochondrial Membrane Potential and Induces Apoptosis. *J. Biol. Chem.* **291**, 582–592 (2016).
30. Wang, X. *et al.* Molecular basis for the formation of ribonucleoprotein complex of Crimean-Congo hemorrhagic fever virus. *J. Struct. Biol.* **196**, 455–465 (2016).
31. Sanchez, A. J., Vincent, M. J. & Nichol, S. T. Characterization of the Glycoproteins of Crimean-Congo Hemorrhagic Fever Virus. *J. Virol.* **76**, 7263 (2002).
32. Erickson, B. R., Deyde, V., Sanchez, A. J., Vincent, M. J. & Nichol, S. T. N-linked glycosylation of Gn (but not Gc) is important for Crimean Congo hemorrhagic fever virus glycoprotein localization and transport. *Virology* **361**, 348–355 (2007).
33. Vincent, M. J. *et al.* Crimean-Congo Hemorrhagic Fever Virus Glycoprotein Proteolytic Processing by Subtilase SKI-1. *J. Virol.* **77**,

8640 (2003).

34. Bergeron, E., Vincent, M. J. & Nichol, S. T. Crimean-Congo Hemorrhagic Fever Virus Glycoprotein Processing by the Endoprotease SKI-1/S1P Is Critical for Virus Infectivity. *J. Virol.* **81**, 13271–13276 (2007).
35. Freitas, N. *et al.* The interplays between Crimean-Congo hemorrhagic fever virus (CCHFV) M segment-encoded accessory proteins and structural proteins promote virus assembly and infectivity. *PLOS Pathog.* **16**, e1008850 (2020).
36. Devignot, S., Bergeron, E., Nichol, S., Mirazimi, A. & Weber, F. A Virus-Like Particle System Identifies the Endonuclease Domain of Crimean-Congo Hemorrhagic Fever Virus. *J. Virol.* **89**, 5957 (2015).
37. Altamura, L. A. *et al.* Identification of a novel C-terminal cleavage of Crimean-Congo hemorrhagic fever virus PreGN that leads to generation of an NSM protein. *J. Virol.* **81**, 6632–42 (2007).
38. Bertolotti-Ciarlet, A. *et al.* Cellular localization and antigenic characterization of crimean-congo hemorrhagic fever virus glycoproteins. *J. Virol.* **79**, 6152–61 (2005).
39. Sanchez, A. J., Vincent, M. J., Erickson, B. R. & Nichol, S. T. Crimean-congo hemorrhagic fever virus glycoprotein precursor is cleaved by Furin-like and SKI-1 proteases to generate a novel 38-kilodalton glycoprotein. *J. Virol.* **80**, 514–25 (2006).
40. Estrada, D. F. & De Guzman, R. N. Structural Characterization of the Crimean-Congo Hemorrhagic Fever Virus Gn Tail Provides Insight into Virus Assembly. *J. Biol. Chem.* **286**, 21678 (2011).
41. Överby, A. K., Popov, V. L., Pettersson, R. F. & Neve, E. P. A. The cytoplasmic tails of Uukuniemi Virus (Bunyaviridae) G(N) and G(C) glycoproteins are important for intracellular targeting and the budding of virus-like particles. *J. Virol.* **81**, 11381–11391 (2007).
42. Garry, C. E. & Garry, R. F. Proteomics computational analyses suggest that the carboxyl terminal glycoproteins of Bunyaviruses are class II viral fusion protein (beta-penetrenes). *Theor. Biol. Med. Model.* **1**, 10 (2004).

43. Fels, J. M. *et al.* Protective neutralizing antibodies from human survivors of Crimean-Congo hemorrhagic fever. *Cell* **184**, 3486–3501.e21 (2021).
44. Hua, B. L. *et al.* A single mutation in Crimean-Congo hemorrhagic fever virus discovered in ticks impairs infectivity in human cells. *Elife* **9**, 1–27 (2020).
45. Mishra, A. K. *et al.* Structural basis of synergistic neutralization of Crimean-Congo hemorrhagic fever virus by human antibodies. *Science (80-.)*. **375**, 104–109 (2022).
46. Garrison, A. R. *et al.* Crimean–Congo hemorrhagic fever virus utilizes a clathrin- and early endosome-dependent entry pathway. *Virology* **444**, 45–54 (2013).
47. Simon, M., Johansson, C., Lundkvist, Å. & Mirazimi, A. Microtubule-dependent and microtubule-independent steps in Crimean-Congo hemorrhagic fever virus replication cycle. *Virology* **385**, 313–322 (2009).
48. Simon, M., Johansson, C. & Mirazimi, A. Crimean-Congo hemorrhagic fever virus entry and replication is clathrin-, pH- and cholesterol-dependent. *J. Gen. Virol.* **90**, 210–215 (2009).
49. Deyde, V. M., Khristova, M. L., Rollin, P. E., Ksiazek, T. G. & Nichol, S. T. Crimean-Congo Hemorrhagic Fever Virus Genomics and Global Diversity. *J. Virol.* **80**, 8834–8842 (2006).
50. Ramírez de Arellano, E. *et al.* Phylogenetic Characterization of Crimean-Congo Hemorrhagic Fever Virus, Spain. *Emerg. Infect. Dis.* **23**, 2078 (2017).
51. Nuttall, P. A. & Labuda, M. Tick-host interactions: Saliva-activated transmission. *Parasitology* **129**, (2004).
52. Rodriguez, S., McAuley, A., Gargili, A. & Bente, D. Interactions of Human Dermal Dendritic Cells and Langerhans Cells Treated with Hyalomma Tick Saliva with Crimean-Congo Hemorrhagic Fever Virus. *Viruses* **10**, 381 (2018).
53. Šimo, L., Kazimirova, M., Richardson, J. & Bonnet, S. I. The essential

- role of tick salivary glands and saliva in tick feeding and pathogen transmission. *Front. Cell. Infect. Microbiol.* **7**, 281 (2017).
54. Rodriguez, S. E. *et al.* Immunobiology of Crimean-Congo hemorrhagic fever. *Antiviral Res.* **199**, 105244 (2022).
 55. Connolly-Andersen, A.-M., Douagi, I., Kraus, A. A. & Mirazimi, A. Crimean Congo hemorrhagic fever virus infects human monocyte-derived dendritic cells. *Virology* **390**, 157–162 (2009).
 56. Bray, M. Pathogenesis of viral hemorrhagic fever. *Curr. Opin. Immunol.* **17**, 399–403 (2005).
 57. Swanepoel, R. *et al.* The clinical pathology of Crimean-Congo hemorrhagic fever. *Rev. Infect. Dis.* **11 Suppl 4**, S794-800
 58. Ergonul, O., Tuncbilek, S., Baykam, N., Celikbas, A. & Dokuzoguz, B. Evaluation of Serum Levels of Interleukin (IL)–6, IL-10, and Tumor Necrosis Factor– α in Patients with Crimean-Congo Hemorrhagic Fever. *J. Infect. Dis.* **193**, 941–944 (2006).
 59. Ergonul, O. O., Celikbas, A., Baykam, N., Eren, S. & Dokuzoguz, B. Analysis of risk-factors among patients with Crimean-Congo haemorrhagic fever virus infection: severity criteria revisited. *Clin. Microbiol. Infect.* **12**, 551–554 (2006).
 60. Saksida, A. *et al.* Interacting roles of immune mechanisms and viral load in the pathogenesis of Crimean-Congo hemorrhagic fever. *Clin. Vaccine Immunol.* **17**, 1086–1093 (2010).
 61. Burt, F. J., Leman, P. A., Abbott, J. C. & Swanepoel, R. Serodiagnosis of Crimean-Congo haemorrhagic fever. *Epidemiol. Infect.* **113**, 551–562 (1994).
 62. Shepherd, A. J., Swanepoel, R. & Leman, P. A. Antibody Response in Crimean-Congo Hemorrhagic Fever. *Rev. Infect. Dis.* **11**, S801–S806 (1989).
 63. Ergunay, K. *et al.* Antibody responses and viral load in patients with Crimean-Congo hemorrhagic fever: a comprehensive analysis during the early stages of the infection. *Diagn. Microbiol. Infect. Dis.* **79**, 31–36 (2014).

64. Haddock, E. *et al.* A cynomolgus macaque model for Crimean-Congo haemorrhagic fever. *Nat. Microbiol.* **3**, 556 (2018).
65. Hawman, D. W. *et al.* Crimean-Congo Hemorrhagic Fever Mouse Model Recapitulating Human Convalescence. *J. Virol.* **93**, (2019).
66. Hawman, D. W. *et al.* T-Cells and Interferon Gamma Are Necessary for Survival Following Crimean-Congo Hemorrhagic Fever Virus Infection in Mice. *Microorganisms* **9**, 1–17 (2021).
67. Duh, D. *et al.* Viral Load as Predictor of Crimean-Congo Hemorrhagic Fever Outcome. *Emerg. Infect. Dis.* **13**, 1769–1772 (2007).
68. Goedhals, D., Paweska, J. T. & Burt, F. J. Long-lived CD8+ T cell responses following Crimean-Congo haemorrhagic fever virus infection. *PLoS Negl. Trop. Dis.* **11**, e0006149 (2017).
69. Bente, D. A. *et al.* Pathogenesis and immune response of Crimean-Congo hemorrhagic fever virus in a STAT-1 knockout mouse model. *J. Virol.* **84**, 11089–11099 (2010).
70. Berezky, S. *et al.* Crimean-Congo hemorrhagic fever virus infection is lethal for adult type I interferon receptor-knockout mice. *J. Gen. Virol.* **91**, 1473–1477 (2010).
71. Zivcec, M. *et al.* Lethal Crimean-Congo hemorrhagic fever virus infection in interferon α/β receptor knockout mice is associated with high viral loads, proinflammatory responses, and coagulopathy. *J. Infect. Dis.* **207**, 1909–1921 (2013).
72. Garrison, A. R. *et al.* A DNA vaccine for Crimean-Congo hemorrhagic fever protects against disease and death in two lethal mouse models. *PLoS Negl. Trop. Dis.* **11**, (2017).
73. Tipih, T. & Burt, F. J. Crimean-congo hemorrhagic fever virus: Advances in vaccine development. *BioResearch Open Access* **9**, 137–150 (2020).
74. Dowall, S. D., Carroll, M. W. & Hewson, R. Development of vaccines against Crimean-Congo haemorrhagic fever virus. *Vaccine* **35**, 6015–6023 (2017).
75. Hinkula, J. *et al.* Immunization with DNA Plasmids Coding for

Crimean-Congo Hemorrhagic Fever Virus Capsid and Envelope Proteins and/or Virus-Like Particles Induces Protection and Survival in Challenged Mice. *J. Virol.* **91**, (2017).

76. Farzani, T. A. *et al.* Co-delivery effect of CD24 on the immunogenicity and lethal challenge protection of a DNA vector expressing nucleocapsid protein of crimean congo hemorrhagic fever virus. *Viruses* **11**, (2019).
77. Suschak, J. J. *et al.* A CCHFV DNA vaccine protects against heterologous challenge and establishes GP38 as immunorelevant in mice. *npj Vaccines* 2021 61 **6**, 1–11 (2021).
78. Hawman, D. W. *et al.* A DNA-based vaccine protects against Crimean-Congo haemorrhagic fever virus disease in a Cynomolgus macaque model. *Nat. Microbiol.* (2020). doi:10.1038/s41564-020-00815-6
79. Buttigieg, K. R. *et al.* A Novel Vaccine against Crimean-Congo Haemorrhagic Fever Protects 100% of Animals against Lethal Challenge in a Mouse Model. *PLoS One* **9**, e91516 (2014).
80. Rodriguez, S. E. *et al.* Vesicular Stomatitis Virus-Based Vaccine Protects Mice against Crimean-Congo Hemorrhagic Fever. *Sci. Rep.* (2019). doi:10.1038/s41598-019-44210-6
81. Farzani, T. A. *et al.* Bovine herpesvirus type 4 (BoHV-4) vector delivering nucleocapsid protein of crimean-congo hemorrhagic fever virus induces comparable protective immunity against lethal challenge in IFN α / β γ R $^{-/-}$ mice models. *Viruses* **11**, (2019).
82. Appelberg, S. *et al.* Nucleoside-Modified mRNA Vaccines Protect IFNAR $^{-/-}$ Mice against Crimean-Congo Hemorrhagic Fever Virus Infection . *J. Virol.* **96**, (2022).
83. Farzani, T. A. *et al.* Immunological analysis of a CCHFV mRNA vaccine candidate in mouse models. *Vaccines* **7**, (2019).
84. Scholte, F. E. M. *et al.* Single-dose replicon particle vaccine provides complete protection against Crimean-Congo hemorrhagic fever virus in mice. *Emerg. Microbes Infect.* **8**, 575 (2019).

85. Dowall, S. D. *et al.* Protective effects of a Modified Vaccinia Ankara-based vaccine candidate against Crimean-Congo Haemorrhagic Fever virus require both cellular and humoral responses. *PLoS One* **11**, e0156637 (2016).
86. Ahmed, A. A. *et al.* Presence of broadly reactive and group-specific neutralizing epitopes on newly described isolates of Crimean-Congo hemorrhagic fever virus. *J. Gen. Virol.* **86**, 3327–3336 (2005).
87. Zivcec, M. *et al.* Identification of broadly neutralizing monoclonal antibodies against Crimean-Congo hemorrhagic fever virus. *Antiviral Res.* **146**, 112–120 (2017).
88. Golden, J. W. *et al.* GP38-targeting monoclonal antibodies protect adult mice against lethal Crimean-Congo hemorrhagic fever virus infection. *Sci. Adv.* (2019). doi:10.1126/sciadv.aaw9535
89. Fritzen, A. *et al.* Epitope-mapping of the glycoprotein from Crimean-Congo hemorrhagic fever virus using a microarray approach. *PLoS Negl. Trop. Dis.* **12**, (2018).
90. Shalitanati, A. *et al.* Fine mapping epitope on glycoprotein-Gn from Crimean-Congo hemorrhagic fever virus. *Comp. Immunol. Microbiol. Infect. Dis.* **59**, 24–31 (2018).
91. Liu, D. *et al.* Fine Epitope Mapping of the Central Immunodominant Region of Nucleoprotein from Crimean-Congo Hemorrhagic Fever Virus (CCHFV). *PLoS One* **9**, e108419 (2014).
92. Lombe, B. P. *et al.* Mapping of Antibody Epitopes on the Crimean-Congo Hemorrhagic Fever Virus Nucleoprotein. *Viruses* 2022, Vol. 14, Page 544 **14**, 544 (2022).
93. Goedhals, D., Paweska, J. T. & Burt, F. J. SHORT REPORT Identification of human linear B-cell epitope sites on the envelope glycoproteins of Crimean-Congo haemorrhagic fever virus. (2014). doi:10.1017/S0950268814002271
94. Zhang, J. *et al.* Fine mapping epitope on glycoprotein Gc from Crimean-Congo hemorrhagic fever virus. *Comp. Immunol. Microbiol. Infect. Dis.* **67**, 101371 (2019).

95. Moming, A. *et al.* Mapping of B-cell epitopes on the N- terminal and C-terminal segment of nucleocapsid protein from Crimean-Congo hemorrhagic fever virus. *PLoS One* **13**, e0204264 (2018).
96. Mousavi-Jazi, M., Karlberg, H., Papa, A., Christova, I. & Mirazimi, A. Healthy individuals' immune response to the Bulgarian Crimean-Congo hemorrhagic fever virus vaccine. *Vaccine* **30**, 6225–6229 (2012).
97. Spengler, J. R. *et al.* A chronological review of experimental infection studies of the role of wild animals and livestock in the maintenance and transmission of Crimean-Congo hemorrhagic fever virus. *Antiviral Res.* **135**, 31–47 (2016).
98. Spengler, J. R. & Estrada-Peña, A. Host preferences support the prominent role of Hyalomma ticks in the ecology of Crimean-Congo hemorrhagic fever. *PLoS Negl. Trop. Dis.* **12**, e0006248 (2018).
99. Gargili, A., Thangamani, S. & Bente, D. Influence of laboratory animal hosts on the life cycle of Hyalomma marginatum and implications for an in vivo transmission model for Crimean-Congo hemorrhagic fever virus. *Front. Cell. Infect. Microbiol.* **4**, (2013).
100. Estrada-Peña, A., Jameson, L., Medlock, J., Vatansever, Z. & Tishkova, F. Unraveling the Ecological Complexities of Tick-Associated Crimean-Congo Hemorrhagic Fever Virus Transmission: A Gap Analysis for the Western Palearctic. <https://home.liebertpub.com/vbz> **12**, 743–752 (2012).
101. Apanaskevich, D. A. Host-parasite relationships of the genus Hyalomma Koch, 1844 (Acari, Ixodidae) and their connection with microevolutionary process. *Parazitologiya* **38**, 515–523 (2004).
102. Jones, L. D., Davies, C. R., Steele, G. M. & Nuttall, P. A. A novel mode of arbovirus transmission involving a nonviremic host. *Science* **237**, 775–777 (1987).
103. Nuttall, P. A. & Labuda, M. Dynamics of infection in tick vectors and at the tick-host interface. *Adv. Virus Res.* **60**, 233–272 (2003).
104. Brossard, M. & Wikel, S. K. Immunology of interactions between ticks and hosts. *Med. Vet. Entomol.* **11**, 270–276 (1997).

105. Willadsen, P. & Kemp, D. H. Vaccination with ‘concealed’ antigens for tick control. *Parasitol. Today* **4**, 196–198 (1988).
106. Nuttall, P. A., Trimmell, A. R., Kazimirova, M. & Labuda, M. Exposed and concealed antigens as vaccine targets for controlling ticks and tick-borne diseases. *Parasite Immunol.* **28**, 155–163 (2006).
107. Francischetti, I. M. B., Sa-Nunes, A., Mans, B. J., Santos, I. M. & Ribeiro, J. M. C. The Role Of Saliva In Tick Feeding. *Front. Biosci.* **14**, 2051 (2009).
108. Franta, Z. *et al.* Dynamics of digestive proteolytic system during blood feeding of the hard tick *Ixodes ricinus*. *Parasites and Vectors* **3**, 1–11 (2010).
109. Sojka, D. *et al.* New insights into the machinery of blood digestion by ticks. *Trends Parasitol.* **29**, 276–285 (2013).
110. Jasinskas, A., Jaworski, D. C. & Barbour, A. G. *Amblyomma americanum*: Specific Uptake of Immunoglobulins into Tick Hemolymph during Feeding. *Exp. Parasitol.* **96**, 213–221 (2000).
111. Wang, H. & Nuttall, P. A. Excretion of host immunoglobulin in tick saliva and detection of IgG-binding proteins in tick haemolymph and salivary glands. *Parasitology* **109**, 525–530 (1994).
112. Ackerman, S., Clare, F. B., McGill, T. W. & Sonenshine, D. E. Passage of host serum components, including antibody, across the digestive tract of *Dermacentor variabilis* (Say). *J. Parasitol.* **67**, 737–740 (1981).
113. Fujisaki, K., Kamio, T. & Kitaoka, S. Passage of host serum components, including antibodies specific for *Theileria sergenti*, across the digestive tract of argasid and ixodid ticks. *Ann. Trop. Med. Parasitol.* **78**, 449–450 (1984).
114. De La Fuente, J. & Contreras, M. Tick vaccines: Current status and future directions. *Expert Review of Vaccines* **14**, 1367–1376 (2015).
115. Graf, J. F. *et al.* Tick control: an industry point of view. *Parasitology* **129**, S427–S442 (2004).
116. de la Fuente, J. *et al.* A ten-year review of commercial vaccine

- performance for control of tick infestations on cattle. *Anim. Heal. Res. Rev.* **8**, 23–28 (2007).
117. Willadsen, P. *et al.* Immunological control of a parasitic arthropod: identification of a protective antigen from *Boophilus microplus*. *J. Immunol.* **143**, 1346–1351 (1989).
 118. Kemp, D. H., Pearson, R. D., Gough, J. M. & Willadsen, P. Vaccination against *Boophilus microplus*: Localization of antigens on tick gut cells and their interaction with the host immune system. *Exp. Appl. Acarol.* **7**, 43–58 (1989).
 119. Merino, O. *et al.* Control of *Rhipicephalus* (*Boophilus*) *microplus* infestations by the combination of subolesin vaccination and tick autocidal control after subolesin gene knockdown in ticks fed on cattle. *Vaccine* **29**, 2248–2254 (2011).
 120. Schetters, T. *et al.* Cattle tick vaccine researchers join forces in CATVAC. in *Parasites and Vectors* **9**, (2016).
 121. De la Fuente, J. & Merino, O. Vaccinomics, the new road to tick vaccines. *Vaccine* **31**, 5923–5929 (2013).
 122. Almazán, C. *et al.* Identification of protective antigens for the control of *Ixodes scapularis* infestations using cDNA expression library immunization. *Vaccine* **21**, 1492–1501 (2003).
 123. Artigas-Jerónimo, S. *et al.* Functional Evolution of Subolesin/Akirin. *Front. Physiol.* **0**, 1612 (2018).
 124. Kumar, B. *et al.* Functional characterization of candidate antigens of *Hyalomma anatolicum* and evaluation of its cross-protective efficacy against *Rhipicephalus microplus*. *Vaccine* **35**, 5682–5692 (2017).
 125. de la Fuente, J. *et al.* Evidence of the role of tick subolesin in gene expression. *BMC Genomics* **9**, 1–16 (2008).
 126. de la Fuente, J. *et al.* Tick-Pathogen Interactions and Vector Competence: Identification of Molecular Drivers for Tick-Borne Diseases. *Front. Cell. Infect. Microbiol.* **0**, 114 (2017).
 127. Naranjo, V. *et al.* Reciprocal Regulation of NF- κ B (Relish) and Subolesin in the Tick Vector, *Ixodes scapularis*. *PLoS One* **8**, e65915

- (2013).
128. Gulia-Nuss, M. *et al.* Genomic insights into the *Ixodes scapularis* tick vector of Lyme disease. *Nat. Commun.* 2016 71 **7**, 1–13 (2016).
 129. Shaw, D. K. *et al.* Infection-derived lipids elicit an immune deficiency circuit in arthropods. *Nat. Commun.* 2017 81 **8**, 1–13 (2017).
 130. Artigas-Jerónimo, S. *et al.* Tick importin- α is implicated in the interactome and regulome of the cofactor subolesin. *Pathogens* **10**, 457 (2021).
 131. Leung, S. W., Harreman, M. T., Hodel, M. R., Hodel, A. E. & Corbett, A. H. Dissection of the Karyopherin α Nuclear Localization Signal (NLS)-binding Groove: Functional Requirements For Nls Binding. *J. Biol. Chem.* **278**, 41947–41953 (2003).
 132. de la Fuente, J. *et al.* The tick protective antigen, 4D8, is a conserved protein involved in modulation of tick blood ingestion and reproduction. *Vaccine* **24**, 4082–4095 (2006).
 133. Galindo, R. C. *et al.* Tick subolesin is an ortholog of the akirins described in insects and vertebrates. *Dev. Comp. Immunol.* **33**, 612–617 (2009).
 134. de la Fuente, J. *et al.* Autocidal control of ticks by silencing of a single gene by RNA interference. *Biochem. Biophys. Res. Commun.* **344**, 332–338 (2006).
 135. Nijhof, A. M. *et al.* Gene silencing of the tick protective antigens, Bm86, Bm91 and subolesin, in the one-host tick *Boophilus microplus* by RNA interference. *Int. J. Parasitol.* **37**, 653–662 (2007).
 136. Kocan, K. M., Manzano-Roman, R. & de la Fuente, J. Transovarial silencing of the subolesin gene in three-host ixodid tick species after injection of replete females with subolesin dsRNA. *Parasitol. Res.* 2007 1006 **100**, 1411–1415 (2007).
 137. Oosterwijk, J. G. van. Anti-tick and pathogen transmission blocking vaccines. *Parasite Immunol.* **43**, e12831 (2021).
 138. de la Fuente, J. & Contreras, M. Additional considerations for anti-tick vaccine research. *Expert Rev. Vaccines* (2022).

doi:10.1080/14760584.2022.2071704

139. de la Fuente, J. *et al.* Subolesin/Akirin Vaccines for the Control of Arthropod Vectors and Vectorborne Pathogens. *Transbound. Emerg. Dis.* **60**, 172–178 (2013).
140. Antunes, S. *et al.* Tick capillary feeding for the study of proteins involved in tick-pathogen interactions as potential antigens for the control of tick infestation and pathogen infection. *Parasites and Vectors* **7**, (2014).
141. De La Fuente, J. & Kocan, K. M. Strategies for development of vaccines for control of ixodid tick species. *Parasite Immunology* **28**, 275–283 (2006).
142. de la Fuente, J. *et al.* Targeting arthropod subolesin/akirin for the development of a universal vaccine for control of vector infestations and pathogen transmission. *Vet. Parasitol.* **181**, 17–22 (2011).
143. Merino, O., Alberdi, P., Pérez de la Lastra, J. M. & de la Fuente, J. Tick vaccines and the control of tick-borne pathogens. *Front. Cell. Infect. Microbiol.* **0**, 30 (2013).
144. Merino, O. *et al.* Vaccination with proteins involved in tick–pathogen interactions reduces vector infestations and pathogen infection. *Vaccine* **31**, 5889–5896 (2013).
145. Merino, O. *et al.* Targeting the tick protective antigen subolesin reduces vector infestations and pathogen infection by *Anaplasma marginale* and *Babesia bigemina*. *Vaccine* **29**, 8575–8579 (2011).
146. Bensaci, M., Bhattacharya, D., Clark, R. & Hu, L. T. Oral vaccination with vaccinia virus expressing the tick antigen subolesin inhibits tick feeding and transmission of *Borrelia burgdorferi*. *Vaccine* **30**, 6040–6046 (2012).
147. Havlíková, S. *et al.* Immunization with recombinant subolesin does not reduce tick infection with tick-borne encephalitis virus nor protect mice against disease. *Vaccine* **31**, 1582–1589 (2013).
148. Levin, M. L., Troughton, D. R. & Loftis, A. D. Duration of tick attachment necessary for transmission of *Anaplasma phagocytophilum*

- by *Ixodes scapularis* (Acari: Ixodidae) nymphs. *Ticks Tick. Borne. Dis.* **12**, 101819 (2021).
149. Kazimírová, M. *et al.* Tick-borne viruses and biological processes at the tick-host-virus interface. *Front. Cell. Infect. Microbiol.* **7**, (2017).
 150. Eisen, L. Pathogen transmission in relation to duration of attachment by *Ixodes scapularis* ticks. *Ticks Tick. Borne. Dis.* **9**, 535 (2018).
 151. Richards, S. L., Langley, R., Apperson, C. S. & Watson, E. Do tick attachment times vary between different tick-pathogen systems? *Environ. - MDPI* **4**, 1–14 (2017).
 152. De La Fuente, J. & Contreras, M. Tick vaccines: Current status and future directions. *Expert Review of Vaccines* **14**, 1367–1376 (2015).
 153. Contreras, M. *et al.* Bacterial membranes enhance the immunogenicity and protective capacity of the surface exposed tick Subolesin-Anaplasma marginale MSP1a chimeric antigen. *Ticks Tick. Borne. Dis.* **6**, 820–828 (2015).
 154. Canales, M., Almazán, C., Pérez de la Lastra, J. M. & de la Fuente, J. Anaplasma marginale major surface protein 1a directs cell surface display of tick BM95 immunogenic peptides on Escherichia coli. *J. Biotechnol.* **135**, 326–332 (2008).
 155. Stanford, M., Werden, S., Mcfadden, G., S, M. M. & W, S. J. Myxoma virus in the European rabbit: interactions between the virus and its susceptible host. doi:10.1051/vetres:2006054i
 156. Kerr, P. J. & Best, S. M. *Myxoma virus in rabbits.* *Rev. sci. tech. Off. int. Epiz* **17**, (1998).
 157. Kerr, P. J. *et al.* Myxoma virus and the Leporipoxviruses: an evolutionary paradigm. *Viruses* **7**, 1020–61 (2015).
 158. Spiesschaert, B., McFadden, G., Hermans, K., Nauwynck, H. & Van de Walle, G. R. The current status and future directions of myxoma virus, a master in immune evasion. *Vet. Res.* **42**, 76 (2011).
 159. Cameron, C. *et al.* The Complete DNA Sequence of Myxoma Virus. *Virology* **264**, 298–318 (1999).

160. McFadden, G. Poxvirus tropism. *Nat. Rev. Microbiol.* 2005 33 **3**, 201–213 (2005).
161. Condit, R. C., Moussatche, N. & Traktman, P. In A Nutshell: Structure and Assembly of the Vaccinia Virion. *Adv. Virus Res.* **66**, 31–124 (2006).
162. Smallwood, S. E., Rahman, M. M., Smith, D. W. & McFadden, G. Myxoma virus: propagation, purification, quantification, and storage. *Curr. Protoc. Microbiol.* **Chapter 14**, Unit 14A.1 (2010).
163. Ball, L. A. High-Frequency Homologous Recombination in Vaccinia Virus DNA. *J. Virol.* **61**, 1788–1795 (1987).
164. Evans, D. H., Stuart, D. & Mcfadden3t, G. High levels of genetic recombination among cotransfected plasmid DNAs in poxvirus-infected mammalian cells. *J. Virol.* **62**, 367 (1988).
165. Pignolet, B. *et al.* Safety and immunogenicity of myxoma virus as a new viral vector for small ruminants. *J. Gen. Virol.* **89**, 1371–1379 (2008).
166. Vrba, S. M., Kirk, N. M., Brisse, M. E., Liang, Y. & Ly, H. Development and Applications of Viral Vected Vaccines to Combat Zoonotic and Emerging Public Health Threats. *Vaccines* **8**, 1–31 (2020).
167. Bertagnoli, S. *et al.* Protection against myxomatosis and rabbit viral hemorrhagic disease with recombinant myxoma viruses expressing rabbit hemorrhagic disease virus capsid protein. *J. Virol.* **70**, 5061–5066 (1996).
168. McCabe, V. J., Tarpey, I. & Spibey, N. Vaccination of cats with an attenuated recombinant myxoma virus expressing feline calicivirus capsid protein. *Vaccine* **20**, 2454–2462 (2002).
169. King, A. A., Fooks, A. R., Aubert, M. & Wandeler, A. I. *Historical Perspective of Rabies in Europe and the Mediterranean Basin*. (World Organisation for Animal Health (OIE), 2004).
170. Fisher, C. R., Streicker, D. G. & Schnell, M. J. The spread and evolution of rabies virus: conquering new frontiers. *Nat. Rev.*

- Microbiol.* **16**, 241 (2018).
171. Pearce, J. M. S. Louis Pasteur and Rabies: a brief note. *J. Neurol. Neurosurg. Psychiatry* **73**, 82–82 (2002).
 172. Fooks, A. R. *et al.* Rabies. *Nat. Rev. Dis. Prim.* 2017 **3**, 1–19 (2017).
 173. Fisher, C. R. & Schnell, M. J. New developments in rabies vaccination. *Rev. Sci. Tech. Off. Int. Epiz* **37**, 657–672 (2018).
 174. Rabies Vaccine Information Statement | CDC. Available at: <https://www.cdc.gov/vaccines/hcp/vis/vis-statements/rabies.html>. (Accessed: 3rd June 2022)
 175. Yang, D.-K., Kim, H.-H., Lee, K.-W. & Song, J.-Y. The present and future of rabies vaccine in animals. *Clin. Exp. Vaccine Res.* **2**, 19 (2013).
 176. Schnell, M. J., Mebatsion, T. & Conzelmann, K. K. Infectious rabies viruses from cloned cDNA. *EMBO J.* **13**, 4195 (1994).
 177. Gomme, E. A., Wanjalla, C. N., Wirblich, C. & Schnell, M. J. Rabies Virus as a Research Tool and Viral Vaccine Vector. *Adv. Virus Res.* **79**, 139 (2011).
 178. Abreu-Mota, T. *et al.* Non-neutralizing antibodies elicited by recombinant Lassa–Rabies vaccine are critical for protection against Lassa fever. *Nat. Commun.* 2018 **9**, 1–16 (2018).
 179. Blaney, J. E. *et al.* Inactivated or Live-Attenuated Bivalent Vaccines That Confer Protection against Rabies and Ebola Viruses. *J. Virol.* **85**, 10605–10616 (2011).
 180. Blaney, J. E. *et al.* Antibody Quality and Protection from Lethal Ebola Virus Challenge in Nonhuman Primates Immunized with Rabies Virus Based Bivalent Vaccine. *PLoS Pathog.* **9**, 1003389 (2013).
 181. Keshwara, R. *et al.* Rabies-based vaccine induces potent immune responses against Nipah virus. *NPJ Vaccines* **4**, (2019).
 182. Kurup, D. *et al.* Inactivated rabies virus vectored SARS-CoV-2 vaccine prevents disease in a Syrian hamster model. *PLoS Pathog.* **17**,

(2021).

183. Spengler, J. R. *et al.* Heterologous protection against Crimean-Congo hemorrhagic fever in mice after a single dose of replicon particle vaccine. *Antiviral Res.* **170**, 104573 (2019).
184. Spengler, J. R. *et al.* Viral replicon particles protect IFNAR^{-/-} mice against lethal Crimean-Congo hemorrhagic fever virus challenge three days after vaccination. *Antiviral Res.* **191**, 105090 (2021).
185. Garcia, G. R. *et al.* The sialotranscriptome of *Amblyomma triste*, *Amblyomma parvum* and *Amblyomma cajennense* ticks, uncovered by 454-based RNA-seq. *Parasites and Vectors* **7**, 1–18 (2014).
186. Anguita, J. *et al.* Salp15, an ixodes scapularis salivary protein, inhibits CD4(+) T cell activation. *Immunity* **16**, 849–859 (2002).
187. Hovius, J. W. R. *et al.* Identification of Salp15 homologues in *Ixodes ricinus* ticks. *Vector Borne Zoonotic Dis.* **7**, 296–303 (2007).
188. Havlíková, S. *et al.* Functional role of 64P, the candidate transmission-blocking vaccine antigen from the tick, *Rhipicephalus appendiculatus*. *Int. J. Parasitol.* **39**, 1485–1494 (2009).
189. Campbell, E. M., Burdin, M., Hoppler, S. & Bowman, A. S. Role of an aquaporin in the sheep tick *Ixodes ricinus*: assessment as a potential control target. *Int. J. Parasitol.* **40**, 15–23 (2010).
190. Hussein, H. E. *et al.* Targeted silencing of the Aquaporin 2 gene of *Rhipicephalus (Boophilus) microplus* reduces tick fitness. *Parasites and Vectors* **8**, 1–12 (2015).
191. Guerrero, F. D. *et al.* *Rhipicephalus (Boophilus) microplus* aquaporin as an effective vaccine antigen to protect against cattle tick infestations. *Parasites and Vectors* **7**, 1–12 (2014).
192. Willadsen, P., Smith, D., Cobon, G. & McKenna, R. V. Comparative vaccination of cattle against *Boophilus microplus* with recombinant antigen Bm86 alone or in combination with recombinant Bm91. *Parasite Immunol.* **18**, 241–246 (1996).
193. García-García, J. C. *et al.* Control of ticks resistant to immunization with Bm86 in cattle vaccinated with the recombinant antigen Bm95

- isolated from the cattle tick, *Boophilus microplus*. *Vaccine* **18**, 2275–2287 (2000).
194. Almazán, C. *et al.* Identification and characterization of *Rhipicephalus* (*Boophilus*) *microplus* candidate protective antigens for the control of cattle tick infestations. *Parasitol. Res.* **106**, 471–479 (2010).
 195. Almazán, C. *et al.* Control of tick infestations in cattle vaccinated with bacterial membranes containing surface-exposed tick protective antigens. *Vaccine* **30**, 265–272 (2012).
 196. Manjunathachar, H. V. *et al.* Identification and characterization of vaccine candidates against *Hyalomma anatolicum* —Vector of Crimean-Congo haemorrhagic fever virus. *Transbound. Emerg. Dis.* **66**, 422–434 (2019).
 197. Das, S. *et al.* SALP16, a gene induced in *Ixodes scapularis* salivary glands during tick feeding. *Am. J. Trop. Med. Hyg.* **62**, 99–105 (2000).
 198. Sukumaran, B. *et al.* An *Ixodes scapularis* protein required for survival of *Anaplasma phagocytophilum* in tick salivary glands. *J. Exp. Med.* **203**, 1507 (2006).
 199. Das, S. *et al.* Salp25D, an *Ixodes scapularis* antioxidant, is 1 of 14 immunodominant antigens in engorged tick salivary glands. *J. Infect. Dis.* **184**, 1056–1064 (2001).
 200. Narasimhan, S. *et al.* A Tick Antioxidant Facilitates the Lyme Disease Agent's Successful Migration from the Mammalian Host to the Arthropod Vector. *Cell Host Microbe* **2**, 7 (2007).
 201. Imamura, S., Vaz, I. D. S., Sugino, M., Ohashi, K. & Onuma, M. A serine protease inhibitor (serpin) from *Haemaphysalis longicornis* as an anti-tick vaccine. *Vaccine* **23**, 1301–1311 (2005).
 202. Imamura, S. *et al.* Two serine protease inhibitors (serpins) that induce a bovine protective immune response against *Rhipicephalus appendiculatus* ticks. *Vaccine* **24**, 2230–2237 (2005).
 203. Dai, J. *et al.* Tick histamine release factor is critical for *Ixodes scapularis* engorgement and transmission of the lyme disease agent. *PLoS Pathog.* **6**, (2010).

204. Schuijt, T. J. *et al.* A tick mannose-binding lectin inhibitor interferes with the vertebrate complement cascade to enhance transmission of the Lyme disease agent. *Cell Host Microbe* **10**, 136–146 (2011).
205. Schuijt, T. J. *et al.* Identification and Characterization of *Ixodes scapularis* Antigens That Elicit Tick Immunity Using Yeast Surface Display. *PLoS One* **6**, e15926 (2011).
206. Pal, U. *et al.* TROSPA, an *Ixodes scapularis* receptor for *Borrelia burgdorferi*. *Cell* **119**, 457–468 (2004).
207. Lu, P. *et al.* RNA interference and the vaccine effect of a subolesin homolog from the tick *Rhipicephalus haemaphysaloides*. *Exp. Appl. Acarol.* **68**, 113–126 (2016).
208. Almazán, C. *et al.* Characterization of three *Ixodes scapularis* cDNAs protective against tick infestations. *Vaccine* **23**, 4403–4416 (2005).
209. Almazán, C., Kocan, K. M., Blouin, E. F. & De La Fuente, J. Vaccination with recombinant tick antigens for the control of *Ixodes scapularis* adult infestations. *Vaccine* **23**, 5294–5298 (2005).
210. Manzano-Román, R., Díaz-Martín, V., Oleaga, A., Siles-Lucas, M. & Pérez-Sánchez, R. Subolesin/akirin orthologs from *Ornithodoros* spp. soft ticks: Cloning, RNAi gene silencing and protective effect of the recombinant proteins. *Vet. Parasitol.* **185**, 248–259 (2012).
211. de la Fuente, J. *et al.* Identification of protective antigens by RNA interference for control of the lone star tick, *Amblyomma americanum*. *Vaccine* **28**, 1786–1795 (2010).
212. Canales, M. *et al.* Conservation and immunogenicity of the mosquito ortholog of the tick-protective antigen, subolesin. *Parasitol. Res.* **105**, 97–111 (2009).
213. Moreno-Cid, J. A. *et al.* Control of multiple arthropod vector infestations with subolesin/akirin vaccines. *Vaccine* **31**, 1187–1196 (2013).
214. Merino, O. *et al.* Control of *Rhipicephalus* (*Boophilus*) *microplus* infestations by the combination of subolesin vaccination and tick autocidal control after subolesin gene knockdown in ticks fed on cattle.

- Vaccine* **29**, 2248–2254 (2011).
215. Carreón, D. *et al.* Vaccination with BM86, subolesin and akirin protective antigens for the control of tick infestations in white tailed deer and red deer. *Vaccine* **30**, 273–279 (2012).
 216. Shakya, M., Kumar, B., Nagar, G., de la Fuente, J. & Ghosh, S. Subolesin: A candidate vaccine antigen for the control of cattle tick infestations in Indian situation. *Vaccine* **32**, 3488–3494 (2014).
 217. Contreras, M. & de la Fuente, J. Control of *Ixodes ricinus* and *Dermacentor reticulatus* tick infestations in rabbits vaccinated with the Q38 Subolesin/Akirin chimera. *Vaccine* **34**, 3010–3013 (2016).
 218. Larsen, M. V. *et al.* Large-scale validation of methods for cytotoxic T-lymphocyte epitope prediction. *BMC Bioinformatics* **8**, 1–12 (2007).
 219. Munderloh, U. & Kurtti, T. Basic Tick Cell Culture Methods.
 220. Munderloh, U. G., Liu, Y., Wang, M., Chen, C. & Kurtti, T. J. Establishment, maintenance and description of cell lines from the tick *Ixodes scapularis*. *J. Parasitol.* **80**, 533–543 (1994).
 221. Dowall, S. D., Carroll, M. W. & Hewson, R. Development of vaccines against Crimean-Congo haemorrhagic fever virus. *Vaccine* **35**, 6015–6023 (2017).
 222. *WHO Task Force Meeting on CCHFV.* (2018).
 223. Top, S. *et al.* Myxomavirus as a vector for the immunisation of sheep: Protection study against challenge with bluetongue virus. *Vaccine* **30**, 1609–1616 (2012).
 224. Nakamura, H. BALB/c Mouse. *Brenner's Encycl. Genet. Second Ed.* 290–292 (2013). doi:10.1016/B978-0-12-374984-0.00133-9
 225. Duncan, R. *et al.* Rubella Virus Capsid Protein Induces Apoptosis in Transfected RK13 Cells. (2000). doi:10.1006/viro.2000.0467
 226. Thorsteinsdóttir, L., Torsteinsdóttir, S. & Svansson, V. Establishment and characterization of fetal equine kidney and lung cells with extended lifespan. Susceptibility to equine gammaherpesvirus infection and transfection efficiency. *Vitr. Cell. Dev. Biol. - Anim.* **52**,

872–877 (2016).

227. Muruve, D. A. *et al.* The inflammasome recognizes cytosolic microbial and host DNA and triggers an innate immune response. *Nat. 2008 4527183* **452**, 103–107 (2008).
228. Wang, F. *et al.* Disruption of Erk-dependent type I interferon induction breaks the myxoma virus species barrier. *Nat. Immunol. 2004 512* **5**, 1266–1274 (2004).
229. MacNeill, A., Doty, Liu, McFadden, D. & Roy. Histological evaluation of intratumoral myxoma virus treatment in an immunocompetent mouse model of melanoma. *Oncolytic Virotherapy* **2**, 1 (2013).
230. Macneill, A. L., Weishaar, K. M., Séguin, B. & Powers, B. E. Safety of an oncolytic myxoma virus in dogs with soft tissue sarcoma. *Viruses* **10**, (2018).
231. Scher, G. & Schnell, M. J. Rhabdoviruses as vectors for vaccines and therapeutics. *Curr. Opin. Virol.* **44**, 169–182 (2020).
232. Smith, M. E. *et al.* Rabies virus glycoprotein as a carrier for anthrax protective antigen. *Virology* **353**, 344 (2006).
233. World Health Organization (WHO). *Oral Vaccination of Dogs Against Rabies: Guidance for research on oral rabies vaccines and Field application of oral vaccination of dogs against rabies.* (2007).
234. European Commission Scientific Committee on Animal Health and Animal Welfare. *The oral vaccination of foxes against rabies.* (2002).
235. McGettigan, J. P. *et al.* Second-Generation Rabies Virus-Based Vaccine Vectors Expressing Human Immunodeficiency Virus Type 1 Gag Have Greatly Reduced Pathogenicity but Are Highly Immunogenic. *J. Virol.* **77**, 237 (2003).
236. Cenna, J. *et al.* Replication-Deficient Rabies Virus–Based Vaccines Are Safe and Immunogenic in Mice and Nonhuman Primates. *J. Infect. Dis.* **200**, 1251 (2009).
237. Albertini, A. A. V., Ruigrok, R. W. H. & Blondel, D. Rabies Virus Transcription and Replication. *Adv. Virus Res.* **79**, 1–22 (2011).

238. Sellers, R. S., Clifford, C. B., Treuting, P. M. & Brayton, C. Immunological variation between inbred laboratory mouse strains: Points to consider in phenotyping genetically immunomodified mice. *Vet. Pathol.* **49**, 32–43 (2012).
239. Spik, K. *et al.* Immunogenicity of combination DNA vaccines for Rift Valley fever virus, tick-borne encephalitis virus, Hantaan virus, and Crimean Congo hemorrhagic fever virus. *Vaccine* **24**, 4657–4666 (2006).
240. Nosrati, M., Behbahani, M. & Mohabatkar, H. Towards the first multi-epitope recombinant vaccine against Crimean-Congo hemorrhagic fever virus: A computer-aided vaccine design approach. *J. Biomed. Inform.* **93**, 103160 (2019).
241. Khan, M. S. A. *et al.* Computational formulation and immune dynamics of a multi-peptide vaccine candidate against Crimean-Congo hemorrhagic fever virus. *Mol. Cell. Probes* **55**, 101693 (2021).
242. Tahir Ul Qamar, M. *et al.* Development of a Novel Multi-Epitope Vaccine Against Crimean-Congo Hemorrhagic Fever Virus: An Integrated Reverse Vaccinology, Vaccine Informatics and Biophysics Approach. *Front. Immunol.* **12**, 2313 (2021).
243. Dowall, S. D. *et al.* A Crimean-Congo hemorrhagic fever (CCHF) viral vaccine expressing nucleoprotein is immunogenic but fails to confer protection against lethal disease. *Hum. Vaccines Immunother.* **12**, 519–527 (2016).
244. Zhao, C. *et al.* Immunogenicity of a multi-epitope DNA vaccine against hantavirus. *Hum. Vaccin. Immunother.* **8**, 208–215 (2012).
245. Zivcec, M., Spiropoulou, C. F. & Spengler, J. R. The use of mice lacking type I or both type I and type II interferon responses in research on hemorrhagic fever viruses. Part 2: Vaccine efficacy studies. *Antiviral Res.* **174**, 104702 (2020).
246. Rodriguez, S. E. Studying the Biology of, and Developing Countermeasures to, a Ticktransmitted Hemorrhagic Fever Virus. (University of Texas Medical Branch, 2018).
247. Garrison, A. R., Smith, D. R. & Golden, J. W. Animal models for

- crimean-congo hemorrhagic fever human disease. *Viruses* **11**, (2019).
248. Mouse Haplotype Table. Affymetrix eBioscience.
249. Trentelman, J. J. A. *et al.* A combination of antibodies against Bm86 and Subolesin inhibits engorgement of *Rhipicephalus australis* (formerly *Rhipicephalus microplus*) larvae in vitro. *Parasit. Vectors* **12**, (2019).
250. Ndawula, C. & Tabor, A. E. Cocktail anti-tick vaccines: The unforeseen constraints and approaches toward enhanced efficacies. *Vaccines* **8**, 1–23 (2020).
251. de la Fuente, J. *et al.* Functional genomic studies of tick cells in response to infection with the cattle pathogen, *Anaplasma marginale*. *Genomics* **90**, 712–722 (2007).
252. de la Fuente, J., Almazán, C., Naranjo, V., Blouin, E. F. & Kocan, K. M. Synergistic effect of silencing the expression of tick protective antigens 4D8 and Rs86 in *Rhipicephalus sanguineus* by RNA interference. *Parasitol. Res.* 2006 992 **99**, 108–113 (2006).
253. Guo, K. *et al.* Monoclonal antibodies target intracellular PRL phosphatases to inhibit cancer metastases in mice. <http://dx.doi.org/10.4161/cbt.7.5.5764> **7**, 750–757 (2008).
254. Wang, X. R., Kurtti, T. J., Oliver, J. D. & Munderloh, U. G. The identification of tick autophagy related genes in *Ixodes scapularis* responding to amino acid starvation. *Ticks Tick. Borne. Dis.* **11**, 101402 (2020).
255. Oliver, J. D., Chávez, A. S. O., Felsheim, R. F., Kurtti, T. J. & Munderloh, U. G. An *Ixodes scapularis* cell line with a predominantly neuron-like phenotype. *Exp. Appl. Acarol.* **66**, 427 (2015).
256. De La Fuente, J., Artigas-Jerónimo, S. & Villar, M. Akirin/Subolesin regulatory mechanisms at host/tick–pathogen interactions. *microLife* **3**, 12 (2022).
257. Franta, Z. *et al.* Dynamics of digestive proteolytic system during blood feeding of the hard tick *Ixodes ricinus*. *Parasites and Vectors* **3**, 1–11 (2010).

258. Mangia, C. *et al.* Exposure to amitraz, fipronil and permethrin affects cell viability and ABC transporter gene expression in an *Ixodes ricinus* cell line. *Parasit. Vectors* **11**, (2018).
259. Hernandez, E. P. *et al.* Induction of intracellular ferritin expression in embryo-derived *Ixodes scapularis* cell line (ISE6). *Sci. Reports 2018* **8**, 1–12 (2018).
260. de la Fuente, J., Almazán, C., Blouin, E. F., Naranjo, V. & Kocan, K. M. Reduction of tick infections with *Anaplasma marginale* and *A. phagocytophilum* by targeting the tick protective antigen subolesin. *Parasitol. Res. 2006 1001* **100**, 85–91 (2006).
261. Vlieghe, I., Yang, G., Hruby, D., Jordan, R. & Neyts, J. Deletion of the vaccinia virus F13L gene results in a highly attenuated virus that mounts a protective immune response against subsequent vaccinia virus challenge. *Antiviral Res.* **93**, 160–166 (2012).
262. Blasco, R. & Moss, B. Extracellular vaccinia virus formation and cell-to-cell virus transmission are prevented by deletion of the gene encoding the 37,000-Dalton outer envelope protein. *J. Virol.* **65**, 5910 (1991).
263. Torina, A. *et al.* Control of tick infestations and pathogen prevalence in cattle and sheep farms vaccinated with the recombinant Subolesin-Major Surface Protein 1a chimeric antigen. *Parasit. Vectors* **7**, 10 (2014).
264. Maki, J. *et al.* Oral vaccination of wildlife using a vaccinia-rabies-glycoprotein recombinant virus vaccine (RABORAL V-RG®): A global review. *Vet. Res.* **48**, 1–26 (2017).

Vita

Megan Mears was born in Ocala, Florida on June 25, 1995 to Sharon and David Mears. During her time as an undergraduate at Georgia Southern University, she discovered her love of infectious disease research while working with Dr. Marina Eremeeva. In May 2017, she graduated *Cum Laude* as a University Honors Program Scholar and received a Bachelor of Science degree in Biology with a minor in Chemistry. Megan then began pursuing her doctorate at the University of Texas Medical Branch in the Experimental Pathology Graduate Program in August 2017. She joined the laboratory of Dr. Dennis Bente in May 2018 to study vaccine development for Crimean-Congo hemorrhagic fever virus. During her studies at UTMB she also completed her Master of Public Health degree with a focus in Epidemiology.

Permanent address: 3222 Antilles Ave, Galveston, TX, 77551

This dissertation was typed by Megan Mears.

Curriculum Vitae

NAME: Megan Mears
PRESENT POSITION

Graduate Research Assistant
Experimental Pathology Graduate Program
Vaccinology Track, Institute for Translational Sciences
Graduate School of Biomedical Sciences
University of Texas Medical Branch (UTMB)
301 University Blvd., Galveston, Texas 77555
Email: memears@utmb.edu
ORCID: 0000-0003-1293-7696

EDUCATION

Aug 2017-Present

Doctor of Philosophy (*Experimental Pathology Graduate Program, Vaccinology Track*), University of Texas Medical Branch, Galveston, Texas

Dec 2021

Master of Public Health (*Epidemiology*), University of Texas Medical Branch, Galveston, Texas

May 2017

Bachelor of Science (*Biology, minor: Chemistry; University Honors Program Scholar; Cum Laude*), Georgia Southern University, Statesboro, Georgia

PROFESSIONAL EXPERIENCE

Aug 2017-Present

Graduate Research Assistant, Department of Pathology, University of Texas Medical Branch, Galveston, Texas

Aug 2019-Dec2019

Intern, Institutional Office of Regulated Nonclinical Studies (ORNcS), University of Texas Medical Branch, Galveston, Texas

May 2015-Jul 2017

Undergraduate Research Assistant, Department of Biostatistics, Epidemiology and Environmental Health Sciences, Georgia Southern University, Statesboro, Georgia

Jun 2016-Aug 2016

Recreational Forestry Technician, Divide Ranger District, US Forest Service, United States Department of Agriculture, Creede, Colorado

Financial Support:

Apr 2022-Aug 2022

NIH NIAID T32 Emerging and Tropical Infectious Diseases Training Program (AI007526-20). Principal Investigator: Dr. Lynn Soong.

Jan 2020-Dec 2021 Pre-Doctoral Fellowship, Sealy Institute for Vaccine Sciences (SIVS), University of Texas Medical Branch, Galveston TX.

CERTIFICATIONS

2020 Approved to work independently at biosafety level 4 (BSL-4)
2018 Approved for Federal Select Agent Work & Tier 1 Clearance
2018 Basics of Good Laboratory Practice (ORNcS, UTMB)
2018 Basics of Good Documentation Practice (ORNcS, UTMB)
2018 Approved to work at biosafety level 3 (BSL-3)
2018 Approved to work at animal biosafety level 2 (ABSL-2)
2017 Approved to work at biosafety level 2 (BSL-2)

HONORS

2021 Poster Award (Edward S. Reynolds Award), Annual Pathology Trainee Research Day, UTMB
2019 Poster Award (Best in Category), 8th Annual UTMB Global Health Education Symposium, UTMB
2019 Poster Award (Edward S. Reynolds Award), Annual Pathology Trainee Research Day, UTMB
2019 Travel Award, Sealy Institute for Vaccine Sciences, UTMB
2018 Travel Award, Institute for Human Infections and Immunity, UTMB
2017-2022 McLaughlin Scholar Award (awarded to graduate students displaying excellence in the areas of infectious disease and immunity), UTMB
2016 Travel Award, American Society for Microbiology
2016 Travel Award, Southeastern Branch of the American Society for Microbiology

ADDITIONAL INVOLVEMENT

Apr 2021 Student Organizer and Moderator, McLaughlin Colloquium Organizing Committee, UTMB
Aug 2020-Aug 2021 President, Experimental Pathology Graduate Student Organization, UTMB
Aug 2019-Aug 2020 Vice President, Experimental Pathology Graduate Student Organization, UTMB
Aug 2019-May 2021 Student Representative, Experimental Pathology Admissions and Recruitment Committee, UTMB

PUBLICATIONS

Published

1. Outlaw V.K., Bovier F.T., **Mears M.C.**, Cajimat M.N.B., Zhu Y., Lin M.J., Addetia A., Lieberman N.A.P., Peddu V., Xie X., Shi P.Y., Greninger A.L., Gellman S.H., Bente D.A., Moscona A., and Porotto M. Inhibition of coronavirus entry *in vitro* and *ex vivo* by a lipid-conjugated peptide derived from the SARS-CoV-2 spike glycoprotein HRC domain. *mBio*. 2020 Oct20; DOI: 0.1128/mBio.01935-20

- Lieberman N.A.P., Peddu V., Xie H., Shrestha L., Huang M., **Mears M.C.**, Cajimat M.N.B., Bente D.A., Shi P.Y., Bovier F., Roychoudhury P., Jerome K.R., Moscona A., Porotto M., Greninger A.L. In vivo antiviral host transcriptional response to SARS-CoV-2 by viral load, sex, and age. *PLoS Biol.* 2020 Sep8; DOI: 10.1371/journal.pbio.3000849
- Kar S., Rodriguez S.E., Akyildiz G., Cajimat M.N.B., Bircan R., **Mears M.C.**, Bente D.A. and Keles A.G. Crimean-Congo hemorrhagic fever virus in tortoises and *Hyalomma aegyptium* ticks in East Thrace, Turkey: potential of a cryptic transmission cycle. *Parasites Vectors.* 2020 Apr19; DOI: 10.1186/s13071-020-04074-6
- Johnson B.A., Hage A., Kalveram B., **Mears M.**, Plante J.A., Rodriguez S.E., Ding Z., Luo X., Bente D., Bradrick S.S., Freiberg A.N., Popov V., Rajsbaum R., Rossi S., Russell W.K., and Menachery V.D. Peptidoglycan associated cyclic lipopeptide disrupts viral infectivity. *J. Virol.* 2019 Aug28; DOI: 10.1128/JVI.01282-19

Submitted

- Mears M.C.***, Rodriguez S.E.*, Schmitz K.S., Padilla A., Biswas S., Cajimat M.N.B., Mire C.E., Welch S.R., Bergeron E., Alabi C.A., Porotto M., and Bente D.A. Design and Evaluation of Neutralizing and Fusion Inhibitory Peptides to Crimean-Congo Hemorrhagic Fever Virus. 2022. *Antiviral Research.* (*Co-first authored)

In Preparation

- Mears M.C.**, de la Fuente J., Barrett A.D.T., and Bente D.A. An *in vitro* approach to evaluate the biological impact of Subolesin antisera.
- Mears M.C.**, and Bente D.A. *In silico* Design of a Crimean-Congo Hemorrhagic Fever Virus Glycoprotein Multi-Epitope Antigen for Vaccine Development.
- Scher G., Bente D.A., **Mears M.C.**, Cajimat M.N.B., and Schnell M.J. GP38 as a Vaccine Target for Crimean-Congo Hemorrhagic Fever Virus.

Theses

- Mears, M.C.** (2021). Gaps, Conflicts, and Recommendations for Application of the Select Agent Regulations Pertaining to Care of Patients with Ebola Virus Disease. Integrative Learning Experience (MPH Thesis). University of Texas Medical Branch.
- Mears, M.C.** (2017). Application of RNA baits for detection and identification of the p120 ortholog of *Ehrlichia ewingii*. University Honors Program Thesis. Georgia Southern University.

ORAL PRESENTATIONS

- Infectious disease and vaccine development research.* Great American Teach-In. Liberty Middle School, Tampa, Florida, November 18, 2021.
- Progress towards a viral-vectored anti-tick vaccine.* Experimental Pathology Student Work in Progress Seminar, University of Texas Medical Branch, Galveston, Texas, September 23, 2021.
- An immunoinformatics guided approach for rational design of a Crimean-Congo hemorrhagic fever virus multi-epitope DNA vaccine.* Experimental Pathology Student

Work in Progress Seminar, University of Texas Medical Branch, Galveston, Texas, December 17, 2020.

4. *Development and evaluation of a bivalent transmissible vaccine targeting Crimean-Congo hemorrhagic fever virus and Hyalomma ticks.* Experimental Pathology Student Work in Progress Seminar, University of Texas Medical Branch, Galveston, Texas, January 16, 2020.
5. *Targeting the reservoir of Crimean-Congo hemorrhagic fever: Development of an anti-tick vaccine.* SaBio, Instituto de Investigación en Recursos Cinegéticos, University of Castilla-La Mancha: Ciudad Real Campus, Ciudad Real, Spain, October 25, 2019.
6. *Development of a reservoir targeted vaccine to control Crimean-Congo hemorrhagic fever.* Experimental Pathology Student Work in Progress Seminar, University of Texas Medical Branch, Galveston, Texas, March 28, 2019.

POSTERS

International

1. **Mears, M.C.**, McFadden, G., de la Fuente, J., Beasley, D.W.C., and Bente, D.A. Targeting the reservoir of Crimean-Congo hemorrhagic fever: Development of an anti-tick vaccine. 2019 International Society for Vaccines (ISV) Annual Congress, Ghent, Belgium, October 27-29, 2019.
2. **Mears M.C.**, Rodriguez S.E., Schmitz K.S., Padilla A.M., Cajimat M.N.B., Schuster I.U.E., Biswas S., Mire C.E., Geisbert T.W., Porotto M., and Bente D.A. Designing and evaluating inhibitory peptides to Crimean-Congo hemorrhagic fever virus. 10th International Global Virus Network Meeting, Les Pensieres Center for Global Health, Veyrier-du-Lac, France, November 28-30, 2018.

National

3. **Mears, M.C.**, McFadden, G., de la Fuente, J., Beasley, D.W.C., and Bente, D.A. Development of a reservoir targeted vaccine to control Crimean-Congo hemorrhagic fever. 17th Annual Ecology and Evolution of Infectious Diseases (EEID) meeting, Princeton University, Princeton, New Jersey, June 10-13, 2019.

Internal

4. **Mears, M.C.**, Scher, G., Rahman, M., McFadden, G., Schnell, M., de la Fuente, J., Barrett, A.D.T., and Bente, D.A. Progress towards a viral-vectored anti-tick vaccine. Twenty-seventh Annual Pathology Department Trainee Research Day, University of Texas Medical Branch, Galveston, Texas, October 7, 2021.
5. **Mears, M.C.**, Cajimat, M.N.B., Barrett, A.D.T., and Bente, D.A. Safety and immunogenicity of a multi-epitope DNA vaccine for Crimean-Congo hemorrhagic fever virus. UTMB McLaughlin Research Colloquium. University of Texas Medical Branch, Galveston, Texas, April 27-30, 2021.
6. **Mears, M.C.**, Cajimat, M.N.B., Barrett, A.D.T., and Bente, D.A. An immunoinformatics guided approach for rational design of a Crimean-Congo hemorrhagic fever virus multi-

epitope DNA vaccine. Twenty-sixth Annual Pathology Department Trainee Research Day, University of Texas Medical Branch, Galveston, Texas, September 21, 2020.

7. **Mears, M.C.**, McFadden, G., de la Fuente, J., Beasley, D.W.C., and Bente, D.A. Targeting the reservoir of Crimean-Congo hemorrhagic fever: Development of an anti-tick vaccine. 8th Annual UTMB Global Health Education Symposium, University of Texas Medical Branch, Galveston, TX, October 12, 2019.
8. **Mears, M.C.**, McFadden, G., de la Fuente, J., Beasley, D.W.C., and Bente, D.A. Development of a reservoir targeted vaccine to control Crimean-Congo hemorrhagic fever. Twenty-fifth Annual Pathology Department Trainee Research Day, University of Texas Medical Branch, Galveston, Texas, October 3, 2019.
9. **Mears, M.C.**, McFadden, G., de la Fuente, J., Beasley, D.W.C., and Bente, D.A. Development of a reservoir targeted vaccine to control Crimean-Congo hemorrhagic fever. UTMB McLaughlin Research Colloquium. University of Texas Medical Branch, Galveston, Texas, March 29, 2019.
10. **Mears M.C.**, Padilla A.M., Schmitz K.S., Rodriguez S.E., Schuster I.U.E., Cajimat M.N.B., Mire C.E., Geisbert T.W., Porotto M., and Bente D.A. Designing and evaluating inhibitory peptides to Crimean-Congo hemorrhagic fever virus. Twenty-fourth Annual Pathology Department Trainee Research Day, University of Texas Medical Branch, Galveston, Texas, May 3, 2018.